UNIVERSIDADE FEDERAL DO RIO GRANDE DO SUL

CENTRO DE BIOTECNOLOGIA

PROGRAMA DE PÓS-GRADUAÇÃO EM BIOLOGIA CELULAR E MOLECULAR

Estudo funcional do fator de transcrição Pdr802 na biologia do patógeno *Cryptococcus neoformans*

Tese de doutorado

Júlia Catarina Vieira Reuwsaat

Porto Alegre, janeiro de 2021.

UNIVERSIDADE FEDERAL DO RIO GRANDE DO SUL

CENTRO DE BIOTECNOLOGIA

PROGRAMA DE PÓS-GRADUAÇÃO EM BIOLOGIA CELULAR E MOLECULAR

Estudo funcional do fator de transcrição Pdr802 na biologia do patógeno *Cryptococcus neoformans*

Júlia Catarina Vieira Reuwsaat

Tese submetida ao Programa de Pós-Graduação em Biologia Celular e Molecular do Centro de Biotecnologia da Universidade Federal do Rio Grande do Sul como requisito parcial para obtenção do Grau de Doutora em Ciências.

Orientadora: Prof. Dra. Lívia Kmetzsch Rosa e Silva

Co-orientadora: Prof. Dra. Marilene Henning Vainstein

Colaboradora: Prof. Dra. Tamara Doering

Porto Alegre, janeiro de 2021.

Este trabalho foi desenvolvido no Laboratório de Biologia Molecular de Patógenos, coordenado pela Professora Lívia Kmetzsch, situado no Centro de Biotecnologia da Universidade Federal do Rio Grande do Sul, e no laboratório da Professora Tamara Doering, da *Washington University School of Medicine, St. Louis*, Estados Unidos da América. Este trabalho contou com fomento do Conselho Nacional de Desenvolvimento Científico e Tecnológico (CNPq, Brasil), da Coordenação de Aperfeiçoamento de Pessoal de Nível Superior (CAPES, Brasil), da Fundação de Amparo à Pesquisa do Estado do Rio Grande do Sul (FAPERGS, Brasil) e do *National Institutes of Health* (NIH, EUA).

AGRADECIMENTOS

Gostaria de agradecer à UFRGS, ao PPGBCM e a todos os professores e funcionários pela oportunidade e ensino de excelência;

Em especial à minha orientadora Lívia Kmetzsch pelos ensinamentos, dedicação, paciência e apoio;

À minha coorientadora Marilene Vainstein pela confiança;

À professora Tamara Doering pela colaboração e oportunidade única;

Ao professor Charley pela revisão da tese e também orientação;

Ao professor Augusto pelas ideias e ensinamentos;

Aos professores Michael Brent, Márcio Rodrigues e Suzana Frases pela colaboração;

Ao professor Itabajara Vaz, membro da comissão de acompanhamento e sempre disposto a conversar, discutir e emprestar reagentes;

Aos meus pais e avós pelo amor incondicional e dedicação, eu não chegaria até aqui sem vocês;

Ao meu irmão, minha inspiração e melhor amigo;

Ao Júnior, meu amor e companheiro, obrigada principalmente pela paciência, incentivo e amor incondicional;

Aos meus companheiros de pesquisa Heryk Motta e Eamim Squizani por toda dedicação, paciência e amizade;

Ao Daniel Agustinho pela amizade e companheirismo;

A todos os colegas (atuais e passados) dos laboratórios 222, 220, 219 e 217 do Centro de Biotecnologia pelo companheirismo e convivência;

A todos os colegas dos laboratórios da professora Tamara Doering e do professor Michael Brent;

À minha família e a todos que contribuíram de alguma forma para a realização desse trabalho;

Aos meus amigos de Porto Alegre e São Leopoldo pelo carinho e amor, mesmo quando distantes a maioria do tempo;

Às agências de fomento CAPES, CNPq, FAPERGS e NIH.

SUMÁRIO

LISTA DE ABREVIATURAS, SÍMBOLOS E UNIDADES

5-FC	5-fluorocitosina/flucitosina
AFLP	polimorfismo de tamanho de fragmento amplificado, do inglês *amplified fragment length polymorphism*
AIDS	síndrome da imunodeficiência adquirida, do inglês *acquired immunodeficiency syndrome*
AMPc	adenosina 3'-5'-monofosfato cíclico
APC	célula apresentadora de antígeno, do inglês *antigen presenting cell*
BHE	barreira hematoencefálica
Ca^{2+}	íon cálcio
CD4+	linfócito T *helper*
CD8+	linfócito T citotóxico
ChIP-Seq	imunoprecipitação de cromatina seguido de sequenciamento, do inglês *chromatin immunoprecipitation followed by sequencing*
DAG	diacilglicerol
DTO	do inglês *dual-threshold optimization*
FT	fator de transcrição
GPI	glicosilfosfatidilinositol
GXM	glucuronoxilomanana
GXMGal	glucuranoxilomanogalactana
HIV	vírus da imunodeficiência humana, do inglês *human immunodeficiency virus*
IFN-γ	interferon gama, do inglês *interferon gamma*
IL-2	interleucina 2
IL-4	interleucina 4
IL-10	interleucina 10
IL-12	interleucina 12
IL-13	interleucina 13
IP3	inositol trifosfato
kDa	quilodalton
L-DOPA	L-3,4-dihidroxifenilalanina

M1	macrófagos tipo 1
M2	macrófagos tipo 2
MAT	do inglês *mating type*
MATα	do inglês *mating type* alpha
MAT**a**	do inglês *mating type* a
MET	microscopia eletrônica de transmissão
MHC	complexo principal de histocompatibilidade, do inglês *major histocompatibility complex*
MLST	do inglês *multi-locus sequence type*
MP	manoproteína
MP84	manoproteína 84
MP88	manoproteína 88
MP98	manoproteína 98
MP115	manoproteína 115
mRNA	RNA mensageiro, do inglês *messenger RNA*
PAMP	padrões moleculares associados a patógenos, do inglês *pathogen-associated molecular pattern*
PCR	reação em cadeia da polimerase, do inglês *polymerase chain reaction*
pH	potencial hidrogeniônico
PIP2	fosfatidilinositol 4,5-bifosfato
RE	retículo endoplasmático
RNA-Seq	sequenciamento de RNA, do inglês *RNA sequencing*
SNC	sistema nervoso central
SRI	síndrome de reconstituição imunológica
Th	T *helper*
Th1	T *helper* 1
Th2	T *helper* 2
TNF-α	fator de necrose tumoral alfa, do inglês *tumor necrosis factor alpha*
UDP	uridina difosfato
var	variedade
VG	do inglês *variety gattii*

VN	do inglês *variety neoformans*
WGA	do inglês *wheat germ agglutinin*

LISTA DE TABELAS

LISTA DE FIGURAS

RESUMO

Cryptococcus neoformans é o agente etiológico da criptococose, enfermidade que afeta principalmente pacientes imunocomprometidos e causa aproximadamente 180.000 óbitos no mundo anualmente. Uma vez em contato com o hospedeiro, este patógeno é exposto à uma variedade de processos adaptativos, os quais são regulados por uma rede de fatores de transcrição (FTs). Dentre eles, destaca-se o FT Pdr802, já previamente caracterizado como um importante regulador da patogênese de *C. neoformans*. Na presente Tese, demonstramos que a expressão do gene codificador de Pdr802 é altamente induzida em condições que mimetizam o ambiente do hospedeiro *in vitro*, e que sua inativação afeta a sobrevivência de *C. neoformans* em um hospedeiro mamífero, no soro murino e em meio de cultura de células. Dois importantes determinantes de virulência deste patógeno são negativamente regulados por Pdr802: a produção da cápsula polissacarídica e de células gigantes (*Titan cells*). Ambos fenótipos elucidam a disseminação limitada do mutante nulo *pdr802* para o Sistema Nervoso Central (SNC) e a consequente redução da virulência dessa linhagem, uma vez que células hipercapsulares e gigantes demonstram taxas de fagocitose por macrófagos reduzidas e ineficiência em ultrapassar diretamente barreiras biológicas. Utilizando ensaio de imunoprecipitação de cromatina seguido de sequenciamento (ChIP-Seq), associado ao sequenciamento de RNA (RNA-Seq), identificamos alvos diretos de Pdr802, que incluem as proteínas relacionadas com *quorum sensing* Pqp1, Opt1 e Liv3 e os fatores de transcrição Stb4, Zfc3 e Bzp4, importantes para a infecção do cérebro e regulação do tamanho da cápsula polissacarídica de *C. neoformans*. Alvos adicionais incluem as proteínas reguladas pela via da calcineurina, Had1 e Crz1, importantes para o remodelamento da parede celular e virulência de *C. neoformans*, e genes envolvidos na resistência à temperatura do hospedeiro, ao estresse oxidativo e atividade de urease. O papel de Pdr802 como regulador negativo da formação de células gigantes e da cápsula polissacarídica, assim como regulador positivo de *quorum sensing*, são críticos para a patogenicidade de *C. neoformans*.

ABSTRACT

Cryptococcus neoformans is the etiological agent of cryptococcosis, an infectious disease that affects mainly immunocompromised patients and causes 180,000 deaths worldwide each year. Once inside the host, cryptococcal cells undergo a variety of adaptative processes that are regulated by a network of transcription factors (TFs). One of these is the TF Pdr802, which have been already shown as an important regulator of *C. neoformans* pathogenicity. In this work, we demonstrated that the Pdr802 coding gene expression is highly induced under host-like conditions *in vitro* and its deletion impairs *C. neoformans* survival in a mammalian host, mouse serum, and tissue culture media. Two important cryptococcal virulence determinants are negatively regulated by Pdr802: the polysaccharide capsule and Titan cells production. Both of these phenotypes explain the limited dissemination of *pdr802* null mutant cells to the central nervous system and the consequently reduced virulence of this strain, as hypercapsular strains and Titan cells are less phagocyted by macrophages and have diminished ability to directly cross biological barriers. Using chromatin immunoprecipitation followed by sequencing (ChIP-Seq), as well as RNA sequencing (RNA-Seq), we identified directly targets of Pdr802, which include the quorum sensing related proteins Pqp1, Opt1, and Liv3 and the transcription factors Stb4, Zfc3 and Bzp4, which regulate cryptococcal brain infectivity and capsule thickness. Additional targets comprise the calcineurin-regulated proteins Had1 and Crz1, important for cell wall remodeling and *C. neoformans* virulence; and genes related to resistance to host temperature and oxidative stress, and to urease activity. The role of Pdr802 as a negative regulator of Titan cell formation and capsule thickness, as well as a positive regulator of quorum sensing are thus critical for cryptococcal pathogenicity.

1. INTRODUÇÃO

1.1. Infecções fúngicas

O reino Fungi engloba inúmeras espécies capazes de rápida adaptação a diferentes ambientes, principalmente a partir da transição entre morfotipos distintos, e compreende muitos organismos degradadores de matéria orgânica (FISHER *et al.*, 2020). Várias enzimas produzidas para decomposição de matéria orgânica também são importantes para possíveis transições de ambientes, como por exemplo, a produção de proteases, fosfolipases e nucleases podem ser decisivas durante uma possível interação com hospedeiros (FISHER *et al.*, 2020). Além disso, os fungos produzem inúmeros metabólitos secundários, entre eles importantes compostos antimicrobianos, pesticidas, micotoxinas e imunosupressores que influenciam diretamente na sua adaptação a diferentes nichos (BILLS; GLOER, 2016; KESWANI *et al.*, 2019).

Dados recentes evidenciam o destacado papel de fungos patogênicos na extinção de espécies, no distúrbio de ecossistemas, na agricultura e na saúde pública (FISHER *et al.*, 2012). Porém, o impacto das infecções fúngicas na saúde humana continua sendo negligenciado, mesmo que estas sejam responsáveis por um maior número de óbitos em comparação à tuberculose ou à malária mundialmente, e que estimativas demonstrem que mais de 300 milhões de pessoas sofrem com infecções fúngicas severas a cada ano (RODRIGUES; NOSANCHUK, 2020). As doenças decorrentes de infecções fúngicas em humanos diferem de outras por inúmeros motivos, como a similaridade entre as células do hospedeiro com o patógeno fúngico, o que dificulta o desenvolvimento de compostos antifúngicos; a capacidade do patógeno de infectar diferentes células do hospedeiro, podendo invadir distintos tecidos simultaneamente; e a ocorrência de potenciais alterações morfológicas durante o período da infecção, impactando diretamente o tratamento, uma vez que morfotipos podem responder distintamente aos compostos administrados (RODRIGUES; NOSANCHUK, 2020).

As infecções fúngicas humanas podem ser classificadas como invasivas (sistêmicas), de pele, mucosa, alérgicas e também crônicas, e causam grande

impacto social e econômico (FUNGAL DISEASE FREQUENCY | GAFFI - GLOBAL ACTION FUND FOR FUNGAL INFECTIONS). As infecções invasivas, mesmo tendo uma incidência menor do que as superficiais, quando chegam ao estágio de desenvolvimento da doença, exibem uma alta taxa de mortalidade, levando mais de um milhão e meio de pessoas à óbito anualmente (BROWN *et al.*, 2012). Dentre os principais fungos causadores de infecções invasivas destacam-se espécies do gênero *Cryptococcus*, *Aspergillus*, *Candida* e *Pneumocystis* (Tabela 1). A incidência de cada uma dessas doenças varia de acordo com condições socioeconômicas, localização geográfica, hábitos culturais e status do sistema imune do hospedeiro (BROWN *et al.*, 2012).

Tabela 1. Principais doenças fúngicas invasivas e impacto global anual.

Doença fúngica	Incidência	Taxa de Fatalidade	Mortes estimadas
Meningite criptocócica	370.000	15-20% EUA; >50% países subdesenvolvidos	>125.000
Pneumonia pneumocística	>500.000	~15% AIDS; ~50% não-AIDS	>250.000
Aspergilose invasiva	>250.000	~50% se tratada	>125.000
Candidíase invasiva	>700.000	~45% se tratada	>350.000
Aspergilose pulmonar crônica	~3 milhões	~15% terceiro mundo	>450.000
Histoplasmose disseminada	>100.000	>30% AIDS, diagnosticada	>80.000
Asma severa por sensibilização fúngica	~10 milhões	>1%	~175.000
Total	**>14.900.000**		**>1.700.000**

Adaptado de Gaffi (FUNGAL DISEASE FREQUENCY | GAFFI - GLOBAL ACTION FUND FOR FUNGAL INFECTIONS).

As micoses sistêmicas são altamente letais se não diagnosticadas e tratadas corretamente. A maioria dessas doenças atingem pacientes que possuem seu sistema imune comprometido, principalmente por infecção pelo vírus HIV resultando na síndrome de imunodeficiência adquirida (AIDS), mas também por câncer e outras condições imunossupressoras (KÖHLER *et al.*, 2017). Uma das principais doenças fúngicas invasivas é a meningite criptocócica, causada pelos patógenos *Cryptococcus neoformans* e *Cryptococcus gattii* (KWON-CHUNG *et al.*, 2014). Também conhecida como criptococose, essa doença leva à óbito aproximadamente 125 mil pacientes anualmente em todo o mundo (Tabela 1).

As infecções causadas por *C. neoformans* são a vasta maioria dos casos consequentes de criptococose (>95%). Até 1950, menos de 300 casos de criptococose tinham sido contabilizados e esses números cresceram significativamente a partir do aumento de quadros de imunossupressão, principalmente devido à AIDS (DUNCAN, 1957; RAJASINGHAM *et al.*, 2017). Nestes pacientes, há uma perda gradual de linfócitos T *helper* (CD4+) (VIJAYAN *et al.*, 2017) e a principal resposta imune contra *Cryptococcus* é através da ativação deste tipo celular (HUFFNAGLE *et al.*, 1994). Algumas linhagens de *C. gattii* são capazes de causar doença em pacientes imunocompetentes, como a R265, responsável pelo surto de criptococose na ilha de Vancouver, Canadá em 1999, sendo considerada um patógeno primário (DATTA; BARTLETT; MARR, 2009; SPEED; DUNT, 1995). No entanto, um estudo de caso-controle evidenciou alguns fatores que predispõe a doença causada por *C. gattii*, como idade avançada, uso de corticoides, doenças pulmonares e fumo (MACDOUGALL *et al.*, 2011). Já *C. neoformans* é considerado um patógeno oportunista ou secundário, mesmo já havendo notificações de casos da doença em pacientes aparentemente imunocompetentes (BEARDSLEY; SORRELL; CHEN, 2019; CASADEVALL; PIROFSKI, 2001; CHEN *et al.*, 2008). Dados epidemiológicos demonstram que as espécies patogênicas do gênero *Cryptococcus* são responsáveis por 60% dos casos de meningite em pacientes HIV positivos mundialmente, levando 15% destes à óbito (RAJASINGHAM *et al.*, 2017).

Um estudo brasileiro demonstrou que *C. neoformans* é o principal causador de micose sistêmica em pacientes com AIDS, com taxa de mortalidade que pode atingir 51% (PRADO *et al.*, 2009). Em 17 de fevereiro de 2020, foi publicada no Diário Oficial da União, portaria nº 264, a inclusão da criptococose como micose sistêmica de notificação compulsória, assim como a esporotricose humana e a paracoccidioidomicose. A partir disso, o impacto da criptococose poderá ser avaliado a nível nacional quanto às suas taxas de incidência e morte, como também seus impactos socioeconômicos.

1.2. Espécies patogênicas do gênero *Cryptococcus*

C. neoformans e *C. gattii* são leveduras encapsuladas do filo Basidiomycota. Estas duas espécies divergiram de um ancestral comum e variam em sua distribuição geográfica, patologia e inúmeros aspectos moleculares (COGLIATI, 2013). A primeira classificação do complexo de espécies de *Cryptococcus* ocorreu em 1950, no qual análises de aglutinação da cápsula polissacarídica as separou em diferentes sorotipos: A, B e C e, posteriormente, os sorotipos D e o híbrido AD também foram descritos (EVANS, 1951; WILSON; BENNETT; BAILEY, 1968). Até então, *C. neoformans* e *C. gattii* eram consideradas linhagens diferentes da mesma espécie quando, em 2002, análises moleculares e epidemiológicas as separaram em duas espécies (KWON-CHUNG *et al.*, 2002; KWON-CHUNG; VARMA, 2006).

A classificação mais utilizada atualmente define as espécies *C. neoformans* e *C. gattii* de acordo com análises de PCR *fingerprinting*, polimorfismo de tamanho de fragmento amplificado (AFLP) e *multilocus sequence type* (MLST) (MEYER *et al.*, 2009). *C. neoformans* é constituído de três variedades: *C. neoformans* var. *grubii* (Sorotipo A, tipos moleculares VNI, VNII e VNB), *C. neoformans* var. *neoformans* (Sorotipo D, tipo molecular VNIV) e híbrido (Sorotipo AD, tipo molecular VNIII) (Tabela 2, classificação usual). Já *C. gattii* é classificado nos sorotipos B (tipos moleculares VGI e VGII) e C (tipos moleculares VGIII e VGIV) (Tabela 2, classificação usual) (LIN; HEITMAN, 2006; MEYER *et al.*, 2009). Contudo, em 2015, uma nova classificação para cada sorotipo de *Cryptococcus* foi proposta, separando *C. neoformans* em duas espécies (complexo de espécies *C. neoformans*) e *C. gattii* em cinco (complexo de espécies *C. gattii*) (HAGEN *et al.*, 2015), além de 4 espécies híbridas (Tabela 2, classificação proposta). Essa nova caracterização é baseada em análises filogenéticas de 11 lócus gênicos (*CAP59*, *GPD1*, *IGS*, *ITS*, *LAC1*, *PLB1*, *RPB1*, *RPB2*, *SOD1*, *TEF1* e *URA5*) de 115 isolados, como também em características como patogenicidade, prevalência de desenvolvimento da doença em cada grupo de pacientes e susceptibilidade a antifúngicos (HAGEN *et al.*, 2015). Porém, o uso dessa nomenclatura ainda não é consenso na literatura (HAGEN *et al.*, 2017; KWON-CHUNG *et al.*, 2017).

Tabela 2. Classificação de *C. neoformans* e *C. gattii*.

Classificação usual	Sorotipo	Tipos moleculares	Classificação proposta
C. neoformans			
var. *grubii*	A	VNI/VNII/VNB (AFLP1, AFLP1A, AFLP1B, VNB)	*C. neoformans*
var. *neoformans*	D	VNIV (AFLP2)	*C. deneoformans*
Híbrido AD	AD	VNIII (AFLP3)	Híbrido *C. neoformans* x *C. deneoformans*
C. gattii	B e C	VGI (AFLP4)	*C. gattii*
		VGII (AFLP6)	*C. deuterogattii*
		VGIII (AFLP5)	*C. bacillisporus*
		VGIV (AFLP7)	*C. tetragattii*
		VGIV/VGIIIc (AFLP10)	*C. decagattii*
Híbrido BD	BD	AFLP8	Híbrido *C. deneoformans* x *C. gattii*
Híbrido AB	AB	AFLP9	Híbrido *C. neoformans* x *C. gattii*
Híbrido AB	AB	AFLP11	Híbrido *C. neoformans* x *C. deuterogattii*

Adaptado de (HAGEN *et al.*, 2015, 2017; KWON-CHUNG *et al.*, 2017).

C. neoformans é uma levedura ambiental encontrada ubiquamente e está presente principalmente em excreta de pombos, solos e árvores (CHOWDHARY *et al.*, 2012; EMMONS, 1955; LITVINTSEVA *et al.*, 2011). Já *C. gattii*, que tinha sua notificação limitada às regiões tropicais e subtropicais (KWON-CHUNG; BENNETT, 1984), passou a ser considera também ubíqua após o surto de infecção em Vancouver, admitindo-se também sua existência em regiões temperadas (DATTA; BARTLETT; MARR, 2009). Esse surto de infecção por *C. gattii* se expandiu pelo Canadá e região noroeste dos Estados Unidos e não atingiu apenas humanos, mas também animais domésticos, terrestres e marinhos (BIELSKA; MAY, 2015). A maioria dos isolados de *C. gattii* são encontradas em vegetais, principalmente árvores de eucaliptos (*Eucalyptus calmadulensis*), amendoeiras (*Terminalia catappa*) e pinheiros (*Pseudotsuga menziesii*) e também em madeiras em decomposição (BIELSKA; MAY, 2015; MA; MAY, 2009).

A reprodução sexual (*mating*) das espécies patogênicas de *Cryptococcus* é bipolar, ou seja, é governado por apenas um lócus genômico conhecido como *MAT*, que possui dois alelos alternativos, *MATα* ou *MAT**a*** (SUN *et al.*, 2019; WICKES, 2002). Muitos dos compostos presentes nos nichos de *Cryptococcus* spp. induzem o *mating*, como inositol (produzido pela maioria das plantas), o hormônio vegetal

ácido indolacético e excreta de pombos (XUE, 2012; XUE *et al.*, 2007). Existem dois tipos de reprodução descritas: unissexual, também conhecida como frutificação monocariótica, e bissexual (SUN *et al.*, 2019). A primeira envolve apenas linhagens *MATα* e a segunda necessita o contato das linhagens *MATα* e *MAT**a*** (Figura 1). Em ambos os casos, há fusão de células haplóides para a produção de filamentos dicarióticos que sofrem meiose, levando à produção de basidiósporos e consequente dispersão dos mesmos (WICKES, 2002). No caso da frutificação monocariótica, há também a possibilidade de endoreplicação, alternativamente à fusão de duas células *MATα* (Figura 1).

A maioria dos isolados naturais e clínicos de *Cryptococcus* spp. são *MATα*, enquanto as linhagens *MAT**a*** estão predominantemente presentes na África, onde encontra-se a maior diversidade genética desse patógeno [Normalmente: α >99% e **a**< 1%; África: α >90% e **a** <10%] (LITVINTSEVA *et al.*, 2003; RANDHAWA *et al.*, 2008; SUN *et al*., 2019; WICKES, 2002). Em relação ao desenvolvimento da criptococose em humanos, os isolados *MATα* são mais virulentos em comparação a isolados *MAT**a*** (KWON-CHUNG; EDMAN; WICKES, 1992). A prevalência de isolados *MATα* demonstra que a reprodução unissexuada de *Cryptococcus* spp. pode ocorrer com maior frequência do que primeiramente proposto, pois a mesma consegue produzir uma grande quantidade de basidiósporos, assim como na reprodução bissexuada (SUN *et al.*, 2019). Essa característica é essencial para a sobrevivência de *Cryptococcus* spp. no ambiente, pois os basidiósporos são mais resistentes à diversos fatores ambientais comparado à forma leveduriforme, e são considerados a principal fonte de infecção (GILES *et al.*, 2009; VELAGAPUDI *et al.*, 2009). Além disso, durante a reprodução, *Cryptococcus* spp. muda sua morfologia de levedura para hifa, sendo a segunda essencial para a sua sobrevivência durante a interação com predadores na natureza, como a ameba *Acanthamoeba castellanii* (CASADEVALL, 2012; LIN; IDNURM; LIN, 2015; MAGDITCH *et al.*, 2012; STEENBERGEN; SHUMAN; CASADEVALL, 2001). É importante ressaltar que ainda não há evidências de reprodução sexuada no interior do hospedeiro humano, apenas no meio ambiente.

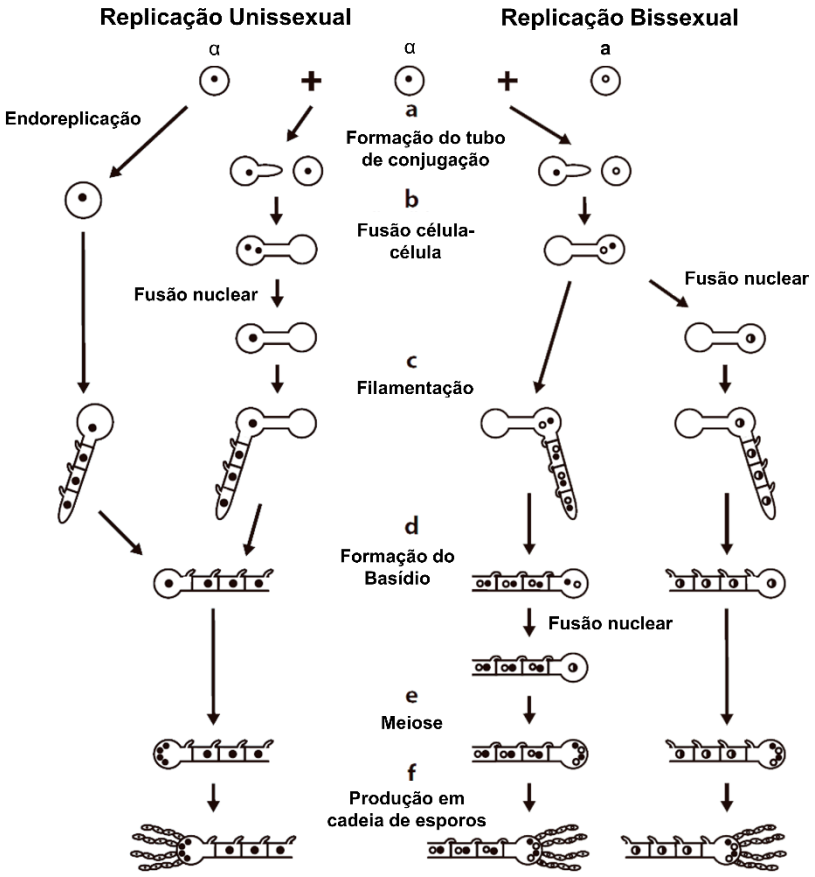

Figura 1. Ciclo sexual de espécies patogênicas de *Cryptococcus*. O ciclo sexual de espécies patogênicas de *Cryptococcus* pode ser dividido em unissexual (envolvendo apenas um único *mating type*) e bissexual (envolvendo dois *mating types* opostos). **(a)** Após o reconhecimento do *mating type* no ambiente apropriado, células fúngicas *MAT*α produzem o tubo de conjugação que cresce e eventualmente se funde com células de *mating type* oposto. **(b)** Após a fusão célula-célula, o filamento se projeta e continua a crescer, **(c, d)** eventualmente se diferenciando em um basídio. **(e, f)** A meiose ocorre dentro do basídio e os produtos meióticos passam por rodadas repetidas de mitose, brotando do basídio como quatro cadeias de basidiósporos. Se a fusão nuclear ocorrer após a fusão célula-célula, o filamento subsequente é monocariótico com fíbulas não fundidas (reprodução bissexuada, painel da direita). Se a fusão nuclear ocorre dentro do basídio, o filamento anterior é dicariótico com fíbulas fundidas (reprodução bissexual, painel da esquerda). Um mecanismo alternativo de reprodução unissexual de *C. neoformans* pode ocorrer dentro de uma célula única, na qual o núcleo sofre endoreplicação; este caminho é representado na reprodução unissexual, painel da esquerda. Adaptado de (SUN *et al.*, 2019).

1.3. Criptococose

A criptococose sistêmica inicia-se a partir da inalação de basidiósporos ou da levedura dessecada do ambiente, que se depositam no pulmão (Figura 2) (MITCHELL; PERFECT, 1995; PERFECT *et al.*, 2010). *C. neoformans* pode ficar latente por indeterminado período de tempo, emergir e se disseminar em um momento de imunossupressão do hospedeiro, apresentando tropismo pelo SNC (ALANIO, 2020; KWON-CHUNG *et al.*, 2014). No tecido cerebral, *C. neoformans* causa o quadro mais grave da doença, a meningite criptocócica, que é fatal se não tratada adequadamente (JARVIS *et al.*, 2014; PERFECT, 2012; SABIITI; MAY, 2012). Já infecções causadas por *C. gattii* tem como característica uma doença centralizada no pulmão do hospedeiro, com formação de grandes massas de infiltrado de células do sistema imune, conhecido como criptococomas, raramente com disseminação para o SNC (NGAMSKULRUNGROJ *et al.*, 2012).

O basidiósporo já foi caracterizado como partícula infecciosa tanto em modelo murino quanto em modelo invertebrado de infecção, e seu tamanho é ideal para inalação e deposição nos alvéolos pulmonares (Figura 2) (KRONSTAD *et al.*, 2011). Após a deposição das células fúngicas no pulmão, a resposta imune do hospedeiro é acionada, diferindo conforme a espécie do agente infeccioso. *C. neoformans* induz uma resposta inflamatória protetora, através da secreção das citocinas TNF-α e IFN-γ, ao contrário de *C. gattii*, que retarda a ativação do sistema imune (CHENG; SHAM; KRONSTAD, 2009). O primeiro contato das células fúngicas com o sistema imune é caracterizado pela interação principalmente com macrófagos alveolares, pois estes representam a maior parte da população de células bronco-alveolares em condições de infecções pulmonares (FU; DRUMMOND, 2020). As ações dessas células incluem fagocitose e eliminação do patógeno, sequestro de polissacarídeos, produção de citocinas e quimiocinas e apresentação de antígenos (GARCÍA-RODAS; ZARAGOZA, 2012). Quando fagocitada por macrófagos, três cenários diferentes podem ser observados: (i) a levedura pode ser eliminada através de mecanismos microbicidas produzidos pela célula do sistema imune ou também pela apresentação de antígenos às células T; (ii) entrar em um estado de latência ou (iii) sobreviver e estabelecer a infecção pulmonar (FU; DRUMMOND, 2020; MCQUISTON; WILLIAMSON, 2012).

É importante ressaltar que a maioria dos estudos, principalmente em modelo murino de infecção, são realizados com células em sua morfologia leveduriforme, e que a resposta imune frente a basidiósporos e leveduras é diferente. Por exemplo, os basidiósporos são rapidamente fagocitados por células do sistema imune como macrófagos, porém conseguem germinar e se replicar no interior dos mesmos. Contudo, se o macrófago é ativado previamente à germinação do basidiósporo, esse é rapidamente eliminado por ser muito sensível às espécies reativas de oxigênio (GILES *et al.*, 2009). Já as células leveduriformes são apenas fagocitadas mediante sua opsonização (interação com anticorpos ou moléculas do sistema complemento, por exemplo), porém, quando internalizadas, também conseguem sobreviver e replicar no interior dos macrófagos (ALVAREZ; CASADEVALL, 2006).

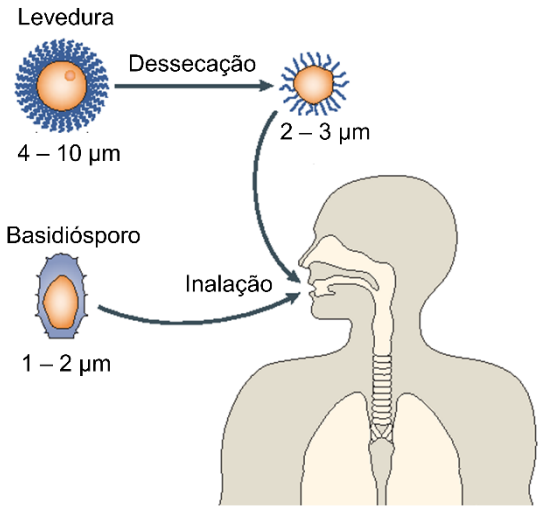

Figura 2. Diferentes tipos morfológicos contribuem para virulência de *C. neoformans* e *C. gattii*. Os basidiósporos e leveduras dessecadas iniciam a infecção após a inalação pelo hospedeiro. Os basidiósporos são resultado de reprodução unissexuada ou bissexuada, enquanto as células da levedura podem dessecar no ambiente e seu tamanho possibilita a inalação profunda no tecido pulmonar. A germinação dos basidiósporos e o crescimento das células leveduriformes nos pulmões resultam na proliferação de *Cryptococcus* spp. e possível colonização do tecido pulmonar. Adaptado de (KRONSTAD *et al.*, 2011).

A capacidade de sobrevivência e replicação de *C. neoformans* no interior de células do sistema imune é correlacionada com sua virulência (ALVAREZ *et al.*, 2009; MA *et al.*, 2009; MANSOUR; LEVITZ, 2002). Após a fagocitose por macrófagos, por exemplo, *C. neoformans* é compartimentalizado nos

fagolisossomos e, neste local, a levedura consegue sobreviver e se replicar mesmo com a normal acidificação da organela (ALVAREZ; CASADEVALL, 2006; ARTAVANIS-TSAKONAS *et al.*, 2006; FELDMESSER; TUCKER; CASADEVALL, 2001; LEVITZ *et al.*, 1999). Essa característica impacta diretamente o desenvolvimento de uma resposta imunológica protetora contra o patógeno e sua disseminação para o SNC, pois um dos mecanismos para a travessia da barreira hematoencefálica (BHE) é conhecido como “Cavalo de Tróia”, em que células de *C. neoformans* são transportadas no interior de macrófagos (Figura 3) (SANTIAGO-TIRADO *et al.*, 2017). *C. neoformans* também consegue transpor a BHE pela via transcelular, a partir da endocitose por células epiteliais cerebrais (CHANG *et al.*, 2004; HUANG *et al.*, 2011; JONG *et al.*, 2008; MARUVADA *et al.*, 2012); ou por via paracelular, no qual a levedura causa danos às junções aderentes das células (Figura 3) (CHEN *et al.*, 2003; OLSZEWSKI *et al.*, 2004; SHI *et al.*, 2010).

O tratamento recomendado para a meningite criptocócica consiste em um regime de três fases chamadas de indução, consolidação e manutenção. A fase de indução dura aproximadamente duas semanas e consiste da administração intravenosa de anfotericina B (0,7 – 1 mg/kg/dia), anfotericina B lipossomal (3 – 4 mg/kg/dia) ou complexo lipídico de anfotericina B (5 mg/kg/dia) e 5-FC oral (100 mg/kg/dia) (PERFECT *et al.*, 2010). No caso da falta de 5-FC, o que é comum nos países com os maiores números de casos de criptococose (PERFECT, 2016), fluconazol pode ser administrado na concentração de 800 mg/dia, porém não é recomendando o uso de fluconazol como monoterapia devido à alta taxa de mortalidade associada (GASKELL *et al.*, 2014; PAPPAS *et al.*, 2009). Já as fases de consolidação e manutenção se caracterizam pela administração de fluconazol, sendo a primeira com 800 mg/dia por 8 semanas e a segunda com 200 mg/dia por 6 a 12 meses em pacientes HIV-negativos e por no mínimo um ano em pacientes HIV-positivos (PAPPAS *et al.*, 2009; PERFECT *et al.*, 2010). É importante ressaltar que mesmo com esse tratamento atual, os índices de mortalidade por meningite criptocócica continuam altos (MOURAD; PERFECT, 2018). Em países de baixa renda, até 70% dos pacientes tratados vão à óbito, enquanto em países europeus ou nos Estados Unidos, esse número varia entre 20 e 30% (RAJASINGHAM *et al.*, 2017).

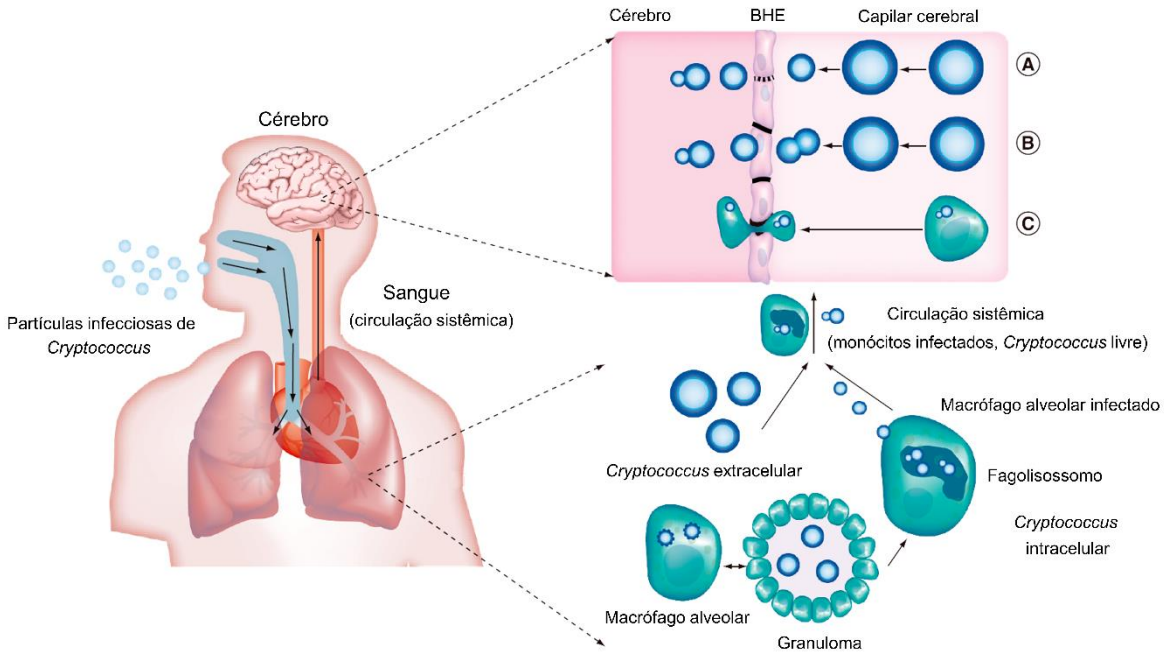

Figura 3. Modelo de disseminação de *C. neoformans* do ambiente para o cérebro humano. Através da inalação basidiósporos ou células dessecadas, *C. neoformans* coloniza o espaço alveolar nos pulmões. Em indivíduos imunocompetentes, macrófagos alveolares ativados fagocitam e eliminam o patógeno ou o envolvem para formar granulomas. Células de *C. neoformans* nos granulomas podem permanecer latentes ou serem reativadas para causar infecção, frente a alterações no estado imunológico do indivíduo. Nos indivíduos imunocomprometidos, macrófagos alveolares infectados pelo patógeno agem como Cavalos de Tróia dentro dos pulmões, desencadeando a disseminação para circulação sistêmica. Células de *C. neoformans* extracelulares podem permanecer nos pulmões ou disseminar transcelularmente na circulação sanguínea. Na circulação sistêmica, células fúngicas se associam com monócitos ou são transportadas livremente para o capilar cerebral. No capilar cerebral, as células leveduriformes podem penetrar na barreira hematoencefálica (BHE) por: **(A)** travessia paracelular entre as células endoteliais, provavelmente permitida por junções aderentes danificadas ou enfraquecidas; **(B)** transcitose - ligação e internalização pelas células endoteliais microvasculares do cérebro; ou **(C)** dentro monócitos/macrófagos infectados (Cavalo de Tróia). Adaptado de (SABIITI; MAY, 2012).

1.4. Patogenicidade

A patogenicidade de microrganismos pode ser definida segundo a teoria de resposta a dano, proposta recentemente em 1999 pelos cientistas Liise-anne Pirofski e Arturo Casadevall (CASADEVALL; PIROFSKI, 1999), a qual propõe que a patogenicidade e virulência de um microrganismo são definidas pelas

contribuições tanto do patógeno quanto do hospedeiro. Essa descrição é fundamental para classificar os patógenos que só causam doença em pacientes com resposta imune deficiente, os quais não são considerados patógenos em hospedeiros sadios. Além disto, essa teoria opõe-se às visões centradas apenas no microrganismo ou hospedeiro individualmente. A visão centrada no microrganismo define que a patogenicidade é uma função da produção de fatores de virulência, ou seja, apenas os microrganismos que os produzem são considerados patogênicos. Nessa visão não se encaixa o próprio *C. neoformans*, o qual possui fatores de virulência definidos, mas não consegue causar doença em humanos com respostas imunes distintas. Já a visão centrada no hospedeiro define que a patogenicidade é apenas consequência do fracasso do sistema imune ao combater a infecção, o que leva a susceptibilidade à determinados microrganismos (CASADEVALL; PIROFSKI, 2003). Essas duas visões são muito importantes, porém as interações patógeno-hospedeiro são dinâmicas, no qual há mudança da resposta imune e do fitness do patógeno constantemente ao longo da interação.

A teoria de resposta a dano define que: (i) a patogênese microbiana é resultado da interação-patógeno hospedeiro; (ii) o resultado dessa interação é determinado pelo dano causado ao hospedeiro; e (iii) os danos podem ser causados pelo microrganismo, pelo hospedeiro ou ambos (CASADEVALL; PIROFSKI, 2003). Um microrganismo patogênico é definido então pela sua capacidade de causar danos ao hospedeiro, principalmente através de seus fatores de virulência e a patogenicidade é medida dentro do hospedeiro. Essa teoria é demonstrada a partir de uma parábola de quantificação de dano, em que o dano é medido em relação à resposta imune do hospedeiro (Figura 4). A curva sugerida para *C. neoformans* em 1999 não incluía danos causados quando a resposta imune do hospedeiro era forte, apenas em respostas imunes fracas ou normais (CASADEVALL; PIROFSKI, 1999). Porém, essa visão já foi alterada, principalmente após a descrição da Síndrome de Reconstituição Imunológica (SRI) associada à criptococose em pacientes com AIDS após a terapia antirretroviral, mostrando que os danos causados em pacientes com criptococose pode ser decorrente de uma resposta inflamatória exacerbada (BOULWARE *et al.*, 2010; HADDOW *et al.*, 2010). Além disso, um estudo recente demonstrou que linfócitos T CD4+ apresentam um papel dicotômico

na criptococose, combatendo e eliminando o patógeno do SNC, mas também induzindo uma resposta neuropatológica devido a hiperinflamação, podendo resultar em morte (NEAL *et al.*, 2017; PIROFSKI; CASADEVALL, 2017).

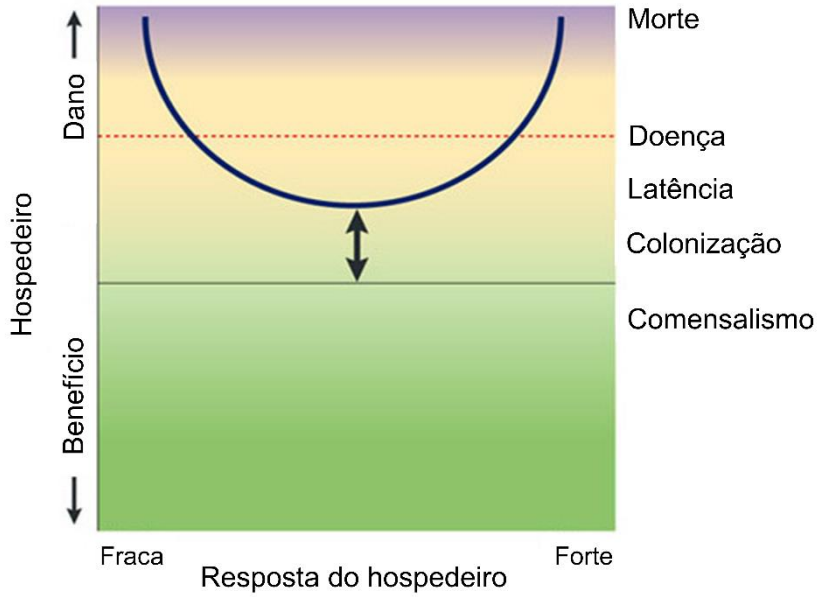

Figura 4. Curva de dano e resposta. Todas as outras curvas específicas de cada microrganismo são derivadas desta curva básica. A seta interna indica que a posição da curva é variável e depende da interação particular hospedeiro-microrganismo. O eixo y denota danos ao hospedeiro em função de sua resposta imune. Nesse esquema, o dano pode ocorrer durante qualquer resposta imune do hospedeiro, mas é ampliado em ambos os extremos. A resposta do hospedeiro é representada por um gradiente de 'fraco' a 'forte'. 'Fraco' e 'forte' são termos que podem abranger características quantitativas e qualitativas da resposta do hospedeiro e são usados como os melhores termos disponíveis para denotar o espectro da resposta do hospedeiro, visto que termos mais precisos são limitados. Respostas fracas são aquelas que são insuficientes, ruins ou inadequadas - ou seja, não são fortes o suficiente para beneficiar o hospedeiro. Respostas fortes são aquelas que são excessivas, robustas ou inadequadas - ou seja, são muito fortes e podem danificar o hospedeiro. Quando um limite de dano é atingido (aqui demonstrado pela linha pontilhada vermelha), o hospedeiro pode tornar-se sintomático e, se o dano for grave, levar à morte. Verde, amarelo e roxo representam saúde, doença e doença grave, respectivamente. Adaptado de (CASADEVALL; PIROFSKI, 2003).

1.4.1. Desenvolvimento à 37ºC

Os fatores de virulência de *C. neoformans* que causam danos ao hospedeiro humano serão descritos a seguir, porém antes é preciso destacar a principal

característica de patógenos humanos, sua capacidade de desenvolvimento a 37ºC. O crescimento na temperatura corporal do hospedeiro está associado à transição da forma filamentosa para leveduriformes de fungos dimórficos capazes de infectar seres humanos como *Histoplasma capsulatum*, *Paracoccidioides brasiliensis* e *Blastomyces dermatidis* (CANNON *et al.*, 1994; MARESCA; KOBAYASHI, 2000). Essa é uma característica que diferencia *C. neoformans* e *C. gattii* de outras espécies do gênero *Cryptococcus* que não conseguem estabelecer a infecção, mas produzem outros fatores de virulência, como a cápsula polissacarídica e produção de melanina (COELHO; BOCCA; CASADEVALL, 2014).

1.4.1.1. Homeostase de cálcio e via de sinalização da calcineurina

O desenvolvimento de *C. neoformans* a 37°C é dependente da atividade da serina/treonina fosfatase calcineurina. Essa proteína é composta pela subunidade catalítica A (Cna1) e uma subunidade reguladora B ligadora à cálcio (Cnb1), formando um heterodímero. A atividade de calcineurina é regulada pelo complexo Ca^{2+}/calmodulina (descrito a seguir), que interage com a subunidade reguladora do heterodímero, alterando sua conformação e o ativando (RAMOS; SYCHROVÁ; KSCHISCHO, 2016). O mutante nulo para calcineurina em *C. neoformans* não é viável a 37°C, mesmo após uma variação de 37°C para 24°C (CHEN *et al.*, 2013). Durante estresse térmico, a proteína calcineurina localiza-se em sítios de processamento de RNA mensageiro (mRNA), conhecidos como corpos de processamento ou corpos-P, sugerindo que calcineurina regula a expressão gênica de alguns alvos após a transcrição dos mesmos (KOZUBOWSKI *et al.*, 2011). Além disso, recentemente foi descrito que a termotolerância de *C. neoformans* é dependente do decaimento de mRNA de proteínas ribossomais e o bloqueio desse processo evita a tradução principalmente de fatores de transcrição essenciais para esta adaptação (BLOOM *et al.*, 2019). A via de sinalização mediada por calcineurina também controla a reprodução sexuada de *C. neoformans*, estabilidade de sua parede celular, resposta a estresses e virulência (CRUZ, 2001; FOX *et al.*, 2001; JUVVADI *et al.*, 2017; KOZUBOWSKI; LEE; HEITMAN, 2009).

A presença de cálcio (Ca^{2+}) é fundamental para a ativação da via de sinalização da calcineurina. Ca^{2+} é considerado o principal segundo mensageiro de células eucarióticas, e em leveduras é capaz de regular diversos processos, como adaptação a pH alcalino, estresse osmótico e salino, danos ao retículo endoplasmático (RE) e resposta à presença de feromônios para o processo de *mating* (RAMOS; SYCHROVÁ; KSCHISCHO, 2016). A manutenção de concentrações intracelulares ideais de Ca^{2+} é regulada por transportadores de membrana, bombas e canais e alterações em suas concentrações podem causar danos irreversíveis à célula, através da ativação constante de vias, possível produção de proteases e ativação de apoptose (CARAFOLI *et al.*, 2001; CARAFOLI; KREBS, 2016; RAMOS; SYCHROVÁ; KSCHISCHO, 2016).

Em *C. neoformans*, íons cálcio entram na célula a partir da atividade do canal permeável Cch1, respondendo principalmente ao estresse do retículo endoplasmático ou depleção do íon nessa organela (VU; BAUTOS; GELLI, 2015). Cch1 é essencial para virulência de *C. neoformans*, e é responsável por captar o íon em ambientes com baixas concentrações de cálcio (LIU *et al.*, 2006). O transportador de cálcio do RE de C*. neoformans* é conhecido como Eca1, uma bomba de Ca^{2+}/ATPase, responsável pela importação do íon do citoplasma para a organela, a qual também é importante para virulência de *C. neoformans* (FAN *et al.*, 2007). É importante ressaltar que a liberação de cálcio de organelas é mediada por inositol trifosfato (IP3), a partir da atividade da enzima fosfolipase C (PLC) na hidrólise de fosfatidilinositol 4,5-bifosfato (PIP2) em IP3 e diacilglicerol (DAG) (ROY *et al.*, 2020) (Figura 5).

O vacúolo é principal organela responsável pelo estoque intracelular de cálcio, o qual pode ser encontrado em sua forma livre ou complexado com fosfatos e polifosfatos (RAMOS; SYCHROVÁ; KSCHISCHO, 2016). Em *C. neoformans*, dois transportadores vacuolares de cálcio responsáveis pela importação do íon, Vcx1 (H^+/Ca^{2+} *exchanger*) e Pmc1 (Ca^{2+}/ATPase), já foram caracterizados (KMETZSCH *et al.*, 2010, 2013; SQUIZANI *et al.*, 2018). O mutante nulo para Vcx1 em *C. neoformans* tem virulência atenuada em modelo murino de infecção, e é sensível à ação de macrófagos alveolares em ensaios de fagocitose *in vitro*. Já o mutante nulo para o transportador de cálcio Pmc1 é avirulento em modelo sistêmico de infecção

em camundongos (SQUIZANI *et al.*, 2018) e é deficiente na disseminação para o SNC (KMETZSCH *et al.*, 2013; SQUIZANI *et al.*, 2018).

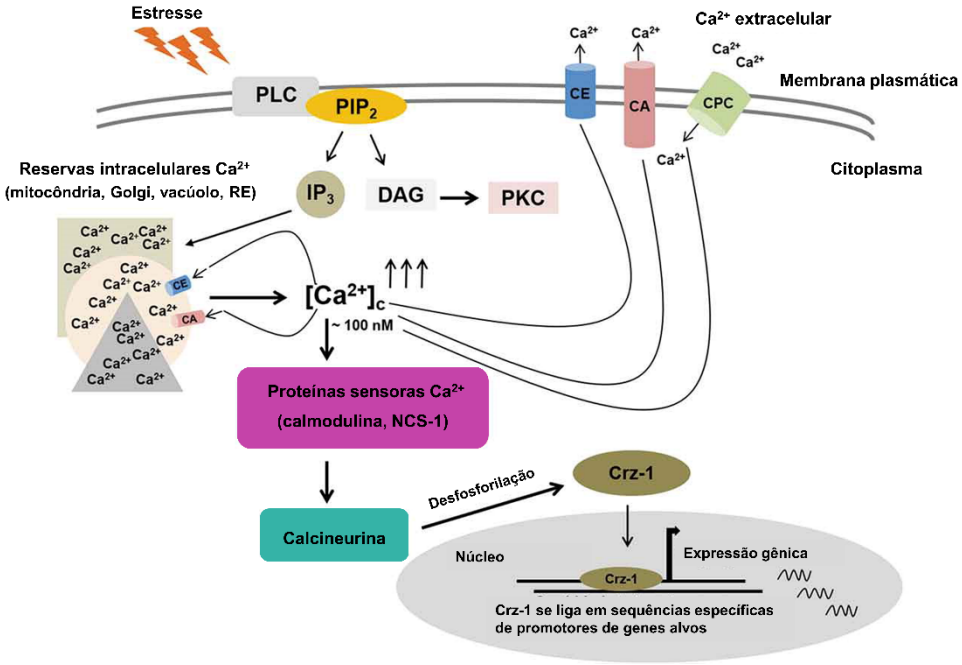

Figura 5. Visão geral da maquinaria de sinalização de cálcio em fungos. A fosfolipase C (PLC) ligada à membrana hidrolisa o fosfatidilinositol-4, 5-bifosfato (PIP2) para produzir duas moléculas importantes: inositol 1,4,5-trifosfatos (IP3) e diacilglicerol (DAG). IP3 induz a liberação de Ca^{2+} dos depósitos intracelulares, incluindo mitocôndrias, Golgi, vacúolos e retículo endoplasmático. O DAG ativa a proteína quinase C (PKC) que está envolvida em vários processos de sinalização. A concentração de Ca^{2+} livre intracelular em repouso ($[Ca^{2+}]c$) é de cerca de 100nM, um aumento de $[Ca^{2+}]c$ é detectado por várias proteínas ligadoras de Ca^{2+}, como calmodulina e Ncs-1, que ativam cascatas de sinalização específicas. O complexo Ca^{2+}/calmodulina ativa a serina/treonina fosfatase calcineurina que desfosforila o fator de transcrição Crz1, o qual se transloca para o núcleo e regula a expressão de genes alvo em resposta a estímulos. O excesso de Ca^{2+} é removido do citosol por Ca^{2+} *exchangers* (CE) e proteínas Ca^{2+}/ATPases (CA), enquanto os canais permeáveis ao Ca^{2+} (CPC) são necessários para o influxo de Ca^{2+} extracelular. Esses processos são necessários para manter a homeostase de Ca^{2+} na célula. Adaptado de *(ROY et al*., 2020).

Ao ocorrer um influxo de cálcio para o interior da célula, este mensageiro secundário liga-se à proteína calmodulina (Cam1), a qual ativa a fosfatase calcineurina (KRAUS; NICHOLS; HEITMAN, 2005). Calmodulina é uma proteína pequena que se liga à cálcio via domínios EF-*hand* e contribui para regulação da mitose, transcrição gênica, rearranjo de citoesqueleto e resposta à estresses

(CHIN; MEANS, 2000). O principal alvo do complexo Ca^{2+}/calmodulina é a fosfatase calcineurina. A ativação da calcineurina ocorre através da interação do complexo com a região C-terminal da subunidade regulatória Cna1, liberando sua auto inibição (HEMENWAY; HEITMAN, 1999) (Figura 5). Calmodulina em *C. neoformans* e em outros fungos também age além da ativação da fosfatase calcineurina, porém sua interação com cálcio é essencial para sua função (JOSEPH; MEANS, 2002; KRAUS; NICHOLS; HEITMAN, 2005; TAKEDA; YAMAMOTO, 1987). Recentemente, foi caracterizada funcionalmente outra proteína ligadora de cálcio em *C. neoformans* chamada Ncs-1. Essa proteína também possui domínios de ligação EF-*hand*, é conservada entre os eucariotos e possui papel importante na divisão celular e virulência dessa levedura (SQUIZANI *et al.*, 2020).

O influxo de cálcio ativa a expressão de genes necessários para responder a estímulos ambientais e manter a homeostase de cálcio na célula. Na levedura modelo *Saccharomyces cerevisiae*, Crz1 (*calcineurin responsive zinc finger 1*) foi identificado como um fator de transcrição ativado por calcineurina, o qual induz a expressão de genes de resposta a estresse (CYERT, 2003; THEWES, 2014). Estudos recentes identificaram o ortólogo de Crz1 em *C. neoformans* e confirmaram que este fator de transcrição é alvo direto de calcineurina (LEV *et al.*, 2012; PARK *et al.*, 2016). Esse FT é desfosforilado por calcineurina e se transloca do citoplasma para o núcleo e regula a expressão gênica de seus alvos (Figura 5). Análises transcricionais revelaram que Crz1 regula a expressão de mais de 100 genes em *C. neoformans*, os quais participam de relevantes processos celulares como síntese da parede celular (*CHS6*, que codifica para quitina sintase 6), transporte de cálcio (*PMC1* e *VCX1*) e virulência (CHOW *et al.*, 2017). É provável que Crz1 não seja o único fator de transcrição ativado por calcineurina. Esta consideração baseia-se na observação e comparação de fenótipos entre linhagens *crz1* e *cna1*, mutantes nulos para Crz1 e calcineurina, respectivamente, e também em análises globais de sequenciamento de RNA do mutante nulo *cna1* que evidenciam a regulação de outros potenciais fatores de transcrição ainda não caracterizados em *C. neoformans* (CHOW *et al.*, 2017).

1.4.2. Determinantes de *C. neoformans* que causam danos ao hospedeiro

1.4.2.1. Cápsula polissacarídica

A cápsula polissacarídica é considerada o principal determinante de virulência de *Cryptococcus* devido a sua alta capacidade de suprimir o sistema imune do hospedeiro, atuando como uma barreira física que interfere diretamente nesta interação (Figura 6) (BOSE *et al.*, 2003; MONARI; BISTONI; VECCHIARELLI, 2006). Esta é uma estrutura muito dinâmica e seus componentes podem ser secretados para o meio extracelular, onde também influenciam interações com células do sistema imune e podem auxiliar na detecção e monitoramento da criptococose (ALSPAUGH, 2015). A cápsula é essencial para a sobrevivência de *Cryptococcus* no hospedeiro e também está presente em isolados ambientais, envolvendo a parede celular da levedura e agindo contra a desidratação (BOSE *et al.*, 2003).

A cápsula é composta por dois polissacarídeos de grande massa molecular, glucuronoxilomanana (GXM), compondo de 90 a 95% da massa capsular e glucuranoxilomanogalactana (GXMGal), compondo de 5 a 10% da massa capsular. Há ainda uma fração minoritária (inferior a 1%) constituída por manoproteínas (MPs) (DOERING, 2009). GXM apresenta uma massa molecular que varia de 1700 a 7000 kDa, dependendo da linhagem, e é composto por monômeros de manose α-1-3 ligadas a moléculas de ácido glucurônico e xilose. Já foram descritas seis estruturas diferentes, sendo que as modificações sempre são em relação à adição dos resíduos de xilose ligadas às manoses e o núcleo manose-β-1-2-ácido glucurônico mantem-se o mesmo entre todos os sorotipos. Esses monômeros se polimerizam e formam as fibras de GXM, que podem ser lineares ou ramificadas (DOERING, 2009; ZARAGOZA *et al.*, 2009). Inclusive, a ramificação do GXM de *C. neoformans* já foi correlacionada com aumento da resistência ao estresse oxidativo e da sobrevivência em soro (CORDERO *et al.*, 2011). Já GXMGal possui uma massa molecular de aproximadamente 100 kDa e é composto por monômeros de galactose α-1-6 ligadas com ligações com manose, xilose e ácido glucurônico

(HEISS *et al.*, 2009). Os resíduos de manose nos dois polímeros também podem estar *O*-acetilados (AGUSTINHO *et al.*, 2018).

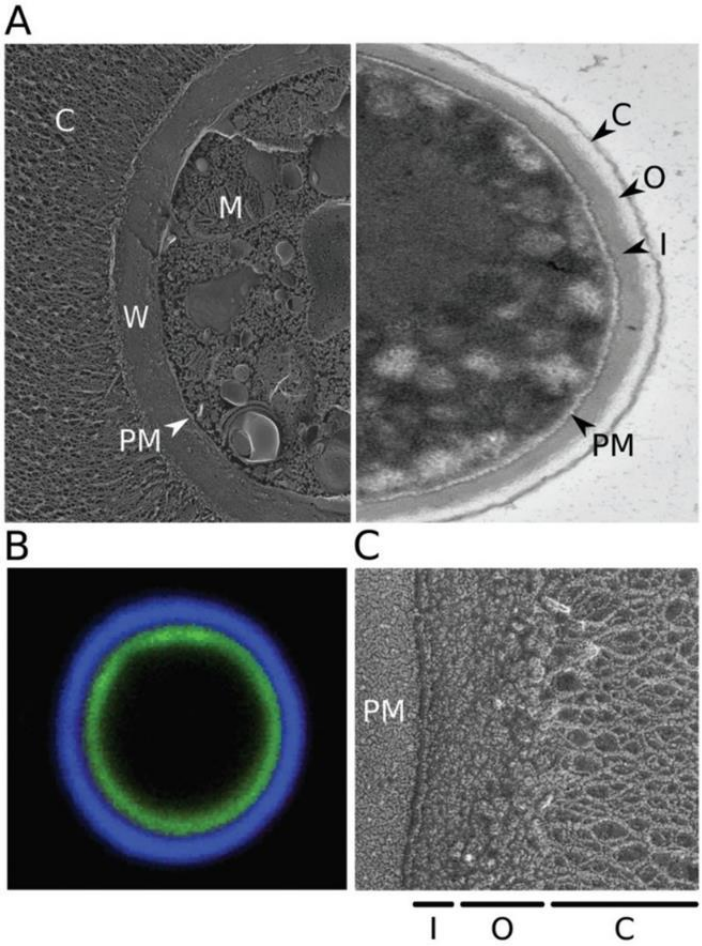

Figura 6. Cápsula e parede celular de *C. neoformans*. (A) Micrografias eletrônicas de *C. neoformans*. À esquerda, imagem de *Quick-freeze deep-etch* de células cultivadas em condições de indução de cápsula; à direita, imagem de transmissão eletrônica de células cultivadas em meio rico (YPD), que produz apenas cápsulas finas. C: cápsula; W: parede celular; PM: membrana plasmática; M: mitocôndria; O: camada externa da parede celular; I: camada interna da parede celular. **(B)** Microscopia fluorescente destacando a parede celular e a cápsula. As células criptocócicas foram induzidas a formar cápsulas e coradas com fluoresceína (verde) para marcar a parede celular e o anticorpo monoclonal 2H1 (azul) foi utilizado para marcar a cápsula. **(C)** *Quick-freeze deep-etch* destacando as duas camadas da parede celular. Adaptado de (ESHER; ZARAGOZA; ALSPAUGH, 2018).

As manoproteínas são glicoproteínas localizadas na parede celular que correspondem a aproximadamente 1% da composição da cápsula de *Cryptococcus* (LEVITZ *et al.*, 2001). Elas possuem uma região rica nos aminoácidos serina e treonina, local no qual ocorre extensiva *O*-glicosilação, e também uma âncora de

glicosilfosfatidilinositol (GPI) e um peptídeo sinal (LEVITZ; SPECHT, 2006). Inúmeros trabalhos exploram o potencial imunoterapêutico das manoproteínas de *C. neoformans*, como MP115, MP88 e MP84, justamente pelo fácil reconhecimento das mesmas como PAMPs (Padrões Moleculares Associados a Patógenos) pelo sistema imune do hospedeiro (BIONDO *et al.*, 2005; HUANG *et al.*, 2002). Além dessa capacidade, já foi demonstrado que a MP84 de *C. neoformans* media a adesão da célula fúngica às células epiteliais do hospedeiro (TEIXEIRA *et al.*, 2014). Uma segunda manoproteína de *C. neoformans* cuja função já foi caracterizada é a Cig1. Ela é secretada ao meio extracelular e tem sua expressão aumentada em condições de privação de ferro. É atribuída como sua função a absorção de componentes hemes para o interior da célula. A deleção do gene *CIG1*, juntamente com o gene codificador da ferroxidase *CFO1*, atenuam a virulência de *C. neoformans* em modelo murino de infecção (CADIEUX *et al.*, 2013). Já a manoproteína MP98 (codificada pelo gene *CDA2*) de *C. neoformans*, é uma das cinco enzimas responsáveis pela síntese de quitosana no fungo, sendo que o mutante quíntuplo para todos os cinco genes possui fenótipo de extremo defeito na integridade da parede celular e também é avirulento em modelo experimental de infecção (BAKER *et al.*, 2007).

A síntese dos polissacarídeos da cápsula ocorre através da atividade de glicosiltransferases e acredita-se que mais de 12 dessas enzimas estejam envolvidas apenas na produção de GXM (DOERING, 2000), sendo que existem 70 genes codificadores de putativas glicosiltransferases no genoma de *C. neoformans* (AGUSTINHO *et al.*, 2018). Os açúcares doadores necessários para síntese de GXM e GXMGal são: GDP-manose, UDP-galactose, UDP-ácido glucurônico, UDP-xilose e UDP-galactofuranose. Mutações nos genes codificadores de enzimas envolvidas na ativação desses açúcares modificam a composição da cápsula e sua estrutura (DOERING, 2009). Por exemplo, a deleção do gene *UGE1*, que codifica uma epimerase que gera UDP-galactose a partir de UDP-glucose, leva à síntese de uma cápsula maior e desestruturada, sem GXMGal. Esse mutante é avirulento e também apresenta defeito na integridade da parede celular, provavelmente devido à falta de modificações nas proteínas da parede (MOYRAND; FONTAINE; JANBON, 2007).

Uma única glicosiltransferase, chamada Cxt1, foi implicada diretamente na síntese da cápsula até o momento. Essa β-1,2-xilosiltransferase é necessária para adição de xilose tanto em GXM, quanto em GXMGal. Sua deleção afeta diretamente a sobrevivência de *C. neoformans* em camundongos (KLUTTS; DOERING, 2008). Outros genes envolvidos na produção da cápsula de *Cryptococcus* são conhecidos como *CAP* e alguns deles também são codificadores de glicosiltransferases, como o gene *CAP59*. O mutante nulo para esse gene não produz cápsula e é avirulento em modelo murino de criptococose, sendo que o produto gênico de *CAP59* tem homologia com α-1-3-manosiltransferase e sua complementação restaura a produção de cápsula e virulência da levedura (CHANG; KWON-CHUNG, 1994). Foram descritos outros genes envolvidos na produção da cápsula, como *CAP64*, *CAP60* e *CAP10*. Os produtos gênicos de *CAP64* e *CAP10* têm similaridade com a subunidade do proteassomo *PRE1* e xilosiltransferase, respectivamente, e *CAP60* tem similaridade com um gene envolvido na capacidade de crescimento da célula fúngica na presença de celulose. A deleção individual desses três genes produz leveduras acapsulares e sem a capacidade de causar morte em camundongos em ensaios de criptococose experimentais (ZARAGOZA *et al.*, 2009).

A síntese de GXM ocorre intracelularmente, especificamente no complexo de Golgi (YONEDA; DOERING, 2006). O transporte desse polissacarídeo é mediado por secreção de vesículas que ultrapassam a parede celular e o liberam no espaço extracelular (RODRIGUES *et al.*, 2007). Esse mecanismo de secreção de GXM via vesículas está relacionado com a biogênese da cápsula, pois, em condições que induzem a expressão dessa estrutura, há maior liberação de vesículas extracelulares contendo o polissacarídeo (RODRIGUES *et al.*, 2007). Porém, mutantes acapsulares continuam secretando as vesículas, mesmo não produzindo GXM e, quando em contato com vesículas de outras linhagens que contém o polissacarídeo, conseguem incorporá-lo em sua superfície (RODRIGUES *et al.*, 2008a).

Além de estarem associadas à secreção de GXM, essas vesículas extracelulares também são conhecidas como *virulence bags*, pois contêm importantes fatores de virulência de *C. neoformans*, como as enzimas fosfolipase,

lacase e urease que serão descritas a seguir (RODRIGUES *et al.*, 2008a). Também já foram identificados diversos lipídeos, manoproteínas e microRNAs no interior de vesículas secretadas por *C. neoformans* (DA SILVA *et al.*, 2015; WOLF *et al.*, 2014) que, quando em contato com o hospedeiro, conseguem modular a função de macrófagos (OLIVEIRA *et al.*, 2010).

Pouco se sabe sobre a montagem dos polissacarídeos após a sua secreção, mas a principal hipótese é de que os mesmos se auto agregam na presença de cátions divalentes (MCFADDEN; DE JESUS; CASADEVALL, 2006; NIMRICHTER *et al.*, 2007). O material capsular recém sintetizado pode se agregar na parte mais externa da cápsula, distante da parede celular, se intercalando com as estruturas mais velhas (ZARAGOZA *et al.*, 2006), ou na parte mais interna da cápsula, próximo à parede celular (CORDERO; BERGMAN; CASADEVALL, 2013; PIERINI; DOERING, 2001). Além disso, a cápsula de *Cryptococcus* é composta por duas partes: a região mais externa, mais permeável e menos densa e a região mais interna, mais densa e que evita o contato de moléculas maiores com a superfície celular criptocócica (FRASES *et al.*, 2009; GATES; THORKILDSON; KOZEL, 2004).

A parede celular é o maior determinante para o ancoramento da cápsula polissacarídica das espécies de *Cryptococcus*. Ainda não se sabe se o ancoramento ocorre diretamente com os componentes clássicos da parede celular, ou se ela promove uma estruturação de proteínas que interagem diretamente com os polissacarídeos da cápsula (O'MEARA; ALSPAUGH, 2012). A parede celular de *C. neoformans* é composta por β-1-3 e β-1-6-glucanos, α-1-3-glucanos, quitina, quitosana, melanina, glicoproteínas e glucosilceramidas derivados da membrana plasmática (NIMRICHTER *et al.*, 2005; RHOME *et al.*, 2007). Como na cápsula polissacarídica, a parede celular de *C. neoformans* também possui duas camadas (Figura 6). A mais interna é formada por fibras paralelas compostas de β-glucanas, quitina e, quando presente, melanina. Esse pigmento confere a porosidade da parede celular (JACOBSON; IKEDA, 2005). Já a camada mais externa da parede é composta principalmente por α e β-glucanas, formando uma rede mais particulada (SAKAGUCHI *et al.*, 1993). Diferentemente de outros fungos, *C. neoformans* possui mais moléculas de β-1-6-glucanas em sua composição do que

β-1-3-glucanas (O'MEARA; ALSPAUGH, 2012). Já foi demonstrado que a inativação da síntese de α-1-3-glucanas não afeta a produção da cápsula, mas o seu ancoramento à parede celular de *C. neoformans*, porém não foi identificada ainda uma ligação direta entre essas duas estruturas (REESE; DOERING, 2003). Moléculas de quitosana, que são formadas a partir da *O*-acetilação de moléculas de quitina, já tiveram sua importância demonstrada na arquitetura correta da cápsula de *C. neoformans*. Umas das enzimas responsáveis pela síntese de quitosana é uma manoproteína conhecida como MP98 (BAKER *et al.*, 2007). Além disso, já foi demonstrado através da marcação de oligômeros de β-1-4-*N*-acetilglucosamina por *wheat germ agglutinin* (WGA), que essas moléculas formam projeções que ligam a cápsula à parede celular (RODRIGUES *et al.*, 2008b).

Como dito anteriormente, a cápsula polissacarídica confere resistência a múltiplos estresses, como desidratação, fagocitose por macrófagos e espécies reativas de oxigênio produzidas pelo fagolisossomo (ESHER; ZARAGOZA; ALSPAUGH, 2018). Sua estrutura, tamanho e composição varia de acordo com o ambiente em que o fungo está inserido. Por exemplo, o desenvolvimento da levedura em meio rico (condições laboratoriais) não induz a produção de cápsula, enquanto a interação com hospedeiros, como camundongos, cultura de células fagocíticas, o modelo invertebrado *Galleria mellonella* e amebas induz a produção da mesma (ESHER; ZARAGOZA; ALSPAUGH, 2018). Estímulos específicos que induzem a produção de cápsula em *C. neoformans* incluem a limitação de nutrientes, principalmente ferro, presença de soro mamífero e altas concentrações de CO_2 (ZARAGOZA *et al.*, 2009). Há evidências de que o tamanho da estrutura polissacarídica varia conforme o local da infecção, sendo que os maiores tamanhos são encontrados em leveduras residentes no pulmão. Além disso, as propriedades imunogênicas da cápsula também variam, evidenciando a adaptação da à diferentes condições (ZARAGOZA *et al.*, 2009).

Durante a infecção, cápsulas maiores evitam a fagocitose mediada pelo sistema complemento e contribui para a sobrevivência intracelular através da resistência a espécies reativas de oxigênio, peptídeos antimicrobianos e antifúngicos (ESHER; ZARAGOZA; ALSPAUGH, 2018). Além disso, as células de *C. neoformans* quando internalizadas por macrófagos liberam GXM, sendo possível

localizar vesículas no citoplasma da célula do sistema imune contendo o polissacarídeo. Esse conteúdo pode levar a célula do hospedeiro à lise, como também afetar a secreção de citocinas e inativar componentes do sistema complemento (BOSE *et al.*, 2003; VECCHIARELLI *et al.*, 1995). Ademais, tanto GXM quanto GXMGal afetam a migração de leucócitos para o local da infecção e induzem a apoptose de linfócitos T (PERICOLINI *et al.*, 2006; YAUCH; LAM; LEVITZ, 2006).

1.4.2.2. Melanina

A produção de melanina é importante para a virulência de *Cryptococcus*, pois protege o fungo dos mecanismos de defesa do sistema imune do hospedeiro. A melanina é um pigmento escuro, hidrofóbico e com carga negativa, proveniente da oxidação de compostos fenólicos, como L-DOPA (WHITE, 1958). Esse pigmento é depositado na parede celular de *Cryptococcus* spp. (Figura 7) e as enzimas responsáveis pela sua síntese são denominadas lacases (CASADEVALL; ROSAS; NOSANCHUK, 2000). *C. neoformans* possui dois genes codificadores dessas proteínas, *LAC1* e *LAC2,* e a inativação de ambos reduz a taxa de sobrevivência da levedura no hospedeiro (MISSALL *et al.*, 2005).

O gene *LAC1* codificada uma enzima glicoproteica de 75 kDa, sendo responsável pela síntese de melanina em praticamente sua totalidade (WILLIAMSON, 1994; ZHU; WILLIAMSON, 2004). Sua síntese é iniciada no interior de vesículas citoplasmáticas (também conhecidas como melanossomos) que contém a enzima Lac1, a qual catalisa a polimerização do pigmento a partir de uma série de reações de oxirredução. Essas vesículas são posteriormente transportadas através da parede celular até a parte interna da parede celular de *C. neoformans* (CAMACHO *et al.*, 2019; CORDERO; CAMACHO; CASADEVALL, 2020; EISENMAN *et al.*, 2005, 2009). Mutantes com defeitos na integridade da parede celular não conseguem manter o pigmento depositado em sua parede, apresentando um fenótipo de *leaky melanin* que contribui para a atenuação da virulência de *C. neoformans* (BAKER *et al.*, 2007). Esse defeito está relacionado especificamente com a rigidez dos polímeros de quitina na parede celular de *C.*

neoformans e *C. gattii* (CHRISSIAN *et al.*, 2020). Dados recentes demonstraram que a enzima Lac1 também possui papel independente da produção do pigmento em *C. neoformans* e influencia a exocitose não lítica de células de macrófagos (FRAZÃO *et al.*, 2020). O gene *LAC2* possui um nível basal de transcrição menor ao de *LAC1*, mas seu produto também é importante para síntese de melanina e proteção no interior de macrófagos (MISSALL *et al.*, 2005). A localização da enzima codificada por *LAC2* ainda não foi determinada.

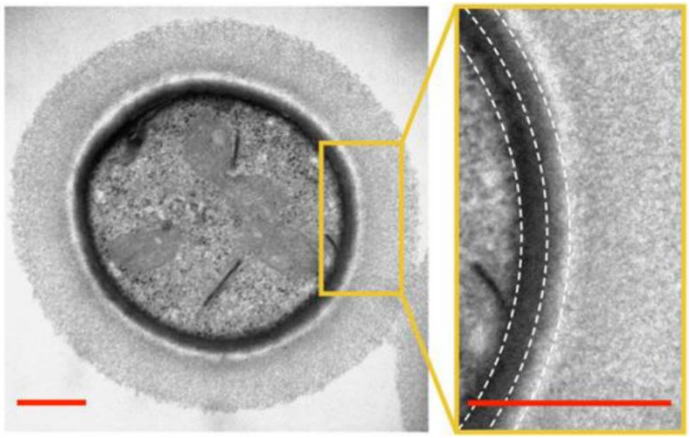

Figura 7. A parede celular de *C. gattii* revela a deposição compacta e uniforme de pigmentos de melanina. Seção transversal representativa de Microscopia Eletrônica de Transmissão (MET) de uma célula de *C. gattii* melanizada. A imagem ampliada à direita ilustra o arranjo do pigmento em camadas na parede celular da levedura. Barra de escala, 500 nm. Adaptado de (CHRISSIAN *et al*., 2020).

No ambiente, a melanização é importante como um mecanismo contra predadores como, por exemplo, amebas, ou contra a radiação ultravioleta e variações térmicas (CORDERO; CASADEVALL, 2017; NOSANCHUK; CASADEVALL, 2003; STEENBERGEN; SHUMAN; CASADEVALL, 2001). Durante a infecção, a síntese de melanina inibe a resposta imune do hospedeiro, protegendo a levedura contra a fagocitose por macrófagos e modulando o perfil de citocinas secretadas (HUFFNAGLE *et al.*, 1995; ZHU; WILLIAMSON, 2004). Esse composto é um dos principais produtos que confere tolerância às espécies reativas de oxigênio e nitrogênio, principalmente quando a levedura se encontra no interior de células do sistema imune e também protege a levedura contra moléculas antifúngicas como anfotericina e caspofungina (CORDERO; CASADEVALL, 2017; NOSANCHUK; CASADEVALL, 2006; TAJIMA *et al.*, 2019; WANG; CASADEVALL,

1994a). *C. neoformans* utiliza componentes exógenos para síntese de melanina, como catecolaminas presentes no sistema nervoso central, o que contribui para o neurotropismo da levedura (WILLIAMSON; WAKAMATSU; ITO, 1998). A produção de melanina também é induzida durante a privação de nutrientes (LEE *et al.*, 2019), o que pode influenciar diretamente a sobrevivência da levedura em determinados ambientes, pois já foi demonstrado que o processo de melanização altera a expressão de genes envolvidos na respiração celular e crescimento (SCHULTZHAUS *et al.*, 2019). Além da melanina ser uma molécula antioxidante, ela também é um importante componente da estrutura da parede celular de *Cryptococcus* spp. e é reconhecida por anticorpos durante modelo murino de infecção experimental (ROSAS; NOSANCHUK; CASADEVALL, 2001).

1.4.2.3. Urease

Urease é um importante fator de virulência de *C. neoformans* e *C. gattii* (COX *et al.*, 2000; FEDER *et al.*, 2015). Essa enzima catalisa a hidrólise de ureia em bicarbonato e amônia, sendo que a amônia gerada por essa via pode ser utilizada como fonte de nitrogênio (CALLAHAN; YUAN; WOLFENDEN, 2005). Como amônia é igualmente distribuída pelo corpo humano, é possível que a mesma sirva como fonte de energia para inúmeros patógenos (RUTHERFORD, 2014). Foi descrito recentemente que a urease de *C. neoformans* tem papel importante no metabolismo da levedura, principalmente em condições de privação de nutrientes a 37ºC, condição na qual o mutante nulo para o gene codificador de Ure1 tem defeito de crescimento. Além disso, esse mutante acumula ureia intracelularmente e tem outras vias metabólicas afetadas, levando a uma desregulação na produção de prolina e espécies reativas de oxigênio. Ademais, esse mutante também tem defeito na produção de melanina a 37ºC (TOPLIS *et al.*, 2020) e é significativo para a virulência em modelo murino de criptococose (COX *et al.*, 2000).

Em *C. neoformans*, urease tem um papel importante na disseminação para o SNC, principalmente pela via paracelular. O mecanismo ainda não foi completamente elucidado, mas é hipotetizado que a atividade de urease causa lesão às junções adjacentes das células endoteliais cerebrais, facilitando a invasão

do SNC pelo patógeno (SHI *et al.*, 2010; SINGH *et al.*, 2013). No entanto, a atividade ureolítica não é necessária para sobrevivência de *C. neoformans* no tecido cerebral (OLSZEWSKI *et al.*, 2004). Além disso, recentemente foi demonstrado que Ure1 de *C. neoformans* promove um aumento do pH no fagolisossomo de macrófagos. Essa característica atrasa a replicação intracelular do patógeno e reduz o dano à membrana do fagolisossomo, e simultaneamente induz a exocitose não lítica da célula do hospedeiro, eventos que podem facilitar a disseminação criptocócica dentro de macrófagos (FU *et al.*, 2018). Ademais, a deleção de Pmc1 leva uma a diminuição da expressão do gene *URE1* e atividade de urease (SQUIZANI *et al.*, 2018), reforçando o papel de Pmc1 no processo de transmigração para o SNC.

1.4.2.4. Fosfolipase

Fosfolipases formam um grupo heterogêneo de enzimas capazes de hidrolisar uma ou mais ligações éster em glicerofosfolipídeos. A ação dessas enzimas resulta na desestabilização de membranas, lise celular e liberação de lipídeos que são reconhecidos como segundos mensageiros e induzem a produção da cápsula polissacarídica em *C. neoformans* quando em contato com o hospedeiro (CHRISMAN *et al.*, 2011; SCHMIEL; MILLER, 1999).

Duas principais fosfolipases são encontradas em *C. neoformans* e têm papel importante na patogenicidade: Plb1 e Plc1. A primeira encontra-se ancorada à parede celular via âncora de GPI (SIAFAKAS *et al.*, 2006), porém exerce papel importante na virulência da levedura quando secretada (SANTANGELO *et al.*, 2004). O mutante nulo para o gene codificador dessa proteína em *C. neoformans* apresenta atenuação da sua virulência, pois possui dificuldade em estabelecer infecção tanto em um modelo murino de infecção quanto em modelo de meningoencefalite induzido em ratos, mostrando o fundamental papel de Plb1 na disseminação do fungo (COX *et al.*, 2001).

No intuito de descrever como a proteína Plb1 era liberada do ancoramento à parede celular, foram caracterizados dois genes codificadores de fosfolipases C (*PLC1* e *PLC2*) em *C. neoformans* (CHAYAKULKEEREE *et al.*, 2008). Ambas

proteínas (Plc1 e Plc2) possuem atividade de clivagem da ligação fosfodiéster de proteínas ancoradas à GPI. Mutantes nulos para ambos os genes demonstraram que apenas a deleção do gene *PLC1* apresenta impacto significativo na secreção de Plb1, porém também ocasiona um fenótipo de deficiência na secreção de melanina e capacidade de crescimento a 37°C, atenuando a virulência da levedura (CHAYAKULKEEREE *et al.*, 2008). Esse resultado evidencia a atividade de Plc1 ligada a outras proteínas componentes da parede celular de *C. neoformans*, não apenas atrelada à Plb1. A atividade de fosfolipase pode estar intimamente ligada à capacidade de replicação no interior de macrófagos, através da permeabilização das membranas dos fagolisossomos (DELEON-RODRIGUEZ; CASADEVALL, 2016; SMITH; DIXON; MAY, 2015).

1.4.3. Resposta imune frente a *Cryptococcus* spp.

Monócitos são células do sistema imune inato com papel fundamental no combate a infecções que correspondem a 10% dos leucócitos circulantes e fornecem vigilância em todos os órgãos do corpo humano (FU; DRUMMOND, 2020). Durante uma infecção, os monócitos infiltram nos tecidos, se diferenciam em macrófagos e células dendríticas e são capazes de fagocitar patógenos, produzir citocinas, e apresentar antígenos. A função dos monócitos é essencial para o controle de infecções causadas pelos fungos *Candida albicans*, *Aspergillus fumigatus* e *H. capsulatum*, porém para outros, como no caso de *C. neoformans*, apresentam um papel dicotômico, pois são importantes para o combate e também patogênese da levedura (FU; DRUMMOND, 2020).

Em infecções causadas por *C. neoformans*, monócitos são responsáveis por mediar o contato com outras células do sistema imune inato e também com o sistema imune adaptativo, através da apresentação de antígenos para linfócitos T e produção de citocinas. Porém, eles também servem como nicho para replicação e sobrevivência de *C. neoformans*, propiciando sua proliferação e disseminação para o SNC (CHARLIER *et al.*, 2009; HEUNG; HOHL, 2019; RETINI *et al.*, 1999; VECCHIARELLI *et al.*, 2000). Os monócitos podem ser diferenciados em (i) clássicos, (ii) intermediários e (iii) não clássicos. Os monócitos clássicos são os

mais abundantes, chegando a quase 90% dos monócitos circulantes e são recrutados rapidamente para locais com infecção ou danos. Eles são responsáveis pelo controle da infecção, regulação da inflamação e reparo de tecidos. Podem se diferenciar em células dendríticas ou macrófagos M1 e M2. As células dendríticas fazem parte do sistema imune inato e são clássicas apresentadoras de antígenos para células do sistema imune adaptativo. Os monócitos são diferenciados em macrófagos M1 a partir do contato com IFN-γ e são responsáveis pela alta produção de óxido nítrico e secreção de citocinas pró-inflamatórias. Esses estão associados à uma resposta de linfócitos T *helper* 1 (Th1). Já macrófagos M2 são definidos pela produção de arginase-1, reparação de tecidos, secreção de citocinas anti-inflamatórias e estão associados a uma resposta adaptativa de linfócitos T *helper* 2 (Th2). Os monócitos não clássicos são responsáveis basicamente pela reparação de tecidos e remoção de células mortas, enquanto os monócitos intermediários apresentam características clássicas e não clássicas, como a secreção de citocinas pró-inflamatórias e expressão de receptores exclusivos de monócitos não clássicos (FU; DRUMMOND, 2020).

A resposta mediada por células T inicia-se nos órgãos linfoides secundários, havendo o reconhecimento do complexo peptídeo-MHC exposto nas células apresentadoras de antígenos (APCs) por células T virgens, pois os linfócitos T não são capazes de reconhecer antígenos na forma nativa. Após a ativação das células T, por reconhecimento de MHC do tipo I ou II, as mesmas se proliferam através da resposta autócrina à interleucina-2 (IL-2) e podem ativar resposta de linfócitos T *helper* ou citotóxico. A principal resposta imune contra células de *C*. *neoformans* é através da ativação de linfócitos T *helper* (CD4+) pela apresentação de antígenos via MHC do tipo II, porém a ativação de linfócitos T citotóxicos (CD8+) não pode ser descartada (HUFFNAGLE *et al.*, 1994).

A resposta Th1 é caracterizada pela secreção de IFN-γ, TNF-α e IL-12, ativação de macrófagos M1 e indução de linfócitos B para opsonização do patógeno, sendo descrita como uma resposta protetora contra a criptococose. Neste caso, *C*. *neoformans* é eliminado pela ativação clássica de macrófagos (HERRING *et al.*, 2002; HOAG *et al.*, 1997; KAWAKAMI *et al.*, 1995; WORMLEY *et al.*, 2007). A

resposta Th2 é caracterizada pela secreção de IL-4, IL-10 e IL-13, ativação de linfócitos B para produção de anticorpos e ativação de macrófagos M2, sendo considera uma resposta prejudicial ao hospedeiro no caso da criptococose (HOAG *et al.*, 1997; KOGUCHI; KAWAKAMI, 2002; WOZNIAK *et al.*, 2012). Já foi demonstrado que a troca de resposta de Th1 para Th2 induz a expressão de fatores de virulência em *C. neoformans* (OSTERHOLZER *et al.*, 2009), porém, apenas a resposta Th1 forte não foi capaz de proteger camundongos contra a infecção e disseminação de *C. neoformans* (linhagem H99) para o sistema nervoso central (ZHANG *et al.*, 2009). Já uma possível explicação para a efetividade de *C. gattii* em causar doença em pacientes imunocompetentes está associada à forte indução de uma resposta imune Th2, a qual favorece a proliferação do fungo intracelularmente, e também diminui a maturação de células dendríticas. Essas células, como apresentadoras de antígenos, são eficazes em internalizar e eliminar células fúngicas de *C. gattii*, porém as células dendríticas infectadas falham ao entrar no processo de maturação, não havendo aumento de expressão de MHC do tipo II, o que leva a uma resposta de células T diminuída (ANGKASEKWINAI *et al.*, 2014; HUSTON *et al.*, 2013).

1.4.4. Resposta de *Cryptococcus* spp. frente ao hospedeiro

1.4.4.1. Inibição da fagocitose

Após a entrada e deposição nos pulmões, as células de *C. neoformans* residem nos alvéolos até serem internalizadas por fagócitos. A fagocitose é uma etapa crítica da patogênese criptocócica, pois o resultado dessa interação pode variar desde a morte celular do fungo até a disseminação do mesmo. Como dito anteriormente, a cápsula criptocócica é o principal determinante de virulência da levedura e atua mascarando a parede celular, a qual é composta por inúmeros carboidratos altamente imunogênicos, como β-glucanos, α-manose e quitina (GAYLORD; CHOY; DOERING, 2020). A cápsula também inibe fisicamente a fagocitose, devido ao aumento do tamanho celular do patógeno. Após a entrada de *C. neoformans* no ambiente hospedeiro, a espessura da cápsula aumenta

drasticamente; conforme o tamanho da cápsula aumenta, a eficácia da fagocitose diminui (SRIKANTA *et al.*, 2011). Além de evitar a fagocitose, o polissacarídeo GXM, quando secretado, induz a produção de IL-10, a qual inibe a expressão de IL-12 em células do sistema imune, o que reprime a secreção de citocinas pró-inflamatórias e afeta diretamente a atividade fungicida de macrófagos (RETINI *et al.*, 2001). A cápsula criptocócica também é importante para a resistência a espécies reativas de oxigênio e radicais livres encontrados no interior de macrófagos (ZARAGOZA *et al.*, 2008).

Algumas proteínas expressas por *C. neoformans* são importantes para evasão da fagocitose independente da cápsula polissacarídica. Uma dessas é a App1 (*Antiphagocytic protein* 1), localizada na parede celular de *C. neoformans*. A deleção do gene codificador de App1 não afeta a produção da cápsula de *C. neoformans*, mas as células da levedura são mais fagocitadas por macrófagos alveolares (LUBERTO *et al.*, 2003). Isso ocorre devido a ligação de App1 ao receptor 3 do sistema complemento (CR3: *complemente receptor* 3) presente na superfície de monócitos, macrófagos e células dendríticas. Essa associação impede a ligação de células da levedura opsonizadas pelo sistema complemento ao receptor CR3, impedindo a fagocitose e internalização desse patógeno (STANO *et al.*, 2009). Outra proteína envolvida em mecanismos anti-fagocíticos dependente e independente da cápsula polissacarídica é o fator de transcrição Gat201. A deleção do gene *GAT201* diminui a produção da cápsula, aumentando o índice de fagocitose dessa linhagem mutante (LIU *et al.*, 2008). Porém, Gat201 também regula a expressão dos genes *GAT204* e *BLP1*, cujos produtos estão envolvidos em mecanismos anti-fagocíticos ainda não elucidados, porém independente da cápsula polissacarídica (CHUN; BROWN; MADHANI, 2011).

O tamanho celular é outra propriedade de *C. neoformans* que influencia a taxa de fagocitose. Dentro de 24 horas após a infecção pulmonar, as células criptocócicas normais podem formar células de gigantes de até 100 µm de largura (GAYLORD; CHOY; DOERING, 2020). As células gigantes, também conhecidas como *Titan cells*, são consideradas um morfotipo e um novo determinante de virulência de *C. neoformans* (Figura 8). Elas apresentam um diâmetro celular entre 10 - 15 µm ou um tamanho total (incluindo a cápsula polissacarídica) maior de 30

µm (GARCÍA-RODAS *et al.*, 2018; ZARAGOZA; NIELSEN, 2013). A formação de *Titan cells* é induzida durante a interação com o hospedeiro e depende do tipo de resposta imune imprimida contra a levedura como também do tempo de infecção. Quando o hospedeiro induz uma resposta imune do tipo Th2, e quanto maior o tempo de sobrevivência de células de *C. neoformans*, maior será o número de células gigantes produzidas (GARCÍA-BARBAZÁN *et al.*, 2016; ZARAGOZA *et al.*, 2010). A baixa densidade celular, privação de nutrientes, baixo pH e hipóxia são os principais indutores da produção de *Titan cells* em *C. neoformans* descritos até o momento (DAMBUZA *et al.*, 2018; HOMMEL *et al.*, 2018; TREVIJANO-CONTADOR *et al.*, 2018). Um mecanismo inibidor da produção de células gigantes é o *quorum sensing*. Essa sinalização é mediada pelo peptídeo Qsp1, o qual é modificado pela protease Pqp1 e internalizado pelo transportador Opt1 (HOMER *et al.*, 2016). A produção de Qsp1, sua secreção e internalização é importante para virulência e *mating* de *C. neoformans* (HOMER *et al.*, 2016; SUMMERS *et al.*, 2020; TIAN *et al.*, 2018) e a deleção dos genes codificadores de Qsp1, Pqp1 e Opt1 induzem a formação de *Titan cells* (HOMMEL *et al.*, 2018; TREVIJANO-CONTADOR *et al.*, 2018).

A produção desse morfotipo celular afeta diretamente o curso da infecção de *C. neoformans*, já que são menos fagocitadas por macrófagos e mais resistentes ao estresse oxidativo quando comparado a células de tamanho padrão, mesmo que disseminem menos para o cérebro (GERSTEIN *et al.*, 2015; OKAGAKI *et al.*, 2010). As células gigantes também conferem proteção contra fagocitose de sua progênie de tamanho normal, por meio de um mecanismo ainda não compreendido (OKAGAKI; NIELSEN, 2012). A importância das células gigantes para proliferação de *C. neoformans* nos pulmões do hospedeiro pode ser explicada pela produção de uma parede celular espessa e de uma cápsula polissacarídica compacta. *In vivo*, essas células apresentam uma parede celular com maior quantidade de glucosamina, manose e xilose em comparação às células de tamanho normal. Já em relação à cápsula polissacarídica, as *Titan cells* apresentam menor quantidade de glicose e galactose e maior conteúdo de manose do que células de tamanho normal (MUKAREMERA *et al.*, 2018). Essas alterações podem mudar constantemente a disponibilidade de PAMPs ao longo da infecção (MUKAREMERA

et al., 2018). Além disso, *Titan cells* apresentam uma grande plasticidade genômica, pois são poliploides e conseguem gerar células filhas (GERSTEIN *et al.*, 2015; OKAGAKI *et al.*, 2010; ZARAGOZA *et al.*, 2010).

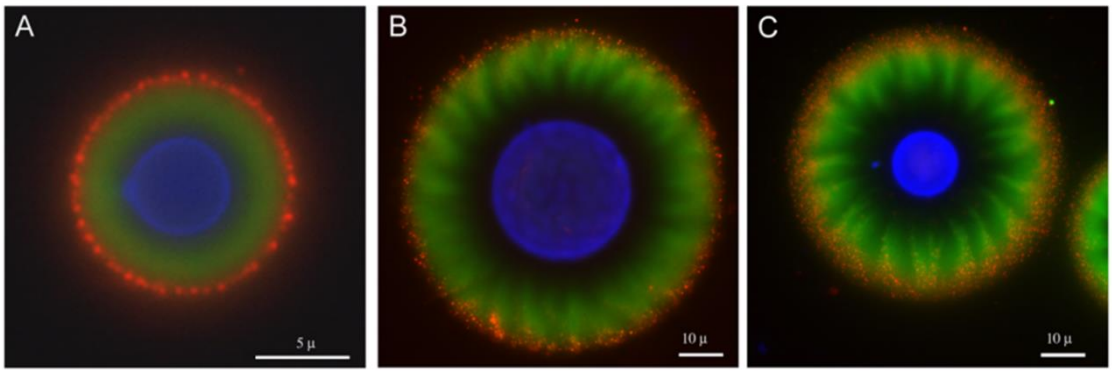

Figura 8. Células gigantes de *C. neoformans* isoladas de diferentes linhagens de camundongos. As células fúngicas foram isoladas do pulmão de camundongos após 14 dias de infecção. (A) Células de tamanho normal de *C. neoformans* H99. (B) Célula gigante (*Titan cell*) isolada de um camundongo C57BL/6J (resposta imune Th2). (C) Célula gigante isolada de um camundongo CD1 (resposta imune Th1). As células foram coradas com *Calcofluor White* (azul) para marcação da parede celular e com os anticorpos anti-GXM IgG1 18B7 (verde) e anti-GXM IgM 2D10 (vermelho). Adaptado de (GARCÍA-BARBAZÁN *et al*., 2016).

1.4.4.2. Sobrevivência e evasão intracelular

Logo após a fagocitose por macrófagos, o fagossomo contendo *C. neoformans* passa pelo processo de maturação, acidificação e fusão com o lisossomo (ARTAVANIS-TSAKONAS *et al.*, 2006; FELDMESSER *et al.*, 2000; LEVITZ *et al.*, 1999). No entanto, *C. neoformans* é capaz de sobreviver e persistir dentro do fagolisossomo (GARCIA-HERMOSO; JANBON; DROMER, 1999). Essa levedura é capaz de manipular a maturação do fagossomo através da indução de danos na membrana, da prevenção de sua completa acidificação e neutralização de atividades antimicrobianas do hospedeiro. Porém, *C. neoformans* não impede a fusão do lisossomo ao fagossomo e sim afeta a correta acidificação do fagolisossomo que consequentemente propicia sua sobrevivência e replicação (ALVAREZ; CASADEVALL, 2006; DAVIS *et al.*, 2015; DE LEON-RODRIGUEZ *et al.*, 2018; JOHNSTON; MAY, 2010; TUCKER; CASADEVALL, 2002). A depleção

de macrófagos é associada com uma maior taxa de sobrevivência de camundongos infectados com o patógeno, suportando a hipótese de que os macrófagos servem como um nicho de sobrevivência, persistência e disseminação de *C. neoformans* (KECHICHIAN; SHEA; DEL POETA, 2007). Em ratos, a latência de *C. neoformans* também está associada à residência em macrófagos (GOLDMAN *et al.*, 2000). A infecção pode ser reativada em condições de imunossupressão, levando à replicação intracelular criptocócica e possível disseminação (ALVAREZ; CASADEVALL, 2006; MA *et al.*, 2006). Consequentemente, a capacidade de *C. neoformans* de se replicar no interior de células do sistema imune contribui para diferentes estágios da patogênese criptocócica (CHARLIER *et al.*, 2009; GILBERT *et al.*, 2017; POETA, 2004).

Os danos induzidos na membrana do fagolisossomo por *C. neoformans* podem ser enzimáticos, a partir da secreção de enzimas, ou mecânicos, pelo próprio crescimento da cápsula polissacarídica (GAYLORD; CHOY; DOERING, 2020). Dois fatores de virulência já discutidos anteriormente, a fosfolipase B1 e a urease, são importantes para sobrevivência no interior de macrófagos. A deleção do gene codificador da fosfolipase diminui o desenvolvimento de *C. neoformans* no interior de macrófagos (COX *et al.*, 2001; DE LEON-RODRIGUEZ *et al.*, 2018), enquanto a urease controla a permeabilização da membrana do fagolisossomo (FU *et al.*, 2018). Além disso, a cápsula polissacarídica e o transportador ABC Afr1 são importantes para a diminuição da acidificação do fagolisossomo (LEON-RODRIGUEZ *et al.*, 2018; ORSI *et al.*, 2009).

A evasão de *C. neoformans* do interior de macrófagos pode ocorrer de três maneiras: exocitose lítica, não-lítica e transferência célula-célula (GAYLORD; CHOY; DOERING, 2020). A exocitose lítica ocorre através da degradação da célula do hospedeiro, potencialmente a partir da secreção de polissacarídeos capsulares ou manoproteínas e também pela rápida proliferação intracelular do patógeno (JOHNSTON; MAY, 2013; O'MEARA *et al.*, 2015). Já a exocitose não-lítica, também conhecida como vomocitose, ocorre a partir da fusão do fagolisossomo contendo *C. neoformans* com a membrana plasmática da célula do sistema imune. Esse mecanismo de evasão é dependente da viabilidade de *C. neoformans* e da produção de alguns de seus determinantes de virulência, como a cápsula

polissacarídica, o pigmento melanina e a fosfolipase Plb1 discutidos anteriormente (GAYLORD; CHOY; DOERING, 2020). Por último, a transferência de *C. neoformans* de uma célula para outra célula do sistema imune compreende menos de 2% da evasão dessa levedura. Esse mecanismo também é dependente da viabilidade de *C. neoformans* e acontece a partir da projeção de estruturas citoplasmáticas dependentes de actina da célula do sistema imune contendo o patógeno em direção à célula aceptora (ALVAREZ; CASADEVALL, 2007; DRAGOTAKES; FU; CASADEVALL, 2019; MA *et al.*, 2007).

1.5. Fatores de transcrição

A regulação da produção de determinantes de virulência de *C. neoformans*, bem como a detecção e resposta a diferentes condições do hospedeiro é regulada por uma rede de fatores de transcrição (JUNG *et al.*, 2015; MAIER *et al.*, 2015). Essa rede é altamente interligada e essencial para adaptação criptocócica ao ambiente pulmonar, inibição da fagocitose por células do sistema imune, resposta ao estresse oxidativo e nutricional e estabilidade da membrana e parede celular. Exemplos de fatores de transcrição de *Cryptococcus* e suas funções estão listados na Tabela 3.

Tabela 3. Fatores de transcrição de *Cryptococcus* e suas funções.

Fatores de transcrição	Função	Referências
Adaptação ao ambiente pulmonar		
Rim101	Importante para o crescimento de *C. neoformans* em altas concentrações salinas, pH alcalino e limitação de ferro. Além disso, é essencial para a formação de células gigantes e o ancoramento da cápsula polissacarídica à parede celular.	(HOMMEL *et al*., 2018; O'MEARA *et al*., 2010; WANG; AISEN; CASADEVALL, 1995)
Produção e secreção da cápsula		
Usv101	Regulador da espessura da cápsula e da liberação de polissacarídeos por regular outros três FTs: Crz1, Gat201 e Rim101, bem como algumas enzimas relacionadas a síntese de carboidratos.	(GISH *et al.*, 2016)
Nrg1	É regulado pela via de sinalização do AMPc e modula a enzima UDP-glicose desidrogenase, necessária para a biossíntese da cápsula.	(CRAMER *et al.*, 2006; HAYNES *et al.*, 2011)
Cir1	Regulador positivo da formação da cápsula.	(HAYNES *et al.*, 2011; JUNG *et al.*, 2006)
Inibição da fagocitose		
Gat201	Regula a proteína anti-fagocítica Blp1e outros fatores de transcrição relacionados com a virulência de *C. neoformans*, como Gat204, Cir1 e Liv3.	(CHUN; BROWN; MADHANI, 2011; LIU *et al.*, 2008)
Resposta a hipóxia e estresse oxidativo		
Sre1	Controla a síntese de ergosterol.	(CHANG *et al.*, 2007)
Yap1	Regula a resistência ao estresse oxidativo e a azóis.	(SO *et al.*, 2019)
Produção de melanina		
Usv101, Bzp4, Hob1, Mbs1	Usv101, Bzp4 e Mbs1 contribuem de forma independente para a melanização, enquanto Hob1 regula positivamente Bzp4 sob privação de nutrientes e a expressão basal de Usv101 e Mbs1.	(GISH *et al.*, 2016; LEE *et al.*, 2019)
Cir1	Regula negativamente a melanização.	(JUNG *et al.*, 2006)
Estabilidade da membrana e parede celular		
Crz1	Regula a estabilidade da membrana e parede celular de forma dependente e independente da via da calcineurina.	(CHOW *et al.*, 2017; LEV *et al.*, 2012; MORANOVA *et al.*, 2014; PARK *et al.*, 2016)
Cir1, Ngr1, Rim101	Regulam a estabilidade da parede celular.	(CRAMER *et al.*, 2006; HAYNES *et al.*, 2011; HOMMEL *et al*., 2018; JUNG *et al.*, 2006; O'MEARA *et al*., 2010; WANG; AISEN;

		CASADEVALL, 1995)
Aquisição de nutrientes		
Zap1	Regula a homeostase de zinco.	(SCHNEIDER *et al.*, 2012)
Cuf1	Regula a homeostase de cobre.	(GARCIA-SANTAMARINA *et al.*, 2018)
Pho4	Regula a homeostase de fosfato.	(LEV *et al.*, 2017)
Cir1	Regula a homeostase de ferro.	(JUNG *et al.*, 2006)

Além dos fatores de transcrição listados acima, o Pdr802 é outro FT importante para a virulência de *C. neoformans*. Seu papel na patogênese desse fungo foi demonstrado por diferentes grupos de pesquisa: (i) a deleção parcial de seu gene codificador (*PDR802*) afetou a virulência de *C. neoformans* em um ensaio de competição em camundongos (LIU *et al.*, 2008); (ii) a deleção completa de *PDR802* também afetou a virulência desse patógeno em um ensaio de curta duração em camundongos e a produção da cápsula polissacarídica (MAIER *et al.*, 2015); (iii) a atividade de Pdr802 foi importante para a sobrevivência do fungo em outro ensaio de competição em modelos murino e invertebrado de infecção (JUNG *et al.*, 2015). Mais recentemente, Pdr802 foi caracterizado como importante para a infecção do SNC (LEE *et al.*, 2020). Entretanto, os alvos deste fator de transcrição, assim como os potenciais mecanismos de ação ainda não foram elucidados.

2. OBJETIVOS

2.1. Objetivo geral

Elucidar os eventos moleculares associados à participação do fator de transcrição Pdr802 na virulência de *C. neoformans*.

2.2. Objetivos específicos

2.2.1. Avaliação da virulência das linhagens selvagem, nula e complementada para o gene *PDR802* em modelo de infecção experimental murino de curta e longa duração;

2.2.2. Ensaios de sobrevivência das linhagens de *C. neoformans* em condições estressoras *in vitro* e que mimetizam o ambiente do hospedeiro;

2.2.3. Análise dos principais determinantes de virulência de *C. neoformans* (produção da cápsula polissacarídica, células gigantes, melanina e urease) pelas linhagens selvagem, nula e complementada para o gene *PDR802*;

2.2.4. Identificação de alvos diretos de Pdr802 através de ensaios de imunoprecipitação de cromatina seguida de sequenciamento (ChIP-Seq) e de expressão gênica (RNA-Seq).

3. Manuscrito publicado junto ao periódico mBio

The Transcription Factor Pdr802 Regulates Titan Cell Formation and Pathogenicity of *Cryptococcus neoformans*

Julia C. V. Reuwsaat[1,2], Daniel P. Agustinho[2], Heryk Motta[1], Holly Brown[2], Andrew L. Chang[2], Michael R. Brent[3], Livia Kmetzsch[1,4,5], and Tamara L. Doering[2,5].

[1]Molecular Biology of Pathogens Laboratory, Biotechnology Center, Universidade Federal do Rio Grande do Sul, Porto Alegre, Brazil.

[2]Department of Molecular Microbiology, Washington University School of Medicine, St. Louis, Missouri, USA.

[3]Center for Genome Sciences and Systems Biology, Washington University School of Medicine, and Departments of Computer Science and Genetics, Washington University, St. Louis, Missouri, USA.

[4]Department of Molecular Biology and Biotechnology, Universidade Federal do Rio Grande do Sul, Porto Alegre, Brazil.

[5]Corresponding authors: livia.kmetzsch@ufrgs.br, doering@wustl.edu

Running head: The role of Pdr802 in *Cryptococcus neoformans* virulence.

AMERICAN SOCIETY FOR MICROBIOLOGY | mBio®

RESEARCH ARTICLE
Host-Microbe Biology

The Transcription Factor Pdr802 Regulates Titan Cell Formation and Pathogenicity of *Cryptococcus neoformans*

Julia C. V. Reuwsaat,[a,b] Daniel P. Agustinho,[b] Heryk Motta,[a] Andrew L. Chang,[b] Holly Brown,[b] Michael R. Brent,[c,d,e] Livia Kmetzsch,[a,f] Tamara L. Doering[b]

[a]Molecular Biology of Pathogens Laboratory, Biotechnology Center, Universidade Federal do Rio Grande do Sul, Porto Alegre, Brazil
[b]Department of Molecular Microbiology, Washington University School of Medicine, St. Louis, Missouri, USA
[c]Center for Genome Sciences and Systems Biology, Washington University School of Medicine, St. Louis, Missouri, USA
[d]Department of Computer Science and Engineering, Washington University, St. Louis, Missouri, USA
[e]Department of Genetics, Washington University, St. Louis, Missouri, USA
[f]Department of Molecular Biology and Biotechnology, Universidade Federal do Rio Grande do Sul, Porto Alegre, Brazil

ABSTRACT *Cryptococcus neoformans* is a ubiquitous, opportunistic fungal pathogen that kills almost 200,000 people worldwide each year. It is acquired when mammalian hosts inhale the infectious propagules; these are deposited in the lung and, in the context of immunocompromise, may disseminate to the brain and cause lethal meningoencephalitis. Once inside the host, *C. neoformans* undergoes a variety of adaptive processes, including secretion of virulence factors, expansion of a polysaccharide capsule that impedes phagocytosis, and the production of giant (Titan) cells. The transcription factor Pdr802 is one regulator of these responses to the host environment. Expression of the corresponding gene is highly induced under host-like conditions *in vitro* and is critical for *C. neoformans* dissemination and virulence in a mouse model of infection. Direct targets of Pdr802 include the quorum sensing proteins Pqp1, Opt1, and Liv3; the transcription factors Stb4, Zfc3, and Bzp4, which regulate cryptococcal brain infectivity and capsule thickness; the calcineurin targets Had1 and Crz1, important for cell wall remodeling and *C. neoformans* virulence; and additional genes related to resistance to host temperature and oxidative stress, and to urease activity. Notably, cryptococci engineered to lack Pdr802 showed a dramatic increase in Titan cells, which are not phagocytosed and have diminished ability to directly cross biological barriers. This explains the limited dissemination of *pdr802* mutant cells to the central nervous system and the consequently reduced virulence of this strain. The role of Pdr802 as a negative regulator of Titan cell formation is thus critical for cryptococcal pathogenicity.

IMPORTANCE The pathogenic yeast *Cryptococcus neoformans* presents a worldwide threat to human health, especially in the context of immunocompromise, and current antifungal therapy is hindered by cost, limited availability, and inadequate efficacy. After the infectious particle is inhaled, *C. neoformans* initiates a complex transcriptional program that integrates cellular responses and enables adaptation to the host lung environment. Here, we describe the role of the transcription factor Pdr802 in the response to host conditions and its impact on *C. neoformans* virulence. We identified direct targets of Pdr802 and also discovered that it regulates cellular features that influence movement of this pathogen from the lung to the brain, where it causes fatal disease. These findings significantly advance our understanding of a serious disease.

KEYWORDS *Cryptococcus neoformans*, Pdr802, Titan cells, capsule, fungal pathogens, pathogenesis, pathogenic yeast, quorum sensing, transcription factors

Citation Reuwsaat JCV, Agustinho DP, Motta H, Chang AL, Brown H, Brent MR, Kmetzsch L, Doering TL. 2021. The transcription factor Pdr802 regulates Titan cell formation and pathogenicity of *Cryptococcus neoformans*. mBio 12:e03457-20. https://doi.org/10.1128/mBio.03457-20.

Address correspondence to Livia Kmetzsch, livia.kmetzsch@ufrgs.br, or Tamara L. Doering, doering@wustl.edu.

Received 9 December 2020
Accepted 28 January 2021
Published 9 March 2021

Cryptococcosis is a fungal infection caused by *Cryptococcus neoformans* and *Cryptococcus gattii*. *C. neoformans* is a ubiquitous opportunistic pathogen that infects mainly immunocompromised patients, while *C. gattii* is capable of infecting immunocompetent individuals (1). Cryptococcosis causes 180,000 deaths worldwide each year, including roughly 15% of all AIDS-related deaths (2), and is initiated by the inhalation of spores or desiccated yeast cells. In immunocompetent individuals, this typically causes an asymptomatic pulmonary infection that is controlled by the host immune response, although a population of *C. neoformans* may remain latent for extended periods of time (3–5).

Under conditions of immunocompromise, cryptococci disseminate from the lung to the brain. Mechanisms that have been suggested to mediate fungal crossing of the blood-brain barrier (BBB) include transcellular migration, in which the yeast cells enter and exit vascular endothelial cells (6–9); paracellular movement, in which they cross the BBB at junctions between endothelial cells (10–12); and "Trojan horse" crossing, whereby macrophages harboring *C. neoformans* enter the brain (13). Cryptococcal meningoencephalitis is difficult to treat and frequently lethal, for reasons that include the availability and cost of therapy (14, 15).

The ability of *C. neoformans* to survive and proliferate in the lung, and subsequently disseminate to the brain, depends on viability at mammalian body temperature and the expression of multiple virulence traits; these include secreted factors (16, 17), a polysaccharide capsule that surrounds the cell wall (18), and the production of giant (Titan) cells (19, 20). One secreted molecule, the pigment melanin, associates with the cell wall, where its antioxidant properties protect fungal cells from reactive oxygen species produced as a host immune defense (21–25). Urease, a secreted metalloenzyme that converts urea to ammonia and CO_2, may affect the course of infection by modulating environmental pH and damaging host tissue structure (11, 12, 26).

The capsule, composed primarily of large polysaccharides (27–29), is a key cryptococcal virulence factor that impairs phagocytosis by immune cells (30–35). This dynamic entity changes its size and structure during interactions with the host or external environment (36–39), contributing to fungal adaptation (40, 41). Capsule polysaccharides that are shed from the cell enable diagnosis of cryptococcal infection and also impede host responses (35, 42).

Titan cells are a cryptococcal morphotype that has been variously characterized as having a cell body diameter (excluding the capsule) greater than 10 or 15 μm or total cell diameter (including the capsule) that exceeds 30 μm (20, 43, 44). These cells are polyploid and produce normal-size cells during infection (19, 45, 46). Titan cell formation is triggered by exposure to the host environment, including nutrient starvation, reduced pH, and hypoxia (47–49), although the extent of induction depends on the host immune response and the duration of infection (45, 50). Titan cell production appears to benefit the development of pulmonary *C. neoformans* infection, since these large cells are less susceptible to internalization by host phagocytes and more resistant to oxidative stress than normal-size cells (19, 46). Some of these effects may be explained by the highly cross-linked capsule and thickened cell wall of Titan cells (51). In contrast to their success in the lungs, Titan cells show impaired dissemination to the brain (19, 46).

C. neoformans experiences a dramatic change in conditions upon entering a host, including altered nutrient levels and pH. To adapt to the new environment, cryptococci activate a network of transcription factors (TFs) (39, 52). For example, imbalances in ion homeostasis trigger transcriptional changes mediated by the TFs Zap1 (53), Cuf1 (54), Pho4 (55), Cir1 (56), and Crz1 (57). Alkaline pH stimulates expression of the TF Rim101, which enables growth under basic conditions and other stresses, such as high salt and iron limitation; it also promotes the association of capsule polysaccharide with the cell and the formation of Titan cells (47, 58).

Overlapping TF circuits regulate cryptococcal virulence determinants, including polysaccharide capsule production and melanin synthesis. For example, Usv101, an

important regulator of capsule thickness and polysaccharide shedding, also regulates three other TFs (Gat201, Crz1, and Rim101) and multiple polysaccharide-related enzymes (59). Gat201 further regulates additional virulence-related transcription factors and the anti-phagocytic protein Blp1 (60), while Crz1 plays a central role in the maintenance of plasma membrane and cell wall stability (57, 61, 62). Crz1 expression is also modulated by the calcineurin signaling pathway, which is required for normal yeast growth at 37°C, virulence, and sexual reproduction (63). A group of TFs, including Usv101, Bzp4, Hob1, and Mbs1 (59, 64), act together to regulate melanin production; deletion of Bzp4 also alters capsule production (52).

In this study, we investigated the TF Pdr802. The corresponding gene has a high rate of nonsynonymous mutations, which suggests that it is evolving rapidly (65). Pdr802 has previously been implicated in *C. neoformans* virulence (39, 52, 66), but its specific role and targets are not known. We discovered that Pdr802 is induced under host-like conditions, is a negative regulator of Titan cell formation, and influences capsule thickness and phagocytosis by macrophages. It also regulates genes whose products act in cell wall remodeling, virulence factor production, resistance to host temperature and oxidative stress, and quorum sensing. These functions make Pdr802 critical for cryptococcal survival in the lung and dissemination to the brain.

RESULTS

Role of Pdr802 in *C. neoformans* virulence. The importance of Pdr802 in *C. neoformans* virulence has been demonstrated in multiple experimental models. Liu and collaborators first reported in 2008 that partial deletion of *PDR802* reduced *C. neoformans* infectivity in a competition assay of pooled *C. neoformans* strains (66). In 2015, Maier et al. showed that a *pdr802* deletion mutant had reduced virulence when tested individually in a short-term mouse model of infection (39). Later that year, Jung and colleagues reported that Pdr802 was required for full virulence in both wax moth larva and short-term mouse infection using pooled strains (52). Most recently, Lee and collaborators showed that Pdr802 was required for brain infection (67).

To further investigate the role of Pdr802 in pathogenesis, we complemented a complete deletion strain in the KN99α background that we had previously generated (*pdr802*) (39) with the intact gene at its native locus (*PDR802*). To examine targets of Pdr802, we also constructed a strain that expresses the protein fused to mCherry at its N terminus (see Fig. S1A in the supplemental material). All of these strains lacked or expressed RNA encoding *PDR802* or its modified forms as expected (Fig. S1B), and *PDR802* was expressed at wild-type levels in the complemented and modified strains (Fig. S1C).

We next assessed the long-term survival of C57BL/6 mice infected with the parental wild-type (WT) strain (KN99α), the deletion mutant (*pdr802*), or the complemented mutant (*PDR802*). In this model, mice infected with the parent or complemented strains survived for roughly 3 weeks, while those infected with the deletion mutant showed a striking increase in survival: all animals survived for at least 65 days, and over half survived to the end of the study (100 days) (Fig. 1A). The lung burden measured at the time of death for *pdr802*-infected mice in this study was approximately 100-fold lower than that of wild-type infections (Fig. S2A), demonstrating the importance of this TF in *C. neoformans* virulence. Mean brain burden at the time of death was more similar between mutant and wild-type infections (Fig. S2A), although we did note some heterogeneity in this measure for *pdr802*-infected mice; animals sacrificed at around 2 months of infection (red symbols) showed brain burdens similar to WT levels, while brain burdens in mice sacrificed at day 100 (blue symbols) ranged between zero fungal cells and the WT level.

We next examined the time course of fungal proliferation in the lungs. As expected, the burdens of WT and the complemented mutant strains increased steadily over an 18-day interval (Fig. 1B), eventually reaching roughly 10^5 times the original inoculum. Towards the end of this period, these cells were also detected in the blood and brain

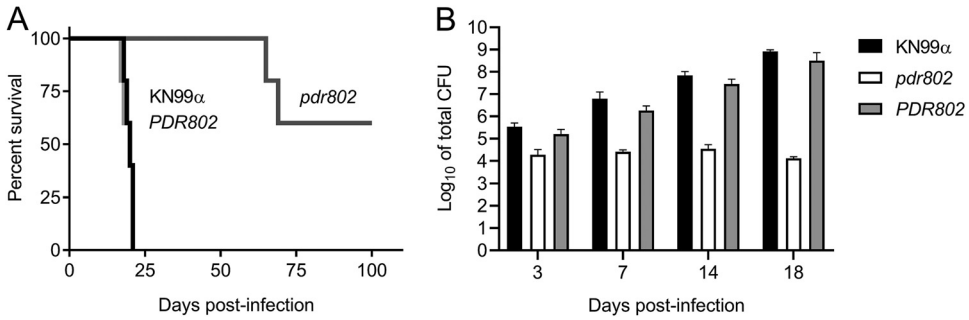

FIG 1 The transcription factor Pdr802 influences *C. neoformans* virulence. (A) Survival of C57BL/6 mice over time after intranasal inoculation with 5×10^4 cryptococci, with sacrifice triggered by weight below 80% of peak. (B) Means and standard deviations (SD) of total colony-forming units (CFU) in lung tissue at various times post-infection. Numbers of CFU inoculated for each strain were 41,400 (KN99α), 42,800 (*pdr802* strain) and 26,600 (*PDR802* strain). $P < 0.05$ for the *pdr802* strain compared to the other strains at all time points.

(Fig. S2B). In contrast, the lung burden of *pdr802* remained close to the inoculum throughout this period, with no mutant cells detected in the blood or brain. At a late time point of *pdr802* infection (75 days), we again noted some heterogeneity of fungal burden: one mouse had high lung burden with no dissemination, another had high lung burden with moderate brain burden, and the third had extremely low lung burden with no dissemination (Fig. S2C). No CFU were detected in the blood of *pdr802*-infected mice at any point during infection. These results suggest that even though the *pdr802* mutant is generally hypovirulent and remains at low levels in the lung, it can occasionally reach the brain and, given enough time, accumulate there (see Discussion).

Given the dramatic effects of Pdr802 on fungal virulence, we wondered about the specific biological processes in which this transcription factor is involved. We first examined the behavior of the *pdr802* strain *in vitro*, including stress conditions that might be encountered in the host. We saw no differences in growth of the mutant compared to WT cells under conditions that challenge cell or cell wall integrity, including the presence of sorbitol, high salt, cell wall dyes, caffeine, sodium dodecyl sulfate (SDS), or ethanol (Fig. S3A to C). The mutant also showed no altered susceptibility to elements of the host response, such as nitrosative or oxidative stresses, or in melanin production. All of these results held when cells were grown on rich medium, whether plates were incubated at 30°C, 37°C, or 37°C in the presence of 5% CO_2, which was recently described as an independent stress for *C. neoformans* (68) (Fig. S3A to C). Finally, the mutant showed no difference from wild-type cells in secretion of urease (Fig. S3D).

Pdr802 is regulated by "host-like" conditions. We next tested the growth of the *pdr802* mutant under conditions more like those encountered inside the mammalian host, using tissue culture medium (Dulbecco's modified Eagle medium [DMEM]) at 37°C in the presence of 5% CO_2. We found that although the *pdr802* mutant grew like WT in rich medium (yeast extract-peptone-dextrose [YPD]), it grew poorly in DMEM (Fig. S4A and B). To test whether the mutant cells were dead or just static after growth in DMEM, we plated aliquots on solid medium to measure CFU over time (Fig. 2A). The *pdr802* culture showed a dramatic decrease in viability compared to WT and the complemented strain, which was greatest in the first 24 h. This is the same time frame in which expression of the *PDR802* gene shows a striking increase, as measured by transcriptome sequencing (RNA-Seq) (Fig. 2B).

Another important feature that is induced by growth in DMEM at 37°C and 5% CO_2 is the polysaccharide capsule, which we previously reported to be regulated by Pdr802, based on negative staining with India ink (39). Fluorescence microscopy confirmed increased capsule thickness of the mutant, which reverted to WT in the

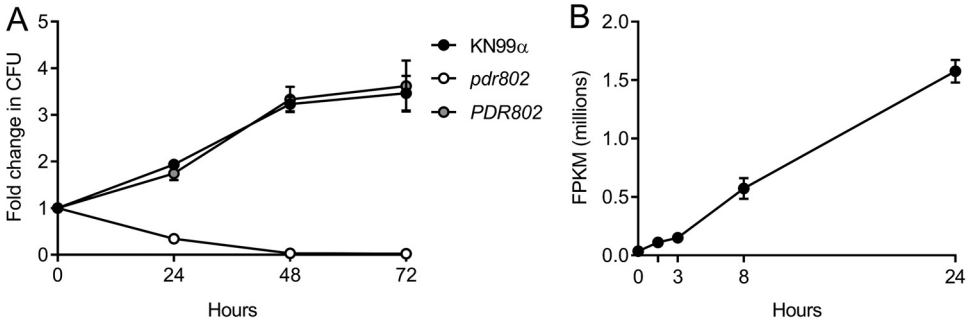

FIG 2 *PDR802* expression is required for cell viability and induced during growth under host-like conditions. (A) Cells grown in DMEM at 37°C and 5% CO_2 were sampled at the times indicated and plated on YPD to assess viability (measured as number of CFU and plotted as fold change from time zero). (B) *PDR802* expression in KN99α cells grown in DMEM at 37°C and 5% CO_2 was assessed by RNA-Seq as in reference 117. FPKM, fragments per kilobase per million. Mean and standard deviation (SD) are shown on both plots.

complemented strain (Fig. 3A). To quantify this change, we took advantage of a semi-automated assay that we have developed (Fig. S5), which measures capsules on a population scale (Fig. 3B) and is therefore very sensitive. This analysis showed that the capsule thickness of *pdr802* cells resembles that of the well-studied hypercapsular mutant *pkr1* (39, 69, 70) and is completely restored to WT by complementation at the native locus (Fig. 3C). Previous studies suggest that capsule thickness upon induction reflects the size of the dominant capsule polymer (glucuronoxylomannan [GXM]) (71, 72), which can be analyzed by agarose gel migration and blotting with anticapsule antibodies (71). Consistent with the difference we observed in capsule thickness by imaging, this method showed decreased mobility of GXM from *pdr802* as capsule induction progressed (Fig. S4C).

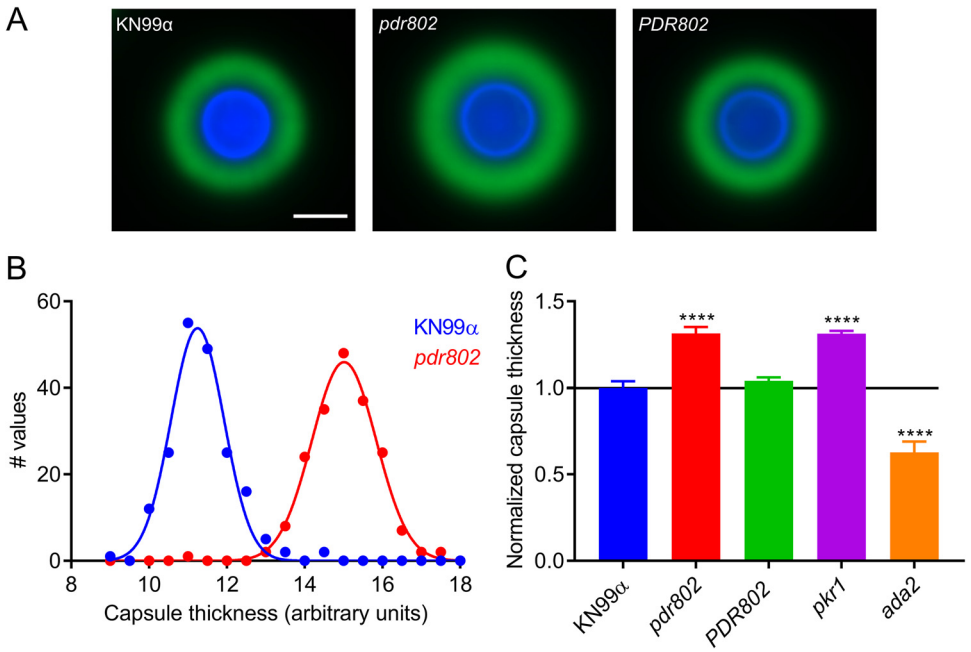

FIG 3 The *pdr802* mutant is hypercapsular. (A) Representative immunofluorescence micrographs of the indicated strains after growth in DMEM (37°C, 5% CO_2) for 24 h. The capsule was stained with anti-GXM monoclonal antibody 302 conjugated with Alexa Fluor 488 (green) and the cell wall with calcofluor white (blue). All images are to the same scale; bar, 5 μm. (B) Capsule thickness distribution for the indicated strains. (C) Mean and SD of capsule size, quantified as detailed in Materials and Methods and Fig. S5, with the *pkr1* (39) and *ada2* (105) strains shown as hypercapsular and hypocapsular controls, respectively. ****, $P < 0.0001$, compared to KN99α by one-way ANOVA with a *post hoc* Dunnett test.

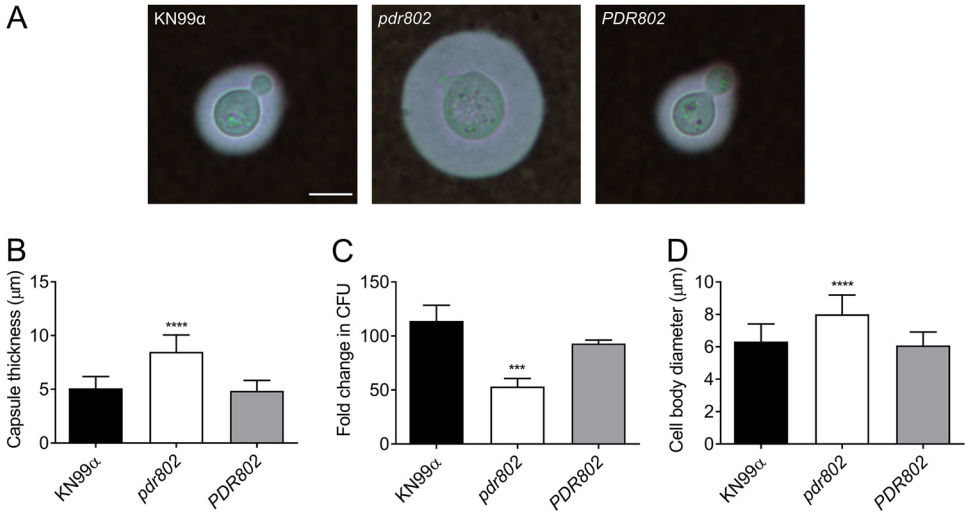

FIG 4 Growth in mouse serum elicits increased capsule thickness and cell body diameter in the *pdr802* mutant. (A) Light micrographs of the indicated strains after growth in mouse serum (at 37°C, 5% CO_2) for 24 h and negative staining with India ink to visualize the capsule. All images are to the same scale; bar, 5 μm. (B) Mean and SD of capsule thickness, assessed by measuring at least 50 cells per strain with ImageJ. (C) Cells grown as described for panel A were plated on YPD to assess CFU. Mean and SD of the fold change compared to 0 h are shown. (D) Mean and SD of cell body diameter, measured as for panel B. ***, $P < 0.001$, and ****, $P < 0.0001$, compared to KN99α by one-way ANOVA with a *post hoc* Dunnett test.

To validate the observations that we had made under standard host-like conditions based on synthetic tissue culture medium, we conducted similar studies in mouse serum at 37°C and 5% CO_2. These conditions induced an even more pronounced hypercapsular phenotype of the *pdr802* mutant (Fig. 4A and B), as well as reduced cell viability (Fig. 4C) and increased cell body diameter (Fig. 4D).

We were intrigued by the enlarged cell body and capsule of the *pdr802* mutant cells under host-like conditions *in vitro* and decided to examine these phenotypes *in vivo*. For these studies, we isolated fungal cells from the lungs of mice at various times after infection and assessed their morphology by negative staining (Fig. 5A). At each time point, the mean mutant cell body diameter was larger than that of the controls. Additionally, while this parameter was stable for WT and complemented strains throughout the infection period, it trended larger at the end of the infection period for the deletion mutant (Fig. 5B). In contrast, mutant capsule thickness, although initially greater than that of control cells, changed little throughout the period, while capsule thickness of control cells increased to that level or beyond (Fig. 5C). Furthermore, although the total diameter of *pdr802* cells consistently exceeded that of WT and complemented cells, their sizes became more comparable late in infection (Fig. S6A). Over time, therefore, the ratio of total cell diameter to cell body diameter for WT and *PDR802* cells steadily increased, while it remained roughly constant for the mutant (Fig. S6B).

Pdr802 negatively regulates Titan cell formation. We were particularly interested in the cell size phenotype of *pdr802* because Titan cells have been strongly implicated in cryptococcal pathogenesis (19). By any definition of this morphotype (cell body diameter greater than 10 or 15 μm or total cell diameter greater than 30 μm), our mutant cell populations were dramatically enriched in Titan cells at every time of infection that we assessed (Fig. S6C).

To specifically test Titan cell formation by the *pdr802* strain, we subjected mutant cells to *in vitro* conditions that induce this process (49) (Fig. 6A) and analyzed the resulting population by flow cytometry. Consistent with our *in vivo* observations, Titan cells constituted a much larger fraction of the population in the mutant culture (8.46%)

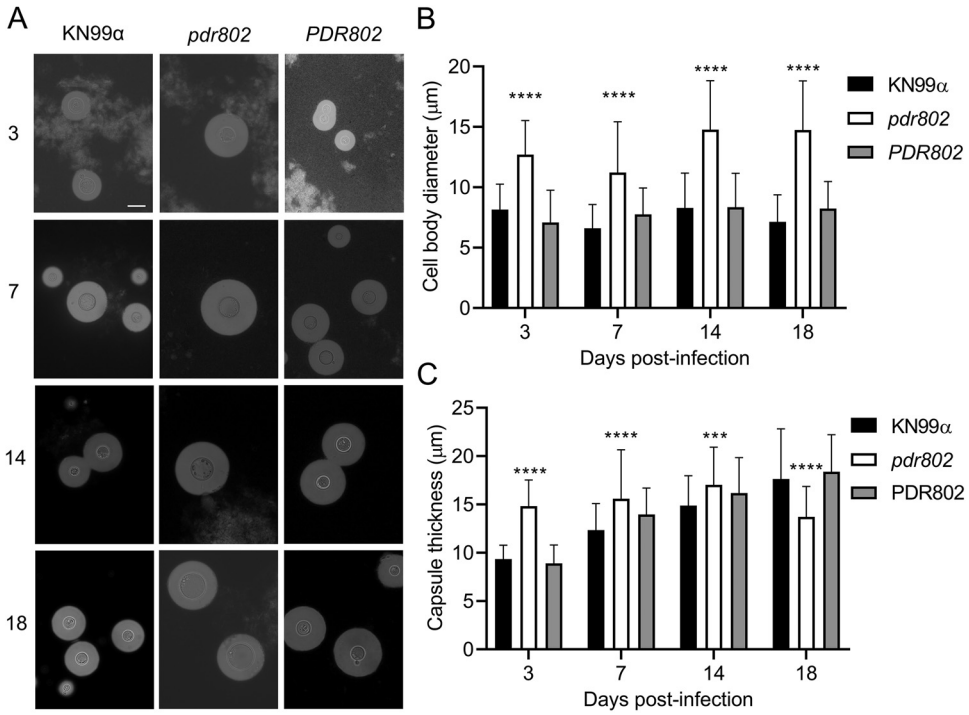

FIG 5 Absence of *PDR802* yields enlarged cells and loss of capsule induction in the context of animal infection. (A) India ink staining of fungi isolated from the lungs of mice infected with the indicated strains. Numbers at left are days post-infection. All images are to the same scale; bar, 10 μm. (B and C) Means and SD of cell body diameter (B) and capsule thickness (C), assessed by measuring at least 50 cells per strain with ImageJ. ****, $P < 0.0001$, and ***, $P < 0.001$, compared to KN99α by one-way ANOVA with a *post hoc* Dunnett test for each day post-infection.

than in the WT and complemented cultures (1.38% and 1.13%, respectively) (Fig. 6B). As expected for Titan cells, these cells are also polyploid (Fig. 6C).

Titan cells are poorly engulfed by host phagocytes (19, 45, 73), which may reflect their increased size as well as alterations in capsule and cell wall (51). We observed this reduced uptake for all strains after growth in conditions that favor Titan cell formation (Fig. 7, Titan versus YPD). Also, all strains showed a reduction in phagocytosis after capsule induction in DMEM (Fig. 7, DMEM versus YPD), which is not surprising, because the capsule is antiphagocytic (31, 73). Notably, the reduction in uptake was greatest for the *pdr802* mutant under both of these conditions, even though it showed normal engulfment when all strains were grown under control conditions (YPD). This is likely because the mutant culture is both hypercapsular and enriched in Titan cells.

Identification of direct, functional targets of Pdr802. To identify direct targets of Pdr802, we next performed chromatin immunoprecipitation followed by sequencing (ChIP-Seq). We compared DNA sequences immunoprecipitated by anti-mCherry monoclonal antibody (MAb) from cells expressing mCherry-Pdr802, which grow similarly to the WT (Fig. S7A), and untagged cells. Both strains were grown for 24 h in DMEM at 37°C and 5% CO_2, as these conditions induce *PDR802* expression dramatically compared to standard YPD growth conditions (Fig. 2).

Using 2-fold-enrichment over control as a cutoff value for peaks with adjusted *P* values of <0.05, we identified 656 binding sites for mCherry-Pdr802 in genomic DNA. Of these, 540 occurred within 1,000 bp upstream of transcription start sites (Data Set S1, sheets 1 and 2), which we used as an approximation of regulatory regions. Notably, ChIP-Seq data for the region upstream of the *PDR802* transcription start site suggested self-regulation, as has been reported for other cryptococcal TFs (74, 75) (Fig. S7B). We further applied discriminative regular expression motif elicitation (DREME) (76) to the

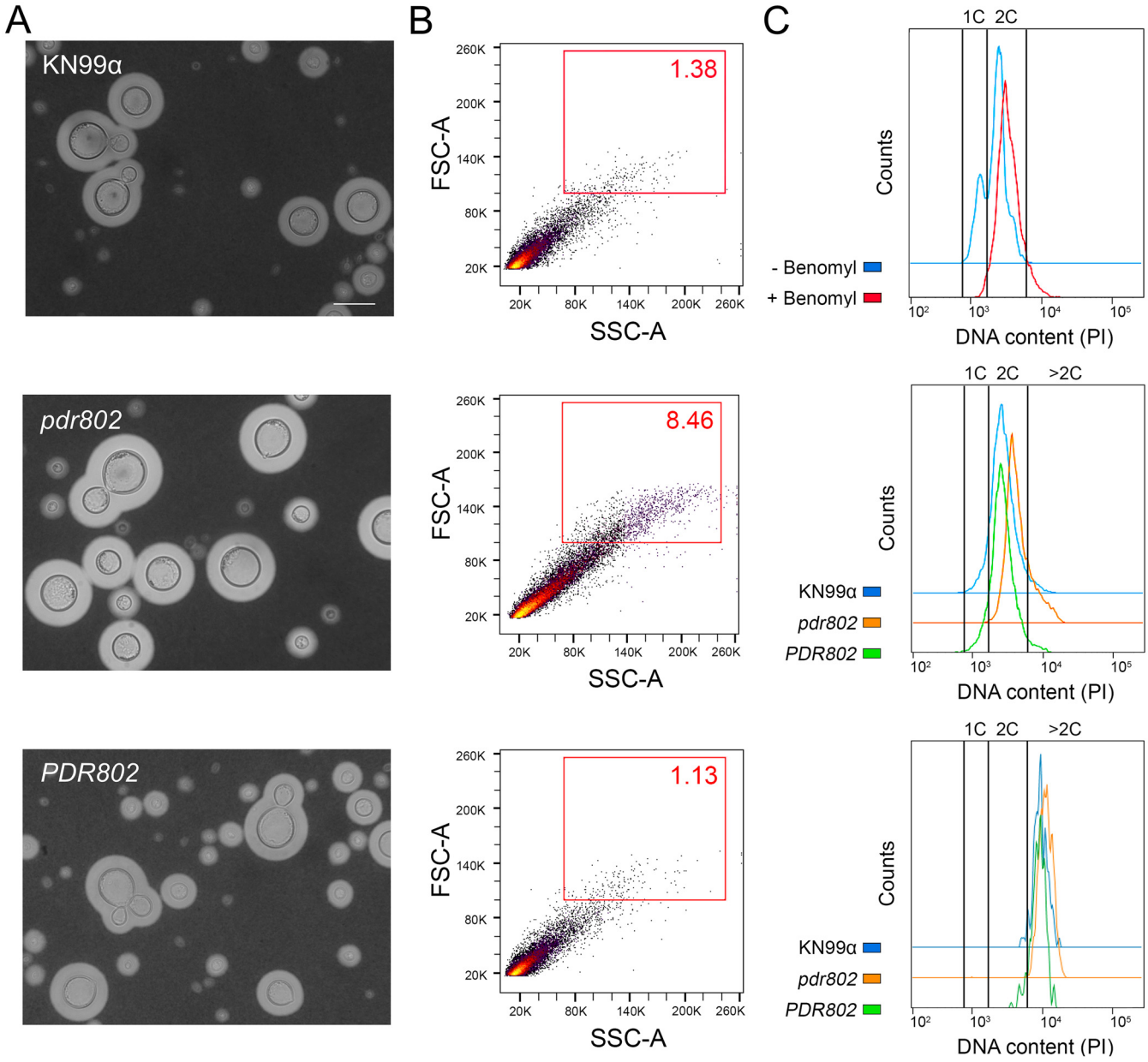

FIG 6 Pdr802 is a negative regulator of Titan cell formation. (A) The indicated strains were subjected to *in vitro* conditions that induce Titan cell formation and imaged with India Ink. All images are to the same scale; bar, 10 μm. Images were selected so that each shows multiple examples of Titan cells, not to reflect abundance of this morphotype. (B) The percentage of Titan cells in each culture was quantified using flow cytometry, gated as indicated by the red square. FSC-A, forward scatter; SSC-A, side scatter. (C) DNA content of cells after staining with propidium iodide (PI) and analysis by flow cytometry. (Top) 1C and 2C gates determined using control cultures of KN99α grown in YNB without or with benomyl, which traps cells at 2C. (Middle) Profiles of the indicated strains after growth under Titan cell-inducing conditions, showing an increased polyploid tail in mutant cultures relative to wild-type cells. (Bottom) DNA content profiles for only the Titan cells (gated as for panel B, red box) for each strain, showing their polyploid nature.

set of 540 upstream regions to identify putative Pdr802 binding motifs; these were highly enriched in GA (TC) (Fig. S7C).

To complement our ChIP studies, we determined the set of genes regulated by Pdr802 under host-like conditions by performing RNA-Seq of WT and *pdr802* cells after growth for 24 h in DMEM at 37°C and 5% CO_2 (Data Set S1, sheet 3). We then used dual-threshold optimization (DTO) to analyze the RNA-Seq and ChIP-Seq data sets together. This statistical method allowed us to combine the evidence from binding and expression studies to converge on a set of direct and functional TF targets (77); because it uses two independent lines of evidence to suggest regulatory relationships, it

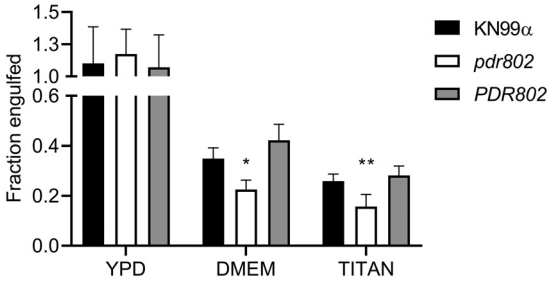

FIG 7 Deletion of *PDR802* affects phagocytosis after growth under conditions that induce capsule and Titan cell formation. *C. neoformans* strains were grown in YPD (18 h), DMEM (24 h), or Titan cell induction medium (72 h) and then incubated for 2 h with J774.16 mouse macrophages; host cells were then washed and lysed to assess fungal burden by CFU. Data shown are normalized to the CFU of the initial inoculum. *, $P < 0.05$, and **, $P < 0.01$, compared to KN99α by one-way ANOVA with a *post hoc* Dunnett test.

increases confidence in highly significant small effects. The Pdr802 target genes yielded by this analysis include key players in multiple processes implicated in cryptococcal virulence, including quorum sensing, Titan cell formation, and stress resistance (Data Set S1, sheets 4 and 5).

Pdr802 regulates the expression of quorum sensing proteins that control Titan cell formation. The most striking phenotype we observed in cells lacking *PDR802* is the marked increase in Titan cell formation. We therefore examined our DTO target list for genes known to influence this phenotype, such as those involved in quorum sensing. Recent studies have shown that the quorum sensing peptide Qsp1 is a negative regulator of Titan cell formation (47, 48); Titan cell formation increases upon deletion of the gene encoding this peptide (*QSP1*) or proteins that mediate its maturation and import (*PQP1* and *OPT1*, respectively). We found that Pdr802 positively regulates *PQP1* and *OPT1* gene expression (Table 1), consistent with its repression of Titan cell formation.

A study of *C. neoformans* cells exposed to Titan cell-inducing conditions *in vitro* reported that 562 genes were upregulated under this condition, while 421 genes were downregulated (48). The overlap of these genes with our DTO set of Pdr802-regulated genes included the TF genes *LIV3*, *STB4*, and *ZFC3* (48) (Data Set S2, sheets 1 and 2). The first two are repressed during Titan cell induction, while *ZFC3* (also known as *CQS2*) is induced. Our analysis showed that Pdr802 positively regulates expression of *LIV3* and *STB4*, while it negatively regulates *ZFC3* (Table 1), in concordance with our phenotypic observations of Titan cell formation. Notably, Liv3 and Zfc3 are responsive to the peptide Qsp1 (74, 75) and are important for *C. neoformans* virulence, while Stb4 influences cryptococcal brain infection (67).

Pdr802 coordinates cryptococcal response to the host environment. *C. neoformans* deploys a variety of proteins to resist the many challenges it experiences upon host entry, which include oxidative and temperature stress. Multiple genes that are central to these responses were identified as direct, functional targets of Pdr802 by our DTO analysis (Table 2). For example, Pdr802 induces the expression of genes whose products detoxify reactive oxygen species (ROS), such as *CAT1*, *CAT2*, and *SOD1* (78, 79), or participate in resistance to these compounds, such as *FZC34*, *MIG1*, and *CCK1* (52, 80, 81) (Table 2). Both the kinase Cck1 (also known as Yck2) and the TF Fzc34 have been implicated in cryptococcal virulence (80, 82).

As noted above, the pigment melanin has important antioxidant properties that promote cryptococcal survival inside the host (16). Under host-like conditions, Pdr802 regulates genes required for melanization, even though it melanizes normally *in vitro*. These genes include *CAC1*, *PKC1*, *CUF1*, and *SNF5* (Table 2). Cac1 is an adenylyl cyclase responsible for cyclic AMP (cAMP) production in *C. neoformans*, which plays a central role in melanin synthesis as well as proper capsule production, mating, and virulence (83). The kinase Pkc1 induces production of the laccase (Lac1) that forms melanin and

TABLE 1 Pdr802 target genes involved in quorum sensing and Titan cell formation

Biological process	CNAG ID[a]	Gene name	Change determined by: ChIP-Seq[b]	Change determined by: RNA-Seq[c]	Description
Quorum sensing	00150	*PQP1*	1.38	−0.78	Peptidase
	03013	*OPT1*	1.25	−0.55	OPT small oligopeptide transporter
Titan cell formation	05835	*LIV3*	1.52	−0.84	Transcription factor
	05785	*STB4*	3.33	−1.71	Transcription factor
	05940	*ZFC3/CQS2*	2.23	0.68	Transcription factor

[a]CNAG, ***C**ryptococcus **n**eoformans* serotype **A** **g**enome project gene identifier (118).
[b]Fold change for mCherry-Pdr802 compared to WT.
[c]Log_2 fold change for *pdr802* compared to WT.

plays a key role in resistance to oxidative and nitrosative stress (84, 85), the TF Cuf1 regulates *LAC1* expression and is important for cryptococcal virulence (86, 87), and *SNF5* is required for full melanization (88). Melanin occurs in the fungal cell wall, which is another key component in fungal stress resistance. Pdr802 is also a direct, functional regulator of several genes whose products influence cell wall glycan content: two chitin deacetylases (Cda3 and Mp98) and the mannoprotein MP88 (Table 2). This is also consistent with the increases in mannose and chitin that occur in Titan cell walls (51).

Pdr802 positively regulates the expression of several proteins required for yeast survival at 37°C, including the kinases Kic1 and Ire1 (Table 2). Ire1 is a regulator of the cryptococcal unfolded-protein response (UPR) pathway and lack of Ire1 or Kic1 impact *C. neoformans* virulence (80, 89). Pdr802 also modulates cryptococcal urease activity, which is required for dissemination to the central nervous system (CNS) (11, 12), by regulating the urea transporter Dur3 and other proteins that influence urease activity

TABLE 2 Genes regulated by Pdr802 involved in adaptation to the host environment

Biological process	CNAG ID[a]	Gene name	Change determined by: ChIP-Seq[b]	Change determined by: RNA-Seq[c]	Description
Oxidative stress resistance	04981	*CAT1*	1.47	−1.60	Catalase 1
	05256	*CAT2*	1.41	−0.42	Catalase 2
	01019	*SOD1*	2.59	−0.53	Superoxide dismutase (Cu-Zn)
	00896	*FZC34*	2.22	−0.82	Transcription factor
	06327	*MIG1*	1.72	−0.78	DNA-binding protein CreA
	00556	*CCK1*	1.78	−0.48	Casein kinase I
Melanin and cell wall formation	03202	*CAC1*	1.60	−0.61	Adenylate cyclase
	01845	*PKC1*	2.00	−0.48	AGC/PKC protein kinase
	07724	*CUF1*	1.27	−0.67	Metal-binding regulatory protein
	00740	*SNF5*	1.28	−0.70	Swi/Snf chromatin-remodeling subunit
	01239	*CDA3*	2.63	1.08	Chitin deacetylase 3
	01230	*MP98*	2.74	0.96	Chitin deacetylase 2
	00776	*MP88*	1.86	1.23	Immunoreactive mannoprotein
Growth at 37°C	00405	*KIC1*	1.88	−0.97	Ste/Ste20/Ysk protein kinase
	03670	*IRE1*	1.66	−1.14	IRE protein kinase
Urease activity	07448	*DUR3*	2.13	−3.05	Urea transporter
	01209	*FAB1*	2.29	−0.49	1-Phosphatidylinositol-3-*P* 5-kinase
	01938	*KIN1*	1.61	−0.34	CAMK/CAMKL/KIN1 protein kinase
	01155	*GUT1*	2.96	0.62	Glycerol kinase
	00791	*HLH1*	1.71	−1.09	Transcription factor
Capsule thickness	02802	*ARG2*	1.56	−0.59	Inositol/phosphatidylinositol kinase
	06809	*IKS1*	2.28	−0.44	IKS protein kinase
	01905	*KSP1*	2.02	−0.64	Serine/threonine protein kinase
	02877	*FZC51*	1.75	−0.69	Transcription factor
	07470	*PDE2*	2.42	−1.80	High-affinity phosphodiesterase
	03346	*BZP4*	3.52	1.30	Transcription factor
Calcineurin signaling	00156	*CRZ1*	1.44	−0.49	Transcription factor
	01744	*HAD1*	2.26	0.47	Phosphatase

[a]CNAG, ***C**ryptococcus **n**eoformans* serotype **A** **g**enome project gene identifier (118).
[b]Fold change for mCherry-Pdr802 compared to WT.
[c]Log_2 fold change for *pdr802* compared to WT.

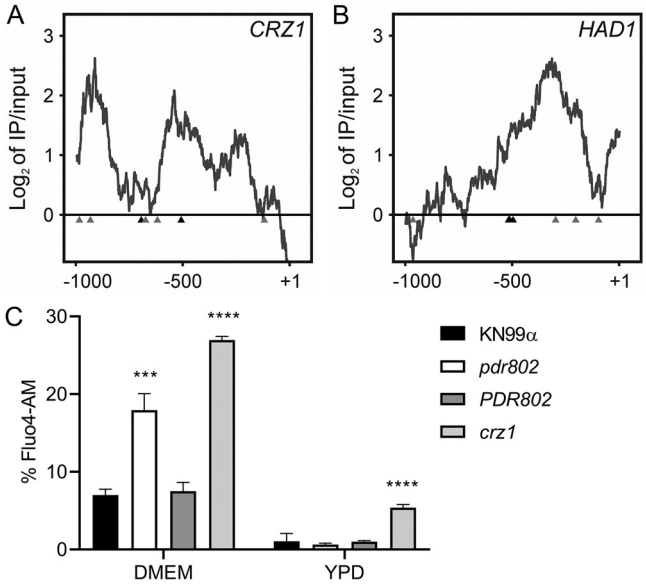

FIG 8 Pdr802 participates in calcineurin signaling. (A and B) Interactions of Pdr802 with upstream regions of the indicated genes. The ratios (log_2) of reads from immunoprecipitated (IP) DNA to input DNA were calculated for 1,000 bp upstream of the first coding nucleotide (+1); shown is the difference in these values between tagged and untagged strains. Black triangles, complete Pdr802 DNA-binding motifs (Fig. S7C); gray triangles, partial motifs. (C) Intracellular calcium measurement by flow cytometry using Fluo-4AM. Each column shows the mean and standard deviation of three biological replicates. ***, $P < 0.001$, and ****, $P < 0.0001$, compared to KN99α by one-way ANOVA with a *post hoc* Dunnett test.

(e.g., the kinases Fab1, Kin1, and Gut1 and the TF Hlh1) (Table 2). Deletion of *FAB1*, *KIN1*, or *HLH1* impaired urease activity in *C. neoformans*, while *GUT1* disruption induced it (52, 80).

Above, we document the role of Pdr802 in capsule synthesis, which is dramatically upregulated in the host environment in general and is further increased in cells lacking this TF. We found that Pdr802 is a positive regulator of multiple genes that have been implicated in reducing cryptococcal capsule thickness. These include the kinases Arg2, Iks1, and Ksp1; the TF Fzc51; and the phosphodiesterase Pde2 (Table 2). Notably, null mutants for those genes are hypercapsular, similar to *pdr802* cells (52, 80, 90). Pdr802 is a negative regulator of the TF Bzp4, which, as mentioned above, positively regulates capsule (Table 2) (52).

Pdr802 regulates calcineurin target genes. The calcineurin signaling pathway is activated by calcium and governs stress response and virulence in *C. neoformans* (91–93). One major mediator of calcineurin signaling is the transcription factor Crz1 mentioned above, which is highly responsive to temperature and influences cryptococcal virulence (57, 62). Upon intracellular calcium influx, calcineurin dephosphorylates Crz1, which then translocates to the nucleus and regulates gene expression (57, 63). We found that Pdr802 binds the *CRZ1* gene promoter and positively regulates its expression (Fig. 8A, Table 2, and Data Set S2, sheet 3). Pdr802 also binds and regulates five other genes whose products are dephosphorylated by calcineurin; these include the phosphatase Had1, which is important for cryptococcal cell wall remodeling and virulence (Fig. 8B, Table 2, and Data Set S2, sheet 3) (63, 94).

Because Crz1 helps maintain normal cryptococcal Ca^{2+} concentrations through the regulation of calcium transporters (57), we wondered about the intracellular calcium levels in *pdr802* cells. We found that indeed, after 24 h of growth in DMEM, the level of cytosolic calcium in the mutant significantly exceeded that of WT or complemented strains (Fig. 8C). It was still, however, below that of a *crz1*-null mutant, supporting the idea that Pdr802 is not the sole regulator of *CRZ1* expression. Notably, *PDR802* deletion

had no effect in rich medium (YPD), which reinforces our hypothesis that Pdr802 acts primarily under host-like conditions. To further explore the relationship of Pdr802 and calcineurin, we compared published gene expression profiles of a calcineurin mutant (57) to our DTO data set. Of the 393 genes that are differently expressed in the calcineurin mutant under thermal stress, 26 are regulated by Pdr802 (Data Set S2, sheet 4).

DISCUSSION

We have shown that Pdr802 is a potent regulator of cryptococcal responses to the host environment. In this context, it influences the formation of capsule and Titan cells as well as cellular responses to temperature and oxidative stress, acts as a downstream effector of calcineurin, and modulates calcium availability. The last function is likely achieved through its positive regulation of the transcription factor Crz1, which in turn modulates the calcium transporters Pmc1 and Vcx1 (57). Since calcium ion is a major second messenger in eukaryotic cells, its accumulation in *pdr802* cells affects multiple processes central to host interactions, including stress responses, cell wall integrity, and capsule size (61, 62, 92, 95, 96).

C. neoformans dissemination to the brain is the main driver of patient mortality (2). We found that dissemination of *pdr802* cells is significantly impaired, although they do occasionally reach the brain. These observations can be explained by a combination of factors. First, the limited accumulation of the *pdr802* mutant in the lungs, due to factors summarized above, may directly affect dissemination (97). Second, this strain survives poorly in mouse serum, as demonstrated directly by our culture experiments and indirectly by our inability to detect it in the blood of infected mice, even 75 days after infection. The latter might occur because the cells do not reach the blood or because they are rapidly eliminated, consistent with previous observations (98). Third, the thick capsules of the *pdr802* mutant reduce its ability to reach the brain. This is true whether fungal entry occurs directly, by the movement of free fungi across the BBB, or indirectly, via a Trojan horse mechanism that requires macrophage uptake (99); such uptake is impeded by enlarged capsules, independent of cell size (31). Fourth, calcium imbalance directly affects cryptococcal transmigration (100). Finally, *pdr802* cells show reduced expression of genes required for urease activity, which promotes *C. neoformans* dissemination to the CNS (11, 12, 100). Interestingly, despite all of these obstacles to dissemination, mutant cells that do reach the brain are able to proliferate to wild-type levels.

Titan cells are a robust and persistent morphotype of *C. neoformans* that contribute to yeast virulence (45). We showed that cells lacking Pdr802 demonstrate increased formation of Titan cells *in vivo* and *in vitro*, suggesting that this TF is a novel repressor of this process. Although Titan cells enhance aspects of cryptococcal pathogenesis (19, 101), their overproduction negatively impacts dissemination to the brain due to their resistance to phagocytosis by macrophages (19, 45) and decreased penetration of biological barriers (19).

Our combined analysis of DNA binding and gene expression data allows us to understand the increase in Titan cell formation that occurs upon deletion of *PDR802*. Under host-like conditions, Pdr802 positively regulates Pqp1, Opt1, and Liv3, all key proteins in the cryptococcal quorum sensing pathway, which represses Titan cell formation (47, 48). In the absence of this TF, quorum sensing is impaired, a situation known to increase Titan cell formation. Pdr802 may also indirectly regulate Titan cell formation by regulating other TFs that impact this process, such as Zfc3 (Cqs2) and Stb4.

We know that capsule, a key virulence factor, is typically highly induced in the host or under host-like conditions (102). Our studies *in vitro*, *ex vivo*, and *in vivo* show that Pdr802 normally reins in this process. This likely occurs via a combination of Pdr802's repression of the TF Bzp4, which positively regulates capsule size, and the induction of other factors (e.g., the TF Fzc1, the phosphodiesterase Pde2, and the kinases Ksp1, Arg2, and Iks1) that negatively regulate capsule size (52, 80, 90).

Overall, we found that Pdr802 influences key cryptococcal phenotypes that

influence virulence, including quorum sensing, stress responses, Titan cell formation, and capsule production (Fig. 9). We have further identified multiple genes that are central in these processes and are directly regulated by Pdr802. Some of these targets are also regulated by calcineurin (e.g., Had1 and Crz1) or by another important TF, Gat201 (e.g., Opt1, Liv3, and Zfc3) (60, 74, 75). Finally, the expression of *PDR802* itself is regulated by the TFs Gat201 and Hob1 (67, 75). The cross talk between all of these regulatory mechanisms remains to be dissected. Nonetheless, it is evident that Pdr802 is critical for both survival in the lung and dissemination to the brain, thus explaining its role in cryptococcal virulence.

MATERIALS AND METHODS

Strain construction and cell growth. We previously reported the *PDR802* deletion mutant (*pdr802*) in the KN99α strain background (103) that was used in this work (39). Complementation of this mutant with the wild-type gene at the native locus (*PDR802*) and construction of a strain that expresses Pdr802 with N-terminal mCherry (mCherry-Pdr802) are detailed in the supplemental methods. For all studies, *C. neoformans* strains were inoculated from single colonies into YPD medium (2% [wt/vol] dextrose, 2% [wt/vol] Bacto peptone, and 1% [wt/vol] yeast extract in double-distilled water [ddH_2O]) and grown overnight at 30°C with shaking at 230 rpm before further handling as detailed below. To assess viability during growth in tissue culture medium, overnight cultures were washed with phosphate-buffered saline (PBS), diluted to 10^6 cells/ml in DMEM (Sigma; D6429), plated (1 ml/well) in triplicate in 24-well plates, and incubated at 37°C and 5% CO_2. At the indicated times, cells were mixed thoroughly, diluted in PBS, and plated on YPD agar (YPD medium, 2% agar [wt/vol]) for assessment of CFU. To assess viability during growth in mouse serum, mouse blood was collected as described below in "Animal experiments"; YPD-grown cryptococcal cells were incubated in 100 μl of serum in 96-well plates for 24 h at 37°C and 5% CO_2, and CFU were counted as described above.

Animal experiments. All animal protocols were approved by the Washington University Institutional Animal Care and Use Committee (reference 20170131) or Comissão de Ética no Uso de Animais (CEUA) (reference 30936), and care was taken to minimize handling and discomfort. For survival studies, groups of five 4- to 6-week-old female C57BL/6 mice (The Jackson Laboratory) were anesthetized by subcutaneous injection of 1.20 mg ketamine and 0.24 mg xylazine in 120 μl sterile water and intranasally infected with 5×10^4 cryptococcal cells. The mice were monitored and humanely sacrificed when their weight decreased to below 80% of initial weight or if they showed signs of disease, at which point organ burden was assessed. The lungs and brains were harvested, homogenized, diluted, and plated on YPD agar. The resulting CFU were enumerated, and survival differences were assessed by Kaplan-Meier analysis.

For timed organ burden studies, *C. neoformans* overnight cultures were centrifuged (1,000 $\times$ *g* for 3 min), washed with sterile PBS, and resuspended in PBS to 1×10^6 cells/ml. Groups of three 4- to 6-week-old female C57BL/6 mice (Centro Multidisciplinar para Investigação Biológica na Área da Ciência em Animais de Laboratório [CEMIB]) were anesthetized as described above, intranasally infected with 5×10^4 cryptococcal cells, and monitored as described above. At set time points post-infection (see above), mice were sacrificed and fungal burden was assessed from organs (as described above) or blood (obtained by cardiac puncture). Organ burden was analyzed by Kruskal-Wallis test with Dunn's multiple comparison *post hoc* test for each day post-infection.

To assess cryptococcal viability in mouse serum, 6 BALB/c mice were anesthetized with isoflurane and blood was collected from the retro-orbital space using a sterile capillary tube. Collected blood was incubated at 37°C for 30 min, and serum was isolated by centrifugation at 1,000 $\times$ *g* for 15 min and then heat inactivated at 56°C for 30 min.

Capsule analysis. To qualitatively assess capsule thickness, strains were grown on YPD medium for 16 h and washed with PBS, and 10^3 cells were incubated in mouse serum for 24 h at 37°C and 5% CO_2. After incubation, cells were fixed in 4% paraformaldehyde and washed three times with PBS. *C. neoformans* cells were placed on glass slides and mixed with similar volumes of India ink, and the capsule was measured as previously described (104).

For population-level capsule measurement, *C. neoformans* strains were grown overnight in YPD, washed with PBS, and diluted to 10^6 cells/ml in DMEM. Aliquots (150 μl) were then plated in quadruplicate in the middle 32 wells of a poly-L-lysine-coated 96-well plate (Fisher; 655936) and incubated at 37°C and 5% CO_2. After 24 h, the cells were washed with PBS and incubated with 150 μl of a staining mixture (100 μg/ml calcofluor white to stain cell walls, 50 μg/ml of the anticapsular monoclonal antibody 302 conjugated to Alexa Fluor 488 [Molecular Probes], and 1.5% goat serum in PBS) for 30 min at room temperature in the dark. The cells were washed again with PBS, fixed with 4% formaldehyde for 10 min at room temperature, and washed with PBS, and each well was refilled with 150 μl PBS. The cells were imaged using a BioTek Cytation 3 imager, which automatically collected 100 images per well in a grid pattern at the well center. Image files were prepared for analysis with GE Healthcare IN Cell Translator and assembled into .xdce image stacks for analysis with GE Healthcare IN Cell Developer Toolbox 1.9. Cell wall and capsule images were first filtered to remove background noise and border objects, and then cells were identified using shape-based object segmentation (3-pixel kernel, 50% sensitivity) followed by watershed clump breaking to prevent apparent connectivity caused by incomplete segmentation. Target linking was performed to assign each cell wall object to one capsule object based on known 1:1 pairing and location, generating a target set. Capsule and cell wall object diameters were calculated

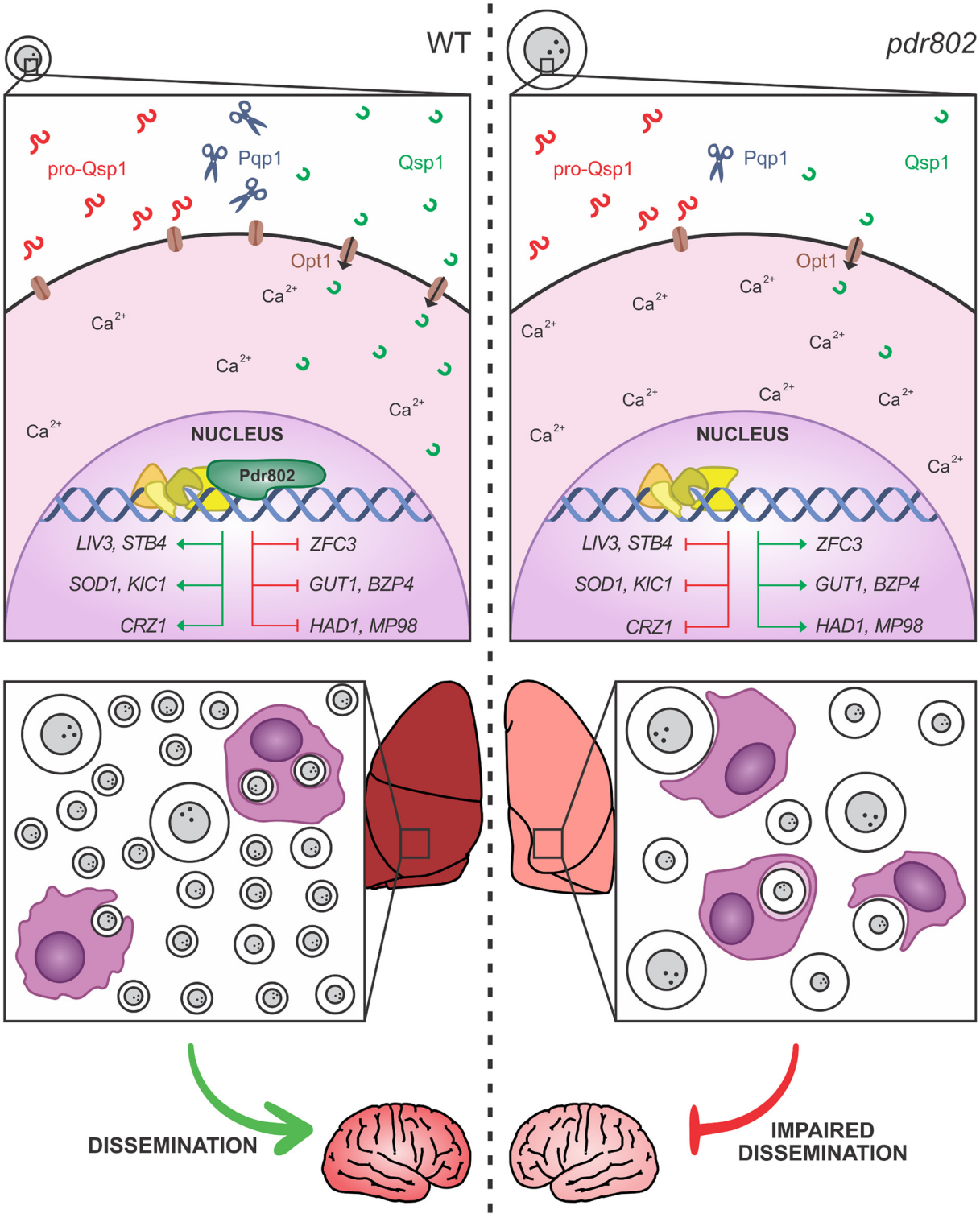

FIG 9 Pdr802 mode of action. (Left) When wild-type *C. neoformans* enters a host, *PDR802* expression is induced and Pdr802 positively regulates elements of the quorum sensing pathway (described in the text) as well as expression of TFs implicated in this pathway (*LIV3*), Titan cell production (*ZFC3*), and brain infectivity (*STB4*). At the same time, Pdr802 regulates two calcineurin targets (*CRZ1* and *HAD1*) and a variety of other genes (see the text). Shown are a few examples of genes involved in the response to oxidative stress (*SOD1*), growth at 37°C (*KIC1*), urease activity (*GUT1*), capsule production (*BZP4*), and cell wall remodeling (*MP98*). (Right) In the absence of these regulatory changes, *pdr802* cells are poorly equipped to survive the stress of the host environment and are subject to increased intracellular calcium levels, dysregulation of capsule production, and impaired stress resistance. As a result, the cryptococcal population in the lung is smaller and is enriched in Titan cells and hypercapsular cells of normal size, both of which demonstrate reduced phagocytosis by host cells and impaired ability to cross biological barriers; these defects reduce dissemination to the central nervous system.

for each target set (hundreds to thousands per well), and the difference between measurements in each pair was defined as the capsule thickness. Data were normalized by the difference in capsule thickness between uninduced and induced WT cells, which were included in each experiment, and compared to data for hypercapsular (*pkr1*) (39) and hypocapsular (*ada2*) (105) control strains in each experiment. Capsule sizes were compared by one-way analysis of variance (ANOVA) with Dunnett's multiple comparison *post hoc* test.

To measure capsule thickness of cryptococcal cells grown in the lungs of infected mice, lung homogenates were filtered through a cell strainer with 40-μm pores using a syringe plunger, fixed in 3.7% formaldehyde, and used for India ink staining and measurement as described above. For the visualization of KN99α and *PDR802* cells from mouse lungs after 18 days of infection, the tissue was treated with 50 μg/ml DNase I for 30 min at 37°C.

GXM immunoblotting was conducted as previously described (71). Briefly, 10^6 cells/ml were grown in DMEM for 24 and 48 h. Culture supernatant fractions were then resolved by gel electrophoresis on 0.6% agarose, transferred onto nylon membranes, and probed with 1 μg/ml anti-GXM antibody 302.

Phenotypic assays. For stress plates, cryptococcal cells were grown overnight in YPD, washed with PBS, and diluted to 10^7 cells/ml in PBS. Aliquots (3 μl) of 10-fold serial dilutions were spotted on YPD or YNB agar supplemented with various stressors (sorbitol, NaCl, $CaCl_2$, LiCl, Congo red, calcofluor white, caffeine, SDS, $NaNO_2$, H_2O_2, and ethanol) at the concentrations indicated in the figures. Melanization was tested on plates made by mixing 10 ml of 2× minimal medium (2 g/liter L-asparagine, 1 g/liter $MgSO_4$ s^2 $7H_2O$, 6 g/liter KH_2PO_4, 2 g/liter thiamine, 2 mM L-3,4-dihydroxyphenylalanine [L-DOPA]; 0.1% dextrose was added for melanization induction, and 0.5% was added for melanization inhibition) with 10 ml of 2% agar-water per plate. A control strain lacking the ability to melanize was used as a control (*lac1*) (88). For the solid urease assay, 10 μl of a 10^7 cells/ml suspension in water was plated on Christensen's urea solid medium (1 g/liter peptone, 1 g/liter dextrose, 5 g/liter NaCl, 0.8 g/liter KH_2PO_4, 1.2 g/liter Na_2HPO_4, 0.012 g/liter phenol red and 15 g/liter agar; pH 6.8). Plates were incubated at 30°C or 37°C.

Titan cells. Titan cell induction was performed in 1× PBS supplemented with 10% heat-inactivated fetal calf serum (FCS) for 72 h at 37°C and 5% CO_2 as recently described (49) and quantified by flow cytometry as previously reported (47, 48). For analysis of DNA content, cells were treated as previously described (47) with a few modifications. Briefly, cultures were fixed with 70% ethanol for 1 h at 24°C and then overnight at 4°C, washed twice with PBS, and then treated with propidium iodide (50 μg/ml) and RNase A (0.5 mg/ml) in PBS for 2 h at 30°C with agitation. Quantification was performed using a FACS ARIA III (BD) cytometer with analysis on the Cytobank platform. A total of 20,000 events were recorded, and doublets were filtered out using comparisons of forward-scatter width (FSC-W) versus forward-scatter height (FSC-H) to exclude events with high FSC-W and FSC-H. To define the 1C and 2C gates, cells were grown in yeast nitrogen base (YNB) (24 h, 30°C, 150 rpm) without or with 80 μg/ml benomyl, which traps cells in 2C, as recently reported (106).

Phagocytosis. J774.16 cells were prepared for uptake experiments by seeding (10^5 cells/well) in a 96-well plate and incubating in DMEM supplemented with 10% fetal bovine serum (FBS) at 37°C and 5% CO_2 for 24 h. *C. neoformans* cells were prepared for uptake experiments by inoculating an overnight culture in YPD into either DMEM or Titan cell induction medium (49) and growing at 37°C and 5% CO_2 for 24 or 72 h, respectively. To initiate the study, cryptococcal cells were washed with PBS and opsonized with anti-capsular antibody 18B7 (1 μg/ml) for 1 h at 37°C, while macrophages were activated with 50 nM phorbol myristate acetate (PMA) for 1 h at 37°C and 5% CO_2; 10^6 cryptococcal cells were then incubated with the macrophages for 2 h at 37°C and 5% CO_2. The wells were then washed three times with warm PBS, and the macrophages were lysed with 0.1% Triton in PBS and plated for CFU enumeration as described above. Fold change in numbers of CFU was assessed by comparison to the CFU of opsonized cells. One-way ANOVA with Dunnett's multiple-comparison *post hoc* test was used to compare phagocytosis of *pdr802* and *PDR802* strains with that of KN99α.

Chromatin immunoprecipitation. ChIP studies were performed as previously described (39, 105). Briefly, wild type and N-terminal-mCherry-Pdr802 strains were cultivated in DMEM for 24 h at 37°C and 5% CO_2. The cells were then fixed with formaldehyde and lysed by mechanical bead-beating, and the cell debris was removed by centrifugation. The supernatant fraction was sheared by sonication and centrifuged, and an aliquot was reserved as "input." The remaining material was incubated with rabbit IgG anti-mCherry antibody (Abcam; ab213511) tethered to protein A Sepharose (IP) or Sepharose alone overnight at 4°C. The beads were then washed, incubated at 65°C to reverse DNA-DNA and DNA-protein cross-links, and the DNA was recovered by phenol-chloroform-isoamyl alcohol (25:24:1) extraction, ethanol precipitation, and resuspension in nuclease-free water.

Samples were submitted to the Washington University Genome Technology Access Center for library preparation, and DNA samples were sequenced using the Illumina NextSeq platform. The first replicate was sequenced using paired-end 2 × 75-bp reads, and replicates 2 and 3 were sequenced using single-end 75-bp reads; the minimum coverage obtained was ~16×. The quality of the reads was evaluated by FastQC (107). Fastq files were aligned to the KN99 genome (108) using NextGenMap 0.5.3 (109). SAM files were converted to bam, reads were sorted and indexed, and read duplicates were removed from the final bam files using SAMtools (110). SAMtools was also used to filter out reads with a mapping quality of less than 20 phreds to guarantee single alignment of the reads. Peaks were called using MACS2 (2.1.1.20160309) (111), filtered by size (maximum threshold of 5 kb and no minimum), and annotated using Homer 4.8 (112). The significant peaks were chosen using the cutoff of fold enrichment above 2 and an adjusted *P* value of <0.05, and read coverage of each peak was obtained using SAMtools (110). Pdr802 binding motifs were identified using DREME (76); partial motifs were defined as at least 5 consecutive base pairs of the motif.

RNA-Seq and DTO. RNA from wild-type and *pdr802* cells grown for 24 h in DMEM (37°C, 5% CO_2) was isolated and sequenced as previously described (39). Briefly, cDNA samples were sequenced using the Illumina NextSeq platform for paired-end 2 × 75 bp reads and read quality was evaluated by FastQC (107). Fastq files were aligned to the KN99 genome (108) using NovoAlign (113), SAM files were converted to bam, reads were sorted and indexed, and read duplicates were removed from the final bam files using SAMtools (110). The number of reads mapped per gene was calculated using HTSeq (114), and differential gene expression was analyzed with DESeq2 (115), using the independent hypothesis weighting (IHW) package to calculate the adjusted *P* values (116). Dual-threshold optimization (DTO) analysis was performed as recently described (77). This is a method for simultaneously finding the best thresholds for significance in a TF binding location data set (e.g., ChIP) and a TF perturbation response data set (e.g., RNA-Seq of a TF mutant). It works by trying out all pairs of thresholds for the two data sets, picking the pair that minimizes the probability of the overlap between the bound and responsive gene sets occurring by chance under a null model, and testing the significance of the overlap by comparison to randomly permuted data. Our application of DTO to our ChIP and RNA-Seq data yielded 1,455 bound genes, 5,186 responsive genes, and 1,167 genes that were both bound and responsive. Based on DTO, Pdr802 has an acceptable convergence from binding and perturbation, with a *P* value of <0.01 from the random permutation test and minimum expected false discovery rate (FDR) less than or equal to 20% at 80% sensitivity. In addition to requiring a statistically significant overlap between the ChIP-Seq and RNA-Seq gene sets, we filtered out any genes for which traditional differential expression analysis yielded an adjusted *P* value of ≤ 0.15 or absolute fold change of ≥ 0.3, leaving 380 bound targets.

Intracellular calcium measurement. To measure intracellular free Ca^{2+}, yeast cells were cultured overnight in YPD at 30°C with shaking, washed three times with deionized water, diluted to 10^6 cells/ml in DMEM (Sigma; D6429), plated (1 ml/well) in triplicate in 24-well plates, and incubated at 37°C and 5% CO_2 for 24 h. At the indicated times, cells were mixed thoroughly, diluted in PBS containing 2 μM Fluo4-AM (Thermo Fisher), incubated at 30°C for 30 min, and analyzed using flow cytometry. The overnight culture was used as a control and treated as above.

Data availability. ChIP-Seq and RNA-Seq data files are available at the NCBI Gene Expression Omnibus under accession numbers GSE153134 and GSE162851, respectively.

SUPPLEMENTAL MATERIAL

Supplemental material is available online only.

DATA SET S1, XLSX file, 2.5 MB.

DATA SET S2, XLSX file, 0.02 MB.

TEXT S1, PDF file, 0.04 MB.

FIG S1, PDF file, 0.5 MB.

FIG S2, PDF file, 0.9 MB.

FIG S3, PDF file, 0.8 MB.

FIG S4, PDF file, 0.6 MB.

FIG S5, PDF file, 0.7 MB.

FIG S6, PDF file, 0.7 MB.

FIG S7, PDF file, 1 MB.

ACKNOWLEDGMENTS

We appreciate helpful discussions with Charley Christian Staats, Augusto Schrank, and members of the Doering, Kmetzsch and Brent labs. We are grateful for assistance from Thomas Hurtaux, Eamim Squizani, and Julia Sperotto with mouse experiments; Guohua Chen with spotting assays; Jessica Plaggenberg with library preparation and sequencing; Chase Mateusiak with RNA-Seq data analysis; and Sandeep Acharya for performing the DTO analysis. We thank Marilene Henning Vainstein and her lab for providing support with *in vivo* experiments. We also thank Liza Miller for comments on the manuscript, Arturo Casadevall for providing the antibody anti-GXM (18B7), and Pedro Brum for the assistance with the DNA analysis of Titan cells on the FACS ARIA III (BD) cytometer from the Department of Genetics of the Universidade Federal do Rio Grande do Sul.

These studies were supported by National Institutes of Health grant AI087794 to T.L.D. and M.R.B.; National Institutes of Health grants AI136688 and AI140979 to T.L.D.; and grants from Coordenação de Aperfeiçoamento de Pessoal de Nível Superior (CAPES, Brazil), Conselho Nacional de Desenvolvimento Científico e Tecnológico (CNPq, Brazil; grant number 310510/2018-0), and Fundação de Amparo à Pesquisa do Estado do Rio Grande do Sul (FAPERGS, Brazil) to L.K. CAPES fully supported J.C.V.R. during her studies in Brazil; her studies in the United States were partially supported by this source

(Advanced Network of Computational Biology, RABICÓ, Biocomputational Grant 23038.010041/2013-13).

Conceived and designed experiments: J.C.V.R., D.P.A., A.L.C., M.R.B., L.K., and T.L.D.; Performed experiments: J.C.V.R., D.P.A., H.M., H.B., and A.L.C; Analyzed data: J.C.V.R., D.P.A., A.L.C., M.R.B., L.K., and T.L.D.; Contributed reagents and materials: M.R.B., L.K., and T.L.D.; Drafted the paper: J.C.V.R, L.K., and T.L.D.; Revised the paper: J.C.V.R., D.P.A., M.R.B., L.K., and T.L.D.

We declare no competing financial interests.

REFERENCES

1. Kwon-Chung KJ, Fraser JA, Doering TL, Wang ZA, Janbon G, Idnurm A, Bahn YS. 2014. *Cryptococcus neoformans* and *Cryptococcus gattii*, the etiologic agents of cryptococcosis. Cold Spring Harb Perspect Med 4: a019760. https://doi.org/10.1101/cshperspect.a019760.
2. Rajasingham R, Smith RM, Park BJ, Jarvis JN, Govender NP, Chiller TM, Denning DW, Loyse A, Boulware DR. 2017. Global burden of disease of HIV-associated cryptococcal meningitis: an updated analysis. Lancet Infect Dis 17:873–881. https://doi.org/10.1016/S1473-3099(17)30243-8.
3. Ballou ER, Johnston SA. 2017. The cause and effect of *Cryptococcus* interactions with the host. Curr Opin Microbiol 40:88–94. https://doi.org/10.1016/j.mib.2017.10.012.
4. Sabiiti W, May RC. 2012. Mechanisms of infection by the human fungal pathogen *Cryptococcus neoformans*. Future Microbiol 7:1297–1313. https://doi.org/10.2217/fmb.12.102.
5. Garcia-Hermoso D, Janbon G, Dromer F. 1999. Epidemiological evidence for dormant *Cryptococcus neoformans* Infection. J Clin Microbiol 37:3204–3209. https://doi.org/10.1128/JCM.37.10.3204-3209.1999.
6. Chang YC, Stins MF, McCaffery MJ, Miller GF, Pare DR, Dam T, Paul-Satyaseela M, Kim KS, Kwon-Chung KJ, Paul-Satyasee M. 2004. Cryptococcal yeast cells invade the central nervous system via transcellular penetration of the blood-brain barrier. Infect Immun 72:4985–4995. https://doi.org/10.1128/IAI.72.9.4985-4995.2004.
7. Huang S-H, Long M, Wu C-H, Kwon-Chung KJ, Chang YC, Chi F, Lee S, Jong A. 2011. Invasion of *Cryptococcus neoformans* into human brain microvascular endothelial cells is mediated through the lipid rafts-endocytic pathway via the dual specificity tyrosine phosphorylation-regulated kinase 3 (DYRK3). J Biol Chem 286:34761–34769. https://doi.org/10.1074/jbc.M111.219378.
8. Jong A, Wu C-H, Shackleford GM, Kwon-Chung KJ, Chang YC, Chen H-M, Ouyang Y, Huang S-H. 2008. Involvement of human CD44 during *Cryptococcus neoformans* infection of brain microvascular endothelial cells. Cell Microbiol 10:1313–1326. https://doi.org/10.1111/j.1462-5822.2008.01128.x.
9. Maruvada R, Zhu L, Pearce D, Zheng Y, Perfect J, Kwon-Chung KJ, Kim KS. 2012. *Cryptococcus neoformans* phospholipase B1 activates host cell Rac1 for traversal across the blood-brain barrier. Cell Microbiol 14:1544–1553. https://doi.org/10.1111/j.1462-5822.2012.01819.x.
10. Chen SHM, Stins MF, Huang S-H, Chen YH, Kwon-Chung KJ, Chang Y, Kim KS, Suzuki K, Jong AY. 2003. *Cryptococcus neoformans* induces alterations in the cytoskeleton of human brain microvascular endothelial cells. J Med Microbiol 52:961–970. https://doi.org/10.1099/jmm.0.05230-0.
11. Olszewski MA, Noverr MC, Chen G-H, Toews GB, Cox GM, Perfect JR, Huffnagle GB. 2004. Urease expression by *Cryptococcus neoformans* promotes microvascular sequestration, thereby enhancing central nervous system invasion. Am J Pathol 164:1761–1771. https://doi.org/10.1016/S0002-9440(10)63734-0.
12. Shi M, Li SS, Zheng C, Jones GJ, Kim KS, Zhou H, Kubes P, Mody CH. 2010. Real-time imaging of trapping and urease-dependent transmigration of *Cryptococcus neoformans* in mouse brain. J Clin Invest 120:1683–1693. https://doi.org/10.1172/JCI41963.
13. Santiago-Tirado FH, Onken MD, Cooper JA, Klein RS, Doering TL. 2017. Trojan horse transit contributes to blood-brain barrier crossing of a eukaryotic pathogen. mBio 8:e02183-16. https://doi.org/10.1128/mBio.02183-16.
14. Jarvis JN, Bicanic T, Loyse A, Namarika D, Jackson A, Nussbaum JC, Longley N, Muzoora C, Phulusa J, Taseera K, Kanyembe C, Wilson D, Hosseinipour MC, Brouwer AE, Limmathurotsakul D, White N, van der Horst C, Wood R, Meintjes G, Bradley J, Jaffar S, Harrison T. 2014. Determinants of mortality in a combined cohort of 501 patients with HIV-associated cryptococcal meningitis: implications for improving outcomes. Clin Infect Dis 58:736–745. https://doi.org/10.1093/cid/cit794.
15. Perfect JR, Dismukes WE, Dromer F, Goldman DL, Graybill JR, Hamill RJ, Harrison TS, Larsen RA, Lortholary O, Nguyen M-H, Pappas PG, Powderly WG, Singh N, Sobel JD, Sorrell TC, TCS. 2010. Clinical practice guidelines for the management of cryptococcal disease: 2010 update by the Infectious Diseases Society of America. Clin Infect Dis 50:291–322. https://doi.org/10.1086/649858.
16. Nosanchuk JD, Casadevall A. 2003. The contribution of melanin to microbial pathogenesis. Cell Microbiol 5:203–223. https://doi.org/10.1046/j.1462-5814.2003.00268.x.
17. Singh A, Panting RJ, Varma A, Saijo T, Waldron KJ, Jong A, Ngamskulrungroj P, Chang YC, Rutherford JC, Kwon-Chung KJ. 2013. Factors required for activation of urease as a virulence determinant in *Cryptococcus neoformans*. mBio 4: e00220-13. https://doi.org/10.1128/mBio.00220-13.
18. Chang YC, Kwon-Chung KJ. 1994. Complementation of a capsule-deficient mutation of *Cryptococcus neoformans* restores its virulence. Mol Cell Biol 14:4912–4919. https://doi.org/10.1128/mcb.14.7.4912.
19. Okagaki LH, Strain AK, Nielsen JN, Charlier C, Baltes NJ, Chrétien F, Heitman J, Dromer F, Nielsen K. 2010. Cryptococcal cell morphology affects host cell interactions and pathogenicity. PLoS Pathog 6: e1000953. https://doi.org/10.1371/journal.ppat.1000953.
20. Zaragoza O, Nielsen K. 2013. Titan cells in *Cryptococcus neoformans*: cells with a giant impact. Curr Opin Microbiol 16:409–413. https://doi.org/10.1016/j.mib.2013.03.006.
21. Wang Y, Aisen P, Casadevall A. 1995. *Cryptococcus neoformans* melanin and virulence: mechanism of action. Infect Immun 63:3131–3136. https://doi.org/10.1128/IAI.63.8.3131-3136.1995.
22. Mednick AJ, Nosanchuk JD, Casadevall A. 2005. Melanization of *Cryptococcus neoformans* affects lung inflammatory responses during cryptococcal infection. Infect Immun 73:2012–2019. https://doi.org/10.1128/IAI.73.4.2012-2019.2005.
23. Wang Y, Casadevall A. 1994. Susceptibility of melanized and nonmelanized *Cryptococcus neoformans* to nitrogen- and oxygen-derived oxidants. Infect Immun 62:3004–3007. https://doi.org/10.1128/IAI.62.7.3004-3007.1994.
24. Doering TL, Nosanchuk JD, Roberts WK, Casadevall A. 1999. Melanin as a potential cryptococcal defence against microbicidal proteins. Med Mycol 37:175–181. https://doi.org/10.1046/j.1365-280X.1999.00218.x.
25. Agustinho DP, Nosanchuk JD. 2017. Functions of fungal melanins: reference module in life sciences. Elsevier, New York, NY.
26. Cox GM, Mukherjee J, Cole GT, Casadevall A, Perfect JR. 2000. Urease as a virulence factor in experimental cryptococcosis. Infect Immun 68:443–448. https://doi.org/10.1128/iai.68.2.443-448.2000.
27. Bose I, Reese AJ, Ory JJ, Janbon G, Doering TL. 2003. A yeast under cover: the capsule of *Cryptococcus neoformans*. Eukaryot Cell 2:655–663. https://doi.org/10.1128/ec.2.4.655-663.2003.
28. Wang ZA, Li LX, Doering TL. 2018. Unraveling synthesis of the cryptococcal cell wall and capsule. Glycobiology 28:719–730. https://doi.org/10.1093/glycob/cwy030.
29. Agustinho DP, Miller LC, Li LX, Doering TL. 2018. Peeling the onion: the outer layers of *Cryptococcus neoformans*. Mem Inst Oswaldo Cruz 113: e180040. https://doi.org/10.1590/0074-02760180040.
30. Bulmer GS, Sans MD. 1967. *Cryptococcus neoformans*. II. Phagocytosis by human leukocytes. J Bacteriol 94:1480–1483. https://doi.org/10.1128/JB.94.5.1480-1483.1967.
31. Bulmer GS, Sans MD. 1968. *Cryptococcus neoformans*. J Bacteriol 95:5–8. https://doi.org/10.1128/JB.95.1.5-8.1968.
32. Tacker JR, Farhi F, Bulmer GS. 1972. Intracellular fate of *Cryptococcus neoformans*. Infect Immun 6:162–167. https://doi.org/10.1128/IAI.6.2.162-167.1972.

33. Monari C, Bistoni F, Vecchiarelli A. 2006. Glucuronoxylomannan exhibits potent immunosuppressive properties. FEMS Yeast Res 6:537–542. https://doi.org/10.1111/j.1567-1364.2006.00072.x.
34. Hayes JB, Sircy LM, Heusinkveld LE, Ding W, Leander RN, McClelland EE, Nelson DE. 2016. Modulation of macrophage inflammatory nuclear factor κB (NF-κB) signaling by intracellular *Cryptococcus neoformans*. J Biol Chem 291:15614–15627. https://doi.org/10.1074/jbc.M116.738187.
35. Fonseca FL, Nohara LL, Cordero RJB, Frases S, Casadevall A, Almeida IC, Nimrichter L, Rodrigues ML. 2010. Immunomodulatory effects of serotype B glucuronoxylomannan from *Cryptococcus gattii* correlate with polysaccharide diameter. Infect Immun 78:3861–3870. https://doi.org/10.1128/IAI.00111-10.
36. Garcia-Hermoso D, Dromer F, Janbon G. 2004. *Cryptococcus neoformans* capsule structure evolution *in vitro* and during murine infection. Infect Immun 72:3359–3365. https://doi.org/10.1128/IAI.72.6.3359-3365.2004.
37. Guimarães AJ, Frases S, Cordero RJB, Nimrichter L, Casadevall A, Nosanchuk JD. 2010. *Cryptococcus neoformans* responds to mannitol by increasing capsule size *in vitro* and *in vivo*. Cell Microbiol 12:740–753. https://doi.org/10.1111/j.1462-5822.2010.01430.x.
38. Cordero RJB, Pontes B, Guimarães AJ, Martinez LR, Rivera J, Fries BC, Nimrichter L, Rodrigues ML, Viana NB, Casadevall A. 2011. Chronological aging is associated with biophysical and chemical changes in the capsule of *Cryptococcus neoformans*. Infect Immun 79:4990–5000. https://doi.org/10.1128/IAI.05789-11.
39. Maier EJ, Haynes BC, Gish SR, Wang ZA, Skowyra ML, Marulli AL, Doering TL, Brent MR. 2015. Model-driven mapping of transcriptional networks reveals the circuitry and dynamics of virulence regulation. Genome Res 25:690–700. https://doi.org/10.1101/gr.184101.114.
40. Santos JRA, Holanda RA, Frases S, Bravim M, Araujo GDS, Santos PC, Costa MC, Ribeiro MJA, Ferreira GF, Baltazar LM, Miranda AS, Oliveira DB, Santos CMA, Fontes ACL, Gouveia LF, Resende-Stoianoff MA, Abrahão JS, Teixeira AL, Paixão TA, Souza DG, Santos DA. 2014. Fluconazole alters the polysaccharide capsule of *Cryptococcus gattii* and leads to distinct behaviors in murine cryptococcosis. PLoS One 9:e112669. https://doi.org/10.1371/journal.pone.0112669.
41. Silveira CP, Piffer AC, Kmetzsch L, Fonseca FL, Soares DA, Staats CC, Rodrigues ML, Schrank A, Vainstein MH. 2013. The heat shock protein (Hsp) 70 of *Cryptococcus neoformans* is associated with the fungal cell surface and influences the interaction between yeast and host cells. Fungal Genet Biol 60:53–63. https://doi.org/10.1016/j.fgb.2013.08.005.
42. Alspaugh JA. 2015. Virulence mechanisms and *Cryptococcus neoformans* pathogenesis. Fungal Genet Biol 78:55–58. https://doi.org/10.1016/j.fgb.2014.09.004.
43. García-Rodas R, de Oliveira H, Trevijano-Contador N, Zaragoza O. 2018. Cryptococcal Titan cells: when yeast cells are all grown up. Curr Top Microbiol Immunol 422:101–120. https://doi.org/10.1007/82_2018_145.
44. Zhou X, Ballou ER. 2018. The *Cryptococcus neoformans* Titan cell: from *in vivo* phenomenon to *in vitro* model. Curr Clin Micro Rpt 5:252–260. https://doi.org/10.1007/s40588-018-0107-9.
45. Zaragoza O, García-Rodas R, Nosanchuk JD, Cuenca-Estrella M, Rodríguez-Tudela JL, Casadevall A. 2010. Fungal cell gigantism during mammalian infection. PLoS Pathog 6:e1000945. https://doi.org/10.1371/journal.ppat.1000945.
46. Gerstein AC, Fu MS, Mukaremera L, Li Z, Ormerod KL, Fraser JA, Berman J, Nielsen K. 2015. Polyploid Titan cells produce haploid and aneuploid progeny to promote stress adaptation. mBio 6:e01340-15. https://doi.org/10.1128/mBio.01340-15.
47. Hommel B, Mukaremera L, Cordero RJB, Coelho C, Desjardins CA, Sturny-Leclère A, Janbon G, Perfect JR, Fraser JA, Casadevall A, Cuomo CA, Dromer F, Nielsen K, Alanio A. 2018. Titan cells formation in *Cryptococcus neoformans* is finely tuned by environmental conditions and modulated by positive and negative genetic regulators. PLoS Pathog 14:e1006982. https://doi.org/10.1371/journal.ppat.1006982.
48. Trevijano-Contador N, de Oliveira HC, García-Rodas R, Rossi SA, Llorente I, Zaballos Á, Janbon G, Ariño J, Zaragoza Ó. 2018. *Cryptococcus neoformans* can form titan-like cells *in vitro* in response to multiple signals. PLoS Pathog 14:e1007007. https://doi.org/10.1371/journal.ppat.1007007.
49. Dambuza IM, Drake T, Chapuis A, Zhou X, Correia J, Taylor-Smith L, LeGrave N, Rasmussen T, Fisher MC, Bicanic T, Harrison TS, Jaspars M, May RC, Brown GD, Yuecel R, MacCallum DM, Ballou ER. 2018. The *Cryptococcus neoformans* Titan cell is an inducible and regulated morphotype underlying pathogenesis. PLoS Pathog 14:e1006978. https://doi.org/10.1371/journal.ppat.1006978.
50. García-Barbazán I, Trevijano-Contador N, Rueda C, de Andrés B, Pérez-Tavárez R, Herrero-Fernández I, Gaspar ML, Zaragoza O. 2016. The formation of titan cells in *Cryptococcus neoformans* depends on the mouse strain and correlates with induction of Th2-type responses. Cell Microbiol 18:111–124. https://doi.org/10.1111/cmi.12488.
51. Mukaremera L, Lee KK, Wagener J, Wiesner DL, Gow NAR, Nielsen K. 2018. Titan cell production in *Cryptococcus neoformans* reshapes the cell wall and capsule composition during infection. Cell Surf 1:15–24. https://doi.org/10.1016/j.tcsw.2017.12.001.
52. Jung K-W, Yang D-H, Maeng S, Lee K-T, So Y-S, Hong J, Choi J, Byun H-J, Kim H, Bang S, Song M-H, Lee J-W, Kim MS, Kim S-Y, Ji J-H, Park G, Kwon H, Cha S, Meyers GL, Wang LL, Jang J, Janbon G, Adedoyin G, Kim T, Averette AK, Heitman J, Cheong E, Lee Y-H, Lee Y-W, Bahn Y-S. 2015. Systematic functional profiling of transcription factor networks in *Cryptococcus neoformans*. Nat Commun 6:6757. https://doi.org/10.1038/ncomms7757.
53. Schneider R, de O, Fogaça N, de SS, Kmetzsch L, Schrank A, Vainstein MH, Staats CC. 2012. Zap1 regulates zinc homeostasis and modulates virulence in *Cryptococcus gattii*. PLoS One 7:e43773. https://doi.org/10.1371/journal.pone.0043773.
54. Garcia-Santamarina S, Festa RA, Smith AD, Yu C-H, Probst C, Ding C, Homer CM, Yin J, Noonan JP, Madhani H, Perfect JR, Thiele DJ. 2018. Genome-wide analysis of the regulation of Cu metabolism in *Cryptococcus neoformans*. Mol Microbiol 108:473–494. https://doi.org/10.1111/mmi.13960.
55. Lev S, Kaufman-Francis K, Desmarini D, Juillard PG, Li C, Stifter SA, Feng CG, Sorrell TC, Grau GER, Bahn Y-S, Djordjevic JT. 2017. Pho4 is essential for dissemination of *Cryptococcus neoformans* to the host brain by promoting phosphate uptake and growth at alkaline pH. mSphere 2:e00381-16. https://doi.org/10.1128/mSphere.00381-16.
56. Jung WH, Sham A, White R, Kronstad JW. 2006. Iron regulation of the major virulence factors in the AIDS-associated pathogen *Cryptococcus neoformans*. PLoS Biol 4:e410. https://doi.org/10.1371/journal.pbio.0040410.
57. Chow EWL, Clancey SA, Billmyre RB, Averette AF, Granek JA, Mieczkowski P, Cardenas ME, Heitman J. 2017. Elucidation of the calcineurin-Crz1 stress response transcriptional network in the human fungal pathogen *Cryptococcus neoformans*. PLoS Genet 13:e1006667. https://doi.org/10.1371/journal.pgen.1006667.
58. O'Meara TR, Norton D, Price MS, Hay C, Clements MF, Nichols CB, Alspaugh JA. 2010. Interaction of *Cryptococcus neoformans* Rim101 and protein kinase A regulates capsule. PLoS Pathog 6:e1000776. https://doi.org/10.1371/journal.ppat.1000776.
59. Gish SR, Maier EJ, Haynes BC, Santiago-Tirado FH, Srikanta DL, Ma CZ, Li LX, Williams M, Crouch EC, Khader SA, Brent MR, Doering TL. 2016. Computational analysis reveals a key regulator of cryptococcal virulence and determinant of host response. mBio 7:e00313-16. https://doi.org/10.1128/mBio.00313-16.
60. Chun CD, Brown JCS, Madhani HD. 2011. A major role for capsule-independent phagocytosis-inhibitory mechanisms in mammalian infection by *Cryptococcus neoformans*. Cell Host Microbe 9:243–251. https://doi.org/10.1016/j.chom.2011.02.003.
61. Moranova Z, Virtudazo E, Hricova K, Ohkusu M, Kawamoto S, Husickova V, Raclavsky V. 2014. The CRZ1/SP1-like gene links survival under limited aeration, cell integrity and biofilm formation in the pathogenic yeast *Cryptococcus neoformans*. Biomed Pap Med Fac Univ Palacky Olomouc Czech Repub 158:212–220. https://doi.org/10.5507/bp.2013.024.
62. Lev S, Desmarini D, Chayakulkeeree M, Sorrell TC, Djordjevic JT. 2012. The Crz1/Sp1 transcription factor of *Cryptococcus neoformans* is activated by calcineurin and regulates cell wall integrity. PLoS One 7:e51403. https://doi.org/10.1371/journal.pone.0051403.
63. Park HS, Chow EWL, Fu C, Soderblom EJ, Moseley MA, Heitman J, Cardenas ME. 2016. Calcineurin targets involved in stress survival and fungal virulence. PLoS Pathog 12:e1005873. https://doi.org/10.1371/journal.ppat.1005873.
64. Lee D, Jang E-H, Lee M, Kim S-W, Lee Y, Lee K-T, Bahn Y-S. 2019. Unraveling melanin biosynthesis and signaling networks in *Cryptococcus neoformans*. mBio 10:e02267-19. https://doi.org/10.1128/mBio.02267-19.
65. Rhodes J, Desjardins CA, Sykes SM, Beale MA, Vanhove M, Sakthikumar S, Chen Y, Gujja S, Saif S, Chowdhary A, Lawson DJ, Ponzio V, Colombo AL, Meyer W, Engelthaler DM, Hagen F, Illnait-Zaragozi MT, Alanio A, Vreulink J-M, Heitman J, Perfect JR, Litvintseva AP, Bicanic T, Harrison TS, Fisher MC, Cuomo CA. 2017. Tracing genetic exchange and biogeography of *Cryptococcus neoformans* var. *grubii* at the global population level. Genetics 207:327–346. https://doi.org/10.1534/genetics.117.203836.
66. Liu OW, Chun CD, Chow ED, Chen C, Madhani HD, Noble SM. 2008. Systematic genetic analysis of virulence in the human fungal pathogen *Cryptococcus neoformans*. Cell 135:174–188. https://doi.org/10.1016/j.cell.2008.07.046.
67. Lee K-T, Hong J, Lee D-G, Lee M, Cha S, Lim Y-G, Jung K-W, Hwangbo A, Lee Y, Yu S-J, Chen Y-L, Lee J-S, Cheong E, Bahn Y-S. 2020. Fungal kinases and

transcription factors regulating brain infection in *Cryptococcus neoformans*. Nat Commun 11:1521. https://doi.org/10.1038/s41467-020-15329-2.
68. Krysan DJ, Zhai B, Beattie SR, Misel KM, Wellington M, Lin X. 2019. Host carbon dioxide concentration is an independent stress for *Cryptococcus neoformans* that affects virulence and antifungal Susceptibility. mBio 10:e01410-19. https://doi.org/10.1128/mBio.01410-19.
69. D'Souza CA, Alspaugh JA, Yue C, Harashima T, Cox GM, Perfect JR, Heitman J. 2001. Cyclic AMP-dependent protein kinase controls virulence of the fungal pathogen *Cryptococcus neoformans*. Mol Cell Biol 21:3179–3191. https://doi.org/10.1128/MCB.21.9.3179-3191.2001.
70. Hu G, Steen BR, Lian T, Sham AP, Tam N, Tangen KL, Kronstad JW. 2007. Transcriptional regulation by protein kinase A in *Cryptococcus neoformans*. PLoS Pathog 3:e42. https://doi.org/10.1371/journal.ppat.0030042.
71. Yoneda A, Doering TL. 2008. Regulation of *Cryptococcus neoformans* capsule size is mediated at the polymer level. Eukaryot Cell 7:546–549. https://doi.org/10.1128/EC.00437-07.
72. Frases S, Pontes B, Nimrichter L, Viana NB, Rodrigues ML, Casadevall A. 2009. Capsule of *Cryptococcus neoformans* grows by enlargement of polysaccharide molecules. Proc Natl Acad Sci U S A 106:1228–1233. https://doi.org/10.1073/pnas.0808995106.
73. Gaylord EA, Choy HL, Doering TL. 2020. Dangerous liaisons: interactions of *Cryptococcus neoformans* with host phagocytes. Pathogens 9:891. https://doi.org/10.3390/pathogens9110891.
74. Summers DK, Perry DS, Rao B, Madhani HD. 2020. Coordinate genomic association of transcription factors controlled by an imported quorum sensing peptide in *Cryptococcus neoformans*. PLoS Genet 16:e1008744. https://doi.org/10.1371/journal.pgen.1008744.
75. Homer CM, Summers DK, Goranov AI, Clarke SC, Wiesner DL, Diedrich JK, Moresco JJ, Toffaletti D, Upadhya R, Caradonna I, Petnic S, Pessino V, Cuomo CA, Lodge JK, Perfect J, Yates JR, III, Nielsen K, Craik CS, Madhani HD. 2016. Intracellular action of a secreted peptide required for fungal virulence. Cell Host Microbe 19:849–864. https://doi.org/10.1016/j.chom.2016.05.001.
76. Bailey TL. 2011. DREME: motif discovery in transcription factor ChIP-seq data. Bioinformatics 27:1653–1659. https://doi.org/10.1093/bioinformatics/btr261.
77. Kang Y, Patel NR, Shively C, Recio PS, Chen X, Wranik BJ, Kim G, Scott McIsaac R, Mitra R, Brent MR. 2020. Dual threshold optimization and network inference reveal convergent evidence from TF binding locations and TF perturbation responses. Genome Res 30:459–471. https://doi.org/10.1101/gr.259655.119.
78. Giles SS, Stajich JE, Nichols C, Gerrald QD, Alspaugh JA, Dietrich F, Perfect JR. 2006. The *Cryptococcus neoformans* catalase gene family and its role in antioxidant defense. Eukaryot Cell 5:1447–1459. https://doi.org/10.1128/EC.00098-06.
79. Cox GM, Harrison TS, McDade HC, Taborda CP, Heinrich G, Casadevall A, Perfect JR. 2003. Superoxide dismutase influences the virulence of *Cryptococcus neoformans* by affecting growth within macrophages. Infect Immun 71:173–180. https://doi.org/10.1128/iai.71.1.173-180.2003.
80. Lee K-T, So Y-S, Yang D-H, Jung K-W, Choi J, Lee D-G, Kwon H, Jang J, Wang LL, Cha S, Meyers GL, Jeong E, Jin J-H, Lee Y, Hong J, Bang S, Ji J-H, Park G, Byun H-J, Park SW, Park Y-M, Adedoyin G, Kim T, Averette AF, Choi J-S, Heitman J, Cheong E, Lee Y-H, Bahn Y-S. 2016. Systematic functional analysis of kinases in the fungal pathogen *Cryptococcus neoformans*. Nat Commun 7:12766. https://doi.org/10.1038/ncomms12766.
81. Caza M, Hu G, Price M, Perfect JR, Kronstad JW. 2016. The zinc finger protein Mig1 regulates mitochondrial function and azole drug susceptibility in the pathogenic fungus *Cryptococcus neoformans*. mSphere 1:e00080-15. https://doi.org/10.1128/mSphere.00080-15.
82. Chen Y, Toffaletti DL, Tenor JL, Litvintseva AP, Fang C, Mitchell TG, McDonald TR, Nielsen K, Boulware DR, Bicanic T, Perfect JR. 2014. The *Cryptococcus neoformans* transcriptome at the site of human meningitis. mBio 5:e01087-13. https://doi.org/10.1128/mBio.01087-13.
83. Alspaugh JA, Pukkila-Worley R, Harashima T, Cavallo LM, Funnell D, Cox GM, Perfect JR, Kronstad JW, Heitman J. 2002. Adenylyl cyclase functions downstream of the Gα protein Gpa1 and controls mating and pathogenicity of *Cryptococcus neoformans*. Eukaryot Cell 1:75–84. https://doi.org/10.1128/ec.1.1.75-84.2002.
84. Heung LJ, Kaiser AE, Luberto C, Del Poeta M. 2005. The role and mechanism of diacylglycerol-protein kinase C1 signaling in melanogenesis by *Cryptococcus neoformans*. J Biol Chem 280:28547–28555. https://doi.org/10.1074/jbc.M503404200.
85. Gerik KJ, Bhimireddy SR, Ryerse JS, Specht CA, Lodge JK. 2008. PKC1 is essential for protection against both oxidative and nitrosative stresses, cell integrity, and normal manifestation of virulence factors in the pathogenic fungus *Cryptococcus neoformans*. Eukaryot Cell 7:1685–1698. https://doi.org/10.1128/EC.00146-08.
86. Waterman SR, Hacham M, Hu G, Zhu X, Park Y-D, Shin S, Panepinto J, Valyi-Nagy T, Beam C, Husain S, Singh N, Williamson PR. 2007. Role of a CUF1/CTR4 copper regulatory axis in the virulence of *Cryptococcus neoformans*. J Clin Invest 117:794–802. https://doi.org/10.1172/JCI30006.
87. Jiang N, Sun N, Xiao D, Pan J, Wang Y, Zhu X. 2009. A copper-responsive factor gene *CUF1* required for copper induction of laccase in *Cryptococcus neoformans*. FEMS Microbiol Lett 296:84–90. https://doi.org/10.1111/j.1574-6968.2009.01619.x.
88. Walton FJ, Idnurm A, Heitman J. 2005. Novel gene functions required for melanization of the human pathogen *Cryptococcus neoformans*. Mol Microbiol 57:1381–1396. https://doi.org/10.1111/j.1365-2958.2005.04779.x.
89. Cheon SA, Jung K-W, Chen Y-L, Heitman J, Bahn Y-S, Kang HA. 2011. Unique evolution of the UPR pathway with a novel bZIP transcription factor, Hxl1, for controlling pathogenicity of *Cryptococcus neoformans*. PLoS Pathog 7:e1002177. https://doi.org/10.1371/journal.ppat.1002177.
90. Hicks JK, Bahn YS, Heitman J. 2005. Pde1 phosphodiesterase modulates cyclic AMP levels through a protein kinase A-mediated negative feedback loop in *Cryptococcus neoformans*. Eukaryot Cell 4:1971–1981. https://doi.org/10.1128/EC.4.12.1971-1981.2005.
91. Kozubowski L, Lee SC, Heitman J. 2009. Signalling pathways in the pathogenesis of *Cryptococcus*. Cell Microbiol 11:370–380. https://doi.org/10.1111/j.1462-5822.2008.01273.x.
92. Fox DS, Cruz MC, Sia RAL, Ke H, Cox GM, Cardenas ME, Heitman J. 2001. Calcineurin regulatory subunit is essential for virulence and mediates interactions with FKBP12-FK506 in *Cryptococcus neoformans*. Mol Microbiol 39:835–849. https://doi.org/10.1046/j.1365-2958.2001.02295.x.
93. Odom A, Muir S, Lim E, Toffaletti DL, Perfect J, Heitman J. 1997. Calcineurin is required for virulence of *Cryptococcus neoformans*. EMBO J 16:2576–2589. https://doi.org/10.1093/emboj/16.10.2576.
94. Jung W-H, Son Y-E, Oh S-H, Fu C, Kim HS, Kwak J-H, Cardenas ME, Heitman J, Park HS. 2018. Had1 is required for cell wall integrity and fungal virulence in *Cryptococcus neoformans*. G3 (Bethesda) 8:643–652. https://doi.org/10.1534/g3.117.300444.
95. Kmetzsch L, Staats CC, Cupertino JB, Fonseca FL, Rodrigues ML, Schrank A, Vainstein MH. 2013. The calcium transporter Pmc1 provides Ca2+ tolerance and influences the progression of murine cryptococcal infection. FEBS J 280:4853–4864. https://doi.org/10.1111/febs.12458.
96. Kmetzsch L, Staats CC, Simon E, Fonseca FL, de Oliveira DL, Sobrino L, Rodrigues J, Leal AL, Nimrichter L, Rodrigues ML, Schrank A, Vainstein MH. 2010. The vacuolar Ca2+ exchanger Vcx1 is involved in calcineurin-dependent Ca2+ tolerance and virulence in *Cryptococcus neoformans*. Eukaryot Cell 9:1798–1805. https://doi.org/10.1128/EC.00114-10.
97. Denham S, Brown J. 2018. Mechanisms of pulmonary escape and dissemination by *Cryptococcus neoformans*. J Fungi (Basel) 4:25. https://doi.org/10.3390/jof4010025.
98. Sun D, Sun P, Li H, Zhang M, Liu G, Strickland AB, Chen Y, Fu Y, Xu J, Yosri M, Nan Y, Zhou H, Zhang X, Shi M. 2019. Fungal dissemination is limited by liver macrophage filtration of the blood. Nat Commun 10:4566. https://doi.org/10.1038/s41467-019-12381-5.
99. Santiago-Tirado FH, Doering TL. 2017. False friends: phagocytes as Trojan horses in microbial brain infections. PLoS Pathog 13:e1006680. https://doi.org/10.1371/journal.ppat.1006680.
100. Squizani ED, Oliveira NK, Reuwsaat JCV, Marques BM, Lopes W, Gerber AL, de Vasconcelos ATR, Lev S, Djordjevic JT, Schrank A, Vainstein MH, Staats CC, Kmetzsch L. 2018. Cryptococcal dissemination to the central nervous system requires the vacuolar calcium transporter Pmc1. Cell Microbiol 20:e12803. https://doi.org/10.1111/cmi.12803.
101. Okagaki LH, Nielsen K. 2012. Titan cells confer protection from phagocytosis in *Cryptococcus neoformans* infections. Eukaryot Cell 11:820–826. https://doi.org/10.1128/EC.00121-12.
102. Srikanta D, Santiago-Tirado FH, Doering TL. 2014. *Cryptococcus neoformans*: historical curiosity to modern pathogen. Yeast 31:47–60. https://doi.org/10.1002/yea.2997.
103. Nielsen K, Cox GM, Wang P, Toffaletti DL, Perfect JR, Heitman J. 2003. Sexual cycle of *Cryptococcus neoformans* var. *grubii* and virulence of congenic a and α isolates. Infect Immun 71:4831–4841. https://doi.org/10.1128/iai.71.9.4831-4841.2003.
104. Reuwsaat JCV, Motta H, Garcia AWA, Vasconcelos CB, Marques BM, Oliveira NK, Rodrigues J, Ferrareze PAG, Frases S, Lopes W, Barcellos VA, Squizani ED, Horta JA, Schrank A, Rodrigues ML, Staats CC, Vainstein MH, Kmetzsch L. 2018. A predicted mannoprotein participates in *Cryptococcus*

gattii capsular structure. mSphere 3:e00023-18. https://doi.org/10.1128/mSphere.00023-18.
105. Haynes BC, Skowyra ML, Spencer SJ, Gish SR, Williams M, Held EP, Brent MR, Doering TL. 2011. Toward an integrated model of capsule regulation in *Cryptococcus neoformans*. PLoS Pathog 7:e1002411. https://doi.org/10.1371/journal.ppat.1002411.
106. Denham ST, Brammer B, Chung KY, Wambaugh MA, Bednarek J, Guo L, Brown JCS. 2020. Phosphate induces a morphological shift that enhances vascular dissemination of *Cryptococcus neoformans*. bioRxiv 2020.08.27.270843.
107. Babraham Bioinformatics. FastQC: a quality control tool for high throughput sequence data. https://www.bioinformatics.babraham.ac.uk/projects/fastqc/. Accessed 24 June 2019.
108. Friedman RZ, Gish SR, Brown H, Brier L, Howard N, Doering TL, Brent MR. 2018. Unintended side effects of transformation are very rare in *Cryptococcus neoformans*. G3 (Bethesda) 8:815–822. https://doi.org/10.1534/g3.117.300357.
109. Sedlazeck FJ, Rescheneder P, von Haeseler A. 2013. NextGenMap: fast and accurate read mapping in highly polymorphic genomes. Bioinformatics 29:2790–2791. https://doi.org/10.1093/bioinformatics/btt468.
110. Li H, Handsaker B, Wysoker A, Fennell T, Ruan J, Homer N, Marth G, Abecasis G, Durbin R, 1000 Genome Project Data Processing Subgroup. 2009. The Sequence Alignment/Map format and SAMtools. Bioinformatics 25:2078–2079. https://doi.org/10.1093/bioinformatics/btp352.
111. Zhang Y, Liu T, Meyer CA, Eeckhoute J, Johnson DS, Bernstein BE, Nusbaum C, Myers RM, Brown M, Li W, Liu XS. 2008. Model-based analysis of ChIP-Seq (MACS). Genome Biol 9:R137. https://doi.org/10.1186/gb-2008-9-9-r137.
112. Heinz S, Benner C, Spann N, Bertolino E, Lin YC, Laslo P, Cheng JX, Murre C, Singh H, Glass CK. 2010. Simple combinations of lineage-determining transcription factors prime cis-regulatory elements required for macrophage and B cell identities. Mol Cell 38:576–589. https://doi.org/10.1016/j.molcel.2010.05.004.
113. Novocraft Technologies. 2014. NovoAlign. http://www.novocraft.com/. Accessed 25 November 2020.
114. Anders S, Pyl PT, Huber W. 2015. HTSeq–a Python framework to work with high-throughput sequencing data. Bioinformatics 31:166–169. https://doi.org/10.1093/bioinformatics/btu638.
115. Love MI, Huber W, Anders S. 2014. Moderated estimation of fold change and dispersion for RNA-seq data with DESeq2. Genome Biol 15:550. https://doi.org/10.1186/s13059-014-0550-8.
116. Ignatiadis N, Klaus B, Zaugg JB, Huber W. 2016. Data-driven hypothesis weighting increases detection power in genome-scale multiple testing. Nat Methods 13:577–580. https://doi.org/10.1038/nmeth.3885.
117. Li LX, Rautengarten C, Heazlewood JL, Doering TL. 2018. Xylose donor transport is critical for fungal virulence. PLoS Pathog 14:e1006765. https://doi.org/10.1371/journal.ppat.1006765.
118. Janbon G, Ormerod KL, Paulet D, Byrnes EJ, Yadav V, Chatterjee G, Mullapudi N, Hon C-C, Billmyre RB, Brunel F, Bahn Y-S, Chen W, Chen Y, Chow EWL, Coppée J-Y, Floyd-Averette A, Gaillardin C, Gerik KJ, Goldberg J, Gonzalez-Hilarion S, Gujja S, Hamlin JL, Hsueh Y-P, Ianiri G, Jones S, Kodira CD, Kozubowski L, Lam W, Marra M, Mesner LD, Mieczkowski PA, Moyrand F, Nielsen K, Proux C, Rossignol T, Schein JE, Sun S, Wollschlaeger C, Wood IA, Zeng Q, Neuvéglise C, Newlon CS, Perfect JR, Lodge JK, Idnurm A, Stajich JE, Kronstad JW, Sanyal K, Heitman J, Fraser JA, Cuomo CA, Dietrich FS. 2014. Analysis of the genome and transcriptome of *Cryptococcus neoformans* var. *grubii* reveals complex RNA expression and microevolution leading to virulence attenuation. PLoS Genet 10:e1004261. https://doi.org/10.1371/journal.pgen.1004261.

SUPPLEMENTARY FIGURES

FIGURE S1

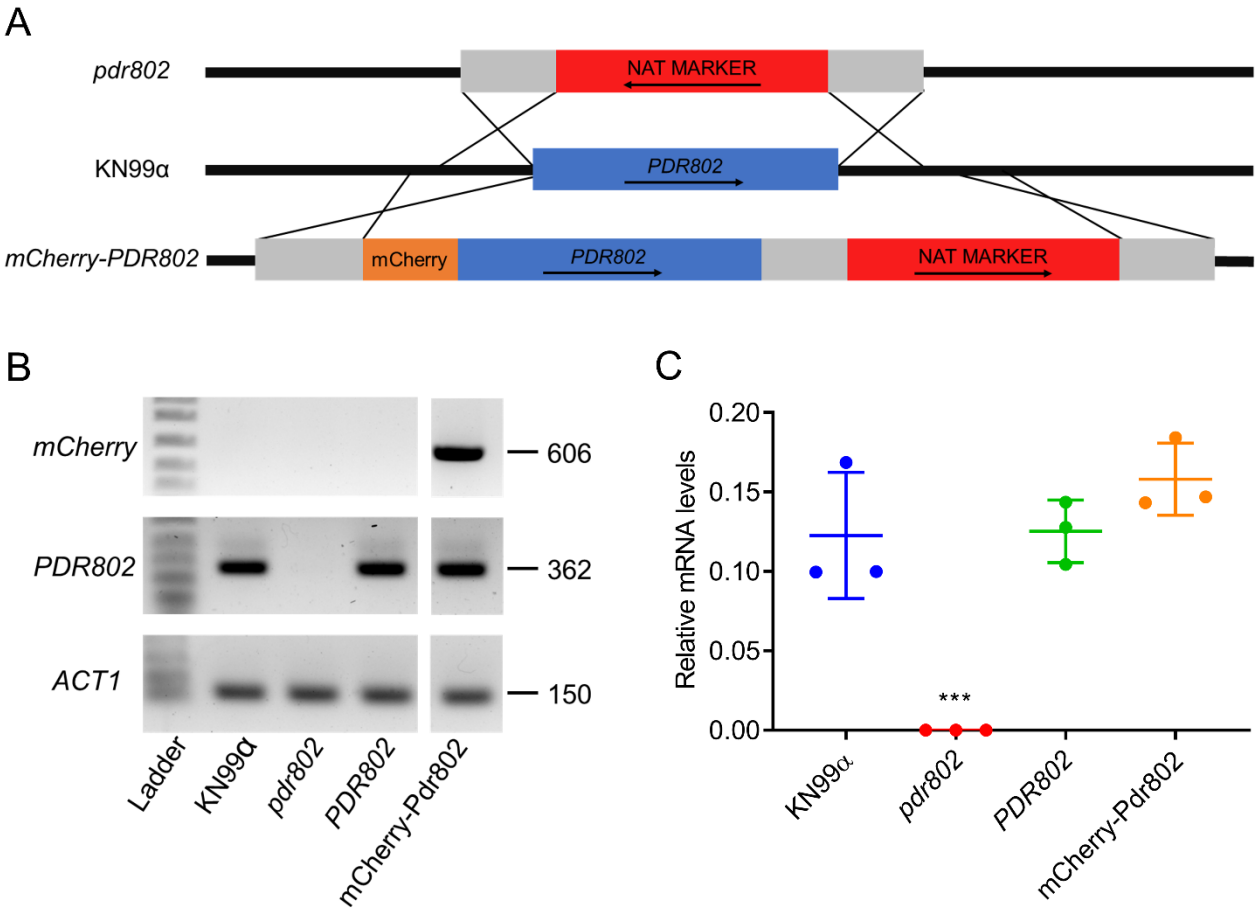

Figure S1. Mutant strain construction and confirmation. A. Scheme for generating *C. neoformans* strains in the KN99α background (middle) that either lack *PDR802* (*pdr802,* top) or encode a tagged copy of the protein (*mCherry-PDR802*). B. Qualitative analysis of gene expression in Panel A strains and the complemented *pdr802* mutant (*PDR802*). Cryptococcal mRNA isolated from cells grown in DMEM (37°C, 5% CO_2, 24 hours) was used to generate cDNA; from this, segments of the genes indicated at the left were amplified using the primers listed in Data Set S2, Sheet 5, and the products were analyzed by agarose gel electrophoresis. Fragment sizes (in bp) are indicated at right and the ladder bands shown are 400, 500, 650, 850 and 1000 bp for the top panel; 200, 300, 400, 500,

and 650 bp for the middle panel; and 100, 200, and 300 bp for the bottom panel. C. Quantitative analysis of *PDR802* expression. Samples of RNA isolated as in B were analyzed for *PDR802* expression by qRT-PCR. All results were normalized to *ACT1* expression. Each symbol represents a biological replicate, with the mean and standard deviation also shown. ***, $p<0.001$ compared to KN99α by one-way ANOVA with posthoc Dunnett test.

FIGURE S2

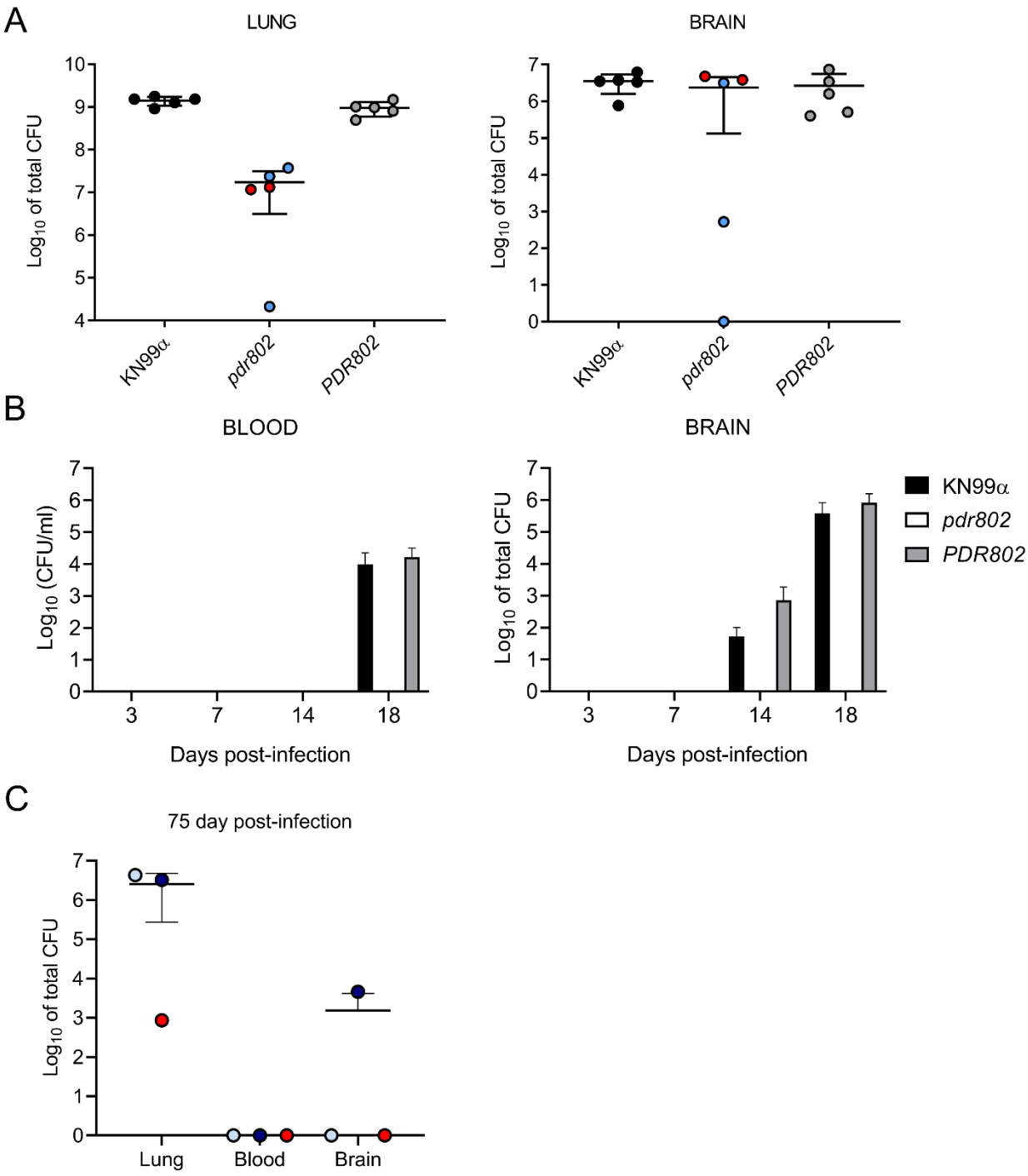

Figure S2. Organ burdens. A. Mean +/- SD values of total colony-forming units (CFU) in the indicated tissue of mice from the Figure 1 survival curve are shown. Each point is the average value for a single animal at the time of death. For *pdr802* infections, red circles

represent mice sacrificed at days 65 and 69, while blue circles represent mice sacrificed at the end of the study (day 100). B. Mean +/- SD of total colony-forming units (CFU) in the blood and brain at the indicated times post-infection. C. Mean +/- SD of total colony-forming units (CFU) in the lung, blood and brain 75 days after infection with *pdr802*. Each color represents one mouse.

FIGURE S3

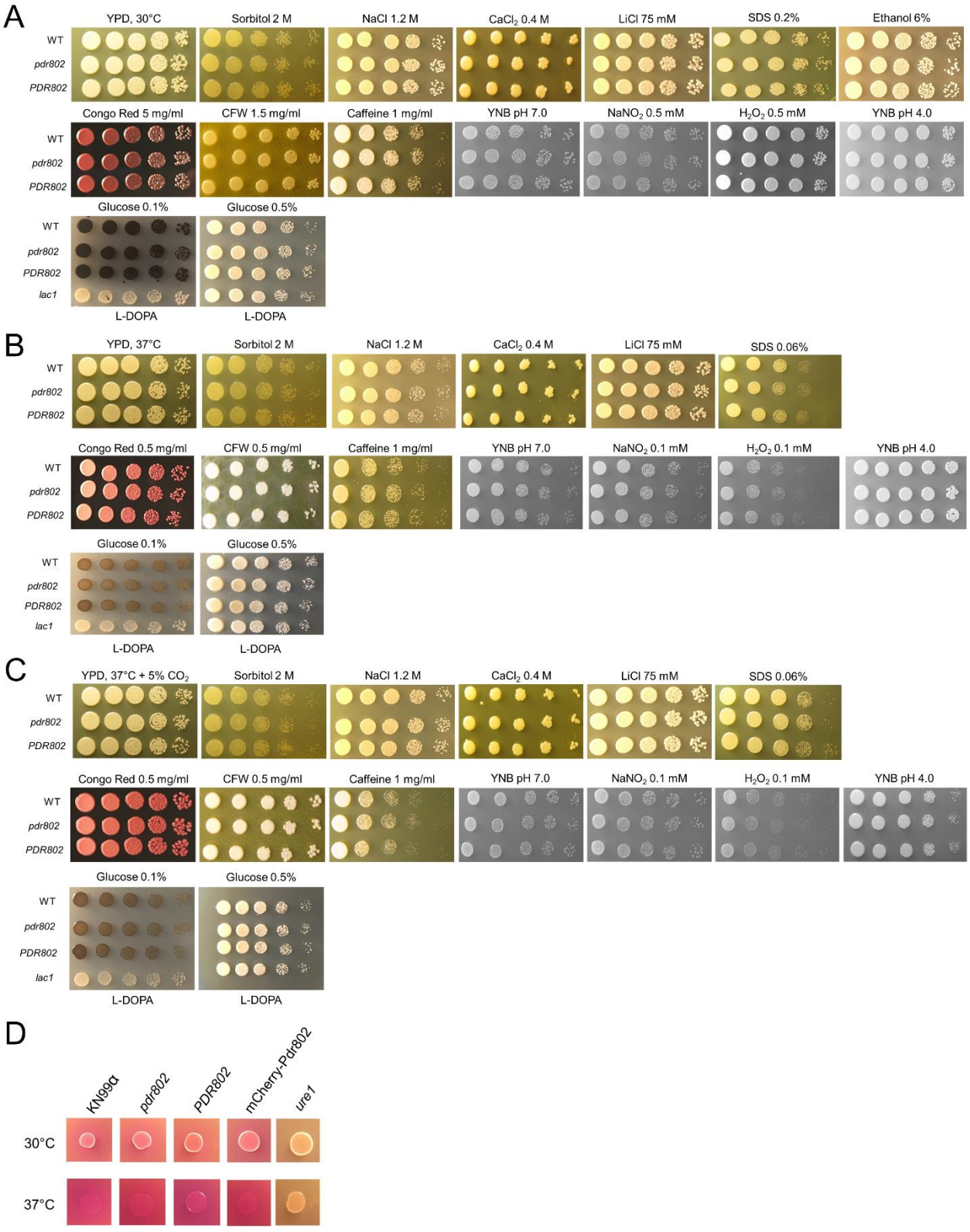
A
YPD, 30°C
Sorbitol 2 M
NaCl 1.2 M
CaCl2 0.4 M
LiCl 75 mM
SDS 0.2%
Ethanol 6%
WT
pdr802
PDR802
Congo Red 5 mg/ml
CFW 1.5 mg/ml
Caffeine 1 mg/ml
YNB pH 7.0
NaNO2 0.5 mM
H2O2 0.5 mM
YNB pH 4.0
Glucose 0.1%
Glucose 0.5%
lac1
L-DOPA
B
YPD, 37°C
SDS 0.06%
Congo Red 0.5 mg/ml
CFW 0.5 mg/ml
NaNO2 0.1 mM
H2O2 0.1 mM
C
YPD, 37°C + 5% CO2
D
KN99α
pdr802
PDR802
mCherry-Pdr802
ure1
30°C
37°C

Figure S3. Characterization of *pdr802* cells. *Panels A-C*.10-fold serial dilutions of WT, *pdr802*, and *PDR802* cells were plated on the media shown and incubated at 30°C (A), 37°C (B), or 37°C in the presence of 5% CO_2 (C). Nitrosative ($NaNO_2$) and oxidative (H_2O_2) stress plates were prepared with YNB medium and melanization plates containing L-DOPA were prepared as in the Methods; all other plates were prepared with YPD medium. *lac1*, a control strain lacking the ability to melanize (88). D. Urease activity of the indicated strains was evaluated using Christensen's urea solid medium (see Methods) at the indicated temperatures. *ure1*, a control strain that does not produce urease (17).

FIGURE S4

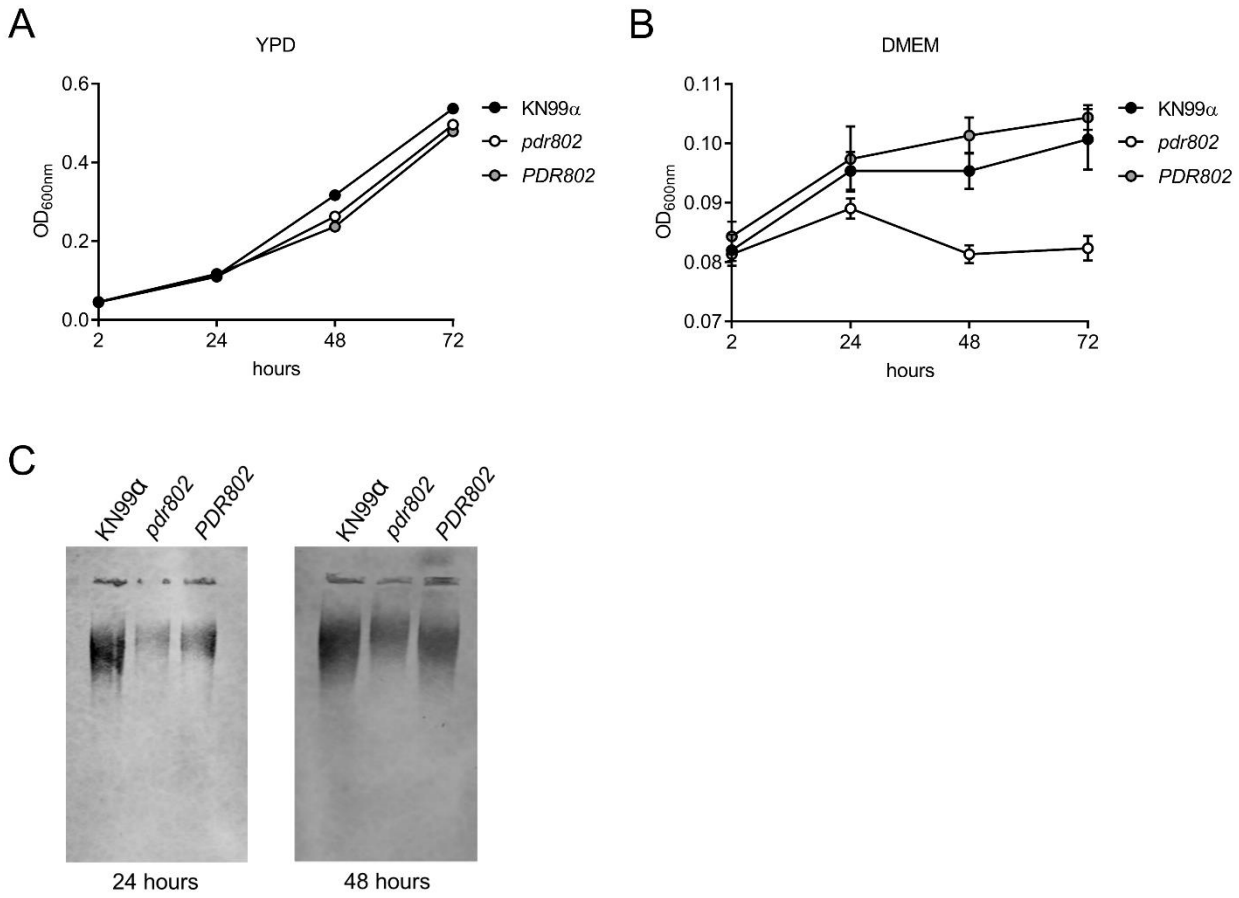

Figure S4. Growth curves and capsule shedding. *Panels A-B*. Growth of the strains indicated in YPD at 30°C (A) or DMEM at 37°C and 5% CO_2 (B) was assessed by OD_{600nm} at the times shown. C. Conditioned medium from the indicated strains was probed for the presence of GXM after growth in DMEM for 24 or 48 hours. Equal volumes of culture supernatant were analyzed without normalization to cell density. Immunoblotting was performed using the anti-GXM monoclonal antibody 302.

FIGURE S5

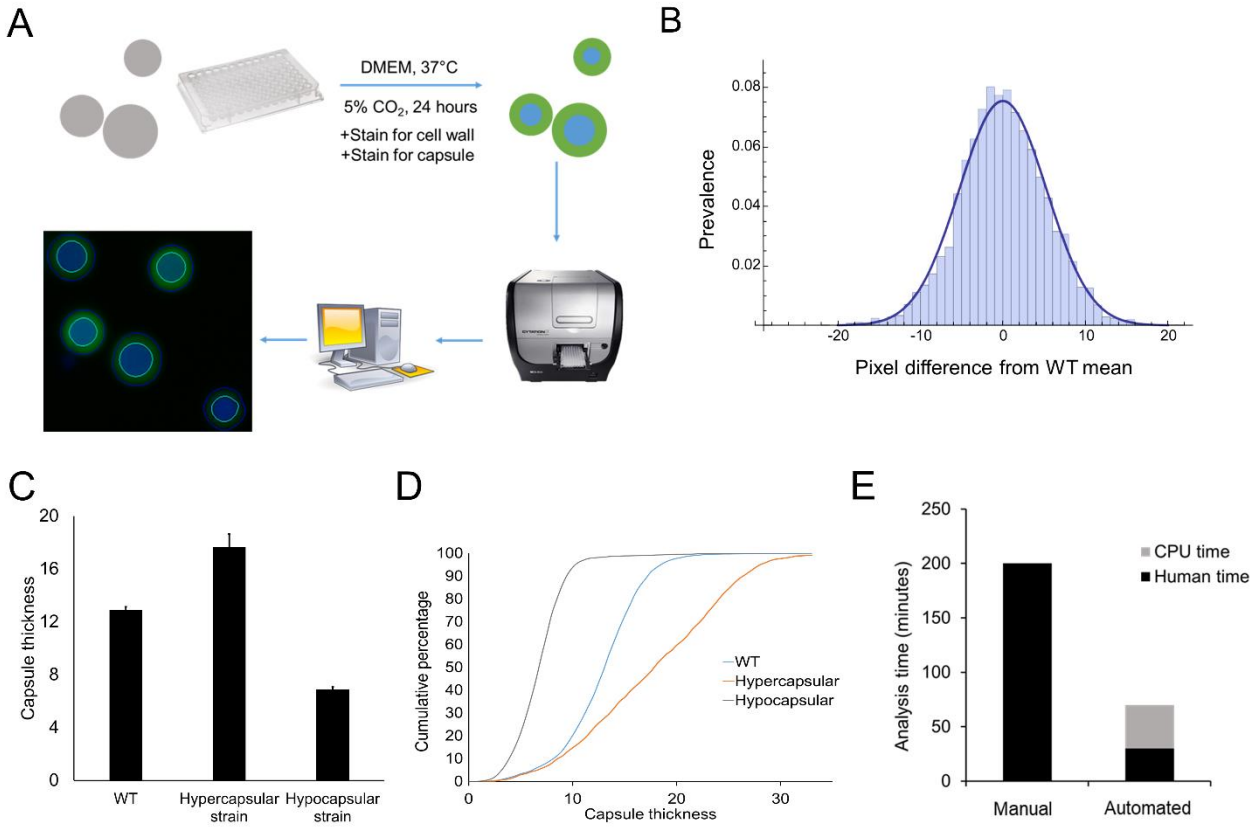

Figure S5. Semi-automated assay for cryptococcal capsule imaging. A. Schematic of applying this method to cryptococcal cells induced to form capsule by growth in DMEM (37°C, 5% CO_2) for 24 h, followed by cell wall and capsule staining. Thousands of cells may be imaged per well and analyzed automatically with software that annotates and measures the capsule (annotated on the micrograph in blue) and cell wall (annotated in bright green). See Methods for details. B. Capsule size distribution of WT cells after induction. Capsule thickness for each cell is the difference between the paired diameters of the cell wall and capsule, which is plotted here with reference to the mean value. C and D. Mean and SD (C) and cumulative percentage (D) analysis of WT compared to hyper and hypocapsular control strains (here *pkr1* and *ada2*, respectively). Capsule thickness is in arbitrary units, related to the pixels measured. E. The time required to analyze the

capsule thickness of 1,000 cells by this method compared to manual assessment of India ink images.

FIGURE S6

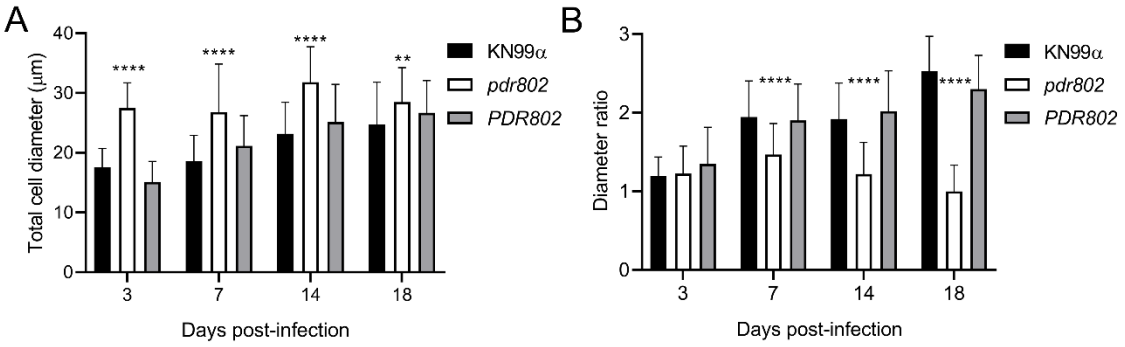

C

3 DPI	KN99α	*pdr802*	*PDR802*
Cell body diameter ≥ 10 μm	20	86.7	11.1
Cell body diameter ≥ 15 μm	0	22.2	0
Total cell diameter ≥ 30 μm	0	31.1	0
7 DPI	**KN99α**	***pdr802***	***PDR802***
Cell body diameter ≥ 10 μm	8.5	57.4	8.5
Cell body diameter ≥ 15 μm	0	19.1	2.1
Total cell diameter ≥ 30 μm	0	31.9	2.1
14 DPI	**KN99α**	***pdr802***	***PDR802***
Cell body diameter ≥ 10 μm	27.1	87.1	24.3
Cell body diameter ≥ 15 μm	2.9	42.9	4.3
Total cell diameter ≥ 30 μm	12.9	57.1	25.7
18 DPI	**KN99α**	***pdr802***	***PDR802***
Cell body diameter ≥ 10 μm	9.1	89.4	15.1
Cell body diameter ≥ 15 μm	0	53.0	1.5
Total cell diameter ≥ 30 μm	21.2	43.9	27.3

Figure S6. *PDR802* deletion induces Titan cell formation. Mean +/- SD of (A) total cell diameter and (B) the ratio of total cell to cell body diameters (diameter ratio), assessed by measuring at least 50 cells per strain with ImageJ. **, $p<0.01$ and ****, $p<0.0001$ for comparison of *pdr802* to KN99α or *PDR802* by one-way ANOVA with posthoc Dunnett test for each day post-infection. C. Percent of Titan cells in the indicated strain, evaluated using various published parameters: cell body diameter above 10 or 15 μm (20) or total cell diameter above 30 μm (43).

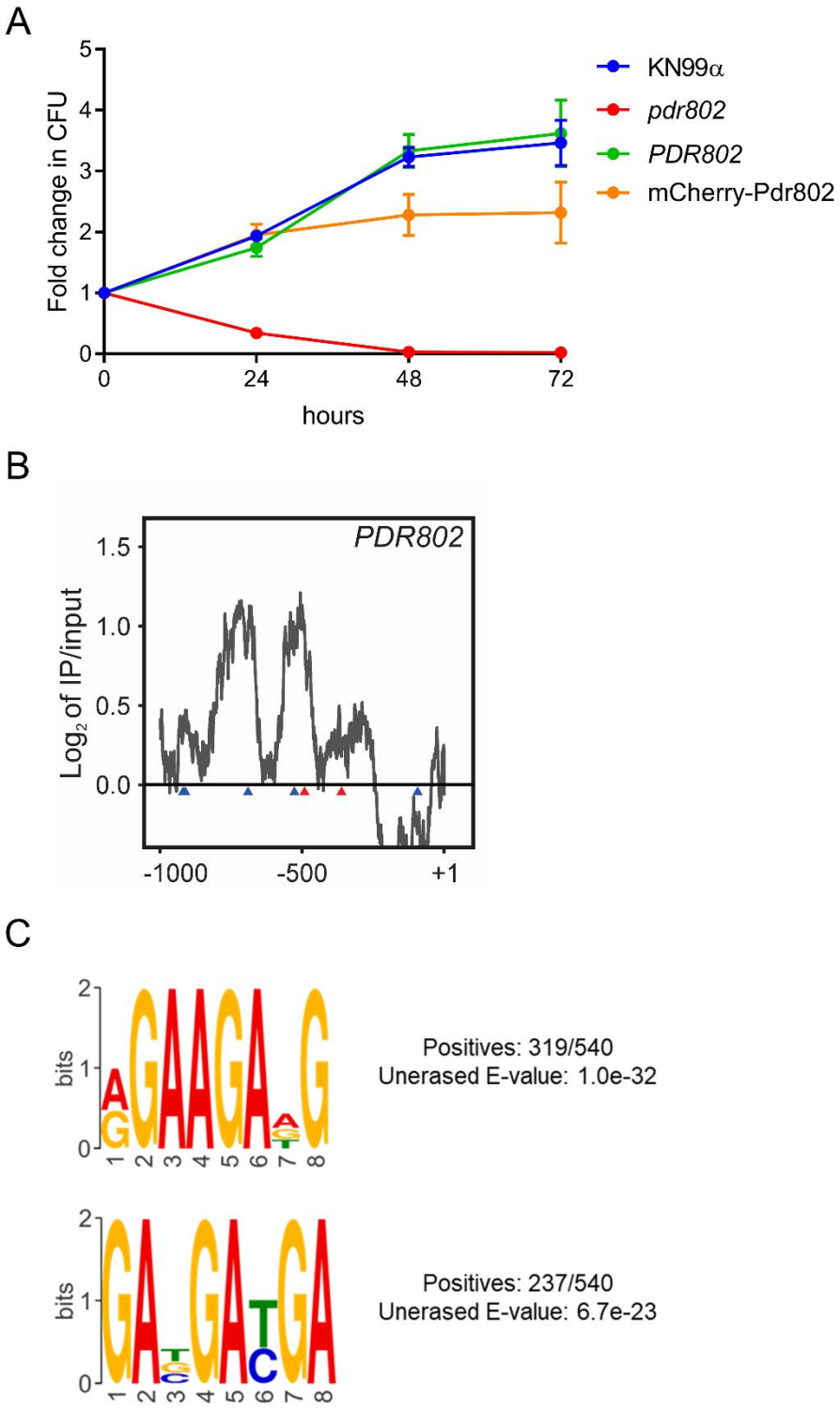

Figure S7. Pdr802 strain viability, putative DNA-binding motifs, and self-regulation.

A. The indicated strains were grown in DMEM at 37°C and 5% CO_2 for the times shown

and samples were tested for their ability to form colonies on YPD medium. Plotted is the fold-change in CFU relative to the initial culture. B. Putative Pdr802-binding motifs determined using DREME (74). Primary and secondary hits are shown for analysis of 1,000 bp upstream of the initiating ATG. C. Pdr802 self-regulation. The ratios (log_2) of reads from immunoprecipitated (IP) DNA to reads from input DNA were calculated for 1,000 bp upstream of the first coding nucleotide (+1) of *PDR802*; shown is the difference in these values between tagged and untagged strains. Red triangles, complete Pdr802 DNA-binding motifs (Figure S7B); blue triangles, partial motifs.

SUPPLEMENTARY METHODS

Strain construction

To complement the *pdr802* deletion mutant at its native locus, we used a split marker strategy (1) to replace the nourseothricin marker with the original *PDR802* sequence (including its native promoter and terminator) followed by a geneticin (G418) resistance marker. To do this we PCR amplified the *PDR802* sequence (4131 bp) with primers JR01/02 and the G418 resistance marker (1627 bp) with primers JR03/04 (see the Data Set S2, Sheet 5 for primer sequences); both amplicons were then gel purified and cloned in tandem into NdeI-digested pUC19, using Gibson Assembly Master Mix (2), to form pUC19+PDR802+G418. This plasmid was digested with NdeI and BssHII to release a 5492-bp fragment containing *PDR802* and a 5' portion of the G418 marker. The 3' portion of the G418 resistance marker (750 bp) was amplified using primers JR05/06 and fused by PCR to a region 3' of *PDR802* (1017 bp; amplified with JR07/08) to yield a 1767 bp product. These fragments were used in biolistic transformation of *pdr802* cells as in ref (3).

To tag Pdr802 with mCherry at the N-terminus, we first fused approximately 1.2 kb upstream of the start codon of *PDR802,* a sequence encoding mCherry, the *PDR802* coding sequence with 500 bp of downstream sequence, and a NAT resistance marker sequence. To generate these segments the *PDR802* promoter (1286 bp) was amplified with primers JR09/10; the mCherry sequence (714 bp) with JR11/12; the *PDR802* coding sequence (2957 bp) with JR13/14; and the NAT marker cassette (1721 bp) with primers JR15/16. All fragments were gel purified and cloned as above into pUC19 digested with Sac1 and Nde1, to form pUC19+mCherry+Pdr+NAT. This was digested with NdeI and

BssHII to release a 5559 bp fragment. The 3' portion of the NAT resistance marker (832 bp) was amplified with primers JR17/18 and fused by PCR to a region 3' of *PDR802* amplified with JR19/20 (1064 bp) to form a 1896-bp product. These fragments were used in biolistic transformation of KN99α cells as above. All strains were confirmed by PCR and sequencing, and further analyzed by RT-PCR and qRT-PCR (see Supplemental Figure 1).

qRT-PCR

RNA from cryptococcal cells grown in DMEM at 37°C with 5% CO_2 for 24 hours was extracted with TriZol® reagent (Invitrogen, MA, USA) according to the manufacturer's instructions. RNA integrity was assessed by electrophoresis on 1% agarose and quantification was performed by absorbance analysis using a NanoDrop™ 2000 spectrophotometer (Thermo Fisher Scientific). cDNAs were prepared from DNase (Promega, WI, USA)-treated total RNA samples (290 ng) using ImProm-II reverse transcriptase (Promega) and oligo-dT. Quantitative real-time PCR (qRT-PCR) was performed on a Fast 7500 real-time PCR system (Applied Biosystems, MA, USA) with the following thermal cycling conditions: 95°C for 10 min followed by 40 cycles of 95°C for 15 s, 55°C for 15 s, and 60°C for 60 s. Platinum® SYBR® green qPCR Supermix (Invitrogen) was used as the reaction mix and supplemented with 5 pmol of each primer (see Data Set S2, Sheet 5, for sequences) and 8 ng of cDNA template for a final volume of 10 µl. All experiments were performed in biological triplicate and each sample was analyzed in triplicate for each primer pair. Melting curve analysis was performed at the end of the reaction to confirm the presence of a single PCR product. Data were

normalized to levels of *ACT1*, which was included in each set of PCR experiments. Relative expression was determined using the $2^{-\Delta Ct}$ method.

REFERENCES

1. Fu J, Hettler E, Wickes BL. 2006. Split marker transformation increases homologous integration frequency in *Cryptococcus neoformans*. Fungal Genet Biol 43:200–212.

2. Gibson DG, Young L, Chuang R-Y, Venter JC, Hutchison CA, Smith HO. 2009. Enzymatic assembly of DNA molecules up to several hundred kilobases. Nat Methods 6:343–345.

3. Friedman RZ, Gish SR, Brown H, Brier L, Howard N, Doering TL, Brent MR. 2018. Unintended Side Effects of Transformation Are Very Rare in *Cryptococcus neoformans*. G3 (Bethesda) 8:815–822.

4. Discussão

A regulação da produção de fatores de virulência é crucial para a patogênese de agentes infecciosos e para o estabelecimento de infecções microbianas. Se esses processos não forem coordenados adequadamente, o patógeno terá menor probabilidade de sobreviver à resposta imunológica e de causar danos ao hospedeiro. Um fator de virulência chave do patógeno *C. neoformans* é a produção de uma cápsula polissacarídica que envolve a parede celular; esta estrutura ajuda as células fúngicas a resistirem ao engulfamento e eliminação pelos fagócitos do hospedeiro. Outro fator de virulência criptocócico importante é a produção de células gigantes que aumenta a resistência dos fungos à fagocitose, estresse oxidativo e tratamento antifúngico. Neste trabalho, identificamos o fator de transcrição Pdr802 como essencial para a adaptação e sobrevivência de *C. neoformans* em condições do hospedeiro *in vitro* e *in vivo*. Células de *C. neoformans* sem Pdr802 exibem cápsulas aumentadas e maior produção de células de células gigantes e, consequentemente, virulência drasticamente reduzida em um modelo murino de infecção. Esses resultados demonstram que mais não é necessariamente melhor quando se trata de fatores de virulência. Em vez disso, a regulação precisa dessas características, para evitar subexpressão ou superexpressão, é crítica para o sucesso desse patógeno frente aos desafios impostos pelo ambiente hospedeiro.

Ao buscar o mecanismo desses fenótipos variados, descobrimos que Pdr802 regula vários genes cujos produtos atuam no remodelamento da parede celular, na resposta ao estresse oxidativo, na resistência à temperatura do hospedeiro e na produção de fatores de virulência. Por exemplo, Pdr802 regula diretamente vários genes que influenciam a espessura da cápsula, de modo que a perda desse fator de transcrição resulta na produção de fibras capsulares alongadas e consequentemente cápsulas aumentadas. Notavelmente, apesar deste fenótipo de hipercapsularidade, o mutante *pdr802* é significativamente menos virulento do que a linhagem controle. Embora parte dessa mudança na patogenicidade seja provavelmente devido a fatores além da cápsula, como a dificuldade de sobrevivência desse mutante em condições que mimetizem o ambiente do

hospedeiro, ela também pode ser influenciada por características da cápsula do mutante que, de alguma forma, podem favorecer uma resposta imune do hospedeiro forte e eficiente. Dentre eles podemos destacar possíveis mudanças estruturais das fibras polissacarídicas, também como sua distribuição ao longo da parede celular e composição.

Como a cápsula, as células gigantes são conhecidas por contribuírem para a virulência criptocócica, mas são paradoxalmente mais produzidas pelo mutante hipovirulento *pdr802*. A principal hipótese é que isso deve-se em grande parte à incapacidade das células do mutante *pdr802* de se comunicarem adequadamente por meio de *quorum sensing*, que normalmente inibe a formação de células gigantes, entre outras funções. Na linhagem selvagem de *C. neoformans*, o fator de transcrição Pdr802 regula positivamente a expressão de genes que codificam a protease Pqp1, o transportador Opt1 e o fator de transcrição Liv3, que respectivamente processam, importam e respondem ao peptídeo de *quorum sensing* Qsp1. Como resultado, as células sem Pdr802 são incapazes de detectar umas às outras normalmente; isso pode prejudicar sua adaptação ao ambiente do hospedeiro, incluindo a modulação da formação de células de gigantes. Essa desregulação, combinada com a expressão perturbada de outros genes que influenciam a formação das células de Titãs, desencadeia uma produção dramática desse morfotipo.

Os exemplos de formação de cápsula e células gigantes destacam o potencial perigo representado para o patógeno pela produção não modulada de até mesmo fatores de virulência valiosos. Embora a inibição ou diminuição da produção de um fator de virulência importante geralmente favoreça a resposta imune e o controle de patógenos pelo hospedeiro *in vivo*, nesses casos, uma resposta fúngica aberrante ao ambiente desafiador do hospedeiro leva ao fracasso da infecção criptocócica. Claramente, a regulação equilibrada dos determinantes de virulência é essencial para *C. neoformans* superar os desafios contínuos que encontra no ambiente de um hospedeiro infectado (Figura 9).

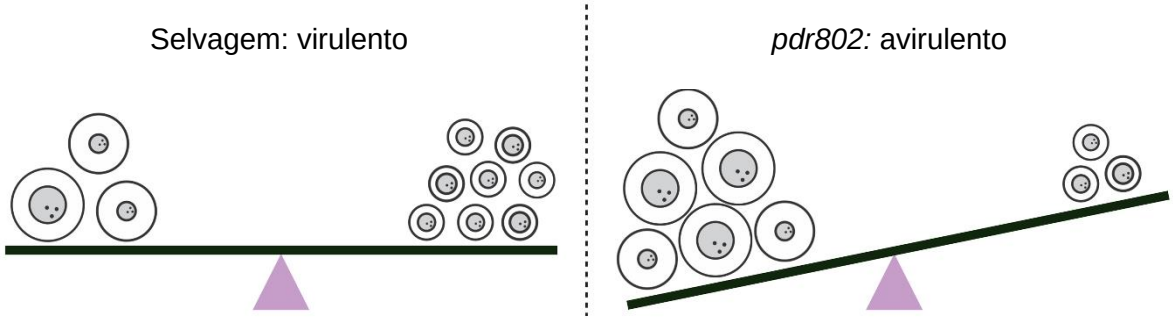

Figura 9. A patogênese efetiva requer uma regulação rígida dos fatores de virulência. Níveis ótimos de produção de cápsula polissacarídica e células gigantes são chave para o sucesso da infecção pela linhagem selvagem (esquerda); perturbação no balanço entre essas características reduz drasticamente a patogenicidade do mutante nulo *pdr802* (direita).

5. Conclusões

5.1. O fator de transcrição Pdr802 é indispensável para a virulência de *C. neoformans* e sua inativação altera o curso da infeção em modelo experimental murino;

5.2. Pdr802 é importante para a sobrevivência da levedura em condições que mimetizam o ambiente do hospedeiro *in vitro*, como em meio DMEM e soro de camundongo;

5.3. Pdr802 regula negativamente a manutenção do tamanho da cápsula polissacarídica e a produção de células gigantes de *C. neoformans*;

5.4. Pdr802 regula positivamente genes envolvidos no *quorum sensing* de *C. neoformans*, como *PQP1*, *OPT1* e *LIV3*;

5.5. Pdr802 regula alvos envolvidos na sinalização da fosfatase calcineurina, como Had1 e Crz1 e na resistência ao estresse oxidativo, produção de melanina, integridade da parede celular, crescimento a 37°C e atividade de urease.

6. Perspectivas

6.1. Determinar sinais específicos que induzam a expressão do gene *PDR802* empregando ensaios de RT-qPCR da linhagem selvagem em meios de cultura de células distintos, em temperaturas diferentes e com e sem adição de componentes específicos, ainda a serem determinados;

6.2. Quantificar a viabilidade da linhagem *pdr802* em DMEM com diferentes concentrações celulares iniciais para avaliação da concentração de Qsp1 na sobrevivência da linhagem;

6.3. Avaliar a relação entre a homeostase de cálcio e a formação de células gigantes em *C. neoformans* a partir da regulação de Pdr802:

6.3.1. Avaliar a expressão gênica global na linhagem selvagem de *C. neoformans* e no mutante nulo *pdr802* em condições de indução de células gigantes *in vitro*;

6.3.2. Avaliar a produção de células gigantes, viabilidade celular e concentração de cálcio citoplasmático em mutantes envolvidos na homeostase de cálcio (*pmc1*, *vcx1*, *pmc1vcx1*, *cch1*, *crz1*, *cna1*, *cnb1*) expostos a condições de indução *in vitro*;

6.3.3. Construir mutantes duplos e/ou de expressão induzida para descrição do mecanismo da interação da via da calcineurina e do fator de transcrição Pdr802 na formação de células gigantes em *C. neoformans*.

7. Anexo 1 – Manuscrito publicado junto ao periódico mSphere

A Predicted Mannoprotein Participates in *Cryptococcus gattii* Capsular Structure

Júlia Catarina Vieira Reuwsaat[1], Heryk Motta de Souza[1], Ane Wichine Acosta Garcia[1], Carolina Bettker Vasconcelos[1], Bárbara Machado Marques[1], Natália Kronbauer Oliveira[1], Jéssica Rodrigues[2], Patrícia Aline Grohns Ferrareze[1], Susana Frases[3], William Lopes[1], Vanessa Abreu Barcellos[1], Eamim Daidrê Squizani[1], José André Horta[4], Augusto Schrank[1,5], Márcio Lourenço Rodrigues[2,6], Charley Christian Staats[1,5], Marilene Henning Vainstein[1,5], Lívia Kmetzsch[5,7].

[1]Laboratório de Fungos de Importância Médica e Biotecnológica, Centro de Biotecnologia, Universidade Federal do Rio Grande do Sul, Porto Alegre, Brazil.

[2]Laboratório de Biologia Celular de Leveduras Patogênicas, Instituto de Microbiologia Paulo de Goés, Universidade Federal do Rio de Janeiro, Rio de Janeiro, Brazil.

[3]Laboratório de Ultraestrutura Celular Hertha Meyer, Instituto de Biofísica Carlos Chagas Filho, Universidade Federal do Rio de Janeiro, Rio de Janeiro, Brazil.

[4]Departamento de Biologia e Farmácia, Universidade de Santa Cruz do Sul (UNISC), Programa de Pós-Graduação em Promoção da Saúde, Santa Cruz do Sul, RS, Brazil.

[5]Departamento de Biologia Molecular e Biotecnologia, Universidade Federal do Rio Grande do Sul, Porto Alegre, Brazil.

[6]Centro de Desenvolvimento Tecnológico em Saúde, Fundação Oswaldo Cruz, Fiocruz, Rio de Janeiro, Brazil.

[7]Laboratório de Fungos de Importância Médica e Biotecnológica, Centro de Biotecnologia, Universidade Federal do Rio Grande do Sul, Porto Alegre, Brazil liviak@cbiot.ufrgs.br.

AMERICAN SOCIETY FOR MICROBIOLOGY | mSphere®

RESEARCH ARTICLE
Host-Microbe Biology

A Predicted Mannoprotein Participates in *Cryptococcus gattii* Capsular Structure

Julia Catarina Vieira Reuwsaat,[a] Heryk Motta,[a] Ane Wichine Acosta Garcia,[a] Carolina Bettker Vasconcelos,[a] Bárbara Machado Marques,[a] Natália Kronbauer Oliveira,[a] Jéssica Rodrigues,[b] Patrícia Aline Gröhns Ferrareze,[a] Susana Frases,[c] William Lopes,[a] Vanessa Abreu Barcellos,[a] Eamim Daidrê Squizani,[a] Jorge André Horta,[d] Augusto Schrank,[a,f] Marcio Lourenço Rodrigues,[b,e*] Charley Christian Staats,[a,f] Marilene Henning Vainstein,[a,f] Lívia Kmetzsch[a,f]

[a]Laboratório de Fungos de Importância Médica e Biotecnológica, Centro de Biotecnologia, Universidade Federal do Rio Grande do Sul, Porto Alegre, Brazil

[b]Laboratório de Biologia Celular de Leveduras Patogênicas, Instituto de Microbiologia Paulo de Goés, Universidade Federal do Rio de Janeiro, Rio de Janeiro, Brazil

[c]Laboratório de Ultraestrutura Celular Hertha Meyer, Instituto de Biofísica Carlos Chagas Filho, Universidade Federal do Rio de Janeiro, Rio de Janeiro, Brazil

[d]Departamento de Biologia e Farmácia, Universidade de Santa Cruz do Sul (UNISC), Programa de Pós-Graduação em Promoção da Saúde, Santa Cruz do Sul, RS, Brazil

[e]Centro de Desenvolvimento Tecnológico em Saúde, Fundação Oswaldo Cruz, Fiocruz, Rio de Janeiro, Brazil

[f]Departamento de Biologia Molecular e Biotecnologia, Universidade Federal do Rio Grande do Sul, Porto Alegre, Brazil

ABSTRACT The yeast-like pathogen *Cryptococcus gattii* is an etiological agent of cryptococcosis. The major cryptococcal virulence factor is the polysaccharide capsule, which is composed of glucuronoxylomannan (GXM), galactoxylomannan (GalXM), and mannoproteins (MPs). The GXM and GalXM polysaccharides have been extensively characterized; however, there is little information about the role of mannoproteins in capsule assembly and their participation in yeast pathogenicity. The present study characterized the function of a predicted mannoprotein from *C. gattii*, designated Krp1. Loss-of-function and gain-of-function mutants were generated, and phenotypes associated with the capsular architecture were evaluated. The null mutant cells were more sensitive to a cell wall stressor that disrupts beta-glucan synthesis. Also, these cells displayed increased GXM release to the culture supernatant than the wild-type strain did. The loss of Krp1 influenced cell-associated cryptococcal polysaccharide thickness and phagocytosis by J774.A1 macrophages in the early hours of interaction, but no difference in virulence in a murine model of cryptococcosis was observed. In addition, recombinant Krp1 was antigenic and differentially recognized by serum from an individual with cryptococcosis, but not with serum from an individual with candidiasis. Taken together, these results indicate that *C. gattii* Krp1 is important for the cell wall structure, thereby influencing capsule assembly, but is not essential for virulence *in vivo*.

IMPORTANCE *Cryptococcus gattii* has the ability to escape from the host's immune system through poorly understood mechanisms and can lead to the death of healthy individuals. The role of mannoproteins in *C. gattii* pathogenicity is not completely understood. The present work characterized a protein, Kpr1, that is essential for the maintenance of *C. gattii* main virulence factor, the polysaccharide capsule. Our data contribute to the understanding of the role of Kpr1 in capsule structuring, mainly by modulating the distribution of glucans in *C. gattii* cell wall.

KEYWORDS *Cryptococcus gattii*, capsular polysaccharide, mannoprotein

Received 12 January 2018 **Accepted** 2 April 2018 **Published** 25 April 2018

Citation Reuwsaat JCV, Motta H, Garcia AWA, Vasconcelos CB, Marques BM, Oliveira NK, Rodrigues J, Ferrareze PAG, Frases S, Lopes W, Barcellos VA, Squizani ED, Horta JA, Schrank A, Rodrigues ML, Staats CC, Vainstein MH, Kmetzsch L. 2018. A predicted mannoprotein participates in *Cryptococcus gattii* capsular structure. mSphere 3:e00023-18. https://doi.org/10.1128/mSphere.00023-18.

Editor Yong-Sun Bahn, Yonsei University

Address correspondence to Lívia Kmetzsch, liviak@cbiot.ufrgs.br.

* Present address: Marcio Lourenço Rodrigues, Instituto Carlos Chagas, Fundação Oswaldo Cruz (Fiocruz), Curitiba-PR, Brazil.

The sibling species *Cryptococcus gattii* and *Cryptococcus neoformans* are the main cause of cryptococcosis in animals and humans (1), a life-threatening disease with an annual incidence of nearly 280,000 cases (2). Globally, cryptococcal meningitis accounts for 15% of AIDS-related deaths and, if not properly threated, can cause up to 70% of the deaths of cryptococcosis patients (2). While *C. gattii* is mostly responsible for the infections of immunocompetent patients, *C. neoformans* has higher infection incidence in immunocompromised hosts (3). *C. gattii* infections were assumed to be restricted to tropical and subtropical areas, but the outbreak in 1999 on Vancouver Island, Canada, altered this view, confirming the presence of this species in temperate regions (4, 5). *C. gattii* is widespread in trees and soil, initiating human infection by the inhalation of spores or dried yeasts, which when they reach the lungs can spread through the bloodstream to the brain, causing meningitis (6).

During the host-pathogen interaction, *Cryptococcus* species use a repertoire of virulence strategies to survive and proliferate, including the production of melanin, secretion of enzymes such as phospholipase B and urease, as well as the production of a polysaccharide capsule that interacts with the cell wall (7). The capsule is considered the major cryptococcal virulence factor due to its immunosuppressive properties (8–12). It is composed of the polysaccharides glucuronoxylomannan (GXM) (90 to 95%) and galactoxylomannan (GalXM) (5 to 10%), with less than 1% of mannoproteins (MPs) (13, 14). Chitooligomers (15) and glucans (16), as well as some cytoplasmic proteins (heat shock proteins) (17), have also been identified as transitory components of the capsule, revealing the dynamics of this structure. *C. neoformans* GXM is the most characterized capsule component (18), and its functional characteristics are usually similar to those of *C. gattii* GXM (19). However, different GXM fractions produced by *C. gattii* and *C. neoformans* could develop distinct innate immune responses in host cells (20, 21), suggesting that *C. gattii* GXM is different from *C. neoformans* to some extent. It is also known that *C. neoformans* strains with mutations in gene products involved in galactose metabolism do not secret GalXM and are easily eradicated from the host, revealing the importance of this polysaccharide in the yeast pathogenicity (22).

The roles of mannoproteins in capsule structure and assembly are still not clear. However, their influence in the induction of T cell responses in the host is well established (23–25), indicating their potential as targets to immunotherapy. Mannoproteins are found in a large variety of fungi (26, 27), and their functions are closely related to cell wall structure (28, 29). Studies have demonstrated the function of mannoproteins in cryptococcal physiology or virulence. *C. neoformans* Cig1 is a mannoprotein that functions as a cell surface hemophore, and cells lacking *CIG1* displayed impaired growth in iron-limiting medium and a small capsule phenotype (30, 31). Moreover, the MP98 protein from *C. neoformans* was characterized as a chitin deacetylase that contributes to the maintenance of cell wall integrity (32). Despite their low abundance in the capsule, the role of mannoproteins in capsular architecture has never been established. This study determined that a *C. gattii* mannoprotein (Krp1) affects capsule assembly in the cell wall but does not influence yeast pathogenicity *in vivo*.

RESULTS

The predicted mannoprotein repertoire of *C. gattii*. In order to characterize the set of predicted mannoproteins encoded by *C. gattii* R265, an *in silico* approach was used to identify proteins with mannoprotein signatures, specifically, the presence of a signal peptide, a glycosylphosphatidylinositol (GPI) anchor, and serine-threonine-rich sites that would comprise the glycosylation site (33). Employing a combination of SignalP (34), PredGPI (35), and GlycoEP (36) analyses, the presence of 34 mannoprotein-coding genes in *C. gattii* R265 genome was predicted (see Table S1 in the supplemental material). Profile assignments employing InterProScan (37) led to the identification of diverse conserved domains in 20 of these predicted proteins, most of them related to enzymes acting on carbohydrates (Table S1). Among such mannoprotein-coding genes, CNBG_4278 is the only one with a Kelch structural domain signature, as revealed by the

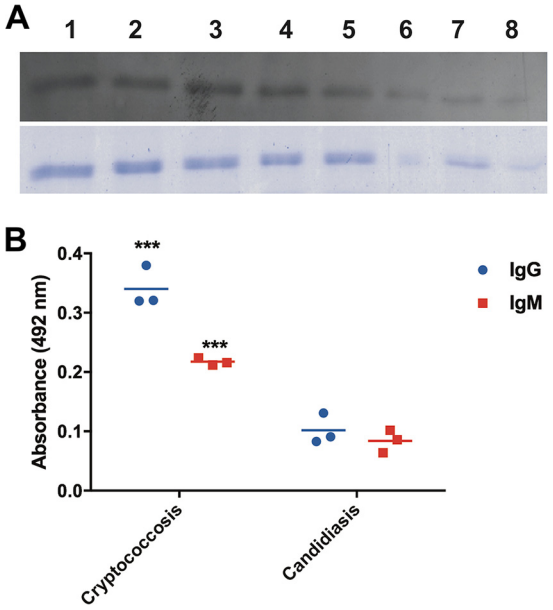

FIG 1 Recombinant Krp1 is antigenic. (A) Western blot. Purified recombinant truncated Krp1 (rKrp1t) expressed in *E. coli* was serially diluted (1:2) and probed with pooled sera from cryptococcal patients (top panel). SDS-PAGE mirror gel (bottom panel). (B) ELISA. One microgram of purified rKrp1t was probed with sera from patients with cryptococcosis and candidiasis. Results were analyzed by unpaired *t* tests. OD readings to determine IgG and IgM are shown. Values that are significantly different ($P < 0.001$) by *t* test are indicated by three asterisks.

superfamily database module of InterProScan. This domain is present in glyoxal and galactose oxidases, enzymes that interact with and modify carbohydrates (38). The CNBG_4278 ortholog in *C. neoformans* (CNAG_05595) was found in extracellular vesicles (EVs) known as "virulence bags" (39, 40), as well as in the cryptococcal secretome (41). Moreover, this gene was found to be differentially expressed in mutants for kinases that govern cell wall integrity (42). Hence, CNBG_4278 was characterized, hereafter described as Kelch repeat-containing protein 1 (Krp1). Despite the presence of a structural domain characteristic of Kelch domain-containing proteins, *C. gattii* Krp1 does not share similarity with these enzymes, not even with *Saccharomyces cerevisiae* and *Candida albicans* Kelch domain-containing protein (Kel1p) (Fig. S1).

Krp1 is antigenic but not essential for *C. gattii* virulence *in vivo*. Considering that the Krp1 ortholog from *C. neoformans* was found in the secretome, it was hypothesized that such a protein could elicit an immune response in the host. The recombinant Krp1 was produced in *Escherichia coli* to evaluate the antigenicity of the predicted mannoprotein Krp1. As the expression of recombinant full-length fungal mannoproteins generally displayed a low yield when expressed in prokaryotic systems (43), a truncated form (rKrp1t) was generated that lacked the signal peptide (first 20 amino acids) and the predicted GPI anchoring signal (last 30 amino acids). Due to the presence of a His_6 tag in the carboxy terminus, the recombinant protein was purified by cobalt affinity chromatography. The purified rKrp1t was serially diluted and submitted to Western blotting using pooled sera from patients with cryptococcosis. A strong recognition signal could be detected with all dilutions of rKrp1t, confirming the Krp1 antigenicity (Fig. 1A). Also, an enzyme-linked immunosorbent assay (ELISA) was performed to confirm the recognition specificity of the recombinant Krp1 using sera from patients infected by other fungal pathogens. Optical density (OD) readings using sera from cryptococcosis patients were at least five times higher (IgG) or three times higher (IgM) than those obtained with sera from patients with candidiasis (Fig. 1B). These results suggest that the predicted mannoprotein is produced during infection and can be recognized by the host.

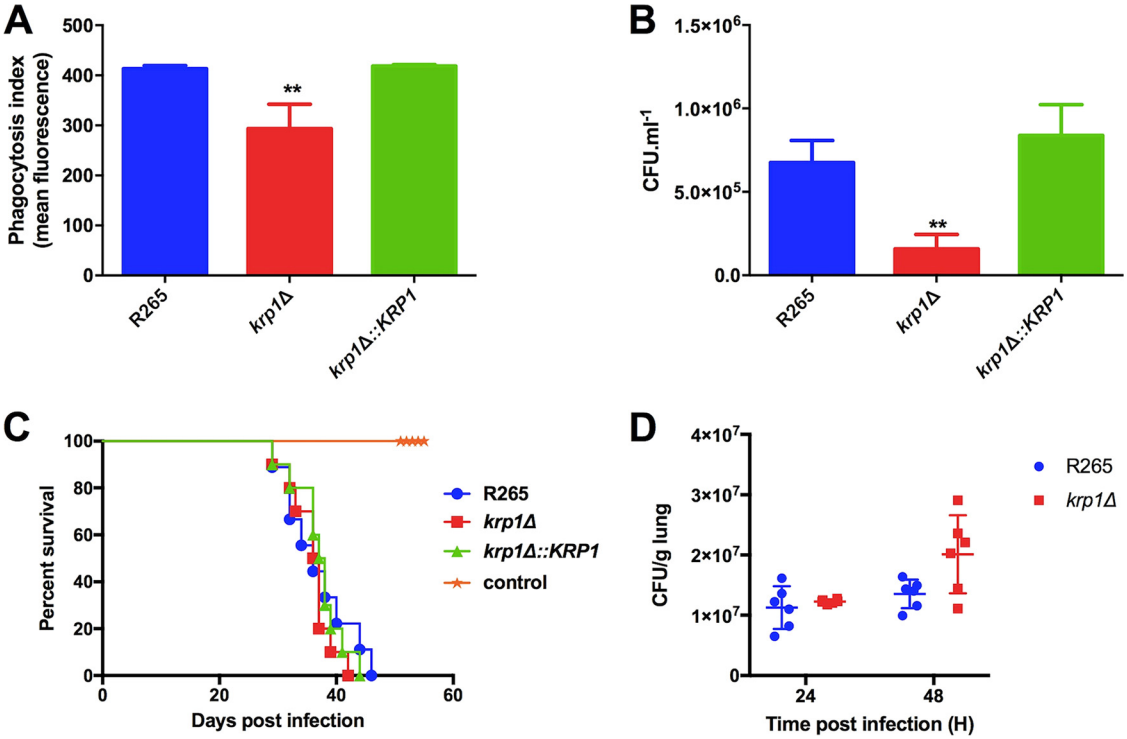

FIG 2 Deletion of the *KRP1* gene alters the yeast phagocytosis rate but is not necessary for the full virulence of *C. gattii*. (A) Phagocytosis index was assessed by flow cytometry after 2 h of interaction of FITC-labeled WT, *krp1*Δ, and *krp1*Δ::*KRP1* strains of cryptococcal cells with J774.A1 macrophages. (B) After 2 h of interaction of WT *C. gattii*, *krp1*Δ, and *krp1*Δ::*KRP1* cells with J774.A1 cells, murine cells were lysed, and the numbers of CFU per milliliter were determined. Data are shown as the means plus standard deviations (SD) for three biological replicates. One-way analysis of variance (ANOVA) followed by posthoc Dunnett test was performed. Values that are significantly different ($P < 0.01$) from the value for the wild-type strain (R265) are indicated by two asterisks. (C) Virulence assay in an intranasal inhalation infection model using BALB/c mice. (D) Fungal load in mouse lungs collected 24 or 48 h postinfection with *C. gattii* WT and *krp1*Δ cells.

To understand the role of Krp1 in *C. gattii* virulence, *krp1*Δ null mutant and *krp1*Δ::*KRP1* complemented mutant strains were constructed (Fig. S2). As macrophages are the host's first line of defense against cryptococcal cells, the outcome of wild-type (WT), mutant, and complemented strains from *in vitro* interactions with phorbol myristate acetate (PMA)-activated J774.A1 macrophages were evaluated. The phagocytosis index of *krp1*Δ cells was lower than those of the WT and complemented strains as seen after 2 h of coincubation either by flow cytometry and by cryptococcal CFU determination analyses (Fig. 2A and B), suggesting that the absence of Krp1 altered the association of cryptococcal cells with macrophages, at least at the early stages of interaction. This was also confirmed by a Giemsa assay (Fig. S3). In order to evaluate whether the lower phagocytosis index of *krp1*Δ cells would reflect an altered virulence, BALB/c mice were intranasally infected with the WT, mutant, and complemented strains. No significant differences in the survival of the mice infected with the different *C. gattii* strains were observed (Fig. 2C), suggesting that Krp1 is not fundamental for cryptococcal virulence. In order to evaluate whether the reduced phagocytosis index determined *in vitro* would be observed *in vivo*, histopathological analysis was conducted using lungs of mice infected with WT and mutant strains. We did not detect a statistically significant difference in the lung fungal burdens from mice infected with the WT or *krp1*Δ strains, either at 24 or 48 h postinfection (Fig. 2D). In addition, histopathological analyses were conducted using lungs collected from mice infected with the WT or *krp1*Δ strain. After 24 h of infection, lungs presented mild neutrophilic and lymphohistiocytic inflammatory infiltrate, independent of the strain used to infect the mice (Fig. S4). These results confirm that the absence of Krp1 did not altered the pathological properties of cryptococcal cells.

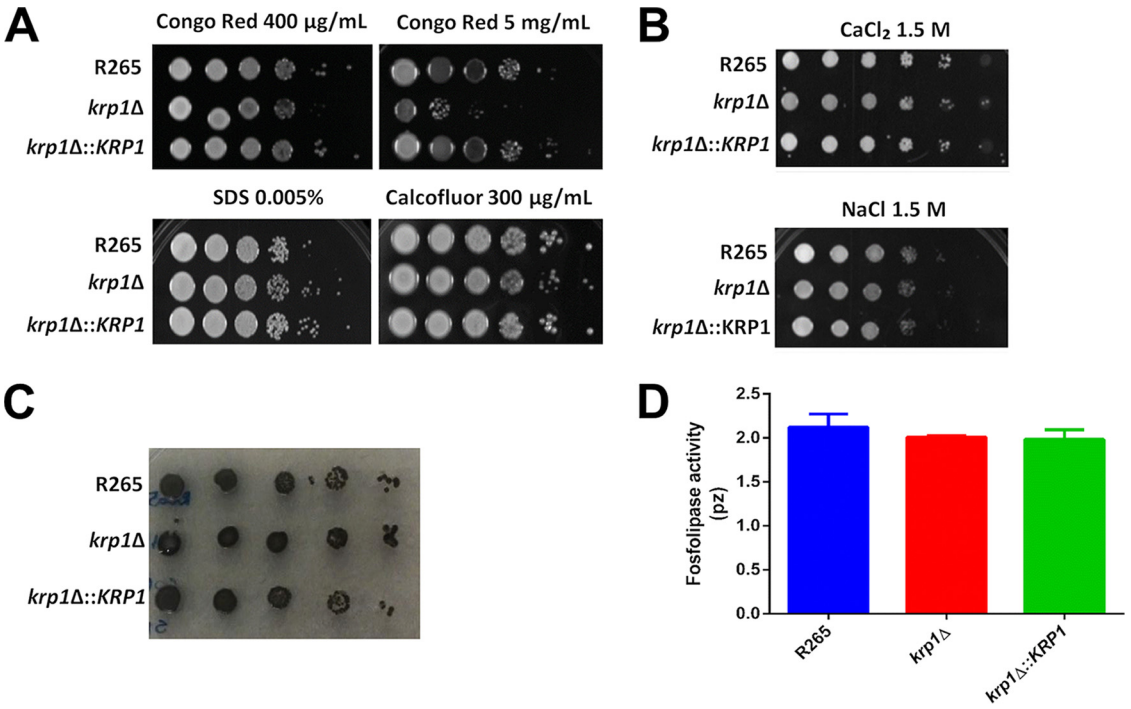

FIG 3 The absence of Krp1 led to defects in the cell wall but does not influence *C. gattii* cell wall-related virulence factors. (A and B) Growth test was performed by plating 3 μl of 10-fold serially diluted suspension of WT, *krp1*Δ, and *krp1*Δ::*KRP1* strains onto YPD agar supplemented with cell wall stressors (Congo red, SDS, and Calcofluor white) (A) or high-osmolarity stressors ($CaCl_2$ and NaCl) (B) as indicated. (C and D) In addition, these dilutions were also spotted onto minimal medium agar supplemented with L-DOPA to evaluate melanization (C) and agar containing egg yolk emulsion to evaluate phospholipase activity (D).

Krp1 absence affects the *C. gattii* cell wall architecture. To further investigate the lower phagocytosis index of *krp1*Δ mutant cells in the early stages of the interaction with macrophages, cell wall alterations that would influence cryptococcal recognition by the host were analyzed. *krp1*Δ cells displayed impaired growth in the presence of high doses of Congo red (Fig. 3A), a dye that may interact with nascent glucan chains and disrupts the balanced cell wall polymerization and crystallization (44). However, all strains grew similarly in the presence of the membrane stressor sodium dodecyl sulfate (SDS) and Calcofluor white (Fig. 3A), which interacts with nascent chitin chains (44, 45). Also, no growth differences were observed under high-osmolarity conditions (Fig. 3B). We also investigated whether the melanization process could be influenced by Krp1 knockout, as cell wall defects influence the deposition of melanin (32). No differences in melanin synthesis and/or deposition could be observed in WT, mutant, and complemented strains cultured in the presence of L-3,4-dihydroxyphenylalanine (L-DOPA) (Fig. 3C). Moreover, the levels of phospholipase B1 activity, an essential virulence factor from *Cryptococcus*, associated with the cell wall-promoting fungal membrane biogenesis and remodeling (46), were also similar in the strains tested (Fig. 3D).

The misdistribution of some cell wall components, including chitooligomers, was shown to be involved in the alteration of the phagocytosis index of *C. neoformans* cells (47). The distribution of some cell wall components was evaluated in the WT, *krp1*Δ, and *krp1*Δ::*KRP1* strains cultured under capsule-inducing conditions. As observed by India ink counterstaining, all strains produced similar capsules with regard to morphology and size (Fig. 4A). Using fluorescence-labeled versions of wheat germ agglutinin (WGA) and concanavalin A (ConA) lectins, the distribution of chitooligomers and α-D-mannosyl groups, respectively, was evaluated. There were no significant differences in the cell wall WGA or ConA staining pattern among the tested strains (Fig. 4B and C). In addition, probing such mutants with the anti-GXM monoclonal antibody (MAb) 18B7 also revealed a similar staining pattern (Fig. 4B and C). Together, these results indicate that

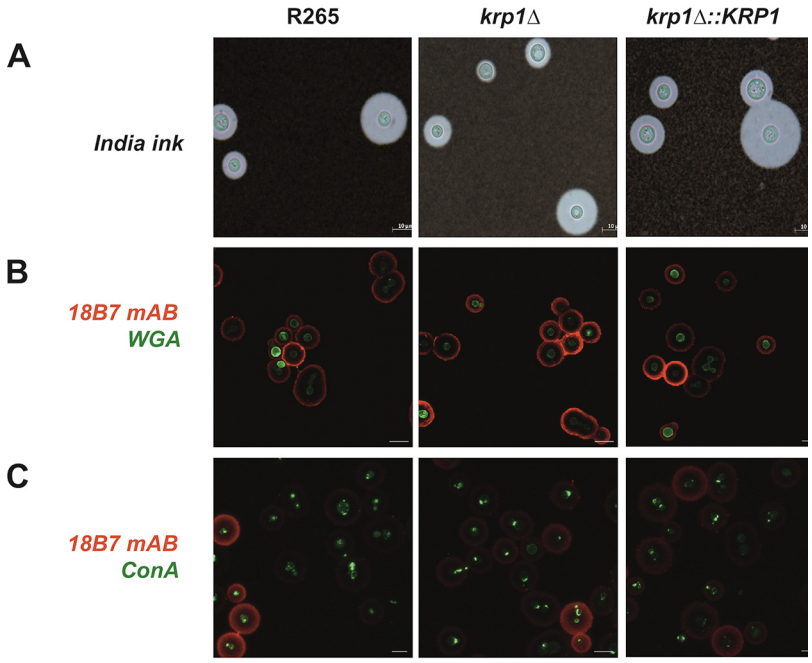

FIG 4 The absence of Krp1 does not alter capsule production nor chitooligomers and mannose distribution in cryptococcal cell surface. (A) India ink staining of *C. gattii* cells grown under capsule-induced conditions. Bars, 10 μm. (B and C) *C. gattii* cells were grown under capsule-induced conditions supplemented with Congo red (625 μg/ml) and labeled with the anti-GXM monoclonal antibody 18B7 to detect capsule (red) and with WGA (green) (B) to detect chitooligomeric structures. Alternatively, such cells were also labeled with the lectin ConA (green) (C) to detect mannosyl residues. Images were captured by a fluorescence confocal microscope. Micrographs were taken at a magnification of ×630.

Krp1 is important for glucan structuration in the *C. gattii* cell wall but does not influence the distribution of important cell wall components and capsule size.

***KRP1* disruption influences interactions of capsular polysaccharides.** As no differences in the distribution of cell wall components were observed that could explain the low levels of *krp1*Δ phagocytosis by macrophages, the biophysical and serological proprieties of the antiphagocytic capsule components were determined. As previously demonstrated, capsule size did not differ among the strains analyzed (Fig. 5A). However, deletion of the *KRP1* gene altered the amount of extracellular GXM, as higher levels of the polysaccharide were detected in *krp1*Δ culture supernatants (Fig. 5B). To further investigate possible alterations in GXM recovered from the different strains that could explain the higher levels of GXM not attached to the cell wall, the serological reactivity of cell-associated and extracellular polysaccharide fractions was evaluated using MAbs that recognize distinct epitopes in the GXM molecule. No significant differences in immunoreactivity to distinct antibodies (MAbs 18B7, 2D10, and 13F1) were found between cell-associated and released GXM recovered from the strains analyzed (Fig. 5C to H).

In order to evaluate possible defects of *krp1*Δ-produced polysaccharides in cell wall attachment, the morphological aspects of GXM incorporation by acapsular *C. neoformans cap67* cells were evaluated by fluorescence microscopy (Fig. 6A). Extracellular polysaccharides were purified from WT, *krp1*Δ, and *krp1*Δ::*KRP1* strains cultured under capsule-inducing conditions and fed to *C. neoformans cap67* cells. Fluorescence microscopy employing the anti-GXM MAb 18B7 did not reveal significant differences in the incorporation of GXM produced by the mutant strain and the WT (Fig. 6A). These results are in agreement with no significant differences among the elemental composition of capsular GXM produced by *krp1*Δ and WT cells (Fig. 6B). As cells lacking Krp1 displayed altered GXM concentration in secreted polysaccharides, it was hypothesized that Krp1 could also influence the physical characteristics of polysaccharide fibers.

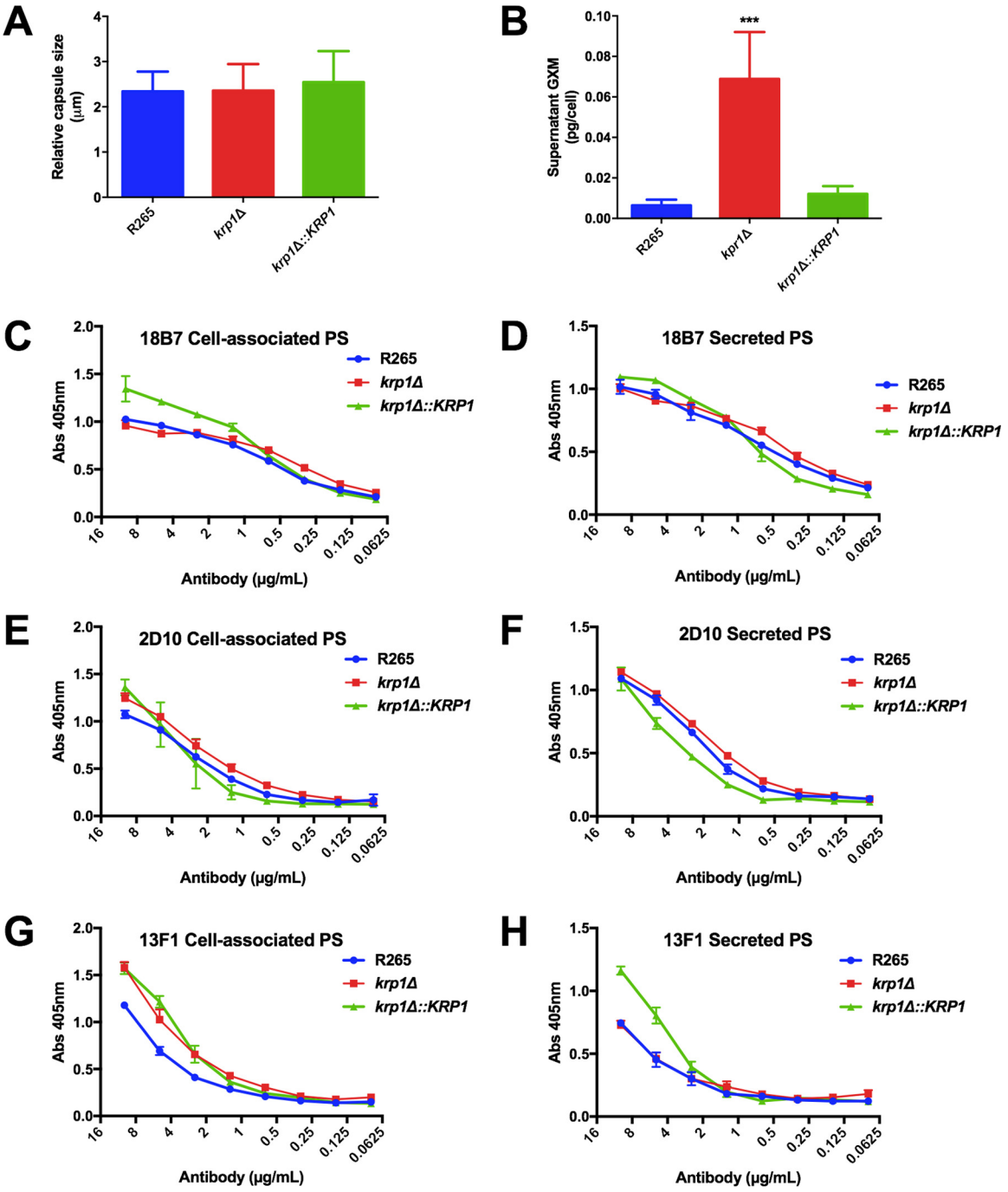

FIG 5 *KRP1* disruption does not affect capsule size or GXM serological proprieties but causes secretion into the extracellular space. (A) Capsule size was measured as the ratio of capsule size to cell diameter from at least 50 cells. (B) Secreted polysaccharides were quantified by ELISA with anti-GXM 18B7. Data are shown as the means plus standard deviations (SD) (error bars) for three biological replicates. One-way ANOVA followed by posthoc Dunnett test was performed. Values that are significantly different ($P < 0.001$) from the value for the wild-type strain (R265) are indicated by three asterisks. (C to H) Serological tests with MAbs 18B7, 2D10, and 13F1 of cell-associated and secreted polysaccharides (PS) from WT and *krp1* null or complemented mutants. Data are shown as the means ± SD for three biological replicates.

Dynamic light scattering (DLS) measurements were used to determine the size distribution of polysaccharide fibers recovered from WT, *krp1*Δ, and *krp1*Δ::*KRP1* strains. While WT cell-associated polysaccharides present a clear bimodal distribution size, ranging from 700 to 820 nm (Fig. 6C), the absence of *KRP1* disorganized the capsule polysaccharide size distribution, leading to a scattered pattern (Fig. 6D). It is noteworthy that such a phenotype was not completely restored by complementation of the WT

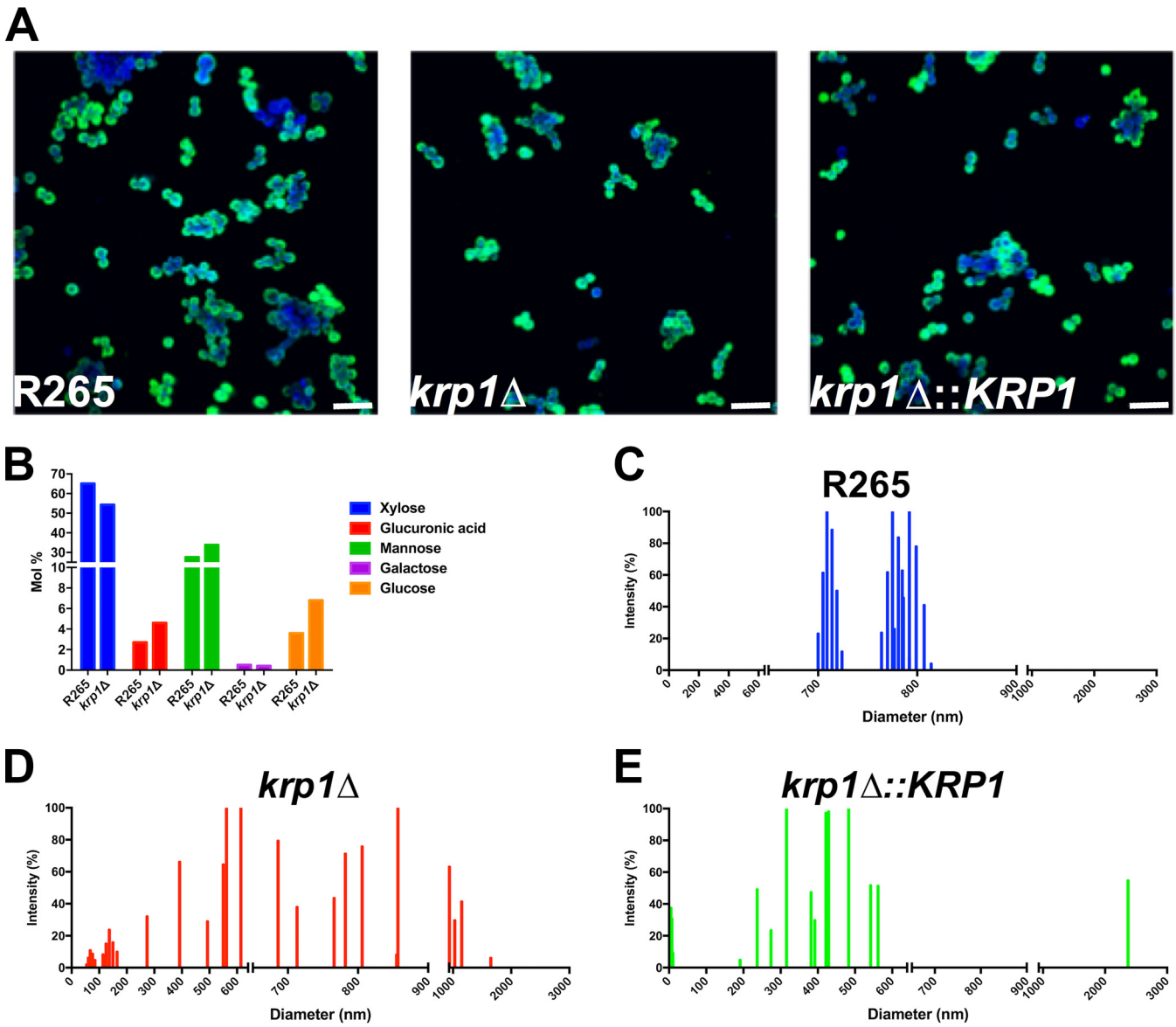

FIG 6 Morphological and structural proprieties of cell-associated and secreted polysaccharides from *C. gattii* strains. (A) Capsule transfer assay. *C. neoformans cap67* cells were grown in YPD medium and incubated with secreted polysaccharides from WT and mutant *C. gattii* strains. For confocal microscopy, *C. neoformans* cells were labeled with Calcofluor white (blue) and MAb 18B7 (green). Bars, 20 μm. (B) Cell-associated polysaccharides were isolated from WT and *krp1*Δ cells, and their elemental composition was determined by GC-MS. (C to E) Cell-associated polysaccharide molecular dimension determination of WT, *krp1*Δ, and *krp1*Δ::*KRP1* strains using DLS analysis. The cells were cultured in minimal medium for 72 h, and the cell-associated polysaccharides were extracted using DMSO. Each graph displays the range of polysaccharide fiber sizes representative of three independent analyses.

gene (Fig. 6E), possibly due to defects in the proper expression of the complementation *KRP1* cassette, which is integrated in an ectopic locus.

To further explore such differences, field emission gun scanning electron microscopy (FEG-SEM) analysis of WT, *krp1*Δ, and *krp1*Δ::*KRP1* strains was performed. A dense array of capsular fibers could be observed in all strains analyzed (Fig. 7A). However, the fibers in the *krp1*Δ cell surface tended to be thicker than those produced by the WT strain ($P < 0.0001$; Fig. 7B). This phenotype was partially reconstituted in the complemented strain ($P < 0.01$; Fig. 7B).

In order to gain insights from the physical-chemical interactions that would be altered in the cells lacking *KRP1*, we performed zeta potential determinations using polysaccharide (PS) isolated from cells, as well from the supernatant. We observed an increased zeta potential in both PS fractions recovered from cells lacking Krp1, suggesting that this mannoprotein is involved in the proper maintenance of capsular

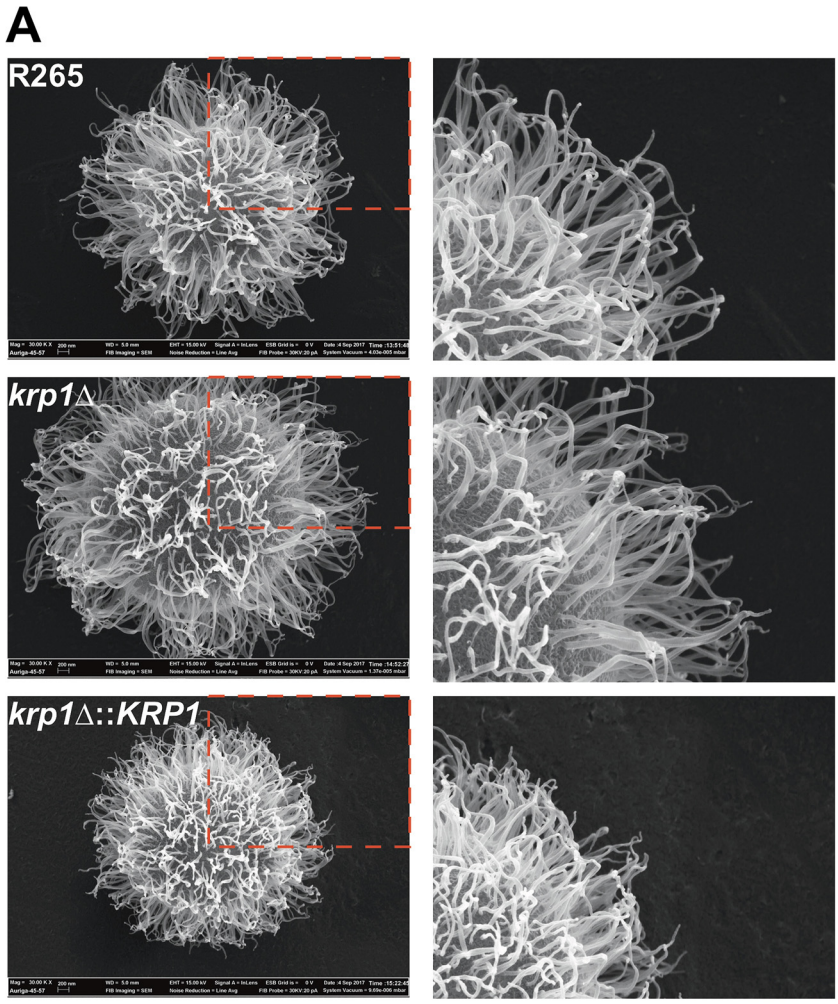

FIG 7 Morphological analysis of WT and Krp1 mutants. (A) FEG-SEM analysis of representative cells belonging to the different genotypes. The right panels represent magnified views of the capsular structures outlined by red broken lines in the left panels. (B) Fiber thickness measured from 20 to 30 cells of WT, *krp1*Δ, and *krp1*Δ::*KRP1* strains. One-way ANOVA followed by posthoc Dunnett test was performed. Values that are significantly different from the value for the wild type (R265) are indicated by asterisks as follows: ****, $P < 0.0001$; **, $P < 0.01$.

charge (Fig. 8). Altogether, these results suggest that Krp1 may prompt interaction of polysaccharides of the *C. gattii* capsule.

DISCUSSION

Mannoproteins are important structural constituents of fungal cell walls (48) and components of the cryptococcal polysaccharide capsule (14). Despite some evidence of

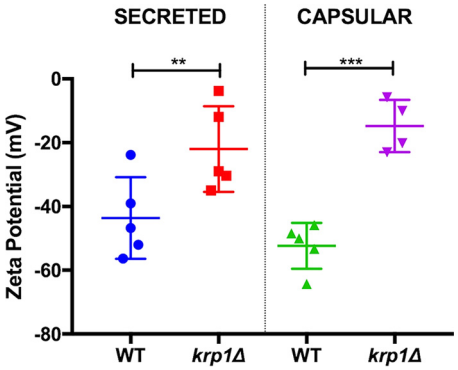

FIG 8 The absence of Krp1 led to altered net charge in capsular polysaccharides. Cells were cultured in minimal medium for 72 h. The cell-associated and secreted polysaccharides were isolated, and their net charge was determined using a zeta potential analyzer. Student's *t* test was performed to evaluate statistical differences (**, $P < 0.01$; ***, $P < 0.001$).

the immunogenicity of these proteins (33, 49), little is known about their role in capsule structuring. Bioinformatic analysis of the predicted proteomes of two clinically important *Cryptococcus* species identified 43 predicted mannoproteins encoded by *C. neoformans* H99 genes. This is in accordance with a previous report that found 53 serine-threonine-rich proteins containing a GPI anchor and signal peptide in the *C. neoformans* var. *neoformans* JEC21 predicted proteome (33). For *C. gattii*, a total of 36 mannoproteins were predicted. Most of the predicted mannoproteins in both species are annotated as hypothetical proteins, with a small proportion of them spanning conserved domains in their sequences. Only two predicted *C. gattii* mannoproteins did not display the *C. neoformans* ortholog, because of the loss of the GPI anchor (see Table S1 in the supplemental material). Similarly, four predicted *C. neoformans* mannoproteins did not have the *C. gattii* ortholog identified as a mannoprotein due to the loss of the signal peptide or GPI anchor (Table S2), including MP88 and *CDA1*. Also, *C. neoformans* genes encode five mannoproteins that do not have an ortholog in *C. gattii* (Table S2). As expected, more than 40% of the predicted mannoproteins do not possess conserved domains, and the majority of the mannoproteins with conserved domains have evidence of carbohydrate modifications (Tables S1 and S2).

The predicted mannoprotein characterized in this study (Krp1) presents a predicted folding found in Kelch repeats, a domain usually associated with galactose or glyoxal oxidases (50, 51) and related to altered cell fusion and morphology in *S. cerevisiae* and *C. albicans* (52). However, our analysis did not reveal conservation among cryptococcal Krp1 and other Kelch repeat-containing proteins from diverse fungal species (Fig. S1). It is noteworthy that the Krp1 ortholog in *C. neoformans* (CNAG_05595) was detected in the secretome and extracellular vesicles (40, 41, 53). As proteins associated with capsule structure were detected in the extracellular space (54), it is possible that Krp1 could also be involved in this process.

Mannoproteins have a potential importance in immunity-based strategies to control cryptococcosis due to their role in T cells and the humoral induction response in the host (55). This study showed that the recombinant Krp1 expressed in *E. coli*, even without glycosylation, was recognized by sera from cryptococcosis patients. The presence of epitopes in the protein sequence irrespective of posttranslational modifications (PTMs) revealed by Western blot analysis is evidence that Krp1 could elicit an immune response. However, at this moment, it is not possible to evaluate whether the native Krp1 would elicit a more intense immune response. It is important to note that such characteristics could also be observed for other *C. neoformans* mannoproteins (56), suggesting the existence of an epitope set that would work without any PTMs. The recombinant Krp1 (rKrp1) was not fully recognized by sera from patients with candidiasis, an important feature for specific cryptococcal antigens that could serve for diagnosis. However, a more in-depth analysis must be performed with sera from

patients infected with different pathogens to confirm the specificity of rKrp1 recognition as a cryptococcal antigen. Importantly, the serological reactivity of rKrp1 with patient sera suggests its production during infection.

Cells lacking the *KRP1* gene displayed impaired phagocytosis by macrophages, at least in the initial stages of coincubation. Cryptococcal uptake by phagocytes is dependent on the recognition of pathogen-associated molecular patterns (PAMPs) present in the yeast cell surface by pattern recognition receptors (PRRs) on host cells (57). Cryptococcal PAMPs include capsule- and cell wall-derived constituents as well as melanin (57). However, one of the several capsule functions is the capability to mask the PAMPs, reducing the recognition of fungal cells by macrophages (58). The first hypothesis for impaired phagocytosis of *krp1*Δ cells was a possible cell wall defect that could have modified the structuration of PAMPs. In line with these assumptions, null mutant cells were found to display higher sensitivity to the cell wall stressor Congo red, a dye that interacts with beta-glucan nascent chains and impairs the activity of assembly enzymes that connect chitin to it (45). As *krp1*Δ cells do not present variations in the distribution of surface components directly associated with host defense, the second hypothesis for its decreased rate of phagocytosis by macrophages was related to its capsule structure and assembly. Even without capsule length differences as measured by the penetration of India ink molecules, *krp1*Δ cells present much more GXM secreted in the culture supernatant. GXM is a known immunoregulatory molecule (58), and the reduced phagocytosis rate of *krp1*Δ cells could be associated with the higher GXM present in the supernatant, which in turn would modulate the activity of macrophages. We do not associate the lower phagocytosis of *krp1*Δ cells to PAMPs as mannose or chitooligomeric structures, as no differences could be observed in cells lacking the *KRP1* gene compared to WT cells. Taken together, these results suggest that higher GXM release modulates macrophage activity, at least during the initial interaction of cryptococci with host cells. Longer incubation periods would buffer this difference by the possible compensatory activity of other proteins. However, this hypothesis needs to be experimentally validated. It is important to note that Krp1 is possibly associated with the onset of infection, demonstrating that alterations in the surfaces of *krp1*Δ cells interfere with the steady activation of macrophages. Nonetheless, Krp1 is not important for *C. gattii* virulence in a murine model of cryptococcosis, which adds a layer of complexity to the function of mannoproteins.

The mechanisms by which capsular components associate with the cryptococcal cell wall in order to build the capsule are still under investigation, but the clear participation of glucans and chitosan has been described (59–62). The *Cryptococcus* cell wall is composed of β-1-3- and β-1-6-glucans, α-1,3-glucans, chitin, chitosan, melanin, glycoproteins and plasma membrane-derived glucosylceramides (63, 64). The innermost part is formed by parallel fibers composed of β-glucans, chitin, and when present, melanin. The outermost layer of the wall is mainly composed of α- and β-glucans, forming a more particulate network (65). Unlike other fungi, *C. neoformans* is composed of more molecules of β-1-6-glucans than β-1-3-glucans (18). Even without proving the direct contact of Krp1 with the cryptococcal capsule, there is evidence to suggest that Krp1 is involved in GXM fiber structuration to the cell wall. (i) Cells lacking Krp1 were hypersensitive to the β-glucan stressor Congo red. (ii) The GXM content of culture supernatants was altered due to the absence of Krp1. (iii) *C. neoformans cap67* cells, which have a Krp1 ortholog, were capable of binding extracellular polysaccharides released by *C. gattii krp1*Δ cells. (iv) Cell-associated cryptococcal polysaccharide diameter and thickness are influenced by the presence of Krp1. Polysaccharide thickness has recently been linked with capsular architecture and pathogenesis (66). Increased fiber thickness is indicative of higher levels of GXM self-aggregation, but other possibilities cannot be ruled out. For instance, altered carbohydrate composition (67) and or branching (68) can affect the thickness of cryptococcal polysaccharide fibers. On the basis of the relatively subtle differences between WT and mutant fibers, as well as of the partial reconstitution of the phenotype in complemented cells, it is still impossible to establish the reasons behind the altered fiber thickness. However, we believe that it is

appropriate to propose that this parameter be included in the analysis of the multiple factors connecting capsular structure with pathogenesis in *Cryptococcus*.

The *Cryptococcus* cell wall matrix is structured by the activity of extracellular cross-linking enzymes that covalently bind carbohydrate polymers and glycoproteins (48) that prepare the structure for capsule attachment. The *Cryptococcus* capsule grows by enlargement of secreted polysaccharide molecules (67), usually secreted by extracellular vesicles, and aggregate in the presence of divalent cations (69). Also, the *C. neoformans* Krp1 ortholog was previously detected in the secretome and extracellular vesicles (39–41). Here, we report the role of Kpr1 in *C. gattii* capsule structuring, mainly by modulating the distribution of glucans in the yeast cell wall.

MATERIALS AND METHODS

Fungal strains, plasmids, and media. The *Cryptococcus gattii* R265 strain used in this study was kindly provided by Wieland Meyer (The University of Sydney, Australia). Plasmid pDNORNAT, which contains the nourseothricin marker cassette, was previously constructed by our group (70). Plasmid pJAF15, which contains the hygromycin resistance marker cassette was a generous gift of Joseph Heitman (Duke University, Durham, NC, USA). The strains were maintained on YPD agar (2% dextrose, 2% peptone, 1% yeast extract, and 1.5% agar). YPD plates containing nourseothricin (100 μg/ml) were used to select *C. gattii* mannoprotein deletion transformants (*krp1*Δ), and YPD plates containing hygromycin (200 μg/ml) were used to select *C. gattii* mannoprotein reconstituted transformants (*krp1*Δ::*KRP1*).

Bioinformatic analysis. The predicted proteomes of *C. gattii* R265 and *C. neoformans* H99 were retrieved from the Broad Institute (71–73) and now available at the FungiDB database (http://fungidb.org/fungidb/). SignalP was used for signal peptide prediction (34), PredGPI was used for glycosylphosphatidylinositol (GPI) anchor prediction (35), and GlycoEP standard was used for O-glycosylation analysis (36). The search for conserved domains was performed using InterProScan (https://www.ebi.ac.uk/interpro/search/sequence-search). For phylogenetic inference, *KRP1* sequence (CNBG_4278) and its orthologs (CGBL_3040C, CNAG_05595, CNH_02380, and CNBL_2400) obtained from FungiDB (http://fungidb.org/fungidb/), were added to sequences of galactose oxidases and glyoxal oxidases described by Yin and colleagues (38). The sequence alignment was performed in MAFFT v7 server with default parameters. The evolutionary model for amino acid substitutions was determined by ProtTest v3.4.2. The tree was constructed with MEGA 6.0 and maximum likelihood method with a bootstrap of 1,000 replicates.

Recombinant expression of Krp1. For expression in *E. coli*, the modified coding sequence of the *KRP1* gene (without signal peptide and GPI anchor site, which refers to amino acids 21 to 381 of the primary sequence) was cloned into pET-23D(+) between the sites of BamHI and HindIII (Invitrogen Corp., Carlsbad, CA, USA). Cloning was confirmed by cleavage and DNA sequencing. For the expression of the recombinant mannoprotein, the *E. coli* BL21(DE3) strain was transformed with the p*LYSs* plasmid, and protein expression was induced with lactose (20 g/liter) for 3 h. Purification was conducted under denaturing conditions with HiTrap immobilized metal affinity chromatography (IMAC) (GE Healthcare Life Sciences) charged with 100 mM $CoCl_2$. Buffers with increasing concentrations of imidazole (50 mM Na_2HPO_4, 300 mM NaCl, 8 M urea, and 10 to 500 mM imidazole) were used for elution of the recombinant protein from the IMAC column.

Western blotting and ELISA with patient sera. The serological properties of recombinant Krp1 were evaluated by Western blotting and ELISA using sera from individuals diagnosed with cryptococcosis. For Western blotting, the purified truncated recombinant Krp1 (rKrp1t) fraction was separated by SDS-PAGE, transferred to a polyvinylidene fluoride membrane, and probed with pooled sera from patients with cryptococcosis at a dilution of 1:10. Detection was performed using a Pierce ECL Western blotting substrate (Thermo Fisher Scientific) according to the manufacturer's instructions using anti-human IgG conjugated to peroxidase. For ELISA, a total of 1 μg of purified rKrp1t was used to sensitize ELISA microplates (BD Falcon 3912) and probed with sera from patients with cryptococcosis and candidiasis for cross-reactivity evaluation at a dilution of 1:200. The IgG and IgM conjugates were quantified using ZyMax goat anti-human IgG H+L and horseradish peroxidase (HRP)-conjugated goat anti-human IgM secondary antibodies according to the manufacturer's instructions.

Disruption and complementation of *KRP1*. Disruption of the *KRP1* gene was achieved by the Delsgate methodology (74). The 5′ and 3′ *KRP1* flanks (781 bp and 771 bp, respectively) were PCR amplified and purified from agarose gels (PureLink quick gel extraction kit; Invitrogen, Germany). *Double-joint* PCR with 1 ng of each fragment was carried out, resulting in a fragment of 1,552 bp. Approximately 200 ng of pDONRNAT and 100 ng of each PCR product were submitted to BP clonase reaction, according to the manufacturer's instructions (Invitrogen, Carlsbad, CA). The product of this reaction was transformed into *E. coli* TG-2. After confirmation of the correct deletion construct, the plasmid was linearized with I-SceI prior to *C. gattii* biolistic transformation (75). The transformants were screened by colony PCR, and the deletion was confirmed by Southern blot and semiquantitative reverse transcription-PCR (RT-PCR) analysis. For complementation, a nearly 3.4-kb genomic PCR fragment containing the wild-type *KRP1* gene was cloned into the EcoRV site of pJAF15. The resulting plasmid was used for *krp1*Δ strain transformation. Genomic insertion of the complemented gene was confirmed by Southern blotting and semiquantitative RT-PCR analysis. The primers used in constructing these plasmids are listed in Table S3 in the supplemental material.

Macrophage assays. Phagocytosis assays were conducted to evaluate the susceptibility of the mutant strains to macrophage antifungal activity. One day before the phagocytosis test, an aliquot of 100,000 J774.A1 cells in DMEM (Dulbecco's modified Eagle medium) supplemented with 10% fetal bovine serum (FBS) was seeded into 96-well culture plates and cultivated for 24 h at 37°C and 5% CO_2. The *C. gattii* strains were inoculated into YPD and allowed to grow at 18 h at 30°C. Then, *C. gattii* cells were washed three times with phosphate-buffered saline (PBS) and counted. A total of 10^7 cells of each strain were opsonized with antiglucuronoxylomannan (anti-GXM) monoclonal antibody (MAb) 18B7 (final concentration of 1 μg/ml) and incubated for 1 h at 37°C. At the same time, macrophage cells were washed once with warm PBS and incubated in FBS-free DMEM with 5 nM phorbol myristate acetate (PMA) for activation for 2 h. Then, macrophages were exposed to yeast cells at a ratio of 1:10 and incubated for 2 h at 37°C and 5% CO_2. At the end of incubation, the wells were washed three times with warm PBS, the macrophage cells were lysed with sterile ice-cold water, and subsequently plated on YPD plates for CFU determination. For the Giemsa assay, at the end of interaction, macrophage cells were fixed with methanol and stained with Griess for 15 min at room temperature. Cells were visualized using a Zeiss Axiovert 200 inverted fluorescence microscope equipped with an AxioCam MRc camera (Carl Zeiss, Jena, Germany). The images were acquired using AxioVision Rel 4.8 software. For flow cytometry analysis, after opsonization, yeast cells were labeled with fluorescein isothiocyanate (FITC) (Sigma). Murine macrophage cells were cultured in a 12-well culture plate. After 2-h incubation, the wells were washed with warm PBS, and trypan blue was added to each well to quench the fluorescence of labeled yeast attached to the outer membranes of the macrophages. Macrophages were detached from the plate using a cell scraper and analyzed by flow cytometry (Millipore Guava software). The phagocytosis index was determined as the ratio of internalized cryptococcal cells to the number of macrophage cells.

Virulence assays. Virulence studies were conducted according to a previously described intranasal inhalation infection model (76, 77) using 10 female BALB/c mice (approximately 4 weeks old) for each strain. Mice were infected with 10^5 yeast cells suspended in 50 μl of PBS and monitored daily. Kaplan-Meier analysis of survival was performed to evaluate survival differences. For determination of the lung fungal burden, mice ($n = 6$) were infected with 10^7 yeast cells. After 24 and 48 postinfection, the animals were euthanized, and the lungs were aseptically excised. The tissues were homogenized in PBS. After removal of host cell debris, the resulting suspensions were plated on YPD for CFU determination.

Histopathology. The lungs of mice infected with wild-type (WT) and *krp1*Δ cells were aseptically collected 24 h postinfection and fixed in 10% neutral buffered formalin. All lungs were then embedded in paraffin, cut into 5-μm-thick slices, and stained with hematoxylin and eosin. All analyses were by Axys Análises Diagnósticos Veterinário (Porto Alegre, Brazil). All slides were examined by light microscopy.

Phenotypic characterization assays. For phenotypic characterization, WT, null, and complemented strains were grown on YPD medium for 16 h, washed with PBS, and adjusted to a cell density of 10^7 cells/ml. The cell suspensions were serially diluted 10-fold, and 3 μl of each dilution was spotted onto YPD agar supplemented with the cell wall stressor Congo red (400 μg/ml and 5 mg/ml), Calcofluor white (300 μg/ml), or SDS (0.005%) (45) and with the salts NaCl (1.5 M) and $CaCl_2$ (1.5 M) (78). The plates were incubated for 2 days at 30°C and photographed. The solid melanization test was performed as described above, mixing 10 ml of 2× minimal medium (2 g/liter L-asparagine, 1 g/liter $MgSO_4 \cdot 7H_2O$, 6 g/liter KH_2PO_4, 2 g/liter thiamine, and 2 mM L-3,4-dihydroxyphenylalanine [L-DOPA]) with 10 ml of 2% agar-water per plate. For the phospholipase test, cells of all strains were spotted in agar containing egg yolk emulsion at a concentration of 8%. After 96 h of incubation at 30°C, the phospholipase activity (pz) was measured as the ratio of the colony diameter by the precipitation zone generated.

Microscopy. Cell surface morphology was analyzed after incubation of yeast cells with Calcofluor white, the monoclonal antibody 18B7 (79), wheat germ agglutinin (WGA), and concanavalin A (ConA). These probes were used to visualize cell wall chitin (Calcofluor white), GXM (MAb 18B7), chitooligomers (WGA), and α-D-mannosyl groups (ConA) by confocal microscopy following a previously described protocol (62). Briefly, 10^6 cells were grown in DMEM for 72 h at 37°C and 5% CO_2. After incubation, cells were fixed in 4% paraformaldehyde and washed three times with PBS. The concentrations of the probes used in this study were 5 μg/ml WGA, 5 μg/ml Calcofluor white, 10 μg/ml MAb 18B7, and 10 μg/ml ConA. The incubations were performed individually for 30 min at 37°C. After each incubation, cells were washed three times with PBS and analyzed with a confocal microscope FV1000, in the Electron Microscopy Center (CME) of the Universidade Federal do Rio Grande do Sul (UFRGS). For scanning electron microscopy, 10^6 cells were grown in minimal medium for 72 h at 30°C and 200 rpm. Sample preparation was conducted as described previously (80), and the capsular structures were visualized with an Auriga field emission gun scanning electron microscopy (FEG-SEM) microscope (Zeiss, Germany). The thickness of WT and *KRP1* mutant fibers was measured in 20 to 30 cells with the ImageJ software as previously described (66).

GXM purification and capsular transfer assay. GXM was isolated from culture supernatant by ultrafiltration as previously described (69). Cellular polysaccharides were extracted with dimethyl sulfoxide (DMSO), following protocols that were established for efficient removal of GXM from *C. neoformans* cells (81). For capsular transfer assay, the *C. neoformans* acapsular *cap67* strain was used as the capsule acceptor. Briefly, 5×10^6 cells/ml were incubated with purified GXM (10 μg/ml in PBS) for 1 h at room temperature followed by extensive washing (59). Cells were stained with MAb 18B7 and Calcofluor white as described above.

Capsule size, GXM quantification, and serological analysis of polysaccharide fractions. For capsule size measurement, WT, null, and complemented strains were grown on YPD medium for 16 h

and washed with PBS, and 10^6 cells were incubated in DMEM for 72 h at 37°C and 5% CO_2. After incubation, cells were fixed in 4% paraformaldehyde and washed three times with PBS. *C. gattii* cells were placed on glass slides and mixed with similar volumes of India ink. Capsule sizes, defined as the distances between the cell wall and the outer border of the capsule in India ink-stained yeast cells, were determined using ImageJ software (version 1.33), elaborated and provided by National Institutes of Health (NIH) (http://rsb.info.nih.gov/ij/). Cell diameters were determined using the same software. The final measurements were presented as ratios of capsule size to cell diameter. Secreted polysaccharides were quantified by ELISA for specific GXM detection (82), and cellular polysaccharides were quantified by the phenol-sulfuric acid method for total carbohydrate determination (83). The serological analysis of polysaccharide fractions from WT and mutant cells was determined by ELISA with different mouse monoclonal antibodies to GXM (MAbs 2D10 and 13F1 [IgM] and 18B7 [IgG]) as previously described (69, 82).

Capsule composition and dynamic light scattering analysis. Glycosyl composition analysis was performed by combined gas chromatography-mass spectrometry (GC-MS) of the per-*O*-trimethylsilyl (TMS) derivatives of the monosaccharide methyl glycosides produced from the sample by acidic methanolysis as described previously (84). The dimensions of polysaccharides were determined by dynamic light scattering (DLS) as described by Frases and colleagues (67).

Zeta potential determination. The zeta potential, particle mobility, and shift frequency of cell-associated and secreted PS samples were calculated in a zeta potential analyzer (ZetaPlus; Brookhaven Instruments Corp., Holtsville, NY), as previously described (9).

Ethics statement. The use of animals in this work was performed with approval of the Universidade Federal do Rio Grande do Sul Ethics Committee for Use of Animals (CEUA 30936). Mice were housed in groups of four and kept in filtered top ventilated cages with food and water *ad libitum*. The animals were cared for according to the Brazilian National Council for Animal Experimentation Control (CONCEA) guidelines. All efforts to minimize animal suffering were made. Before infection assays, mice were intraperitoneally anesthetized with ketamine (100 mg/kg of body weight) and xylazine (16 mg/kg). Mice were monitored twice daily for any signs of suffering, defined by weight loss, weakness, or inability to obtain food or water. At the first signs of suffering, mice were euthanized with an overdose of thiopental (140 mg/kg) and lidocaine (10 mg/kg). The utilization of patients' sera was approved by UFRGS Ethics Committee (CEP 19812). Informed consent was obtained from all participants.

SUPPLEMENTAL MATERIAL

Supplemental material for this article may be found at https://doi.org/10.1128/mSphere.00023-18.

FIG S1, TIF file, 2.1 MB.
FIG S2, JPG file, 2.8 MB.
FIG S3, TIF file, 0.1 MB.
FIG S4, JPG file, 1.4 MB.
TABLE S1, DOCX file, 0.1 MB.
TABLE S2, DOCX file, 0.1 MB.
TABLE S3, DOCX file, 0.1 MB.

ACKNOWLEDGMENTS

L.K., M.H.V., C.C.S., M.L.R., and A.S. were supported by grants from Coordenação de Aperfeiçoamento de Pessoal de Nível Superior (CAPES, Brazil), Conselho Nacional de Desenvolvimento Científico e Tecnológico (CNPq, Brazil), Fundação de Amparo à Pesquisa do Estado do Rio de Janeiro (FAPERJ, Brazil), and Fundação de Amparo à Pesquisa do Estado do Rio Grande do Sul (FAPERGS, Brazil). M.L.R. also acknowledges support from the Instituto Nacional de Ciência e Tecnologia de Inovação em Doenças de Populações Negligenciadas (INCT-IDPN).

We thank Arturo Casadevall for providing anti-GXM monoclonal antibodies (18B7, 2D10, and 13F1). We also thank the Electron Microscopy Center (CME) of the Federal University of Rio Grande do Sul (UFRGS) for the confocal and scanning electron microscopy analysis, as well as Henrique Biehl and Diego Muszinski for technical assistance.

J.C.V.R., M.L.R., C.C.S., M.H.V., and L.K. conceived and designed the experiments. J.C.V.R., H.M., A.W.A.G., C.B.V., B.M.M., J.R., P.A.G.F., S.F., W.L., V.A.B., E.D.S., and J.A.H. performed the experiments. J.C.V.R., M.L.R., C.C.S., M.H.V., and L.K. analyzed the data. M.L.R., A.S., C.C.S., M.H.V., and L.K. contributed reagents and materials. J.C.V.R., C.C.S., and L.K. wrote the paper.

We declare that we have no competing financial interests.

REFERENCES

1. Lin X, Heitman J. 2006. The biology of the *Cryptococcus neoformans* species complex. Annu Rev Microbiol 60:69–105. https://doi.org/10.1146/annurev.micro.60.080805.142102.
2. Rajasingham R, Smith RM, Park BJ, Jarvis JN, Govender NP, Chiller TM, Denning DW, Loyse A, Boulware DR. 2017. Global burden of disease of HIV-associated cryptococcal meningitis: an updated analysis. Lancet Infect Dis 17:873–881. https://doi.org/10.1016/S1473-3099(17)30243-8.
3. Chen SC, Meyer W, Sorrell TC. 2014. *Cryptococcus gattii* infections. Clin Microbiol Rev 27:980–1024. https://doi.org/10.1128/CMR.00126-13.
4. Kwon-Chung KJ, Bennett JE. 1984. High prevalence of *Cryptococcus neoformans* var. *gattii* in tropical and subtropical regions. Zentralbl Bakteriol Mikrobiol Hyg A 257:213–218.
5. Datta K, Bartlett KH, Marr KA. 2009. *Cryptococcus gattii*: emergence in western North America: exploitation of a novel ecological niche. Interdiscip Perspect Infect Dis 2009:176532. https://doi.org/10.1155/2009/176532.
6. Bielska E, May RC. 2016. What makes *Cryptococcus gattii* a pathogen? FEMS Yeast Res 16:fov106. https://doi.org/10.1093/femsyr/fov106.
7. Ma H, May RC. 2009. Virulence in *Cryptococcus* species. Adv Appl Microbiol 67:131–190. https://doi.org/10.1016/S0065-2164(08)01005-8.
8. Hayes JB, Sircy LM, Heusinkveld LE, Ding W, Leander RN, McClelland EE, Nelson DE. 2016. Modulation of macrophage inflammatory nuclear factor κB (NF-κB) signaling by intracellular *Cryptococcus neoformans*. J Biol Chem 291:15614–15627. https://doi.org/10.1074/jbc.M116.738187.
9. Frases S, Nimrichter L, Viana NB, Nakouzi A, Casadevall A. 2008. *Cryptococcus neoformans* capsular polysaccharide and exopolysaccharide fractions manifest physical, chemical, and antigenic differences. Eukaryot Cell 7:319–327. https://doi.org/10.1128/EC.00378-07.
10. Monari C, Bistoni F, Vecchiarelli A. 2006. Glucuronoxylomannan exhibits potent immunosuppressive properties. FEMS Yeast Res 6:537–542. https://doi.org/10.1111/j.1567-1364.2006.00072.x.
11. Vecchiarelli A. 2005. The cellular responses induced by the capsular polysaccharide of *Cryptococcus neoformans* differ depending on the presence or absence of specific protective antibodies. Curr Mol Med 5:413–420. https://doi.org/10.2174/1566524054022585.
12. Vecchiarelli A, Monari C. 2012. Capsular material of *Cryptococcus neoformans*: virulence and much more. Mycopathologia 173:375–386. https://doi.org/10.1007/s11046-011-9513-8.
13. Rakesh V, Schweitzer AD, Zaragoza O, Bryan R, Wong K, Datta A, Casadevall A, Dadachova E. 2008. Finite-element model of interaction between fungal polysaccharide and monoclonal antibody in the capsule of *Cryptococcus neoformans*. J Phys Chem B 112:8514–8522. https://doi.org/10.1021/jp8018205.
14. Levitz SM, Nong S, Mansour MK, Huang C, Specht CA. 2001. Molecular characterization of a mannoprotein with homology to chitin deacetylases that stimulates T cell responses to *Cryptococcus neoformans*. Proc Natl Acad Sci U S A 98:10422–10427. https://doi.org/10.1073/pnas.181331398.
15. Rodrigues ML, Alvarez M, Fonseca FL, Casadevall A. 2008. Binding of the wheat germ lectin to *Cryptococcus neoformans* suggests an association of chitinlike structures with yeast budding and capsular glucuronoxylomannan. Eukaryot Cell 7:602–609. https://doi.org/10.1128/EC.00307-07.
16. Cordero RJ, Pontes B, Guimarães AJ, Martinez LR, Rivera J, Fries BC, Nimrichter L, Rodrigues ML, Viana NB, Casadevall A. 2011. Chronological aging is associated with biophysical and chemical changes in the capsule of *Cryptococcus neoformans*. Infect Immun 79:4990–5000. https://doi.org/10.1128/IAI.05789-11.
17. Silveira CP, Piffer AC, Kmetzsch L, Fonseca FL, Soares DA, Staats CC, Rodrigues ML, Schrank A, Vainstein MH. 2013. The heat shock protein (Hsp) 70 of *Cryptococcus neoformans* is associated with the fungal cell surface and influences the interaction between yeast and host cells. Fungal Genet Biol 60:53–63. https://doi.org/10.1016/j.fgb.2013.08.005.
18. O'Meara TR, Alspaugh JA. 2012. The *Cryptococcus neoformans* capsule: a sword and a shield. Clin Microbiol Rev 25:387–408. https://doi.org/10.1128/CMR.00001-12.
19. Kwon-Chung KJ, Fraser JA, Doering TL, Wang Z, Janbon G, Idnurm A, Bahn YS. 2014. *Cryptococcus neoformans* and *Cryptococcus gattii*, the etiologic agents of cryptococcosis. Cold Spring Harb Perspect Med 4:a019760. https://doi.org/10.1101/cshperspect.a019760.
20. Fonseca FL, Nohara LL, Cordero RJ, Frases S, Casadevall A, Almeida IC, Nimrichter L, Rodrigues ML. 2010. Immunomodulatory effects of serotype B glucuronoxylomannan from *Cryptococcus gattii* correlate with polysaccharide diameter. Infect Immun 78:3861–3870. https://doi.org/10.1128/IAI.00111-10.
21. Urai M, Kaneko Y, Ueno K, Okubo Y, Aizawa T, Fukazawa H, Sugita T, Ohno H, Shibuya K, Kinjo Y, Miyazaki Y. 2015. Evasion of innate immune responses by the highly virulent *Cryptococcus gattii* by altering capsule glucuronoxylomannan structure. Front Cell Infect Microbiol 5:101. https://doi.org/10.3389/fcimb.2015.00101.
22. Moyrand F, Fontaine T, Janbon G. 2007. Systematic capsule gene disruption reveals the central role of galactose metabolism on *Cryptococcus neoformans* virulence. Mol Microbiol 64:771–781. https://doi.org/10.1111/j.1365-2958.2007.05695.x.
23. Specht CA, Nong S, Dan JM, Lee CK, Levitz SM. 2007. Contribution of glycosylation to T cell responses stimulated by recombinant *Cryptococcus neoformans* mannoprotein. J Infect Dis 196:796–800. https://doi.org/10.1086/520536.
24. Pietrella D, Corbucci C, Perito S, Bistoni G, Vecchiarelli A. 2005. Mannoproteins from *Cryptococcus neoformans* promote dendritic cell maturation and activation. Infect Immun 73:820–827. https://doi.org/10.1128/IAI.73.2.820-827.2005.
25. Mansour MK, Latz E, Levitz SM. 2006. *Cryptococcus neoformans* glycoantigens are captured by multiple lectin receptors and presented by dendritic cells. J Immunol 176:3053–3061. https://doi.org/10.4049/jimmunol.176.5.3053.
26. Zhang WJ, Ballou CE. 1981. Saccharomyces kluyveri cell wall mannoprotein. Structures of the O- and N-linked carbohydrate components. J Biol Chem 256:10073–10079.
27. Nguyen TH, Fleet GH, Rogers PL. 1998. Composition of the cell walls of several yeast species. Appl Microbiol Biotechnol 50:206–212. https://doi.org/10.1007/s002530051278.
28. Teparić R, Mrsa V. 2013. Proteins involved in building, maintaining and remodeling of yeast cell walls. Curr Genet 59:171–185. https://doi.org/10.1007/s00294-013-0403-0.
29. Hagen I, Ecker M, Lagorce A, Francois JM, Sestak S, Rachel R, Grossmann G, Hauser NC, Hoheisel JD, Tanner W, Strahl S. 2004. Sed1p and Srl1p are required to compensate for cell wall instability in *Saccharomyces cerevisiae* mutants defective in multiple GPI-anchored mannoproteins. Mol Microbiol 52:1413–1425. https://doi.org/10.1111/j.1365-2958.2004.04064.x.
30. Lian T, Simmer MI, D'Souza CA, Steen BR, Zuyderduyn SD, Jones SJ, Marra MA, Kronstad JW. 2005. Iron-regulated transcription and capsule formation in the fungal pathogen *Cryptococcus neoformans*. Mol Microbiol 55:1452–1472. https://doi.org/10.1111/j.1365-2958.2004.04474.x.
31. Cadieux B, Lian T, Hu G, Wang J, Biondo C, Teti G, Liu V, Murphy ME, Creagh AL, Kronstad JW. 2013. The mannoprotein Cig1 supports iron acquisition from heme and virulence in the pathogenic fungus *Cryptococcus neoformans*. J Infect Dis 207:1339–1347. https://doi.org/10.1093/infdis/jit029.
32. Baker LG, Specht CA, Donlin MJ, Lodge JK. 2007. Chitosan, the deacetylated form of chitin, is necessary for cell wall integrity in *Cryptococcus neoformans*. Eukaryot Cell 6:855–867. https://doi.org/10.1128/EC.00399-06.
33. Levitz SM, Specht CA. 2006. The molecular basis for the immunogenicity of *Cryptococcus neoformans* mannoproteins. FEMS Yeast Res 6:513–524. https://doi.org/10.1111/j.1567-1364.2006.00071.x.
34. Petersen TN, Brunak S, von Heijne G, Nielsen H. 2011. SignalP 4.0: discriminating signal peptides from transmembrane regions. Nat Methods 8:785–786. https://doi.org/10.1038/nmeth.1701.
35. Pierleoni A, Martelli PL, Casadio R. 2008. PredGPI: a GPI-anchor predictor. BMC Bioinformatics 9:392. https://doi.org/10.1186/1471-2105-9-392.
36. Chauhan JS, Rao A, Raghava GP. 2013. In silico platform for prediction of N-, O- and C-glycosites in eukaryotic protein sequences. PLoS One 8:e67008. https://doi.org/10.1371/journal.pone.0067008.
37. Jones P, Binns D, Chang HY, Fraser M, Li W, McAnulla C, McWilliam H, Maslen J, Mitchell A, Nuka G, Pesseat S, Quinn AF, Sangrador-Vegas A, Scheremetjew M, Yong SY, Lopez R, Hunter S. 2014. InterProScan 5: genome-scale protein function classification. Bioinformatics 30:1236–1240. https://doi.org/10.1093/bioinformatics/btu031.
38. Yin DT, Urresti S, Lafond M, Johnston EM, Derikvand F, Ciano L, Berrin JG, Henrissat B, Walton PH, Davies GJ, Brumer H. 2015. Structure-function characterization reveals new catalytic diversity in the galactose oxidase

and glyoxal oxidase family. Nat Commun 6:10197. https://doi.org/10.1038/ncomms10197.
39. Rodrigues ML, Nimrichter L, Oliveira DL, Frases S, Miranda K, Zaragoza O, Alvarez M, Nakouzi A, Feldmesser M, Casadevall A. 2007. Vesicular polysaccharide export in Cryptococcus neoformans is a eukaryotic solution to the problem of fungal trans-cell wall transport. Eukaryot Cell 6:48–59. https://doi.org/10.1128/EC.00318-06.
40. Wolf JM, Espadas-Moreno J, Luque-Garcia JL, Casadevall A. 2014. Interaction of Cryptococcus neoformans extracellular vesicles with the cell wall. Eukaryot Cell 13:1484–1493. https://doi.org/10.1128/EC.00111-14.
41. Geddes JM, Croll D, Caza M, Stoynov N, Foster LJ, Kronstad JW. 2015. Secretome profiling of *Cryptococcus neoformans* reveals regulation of a subset of virulence-associated proteins and potential biomarkers by protein kinase A. BMC Microbiol 15:206. https://doi.org/10.1186/s12866-015-0532-3.
42. Donlin MJ, Upadhya R, Gerik KJ, Lam W, VanArendonk LG, Specht CA, Sharma NK, Lodge JK. 2014. Cross talk between the cell wall integrity and cyclic AMP/protein kinase A pathways in *Cryptococcus neoformans*. mBio 5:e01573-14. https://doi.org/10.1128/mBio.01573-14.
43. La Valle R, Sandini S, Gomez MJ, Mondello F, Romagnoli G, Nisini R, Cassone A. 2000. Generation of a recombinant 65-kilodalton mannoprotein, a major antigen target of cell-mediated immune response to *Candida albicans*. Infect Immun 68:6777–6784. https://doi.org/10.1128/IAI.68.12.6777-6784.2000.
44. Roncero C, Durán A. 1985. Effect of Calcofluor white and Congo red on fungal cell wall morphogenesis: in vivo activation of chitin polymerization. J Bacteriol 163:1180–1185.
45. Ram AF, Klis FM. 2006. Identification of fungal cell wall mutants using susceptibility assays based on Calcofluor white and Congo red. Nat Protoc 1:2253–2256. https://doi.org/10.1038/nprot.2006.397.
46. Siafakas AR, Sorrell TC, Wright LC, Wilson C, Larsen M, Boadle R, Williamson PR, Djordjevic JT. 2007. Cell wall-linked cryptococcal phospholipase B1 is a source of secreted enzyme and a determinant of cell wall integrity. J Biol Chem 282:37508–37514. https://doi.org/10.1074/jbc.M707913200.
47. Ost KS, Esher SK, Leopold Wager CM, Walker L, Wagener J, Munro C, Wormley FL, Jr, Alspaugh JA. 2017. Rim pathway-mediated alterations in the fungal cell wall influence immune recognition and inflammation. mBio 8:e02290-16. https://doi.org/10.1128/mBio.02290-16.
48. Free SJ. 2013. Fungal cell wall organization and biosynthesis. Adv Genet 81:33–82. https://doi.org/10.1016/B978-0-12-407677-8.00002-6.
49. Lam JS, Mansour MK, Specht CA, Levitz SM. 2005. A model vaccine exploiting fungal mannosylation to increase antigen immunogenicity. J Immunol 175:7496–7503. https://doi.org/10.4049/jimmunol.175.11.7496.
50. Whittaker JW. 2005. The radical chemistry of galactose oxidase. Arch Biochem Biophys 433:227–239. https://doi.org/10.1016/j.abb.2004.08.034.
51. Daou M, Faulds CB. 2017. Glyoxal oxidases: their nature and properties. World J Microbiol Biotechnol 33:87. https://doi.org/10.1007/s11274-017-2254-1.
52. Philips J, Herskowitz I. 1998. Identification of Kel1p, a kelch domain-containing protein involved in cell fusion and morphology in *Saccharomyces cerevisiae*. J Cell Biol 143:375–389. https://doi.org/10.1083/jcb.143.2.375.
53. Peres da Silva R, Puccia R, Rodrigues ML, Oliveira DL, Joffe LS, César GV, Nimrichter L, Goldenberg S, Alves LR. 2015. Extracellular vesicle-mediated export of fungal RNA. Sci Rep 5:7763. https://doi.org/10.1038/srep07763.
54. Joffe LS, Nimrichter L, Rodrigues ML, Del Poeta M. 2016. Potential roles of fungal extracellular vesicles during infection. mSphere 1:e00099-16. https://doi.org/10.1128/mSphere.00099-16.
55. Mansour MK, Yauch LE, Rottman JB, Levitz SM. 2004. Protective efficacy of antigenic fractions in mouse models of cryptococcosis. Infect Immun 72:1746–1754. https://doi.org/10.1128/IAI.72.3.1746-1754.2004.
56. Biondo C, Messina L, Bombaci M, Mancuso G, Midiri A, Beninati C, Cusumano V, Gerace E, Papasergi S, Teti G. 2005. Characterization of two novel cryptococcal mannoproteins recognized by immune sera. Infect Immun 73:7348–7355. https://doi.org/10.1128/IAI.73.11.7348-7355.2005.
57. Erwig LP, Gow NA. 2016. Interactions of fungal pathogens with phagocytes. Nat Rev Microbiol 14:163–176. https://doi.org/10.1038/nrmicro.2015.21.
58. Huston SM, Ngamskulrungroj P, Xiang RF, Ogbomo H, Stack D, Li SS, Timm-McCann M, Kyei SK, Oykhman P, Kwon-Chung KJ, Mody CH. 2016. *Cryptococcus gattii* capsule blocks surface recognition required for dendritic cell maturation independent of internalization and antigen processing. J Immunol 196:1259–1271. https://doi.org/10.4049/jimmunol.1501089.
59. Reese AJ, Doering TL. 2003. Cell wall alpha-1,3-glucan is required to anchor the Cryptococcus neoformans capsule. Mol Microbiol 50:1401–1409. https://doi.org/10.1046/j.1365-2958.2003.03780.x.
60. Reese AJ, Yoneda A, Breger JA, Beauvais A, Liu H, Griffith CL, Bose I, Kim MJ, Skau C, Yang S, Sefko JA, Osumi M, Latge JP, Mylonakis E, Doering TL. 2007. Loss of cell wall alpha(1-3) glucan affects Cryptococcus neoformans from ultrastructure to virulence. Mol Microbiol 63:1385–1398. https://doi.org/10.1111/j.1365-2958.2006.05551.x.
61. Gilbert NM, Donlin MJ, Gerik KJ, Specht CA, Djordjevic JT, Wilson CF, Sorrell TC, Lodge JK. 2010. KRE genes are required for beta-1,6-glucan synthesis, maintenance of capsule architecture and cell wall protein anchoring in *Cryptococcus neoformans*. Mol Microbiol 76:517–534. https://doi.org/10.1111/j.1365-2958.2010.07119.x.
62. Fonseca FL, Nimrichter L, Cordero RJ, Frases S, Rodrigues J, Goldman DL, Andruszkiewicz R, Milewski S, Travassos LR, Casadevall A, Rodrigues ML. 2009. Role for chitin and chitooligomers in the capsular architecture of *Cryptococcus neoformans*. Eukaryot Cell 8:1543–1553. https://doi.org/10.1128/EC.00142-09.
63. Nimrichter L, Cerqueira MD, Leitão EA, Miranda K, Nakayasu ES, Almeida SR, Almeida IC, Alviano CS, Barreto-Bergter E, Rodrigues ML. 2005. Structure, cellular distribution, antigenicity, and biological functions of *Fonsecaea pedrosoi* ceramide monohexosides. Infect Immun 73:7860–7868. https://doi.org/10.1128/IAI.73.12.7860-7868.2005.
64. Rhome R, McQuiston T, Kechichian T, Bielawska A, Hennig M, Drago M, Morace G, Luberto C, Del Poeta M. 2007. Biosynthesis and immunogenicity of glucosylceramide in *Cryptococcus neoformans* and other human pathogens. Eukaryot Cell 6:1715–1726. https://doi.org/10.1128/EC.00208-07.
65. Sakaguchi N, Baba T, Fukuzawa M, Ohno S. 1993. Ultrastructural study of *Cryptococcus neoformans* by quick-freezing and deep-etching method. Mycopathologia 121:133–141. https://doi.org/10.1007/BF01104068.
66. Ramos CL, Gomes FM, Girard-Dias W, Almeida FP, Albuquerque PC, Kretschmer M, Kronstad JW, Frases S, de Souza W, Rodrigues ML, Miranda K. 2017. Phosphorus-rich structures and capsular architecture in *Cryptococcus neoformans*. Future Microbiol 12:227–238. https://doi.org/10.2217/fmb-2017-0060.
67. Frases S, Pontes B, Nimrichter L, Viana NB, Rodrigues ML, Casadevall A. 2009. Capsule of *Cryptococcus neoformans* grows by enlargement of polysaccharide molecules. Proc Natl Acad Sci U S A 106:1228–1233. https://doi.org/10.1073/pnas.0808995106.
68. Cordero RJ, Frases S, Guimarães AJ, Rivera J, Casadevall A. 2011. Evidence for branching in cryptococcal capsular polysaccharides and consequences on its biological activity. Mol Microbiol 79:1101–1117. https://doi.org/10.1111/j.1365-2958.2010.07511.x.
69. Nimrichter L, Frases S, Cinelli LP, Viana NB, Nakouzi A, Travassos LR, Casadevall A, Rodrigues ML. 2007. Self-aggregation of *Cryptococcus neoformans* capsular glucuronoxylomannan is dependent on divalent cations. Eukaryot Cell 6:1400–1410. https://doi.org/10.1128/EC.00122-07.
70. Schneider RDO, Fogaça NDS, Kmetzsch L, Schrank A, Vainstein MH, Staats CC. 2012. Zap1 regulates zinc homeostasis and modulates virulence in *Cryptococcus gattii*. PLoS One 7:e43773. https://doi.org/10.1371/journal.pone.0043773.
71. D'Souza CA, Kronstad JW, Taylor G, Warren R, Yuen M, Hu G, Jung WH, Sham A, Kidd SE, Tangen K, Lee N, Zeilmaker T, Sawkins J, McVicker G, Shah S, Gnerre S, Griggs A, Zeng Q, Bartlett K, Li W, Wang X, Heitman J, Stajich JE, Fraser JA, Meyer W, Carter D, Schein J, Krzywinski M, Kwon-Chung KJ, Varma A, Wang J, Brunham R, Fyfe M, Ouellette BF, Siddiqui A, Marra M, Jones S, Holt R, Birren BW, Galagan JE, Cuomo CA. 2011. Genome variation in *Cryptococcus gattii*, an emerging pathogen of immunocompetent hosts. mBio 2:e00342-10. https://doi.org/10.1128/mBio.00342-10.
72. Farrer RA, Desjardins CA, Sakthikumar S, Gujja S, Saif S, Zeng Q, Chen Y, Voelz K, Heitman J, May RC, Fisher MC, Cuomo CA. 2015. Genome evolution and innovation across the four major lineages of *Cryptococcus gattii*. mBio 6:e00868-15. https://doi.org/10.1128/mBio.00868-15.
73. Janbon G, Ormerod KL, Paulet D, Byrnes EJ, Yadav V, Chatterjee G, Mullapudi N, Hon CC, Billmyre RB, Brunel F, Bahn YS, Chen W, Chen Y, Chow EW, Coppée JY, Floyd-Averette A, Gaillardin C, Gerik KJ, Goldberg J, Gonzalez-Hilarion S, Gujja S, Hamlin JL, Hsueh YP, Ianiri G, Jones S, Kodira CD, Kozubowski L, Lam W, Marra M, Mesner LD, Mieczkowski PA,

Moyrand F, Nielsen K, Proux C, Rossignol T, Schein JE, Sun S, Wollschlaeger C, Wood IA, Zeng Q, Neuvéglise C, Newlon CS, Perfect JR, Lodge JK, Idnurm A, Stajich JE, Kronstad JW, Sanyal K, Heitman J, Fraser JA, Cuomo CA, Dietrich FS. 2014. Analysis of the genome and transcriptome of *Cryptococcus neoformans* var. *grubii* reveals complex RNA expression and microevolution leading to virulence attenuation. PLoS Genet 10: e1004261. https://doi.org/10.1371/journal.pgen.1004261.

74. García-Pedrajas MD, Nadal M, Kapa LB, Perlin MH, Andrews DL, Gold SE. 2008. DelsGate, a robust and rapid gene deletion construction method. Fungal Genet Biol 45:379–388. https://doi.org/10.1016/j.fgb.2007.11.001.
75. Toffaletti DL, Rude TH, Johnston SA, Durack DT, Perfect JR. 1993. Gene transfer in *Cryptococcus neoformans* by use of biolistic delivery of DNA. J Bacteriol 175:1405–1411. https://doi.org/10.1128/jb.175.5.1405-1411.1993.
76. Kmetzsch L, Staats CC, Simon E, Fonseca FL, de Oliveira DL, Sobrino L, Rodrigues J, Leal AL, Nimrichter L, Rodrigues ML, Schrank A, Vainstein MH. 2010. The vacuolar Ca^{2+} exchanger Vcx1 is involved in calcineurin-dependent Ca^{2+} tolerance and virulence in *Cryptococcus neoformans*. Eukaryot Cell 9:1798–1805. https://doi.org/10.1128/EC.00114-10.
77. Kmetzsch L, Staats CC, Cupertino JB, Fonseca FL, Rodrigues ML, Schrank A, Vainstein MH. 2013. The calcium transporter Pmc1 provides Ca2+ tolerance and influences the progression of murine cryptococcal infection. FEBS J 280:4853–4864. https://doi.org/10.1111/febs.12458.
78. Lev S, Desmarini D, Chayakulkeeree M, Sorrell TC, Djordjevic JT. 2012. The Crz1/Sp1 transcription factor of *Cryptococcus neoformans* is activated by calcineurin and regulates cell wall integrity. PLoS One 7:e51403. https://doi.org/10.1371/journal.pone.0051403.
79. Casadevall A, Cleare W, Feldmesser M, Glatman-Freedman A, Goldman DL, Kozel TR, Lendvai N, Mukherjee J, Pirofski LA, Rivera J, Rosas AL, Scharff MD, Valadon P, Westin K, Zhong Z. 1998. Characterization of a murine monoclonal antibody to *Cryptococcus neoformans* polysaccharide that is a candidate for human therapeutic studies. Antimicrob Agents Chemother 42:1437–1446.
80. Araújo GR, Fontes GN, Leão D, Rocha GM, Pontes B, Sant'Anna C, de Souza W, Frases S. 2016. *Cryptococcus neoformans* capsular polysaccharides form branched and complex filamentous networks viewed by high-resolution microscopy. J Struct Biol 193:75–82. https://doi.org/10.1016/j.jsb.2015.11.010.
81. Bryan RA, Zaragoza O, Zhang T, Ortiz G, Casadevall A, Dadachova E. 2005. Radiological studies reveal radial differences in the architecture of the polysaccharide capsule of *Cryptococcus neoformans*. Eukaryot Cell 4:465–475. https://doi.org/10.1128/EC.4.2.465-475.2005.
82. Casadevall A, Mukherjee J, Scharff MD. 1992. Monoclonal antibody based ELISAs for cryptococcal polysaccharide. J Immunol Methods 154: 27–35. https://doi.org/10.1016/0022-1759(92)90209-C.
83. Dubois M, Gilles K, Hamilton JK, Rebers PA, Smith F. 1951. A colorimetric method for the determination of sugars. Nature 168:167. https://doi.org/10.1038/168167a0.
84. Santander J, Martin T, Loh A, Pohlenz C, Gatlin DM, Curtiss R. 2013. Mechanisms of intrinsic resistance to antimicrobial peptides of *Edwardsiella ictaluri* and its influence on fish gut inflammation and virulence. Microbiology 159:1471–1486. https://doi.org/10.1099/mic.0.066639-0.

8. Referências

AGUSTINHO, D. P. *et al.* Peeling the onion: the outer layers of *Cryptococcus neoformans*. **Memórias do Instituto Oswaldo Cruz**, *[S. l.]*, v. 113, n. 7, p. e180040, 2018. Disponível em: https://doi.org/10.1590/0074-02760180040

ALANIO, A. Dormancy in *Cryptococcus neoformans*: 60 years of accumulating evidence. **American Society for Clinical Investigation**, *[S. l.]*, v. 130, n. 7, p. 3353-3360, 2020. Disponível em: https://doi.org/10.1172/JCI136223

ALSPAUGH, J. A. Virulence mechanisms and *Cryptococcus neoformans* pathogenesis. **Fungal Genetics and Biology**, *[S. l.]*, v. 78, p. 55–58, 2015. Disponível em: https://doi.org/10.1016/j.fgb.2014.09.004

ALVAREZ, M. *et al.* The outcome of *Cryptococcus neoformans* intracellular pathogenesis in human monocytes. **BMC Microbiology**, *[S. l.]*, v. 9, 2009. Disponível em: https://doi.org/10.1186/1471-2180-9-51

ALVAREZ, M.; CASADEVALL, A. Phagosome Extrusion and Host-Cell Survival after *Cryptococcus neoformans* Phagocytosis by Macrophages. **Current Biology**, *[S. l.]*, v. 16, n. 21, p. 2161–2165, 2006. Disponível em: https://doi.org/10.1016/j.cub.2006.09.061

ALVAREZ, M.; CASADEVALL, A. Cell-to-cell spread and massive vacuole formation after *Cryptococcus neoformans* infection of murine macrophages. **BMC Immunology**, *[S. l.]*, v. 8, p. 1–7, 2007. Disponível em: https://doi.org/10.1186/1471-2172-8-16

ANGKASEKWINAI, P. *et al. Cryptococcus gattii* Infection Dampens Th1 and Th17 Responses by Attenuating Dendritic Cell Function and Pulmonary Chemokine Expression in the Immunocompetent Hosts. **Infection and Immunity**, *[S. l.]*, v. 82, n. 9, p. 3880–3890, 2014. Disponível em: https://doi.org/10.1128/IAI.01773-14

ARTAVANIS-TSAKONAS, K. *et al.* Recruitment of CD63 to *Cryptococcus neoformans* phagosomes requires acidification. **Proceedings of the National Academy of Sciences of the United States of America**, *[S. l.]*, v. 103, n. 43, p. 15945–15950, 2006. Disponível em: https://doi.org/10.1073/pnas.0607528103

BAKER, L. G. *et al.* Chitosan, the Deacetylated Form of Chitin, Is Necessary for Cell Wall Integrity in *Cryptococcus neoformans*. **Eukaryotic Cell**, *[S. l.]*, v. 6, n. 5, p. 855–867, 2007. Disponível em: https://doi.org/10.1128/EC.00399-06

BEARDSLEY, J.; SORRELL, T. C.; CHEN, S. C. A. Central Nervous System Cryptococcal Infections in Non-HIV Infected Patients. **Journal of Fungi**, *[S. l.]*, v. 5, n. 3, p. 71, 2019. Disponível em: https://doi.org/10.3390/jof5030071

BIELSKA, E.; MAY, R. C. What makes *Cryptococcus gattii* a pathogen?. **Oxford University Press**, *[S. l.]*, v. 16, n. 1, p. 106, 2015. Disponível em: https://doi.org/10.1093/femsyr/fov106

BILLS, G. F.; GLOER, J. B. Biologically Active Secondary Metabolites from the Fungi. *In*: **The Fungal Kingdom**. *[S. l.]*: American Society of Microbiology, 2016. v. 4p. 1087–1119. *E-book*. Disponível em: https://doi.org/10.1128/microbiolspec.funk-

0009-2016

BIONDO, C. *et al.* Characterization of Two Novel Cryptococcal Mannoproteins Recognized by Immune Sera. **Infection and Immunity**, *[S. l.]*, v. 73, n. 11, p. 7348–7355, 2005. Disponível em: https://doi.org/10.1128/IAI.73.11.7348-7355.2005

BLOOM, A. L. M. *et al.* Thermotolerance in the pathogen *Cryptococcus neoformans* is linked to antigen masking via mRNA decay-dependent reprogramming. **Nature Communications**, *[S. l.]*, v. 10, n. 1, 2019. Disponível em: https://doi.org/10.1038/s41467-019-12907-x

BOSE, I. *et al.* A Yeast under Cover: the Capsule of *Cryptococcus neoformans*. **Eukaryotic Cell**, *[S. l.]*, v. 2, n. 4, p. 655–663, 2003. Disponível em: https://doi.org/10.1128/EC.2.4.655-663.2003

BOULWARE, D. R. *et al.* Paucity of initial cerebrospinal fluid inflammation in cryptococcal meningitis is associated with subsequent immune reconstitution inflammatory syndrome. **Journal of Infectious Diseases**, *[S. l.]*, v. 202, n. 6, p. 962–970, 2010. Disponível em: https://doi.org/10.1086/655785

BROWN, G. D. *et al.* Hidden killers: Human fungal infections. **American Association for the Advancement of Science**, *[S. l.]*, v. 4, n. 165, p. 165rv13 , 2012. Disponível em: https://doi.org/10.1126/scitranslmed.3004404

CADIEUX, B. *et al.* The Mannoprotein Cig1 Supports Iron Acquisition From Heme and Virulence in the Pathogenic Fungus *Cryptococcus neoformans*. **Journal of Infectious Diseases**, *[S. l.]*, v. 207, n. 8, p. 1339–1347, 2013. Disponível em: https://doi.org/10.1093/infdis/jit029

CALLAHAN, B. P.; YUAN, Y.; WOLFENDEN, R. The Burden Borne by Urease. **Journal of the American Chemical Society**, *[S. l.]*, v. 127, n. 31, p. 10828–10829, 2005. Disponível em: https://doi.org/10.1021/ja0525399

CAMACHO, E. *et al.* The structural unit of melanin in the cell wall of the fungal pathogen *Cryptococcus neoformans*. **Journal of Biological Chemistry**, *[S. l.]*, v. 294, n. 27, p. 10471–10489, 2019. Disponível em: https://doi.org/10.1074/jbc.RA119.008684

CANNON, R. D. *et al.* Molecular biological and biochemical aspects of fungal dimorphism. **Medical Mycology**, *[S. l.]*, v. 32, n. s1, p. 53–64, 1994. Disponível em: https://doi.org/10.1080/02681219480000721

CARAFOLI, E. *et al.* Generation, Control, and Processing of Cellular Calcium Signals. **CRC Press LLC**, *[S. l.]*, v. 36, n. 2, p. 107-206, 2001. Disponível em: https://doi.org/10.1080/20014091074183

CARAFOLI, E.; KREBS, J. Why Calcium? How Calcium Became the Best Communicator. **Journal of Biological Chemistry**, *[S. l.]*, v. 291, n. 40, p. 20849–20857, 2016. Disponível em: https://doi.org/10.1074/jbc.R116.735894

CASADEVALL, A. Amoeba Provide Insight into the Origin of Virulence in Pathogenic Fungi. **Advances in Experimental Medicine and Biology**, *[S. l.]*, v. 710, p. 1–10, 2012. Disponível em: https://doi.org/10.1007/978-1-4419-5638-5_1

CASADEVALL, A.; PIROFSKI, L. Host-Pathogen Interactions: The Attributes of Virulence. **The Journal of Infectious Diseases**, *[S. l.]*, v. 184, n. 3, p. 337–344, 2001. Disponível em: https://doi.org/10.1086/322044

CASADEVALL, A.; PIROFSKI, L. A. Host-Pathogen Interactions: Redefining the Basic Concepts of Virulence and Pathogenicity. **Infection and Immunity**, *[S. l.]*, v. 67, n. 8, p. 3703-3713, 1999. Disponível em: https://doi.org/10.1128/iai.67.8.3703-3713.1999

CASADEVALL, A.; PIROFSKI, L. A. The damage-response framework of microbial pathogenesis. **Nature Reviews Microbiology**, *[S. l.]*, v. 1, n. 1, p. 17–24, 2003. Disponível em: https://doi.org/10.1038/nrmicro732

CASADEVALL, A.; ROSAS, A. L.; NOSANCHUK, J. D. Melanin and virulence in *Cryptococcus neoformans*. **Current Biology Ltd**, *[S. l.]*, v. 3, n. 4, p. 354-358, 2000. Disponível em: https://doi.org/10.1016/S1369-5274(00)00103-X

CAZA, M.; KRONSTAD, J. W. The cAMP/Protein Kinase A Pathway Regulates Virulence and Adaptation to Host Conditions in *Cryptococcus neoformans*. **Frontiers Media S.A.**, *[S. l.]*, v. 9, n. 1, p. 212-220, 2019. Disponível em: https://doi.org/10.3389/fcimb.2019.00212

CHANG, Y. C. *et al.* Cryptococcal Yeast Cells Invade the Central Nervous System via Transcellular Penetration of the Blood-Brain Barrier. **Infection and Immunity**, *[S. l.]*, v. 72, n. 9, p. 4985–4995, 2004. Disponível em: https://doi.org/10.1128/IAI.72.9.4985-4995.2004

CHANG, Y. C. *et al.* Sre1p, a regulator of oxygen sensing and sterol homeostasis, is required for virulence in *Cryptococcus neoformans*. **Molecular Microbiology**, *[S. l.]*, v. 64, n. 3, p. 614–629, 2007. Disponível em: https://doi.org/10.1111/j.1365-2958.2007.05676.x

CHANG, Y. C.; KWON-CHUNG, K. J. Complementation of a capsule-deficient mutation of *Cryptococcus neoformans* restores its virulence. **Molecular and Cellular Biology**, *[S. l.]*, v. 14, n. 7, p. 4912–4919, 1994. Disponível em: https://doi.org/10.1128/MCB.14.7.4912

CHARLIER, C. *et al.* Evidence of a Role for Monocytes in Dissemination and Brain Invasion by *Cryptococcus neoformans*. **Infection and immunity**, *[S. l.]*, v. 77, n. 1, p. 120–7, 2009. Disponível em: https://doi.org/10.1128/IAI.01065-08

CHAYAKULKEEREE, M. *et al.* Role and mechanism of phosphatidylinositol-specific phospholipase C in survival and virulence of *Cryptococcus neoformans*. **Molecular Microbiology**, *[S. l.]*, v. 69, n. 4, p. 809–826, 2008. Disponível em: https://doi.org/10.1111/j.1365-2958.2008.06310.x

CHEN, J. *et al. Cryptococcus neoformans* Strains and Infection in Apparently Immunocompetent Patients, China. **Emerging Infectious Diseases**, *[S. l.]*, v. 14, n. 5, p. 755–762, 2008. Disponível em: https://doi.org/10.3201/eid1405.071312

CHEN, S. H. M. *et al. Cryptococcus neoformans* induces alterations in the cytoskeleton of human brain microvascular endothelial cells. **Journal of Medical Microbiology**, *[S. l.]*, v. 52, n. 11, p. 961–970, 2003. Disponível em:

https://doi.org/10.1099/jmm.0.05230-0

CHEN, Y. L. *et al.* Calcineurin Governs Thermotolerance and Virulence of *Cryptococcus gattii*. **G3: Genes, Genomes, Genetics**, *[S. l.]*, v. 3, n. 3, p. 527–539, 2013. Disponível em: https://doi.org/10.1534/g3.112.004242

CHENG, P. Y.; SHAM, A.; KRONSTAD, J. W. *Cryptococcus gattii* Isolates from the British Columbia Cryptococcosis Outbreak Induce Less Protective Inflammation in a Murine Model of Infection than *Cryptococcus neoformans*. **Infection and Immunity**, *[S. l.]*, v. 77, n. 10, p. 4284–4294, 2009. Disponível em: https://doi.org/10.1128/IAI.00628-09

CHIN, D.; MEANS, A. R. Calmodulin: A prototypical calcium sensor. **Trends Cell Biol**, *[S. l.]*, v. 10, n. 8, p. 322-328, 2000. Disponível em: https://doi.org/10.1016/S0962-8924(00)01800-6

CHOW, E. W. L. *et al.* Elucidation of the calcineurin-Crz1 stress response transcriptional network in the human fungal pathogen *Cryptococcus neoformans*. **PLOS Genetics**, *[S. l.]*, v. 13, n. 4, p. e1006667, 2017. Disponível em: https://doi.org/10.1371/journal.pgen.1006667

CHOWDHARY, A. *et al.* Environmental prevalence of *Cryptococcus neoformans* and *Cryptococcus gattii* in India: An update. **Taylor & Francis**, *[S. l.]*, v. 38, n. 1, p. 1-16, 2012. Disponível em: https://doi.org/10.3109/1040841X.2011.606426

CHRISMAN, C. J. *et al.* Phospholipids Trigger *Cryptococcus neoformans* Capsular Enlargement during Interactions with Amoebae and Macrophages. **PLoS Pathogens**, *[S. l.]*, v. 7, n. 5, 2011. Disponível em: https://doi.org/10.1371/journal.ppat.1002047

CHRISSIAN, C. *et al.* Melanin deposition in two *Cryptococcus* species depends on cell-wall composition and flexibility. **Journal of Biological Chemistry**, *[S. l.]*, v. 295, n. 7, p. 1815–1828, 2020. Disponível em: https://doi.org/10.1074/jbc.RA119.011949

CHUN, C. D.; BROWN, J. C. S.; MADHANI, H. D. A Major Role for Capsule-Independent Phagocytosis-Inhibitory Mechanisms in Mammalian Infection by *Cryptococcus neoformans*. **Cell Host & Microbe**, *[S. l.]*, v. 9, n. 3, p. 243–251, 2011. Disponível em: https://doi.org/10.1016/j.chom.2011.02.003

COELHO, C.; BOCCA, A. L.; CASADEVALL, A. The Tools for Virulence of *Cryptococcus neoformans*. *In*: **Advances in Applied Microbiology**. *[S. l.]*: Academic Press Inc., 2014. v. 87p. 1–41. *E-book*. Disponível em: https://doi.org/10.1016/B978-0-12-800261-2.00001-3

COGLIATI, M. Global Molecular Epidemiology of *Cryptococcus neoformans* and *Cryptococcus gattii*: An Atlas of the Molecular Types. **Scientifica**, *[S. l.]*, v. 2013, p. 1–23, 2013. Disponível em: https://doi.org/10.1155/2013/675213

CORDERO, R. J. B. *et al.* Evidence for branching in cryptococcal capsular polysaccharides and consequences on its biological activity. **Molecular Microbiology**, *[S. l.]*, v. 79, n. 4, p. 1101–1117, 2011. Disponível em: https://doi.org/10.1111/j.1365-2958.2010.07511.x

CORDERO, R. J. B.; BERGMAN, A.; CASADEVALL, A. Temporal Behavior of Capsule Enlargement by *Cryptococcus neoformans*. **Eukaryotic Cell**, *[S. l.]*, v. 12, n. 10, p. 1383–1388, 2013. Disponível em: https://doi.org/10.1128/EC.00163-13

CORDERO, R. J. B.; CAMACHO, E.; CASADEVALL, A. Melanization in *Cryptococcus neoformans* Requires Complex Regulation. **American Society for Microbiology**, *[S. l.]*, v. 11, n. 1, p. 1-3, 2020. Disponível em: https://doi.org/10.1128/mBio.03313-19

CORDERO, R. J. B.; CASADEVALL, A. Functions of fungal melanin beyond virulence. **Fungal Biology Reviews**, *[S. l.]*, v. 31, n. 2, p. 99-112, 2017. Disponível em: https://doi.org/10.1016/j.fbr.2016.12.003

COX, G. M. *et al.* Urease as a Virulence Factor in Experimental Cryptococcosis. **Infection and immunity**, *[S. l.]*, v. 68, n. 2, p. 443–8, 2000. Disponível em: https://doi.org/10.1128/IAI.68.2.443-448.2000

COX, G. M. *et al.* Extracellular phospholipase activity is a virulence factor for *Cryptococcus neoformans*. **Molecular Microbiology**, *[S. l.]*, v. 39, n. 1, p. 166–175, 2001. Disponível em: https://doi.org/10.1046/j.1365-2958.2001.02236.x

CRAMER, K. L. *et al.* Transcription Factor Nrg1 Mediates Capsule Formation, Stress Response, and Pathogenesis in *Cryptococcus neoformans*. **Eukaryotic Cell**, *[S. l.]*, v. 5, n. 7, p. 1147–1156, 2006. Disponível em: https://doi.org/10.1128/EC.00145-06

CRUZ, M. C.; FOX, D. S.; HEITMAN, J. Calcineurin is required for hyphal elongation during mating and haploid fruiting in *Cryptococcus neoformans*. **The EMBO Journal**, *[S. l.]*, v. 20, n. 5, p. 1020–1032, 2001. Disponível em: https://doi.org/10.1093/emboj/20.5.1020

CYERT, M. S. Calcineurin signaling in *Saccharomyces cerevisiae*: How yeast go crazy in response to stress. **Biochemical and Biophysical Research Communications**, *[S. l.]*, v. 311, n. 4, p. 1143–1150, 2003. Disponível em: https://doi.org/10.1016/S0006-291X(03)01552-3

DA SILVA, R. P. *et al.* Extracellular vesicle-mediated export of fungal RNA. **Scientific Reports**, *[S. l.]*, v. 5, 2015. Disponível em: https://doi.org/10.1038/srep07763

DAMBUZA, I. M. *et al.* The *Cryptococcus neoformans* Titan cell is an inducible and regulated morphotype underlying pathogenesis. **PLOS Pathogens**, *[S. l.]*, v. 14, n. 5, p. e1006978, 2018. Disponível em: https://doi.org/10.1371/journal.ppat.1006978

DATTA, K.; BARTLETT, K. H.; MARR, K. A. *Cryptococcus gattii*: Emergence in Western North America: Exploitation of a Novel Ecological Niche. **Interdisciplinary Perspectives on Infectious Diseases**, *[S. l.]*, v. 2009, p. 1–8, 2009. Disponível em: https://doi.org/10.1155/2009/176532

DAVIS, M. J. *et al. Cryptococcus neoformans* – Induced Macrophage Lysosome Damage Crucially Contributes to Fungal Virulence. **The Journal of Immunology**, *[S. l.]*, v. 194, n. 5, p. 2219–2231, 2015. Disponível em: https://doi.org/10.4049/jimmunol.1402376

DE LEON-RODRIGUEZ, C. M. *et al.* The Outcome of the *Cryptococcus neoformans* – Macrophage Interaction Depends on Phagolysosomal Membrane Integrity. **The Journal of Immunology**, *[S. l.]*, v. 201, n. 2, p. 583–603, 2018. Disponível em: https://doi.org/10.4049/jimmunol.1700958

DELEON-RODRIGUEZ, C. M.; CASADEVALL, A. *Cryptococcus neoformans*: Tripping on Acid in the Phagolysosome. **Frontiers in Microbiology**, *[S. l.]*, v. 7, 2016. Disponível em: https://doi.org/10.3389/fmicb.2016.00164

DOERING, T. L. *et al.* Melanin as a potential cryptococcal defence against microbicidal proteins. **Medical mycology**, *[S. l.]*, v. 37, n. 3, p. 175–81, 1999. Disponível em: https://doi.org/10.1080/j.1365-280x.1999.00218.x

DOERING, T. L. How does *Cryptococcus* get its coat?. **Trends Microbiol**, *[S. l.]*, v. 8, n. 12, p. 547-553, 2000. Disponível em: https://doi.org/10.1016/S0966-842X(00)01890-4

DOERING, T. L. How Sweet it is! Cell Wall Biogenesis and Polysaccharide Capsule Formation in *Cryptococcus neoformans*. **Annual review of microbiology**, *[S. l.]*, v. 63, p. 223–47, 2009. Disponível em: https://doi.org/10.1146/annurev.micro.62.081307.162753

DRAGOTAKES, Q.; FU, M. S.; CASADEVALL, A. Dragotcytosis: Elucidation of the Mechanism for *Cryptococcus neoformans* Macrophage-to-Macrophage Transfer. **The Journal of Immunology**, *[S. l.]*, v. 202, n. 9, p. 2661–2670, 2019. Disponível em: https://doi.org/10.4049/jimmunol.1801118

DUNCAN, J. T. Cryptococcosis, Torulosis or European Blastomycosis. **The American Journal of Tropical Medicine and Hygiene**, *[S. l.]*, v. 6, n. 1, p. 192–192, 1957. Disponível em: https://doi.org/10.4269/ajtmh.1957.6.1.tm0060010192b

EISENMAN, H. C. *et al.* Microstructure of Cell Wall-Associated Melanin in the Human Pathogenic Fungus *Cryptococcus neoformans*. **Biochemistry**, *[S. l.]*, v. 44, n. 10, p. 3683–3693, 2005. Disponível em: https://doi.org/10.1021/bi047731m

EISENMAN, H. C. *et al.* Vesicle-associated melanization in *Cryptococcus neoformans*. **Microbiology**, *[S. l.]*, v. 155, n. 12, p. 3860–3867, 2009. Disponível em: https://doi.org/10.1099/mic.0.032854-0

EMMONS, C. W. Saprophytic sources of *Cryptococcus neoformans* associated with the pigeon (*Columba livia*). **American Journal of Epidemiology**, *[S. l.]*, v. 62, n. 3, p. 227–232, 1955. Disponível em: https://doi.org/10.1093/oxfordjournals.aje.a119775

ESHER, S. K.; ZARAGOZA, O.; ALSPAUGH, J. A. Cryptococcal pathogenic mechanisms: A dangerous trip from the environment to the brain. **Memorias do Instituto Oswaldo Cruz**, *[S. l.]*, v. 113, n. 7, p. 1–15, 2018. Disponível em: https://doi.org/10.1590/0074-02760180057

EVANS, E. E. The Antigenic Composition of *Cryptococcus neoformans*. II. Serologic Studies with the Capsular Polysaccharide. **The Journal of Immunology**, *[S. l.]*, v. 67, n. 2, p. 109–114, 1951. Disponível em: https://doi.org/10.1128/JB.66.3.287-293.1953

FAN, W. *et al.* Eca1, a Sarcoplasmic/Endoplasmic Reticulum Ca2+-ATPase, Is Involved in Stress Tolerance and Virulence in *Cryptococcus neoformans*. **Infection and Immunity**, *[S. l.]*, v. 75, n. 7, p. 3394–3405, 2007. Disponível em: https://doi.org/10.1128/IAI.01977-06

FEDER, V. *et al. Cryptococcus gattii* urease as a virulence factor and the relevance of enzymatic activity in cryptococcosis pathogenesis. **FEBS Journal**, *[S. l.]*, v. 282, n. 8, p. 1406–1418, 2015. Disponível em: https://doi.org/10.1111/febs.13229

FELDMESSER, M. *et al. Cryptococcus neoformans* Is a Facultative Intracellular Pathogen in Murine Pulmonary Infection. **Infection and Immunity**, *[S. l.]*, v. 68, n. 7, p. 4225–4237, 2000. Disponível em: https://doi.org/10.1128/IAI.68.7.4225-4237.2000

FELDMESSER, M.; TUCKER, S.; CASADEVALL, A. Intracellular parasitism of macrophages by *Cryptococcus neoformans*. **Trends Microbiol**, *[S. l.]*, v. 9, n. 6, p. 273-278, 2001. Disponível em: https://doi.org/10.1016/S0966-842X(01)02035-2

FISHER, M. C. *et al.* Emerging fungal threats to animal, plant and ecosystem health. **Nature**, *[S. l.]*, v. 484, n. 7393, p. 186-194, 2012. Disponível em: https://doi.org/10.1038/nature10947

FISHER, M. C. *et al.* Threats Posed by the Fungal Kingdom to Humans, Wildlife, and Agriculture. **mBio**, *[S. l.]*, v. 11, n. 3, 2020. Disponível em: https://doi.org/10.1128/mBio.00449-20

FOX, D. S. *et al.* Calcineurin regulatory subunit is essential for virulence and mediates interactions with FKBP12-FK506 in *Cryptococcus neoformans*. **Molecular Microbiology**, *[S. l.]*, v. 39, n. 4, p. 835–849, 2001. Disponível em: https://doi.org/10.1046/j.1365-2958.2001.02295.x

FRASES, S. *et al.* Capsule of *Cryptococcus neoformans* grows by enlargement of polysaccharide molecules. **Proceedings of the National Academy of Sciences of the United States of America**, *[S. l.]*, v. 106, n. 4, p. 1228–1233, 2009. Disponível em: https://doi.org/10.1073/pnas.0808995106

FRAZÃO, S. de O. *et al.* Laccase Affects the Rate of *Cryptococcus neoformans* Nonlytic Exocytosis from Macrophages. **mBio**, *[S. l.]*, v. 11, n. 5, p. 1–6, 2020. Disponível em: https://doi.org/10.1128/mBio.02085-20

FU, M. S. *et al. Cryptococcus neoformans* urease affects the outcome of intracellular pathogenesis by modulating phagolysosomal pH. **PLOS Pathogens**, *[S. l.]*, v. 14, n. 6, p. e1007144, 2018. Disponível em: https://doi.org/10.1371/journal.ppat.1007144

FU, M. S.; DRUMMOND, R. A. The Diverse Roles of Monocytes in Cryptococcosis. **Journal of Fungi**, *[S. l.]*, v. 6, n. 3, p. 111, 2020. Disponível em: https://doi.org/10.3390/jof6030111

Fungal Disease Frequency | Gaffi - Global Action Fund for Fungal Infections, *[s. l.]*, *[s. d.]*. Disponível em: https://www.gaffi.org/why/fungal-disease-frequency/.

GARCÍA-BARBAZÁN, I. *et al.* The formation of titan cells in *Cryptococcus*

neoformans depends on the mouse strain and correlates with induction of Th2-type responses. **Cellular Microbiology**, *[S. l.]*, v. 18, n. 1, p. 111–124, 2016. Disponível em: https://doi.org/10.1111/cmi.12488

GARCIA-HERMOSO, D.; JANBON, G.; DROMER, F. Epidemiological Evidence for Dormant *Cryptococcus neoformans* Infection. **Journal of Clinical Microbiology**, *[S. l.]*, v. 37, n. 10, p. 3204–3209, 1999. Disponível em: https://doi.org/10.1128/jcm.37.10.3204-3209.1999

GARCÍA-RODAS, R. *et al.* Cryptococcal Titan Cells: When Yeast Cells Are All Grown up. *In*: **Current Topics in Microbiology and Immunology**. *[S. l.]*, 2018. v. 422p. 101–120. *E-book*. Disponível em: https://doi.org/10.1007/82_2018_145

GARCÍA-RODAS, R.; ZARAGOZA, O. Catch me if you can: Phagocytosis and killing avoidance by *Cryptococcus neoformans*. **FEMS Immunology and Medical Microbiology**, *[S. l.]*, v. 64, n. 2, p. 147–161, 2012. Disponível em: https://doi.org/10.1111/j.1574-695X.2011.00871.x

GARCIA-SANTAMARINA, S. *et al.* Genome-wide analysis of the regulation of Cu metabolism in *Cryptococcus neoformans*. **Molecular Microbiology**, *[S. l.]*, v. 108, n. 5, p. 473–494, 2018. Disponível em: https://doi.org/10.1111/mmi.13960

GASKELL, K. M. *et al.* A Prospective Study of Mortality from Cryptococcal Meningitis following Treatment Induction with 1200mg Oral Fluconazole in Blantyre, Malawi. **PLoS ONE**, *[S. l.]*, v. 9, n. 11, 2014. Disponível em: https://doi.org/10.1371/journal.pone.0110285

GATES, M. A.; THORKILDSON, P.; KOZEL, T. R. Molecular architecture of the *Cryptococcus neoformans* capsule. **Molecular Microbiology**, *[S. l.]*, v. 52, n. 1, p. 13–24, 2004. Disponível em: https://doi.org/10.1111/j.1365-2958.2003.03957.x

GAYLORD, E. A.; CHOY, H. L.; DOERING, T. L. Dangerous Liaisons: Interactions of *Cryptococcus neoformans* with Host Phagocytes. **Pathogens**, *[S. l.]*, v. 9, n. 11, p. 891, 2020. Disponível em: https://doi.org/10.3390/pathogens9110891

GERSTEIN, A. C. *et al.* Polyploid Titan Cells Produce Haploid and Aneuploid Progeny To Promote Stress Adaptation. **mBio**, *[S. l.]*, v. 6, n. 5, p. e01340-15, 2015. Disponível em: https://doi.org/10.1128/mBio.01340-15

GILBERT, A. S. *et al.* Vomocytosis of live pathogens from macrophages is regulated by the atypical MAP kinase ERK5. **Science Advances**, *[S. l.]*, v. 3, n. 8, 2017. Disponível em: https://doi.org/10.1126/sciadv.1700898

GILES, S. S. *et al.* Elucidating the Pathogenesis of Spores from the Human Fungal Pathogen *Cryptococcus neoformans*. **Infection and Immunity**, *[S. l.]*, v. 77, n. 8, p. 3491–3500, 2009. Disponível em: https://doi.org/10.1128/IAI.00334-09

GISH, S. R. *et al.* Computational Analysis Reveals a Key Regulator of Cryptococcal Virulence and Determinant of Host Response. **mBio**, *[S. l.]*, v. 7, n. 2, p. e00313-16, 2016. Disponível em: https://doi.org/10.1128/mBio.00313-16

GOLDMAN, D. L. *et al.* Persistent *Cryptococcus neoformans* Pulmonary Infection in the Rat Is Associated with Intracellular Parasitism, Decreased Inducible Nitric Oxide

Synthase Expression, and Altered Antibody Responsiveness to Cryptococcal Polysaccharide. **Infection and Immunity**, *[S. l.]*, v. 68, n. 2, p. 832–838, 2000. Disponível em: https://doi.org/10.1128/IAI.68.2.832-838.2000

HADDOW, L. J. *et al.* Cryptococcal immune reconstitution inflammatory syndrome in HIV-1-infected individuals: proposed clinical case definitions. **The Lancet Infectious Diseases**, *[S. l.]*, v. 10, n. 11, p. 791-802, 2010. Disponível em: https://doi.org/10.1016/S1473-3099(10)70170-5

HAGEN, F. *et al.* Recognition of seven species in the *Cryptococcus gattii*/*Cryptococcus neoformans* species complex. **Fungal Genetics and Biology**, *[S. l.]*, v. 78, p. 16–48, 2015. Disponível em: https://doi.org/10.1016/j.fgb.2015.02.009

HAGEN, F. *et al.* Importance of Resolving Fungal Nomenclature: the Case of Multiple Pathogenic Species in the *Cryptococcus* Genus. **mSphere**, *[S. l.]*, v. 2, n. 4, p. 238–255, 2017. Disponível em: https://doi.org/10.1128/msphere.00238-17

HAYNES, B. C. *et al.* Toward an Integrated Model of Capsule Regulation in *Cryptococcus neoformans*. **PLoS Pathogens**, *[S. l.]*, v. 7, n. 12, p. e1002411, 2011. Disponível em: https://doi.org/10.1371/journal.ppat.1002411

HEISS, C. *et al.* The structure of *Cryptococcus neoformans* galactoxylomannan contains β-d-glucuronic acid. **Carbohydrate Research**, *[S. l.]*, v. 344, n. 7, p. 915–920, 2009. Disponível em: https://doi.org/10.1016/j.carres.2009.03.003

HEMENWAY, C. S.; HEITMAN, J. Calcineurin: Structure, function, and inhibition. **Cell Biochemistry and Biophysics**, *[S. l.]*, v. 30, n. 1, p. 115–151, 1999. Disponível em: https://doi.org/10.1007/BF02737887

HERRING, A. C. *et al.* Induction of Interleukin-12 and Gamma Interferon Requires Tumor Necrosis Factor Alpha for Protective T1-Cell-Mediated Immunity to Pulmonary *Cryptococcus neoformans* Infection. **Infection and Immunity**, *[S. l.]*, v. 70, n. 6, p. 2959–2964, 2002. Disponível em: https://doi.org/10.1128/IAI.70.6.2959-2964.2002

HEUNG, L. J.; HOHL, T. M. Inflammatory monocytes are detrimental to the host immune response during acute infection with *Cryptococcus neoformans*. **PLoS Pathogens**, *[S. l.]*, v. 15, n. 3, p. e1007627, 2019. Disponível em: https://doi.org/10.1371/journal.ppat.1007627

HOAG, K. A. *et al.* IL-12 and IFN- γ Are Required for Initiating the Protective Th1 Response to Pulmonary Cryptococcosis in Resistant C.B-17 Mice. **American Journal of Respiratory Cell and Molecular Biology**, *[S. l.]*, v. 17, n. 6, p. 733–739, 1997. Disponível em: https://doi.org/10.1165/ajrcmb.17.6.2879

HOMER, C. M. *et al.* Intracellular Action of a Secreted Peptide Required for Fungal Virulence. **Cell Host and Microbe**, *[S. l.]*, v. 19, n. 6, p. 849–864, 2016. Disponível em: https://doi.org/10.1016/j.chom.2016.05.001

HOMMEL, B. *et al.* Titan cells formation in *Cryptococcus neoformans* is finely tuned by environmental conditions and modulated by positive and negative genetic regulators. **PLOS Pathogens**, *[S. l.]*, v. 14, n. 5, p. e1006982, 2018. Disponível em:

https://doi.org/10.1371/journal.ppat.1006982

HOOD, M. I.; SKAAR, E. P. Nutritional immunity: transition metals at the pathogen–host interface. **Nature Reviews Microbiology**, *[S. l.]*, v. 10, n. 8, p. 525-537, 2012. Disponível em: https://doi.org/10.1038/nrmicro2836

HUANG, C. *et al.* Purification and Characterization of a Second Immunoreactive Mannoprotein from *Cryptococcus neoformans* That Stimulates T-Cell Responses. **Infection and Immunity**, *[S. l.]*, v. 70, n. 10, p. 5485–5493, 2002. Disponível em: https://doi.org/10.1128/IAI.70.10.5485-5493.2002

HUANG, S.-H. *et al.* Invasion of *Cryptococcus neoformans* into Human Brain Microvascular Endothelial Cells Is Mediated through the Lipid Rafts-Endocytic Pathway via the Dual Specificity Tyrosine Phosphorylation-regulated Kinase 3 (DYRK3). **Journal of Biological Chemistry**, *[S. l.]*, v. 286, n. 40, p. 34761–34769, 2011. Disponível em: https://doi.org/10.1074/jbc.M111.219378

HUFFNAGLE, G. B. *et al.* The role of CD4+ and CD8+ T cells in the protective inflammatory response to a pulmonary cryptococcal infection. **Journal of Leukocyte Biology**, *[S. l.]*, v. 55, n. 1, p. 35–42, 1994. Disponível em: https://doi.org/10.1002/jlb.55.1.35

HUFFNAGLE, G. B. *et al.* Down-regulation of the afferent phase of T cell-mediated pulmonary inflammation and immunity by a high melanin-producing strain of *Cryptococcus neoformans*. **The Journal of Immunology**, *[S. l.]*, v. 155, n. 7, 1995.

HUSTON, S. M. *et al. Cryptococcus gattii* Is Killed by Dendritic Cells, but Evades Adaptive Immunity by Failing To Induce Dendritic Cell Maturation. **The Journal of Immunology**, *[S. l.]*, v. 191, n. 1, p. 249–261, 2013. Disponível em: https://doi.org/10.4049/jimmunol.1202707

JACOBSON, E. S.; IKEDA, R. Effect of melanization upon porosity of the cryptococcal cell wall. **Medical Mycology**, *[S. l.]*, v. 43, n. 4, p. 327–333, 2005. Disponível em: https://doi.org/10.1080/13693780412331271081

JARVIS, J. N. *et al.* Determinants of Mortality in a Combined Cohort of 501 Patients With HIV-Associated Cryptococcal Meningitis: Implications for Improving Outcomes. **Clinical Infectious Diseases**, *[S. l.]*, v. 58, n. 5, p. 736–745, 2014. Disponível em: https://doi.org/10.1093/cid/cit794

JOHNSTON, S. A.; MAY, R. C. The Human Fungal Pathogen *Cryptococcus neoformans* Escapes Macrophages by a Phagosome Emptying Mechanism That Is Inhibited by Arp2/3 Complex-Mediated Actin Polymerisation. **PLoS Pathogens**, *[S. l.]*, v. 6, n. 8, p. e1001041, 2010. Disponível em: https://doi.org/10.1371/journal.ppat.1001041

JOHNSTON, S. A.; MAY, R. C. *Cryptococcus* interactions with macrophages: evasion and manipulation of the phagosome by a fungal pathogen. **Cellular Microbiology**, *[S. l.]*, v. 15, n. 3, p. 403–411, 2013. Disponível em: https://doi.org/doi.org/10.1111/cmi.12067

JONG, A. *et al.* Involvement of human CD44 during *Cryptococcus neoformans* infection of brain microvascular endothelial cells. **Cellular Microbiology**, *[S. l.]*, v.

10, n. 6, p. 1313–1326, 2008. Disponível em: https://doi.org/10.1111/j.1462-5822.2008.01128.x

JOSEPH, J. D.; MEANS, A. R. Calcium Binding Is Required for Calmodulin Function in *Aspergillus nidulans*. **Eukaryotic Cell**, *[S. l.]*, v. 1, n. 1, p. 119–125, 2002. Disponível em: https://doi.org/10.1128/EC.01.1.119-125.2002

JUNG, K.-W. *et al.* Systematic functional profiling of transcription factor networks in *Cryptococcus neoformans*. **Nature Communications**, *[S. l.]*, v. 6, n. 1, p. 6757, 2015. Disponível em: https://doi.org/10.1038/ncomms7757

JUNG, W. H. *et al.* Iron Regulation of the Major Virulence Factors in the AIDS-Associated Pathogen *Cryptococcus neoformans*. **PLoS Biology**, *[S. l.]*, v. 4, n. 12, p. e410, 2006. Disponível em: https://doi.org/10.1371/journal.pbio.0040410

JUVVADI, P. R. *et al.* Calcineurin in fungal virulence and drug resistance: Prospects for harnessing targeted inhibition of calcineurin for an antifungal therapeutic approach. **Virulence**, *[S. l.]*, v. 8, n. 2, p. 186–197, 2017. Disponível em: https://doi.org/10.1080/21505594.2016.1201250

KAWAKAMI, K. *et al.* T Cell-Dependent Activation of Macrophages and Enhancement of Their Phagocytic Activity in the Lungs of Mice Inoculated with Heat-Killed *Cryptococcus neoformans*: Involvement of IFN-γ and Its Protective Effect against Cryptococcal Infection. **Microbiology and Immunology**, *[S. l.]*, v. 39, n. 2, p. 135–143, 1995. Disponível em: https://doi.org/10.1111/j.1348-0421.1995.tb02180.x

KECHICHIAN, T. B.; SHEA, J.; DEL POETA, M. Depletion of Alveolar Macrophages Decreases the Dissemination of a Glucosylceramide-Deficient Mutant of *Cryptococcus neoformans* in Immunodeficient Mice. **Infection and Immunity**, *[S. l.]*, v. 75, n. 10, p. 4792–4798, 2007. Disponível em: https://doi.org/10.1128/IAI.00587-07

KESWANI, C. *et al.* Antimicrobial secondary metabolites from agriculturally important fungi as next biocontrol agents. **Applied Microbiology and Biotechnology**, *[S. l.]*, v. 103, n. 23-24, p. 9287-9303, 2019. Disponível em: https://doi.org/10.1007/s00253-019-10209-2

KLUTTS, J. S.; DOERING, T. L. Cryptococcal Xylosyltransferase 1 (Cxt1p) from *Cryptococcus neoformans* Plays a Direct Role in the Synthesis of Capsule Polysaccharides. **Journal of Biological Chemistry**, *[S. l.]*, v. 283, n. 21, p. 14327–14334, 2008. Disponível em: https://doi.org/10.1074/jbc.M708927200

KMETZSCH, L. *et al.* The Vacuolar Ca2+ Exchanger Vcx1 Is Involved In Calcineurin-Dependent Ca2+ Tolerance and Virulence in *Cryptococcus neoformans*. **Eukaryotic Cell**, *[S. l.]*, v. 9, n. 11, p. 1798–1805, 2010. Disponível em: https://doi.org/10.1128/EC.00114-10

KMETZSCH, L. *et al.* The calcium transporter Pmc1 provides Ca2+ tolerance and influences the progression of murine cryptococcal infection. **FEBS Journal**, *[S. l.]*, v. 280, n. 19, p. 4853–4864, 2013. Disponível em: https://doi.org/10.1111/febs.12458

KOGUCHI, Y.; KAWAKAMI, K. Cryptococcal infection and Th1-Th2 cytokine balance. **International Reviews of Immunology**, *[S. l.]*, v. 21, n. 4–5, p. 423–428, 2002. Disponível em: https://doi.org/10.1080/08830180213274

KÖHLER, J. R. *et al.* Fungi that Infect Humans. *In*: **The Fungal Kingdom**. *[S. l.]*: American Society of Microbiology, 2017. v. 5p. 813–843. *E-book*. Disponível em: https://doi.org/10.1128/microbiolspec.funk-0014-2016

KOZUBOWSKI, L. *et al.* Calcineurin Colocalizes with P-Bodies and Stress Granules during Thermal Stress in *Cryptococcus neoformans*. **Eukaryotic Cell**, *[S. l.]*, v. 10, n. 11, p. 1396–1402, 2011. Disponível em: https://doi.org/10.1128/EC.05087-11

KOZUBOWSKI, L.; LEE, S. C.; HEITMAN, J. Signalling pathways in the pathogenesis of *Cryptococcus*. **Cellular Microbiology**, *[S. l.]*, v. 11, n. 3, p. 370–380, 2009. Disponível em: https://doi.org/10.1111/j.1462-5822.2008.01273.x

KRAUS, P. R.; NICHOLS, C. B.; HEITMAN, J. Calcium- and Calcineurin-Independent Roles for Calmodulin in *Cryptococcus neoformans* Morphogenesis and High-Temperature Growth. **Eukaryotic Cell**, *[S. l.]*, v. 4, n. 6, p. 1079–1087, 2005. Disponível em: https://doi.org/10.1128/EC.4.6.1079-1087.2005

KRONSTAD, J. W. *et al.* Expanding fungal pathogenesis: *Cryptococcus* breaks out of the opportunistic box. **Nature Reviews Microbiology**, *[S. l.]*, v. 9, n. 3, p. 193–203, 2011. Disponível em: https://doi.org/10.1038/nrmicro2522

KWON-CHUNG, K. J. *et al.* Proposal to conserve the name *Cryptococcus gattii* against *C. hondurianus* and *C. bacillisporus* (*Basidiomycota*, *Hymenomycetes*, *Tremellomycetidae*). **Taxon**, *[S. l.]*, v. 51, n. 4, p. 804–806, 2002. Disponível em: https://doi.org/10.2307/1555045

KWON-CHUNG, K. J. *et al. Cryptococcus neoformans* and *Cryptococcus gattii*, the Etiologic Agents of Cryptococcosis. **Cold Spring Harbor Perspectives in Medicine**, *[S. l.]*, v. 4, n. 7, p. a019760, 2014. Disponível em: https://doi.org/10.1101/cshperspect.a019760

KWON-CHUNG, K. J. *et al.* The Case for Adopting the “Species Complex” Nomenclature for the Etiologic Agents of Cryptococcosis. **mSphere**, *[S. l.]*, v. 2, n. 1, 2017. Disponível em: https://doi.org/10.1128/msphere.00357-16

KWON-CHUNG, K. J.; BENNETT, J. E. Epidemiologic Differences Between the Two Varieties of *Cryptococcus neoformans*. **American Journal of Epidemiology**, *[S. l.]*, v. 120, n. 1, p. 123–130, 1984. Disponível em: https://doi.org/10.1093/oxfordjournals.aje.a113861

KWON-CHUNG, K. J.; EDMAN, J. C.; WICKES, B. L. Genetic association of mating types and virulence in *Cryptococcus neoformans*. **Infection and Immunity**, *[S. l.]*, v. 60, n. 2, 1992. Disponível em: https://doi.org/10.1128/IAI.60.2.602-605.1992

KWON-CHUNG, K. J.; VARMA, A. Do major species concepts support one, two or more species within *Cryptococcus neoformans*?. **FEMS Yeast Res**, *[S. l.]*, v. 6, n. 4, p. 574-587, 2006. Disponível em: https://doi.org/10.1111/j.1567-1364.2006.00088.x

LEE, D. *et al.* Unraveling Melanin Biosynthesis and Signaling Networks in *Cryptococcus neoformans*. **mBio**, *[S. l.]*, v. 10, n. 5, p. e02267-19, 2019. Disponível em: https://doi.org/10.1128/mBio.02267-19

LEE, K.-T. *et al.* Fungal kinases and transcription factors regulating brain infection in *Cryptococcus neoformans*. **Nature Communications**, *[S. l.]*, v. 11, n. 1, p. 1521, 2020. Disponível em: https://doi.org/10.1038/s41467-020-15329-2

LEON-RODRIGUEZ, C. M. De *et al.* The Capsule of *Cryptococcus neoformans* Modulates Phagosomal pH through Its Acid-Base Properties. **mSphere**, *[S. l.]*, v. 3, n. 5, p. 1–8, 2018. Disponível em: https://doi.org/10.1128/mSphere.00437-18

LEV, S. *et al.* The Crz1/Sp1 Transcription Factor of *Cryptococcus neoformans* Is Activated by Calcineurin and Regulates Cell Wall Integrity. **PLoS ONE**, *[S. l.]*, v. 7, n. 12, p. e51403, 2012. Disponível em: https://doi.org/10.1371/journal.pone.0051403

LEV, S. *et al.* Pho4 Is Essential for Dissemination of *Cryptococcus neoformans* to the Host Brain by Promoting Phosphate Uptake and Growth at Alkaline pH. **mSphere**, *[S. l.]*, v. 2, n. 1, p. e00381-16, 2017. Disponível em: https://doi.org/10.1128/mSphere.00381-16

LEVITZ, S. M. *et al. Cryptococcus neoformans* Resides in an Acidic Phagolysosome of Human Macrophages. **Infection and Immunity**, *[S. l.]*, v. 67, n. 2, p. 885–890, 1999. Disponível em: https://doi.org/10.1128/iai.67.2.885-890.1999

LEVITZ, S. M. *et al.* Molecular characterization of a mannoprotein with homology to chitin deacetylases that stimulates T cell responses to *Cryptococcus neoformans*. **Proceedings of the National Academy of Sciences of the United States of America**, *[S. l.]*, v. 98, n. 18, p. 10422–10427, 2001. Disponível em: https://doi.org/10.1073/pnas.181331398

LEVITZ, S. M.; SPECHT, C. A. The molecular basis for the immunogenicity of *Cryptococcus neoformans* mannoproteins. FEMS Yeast Res, *[S. l.]*, v. 6, n. 4, p. 513-524, 2006. Disponível em: https://doi.org/10.1111/j.1567-1364.2006.00071.x

LIN, J.; IDNURM, A.; LIN, X. Morphology and its underlying genetic regulation impact the interaction between *Cryptococcus neoformans* and its hosts. **Medical Mycology**, *[S. l.]*, v. 53, n. 5, p. 493–504, 2015. Disponível em: https://doi.org/10.1093/mmy/myv012

LIN, X.; HEITMAN, J. The Biology of the *Cryptococcus neoformans* Species Complex. **Annual Review of Microbiology**, *[S. l.]*, v. 60, n. 1, p. 69–105, 2006. Disponível em: https://doi.org/10.1146/annurev.micro.60.080805.142102

LITVINTSEVA, A. P. *et al.* Evidence of Sexual Recombination among *Cryptococcus neoformans* Serotype A Isolates in Sub-Saharan Africa. **Eukaryotic Cell**, *[S. l.]*, v. 2, n. 6, p. 1162–1168, 2003. Disponível em: https://doi.org/10.1128/EC.2.6.1162-1168.2003

LITVINTSEVA, A. P. *et al.* Evidence that the Human Pathogenic Fungus *Cryptococcus neoformans* var. *grubii* May Have Evolved in Africa. **PLoS ONE**, *[S. l.]*, v. 6, n. 5, p. e19688, 2011. Disponível em:

https://doi.org/10.1371/journal.pone.0019688

LIU, M. *et al.* Cch1 Mediates Calcium Entry in *Cryptococcus neoformans* and Is Essential in Low-Calcium Environments. **Eukaryotic Cell**, *[S. l.]*, v. 5, n. 10, p. 1788–1796, 2006. Disponível em: https://doi.org/10.1128/EC.00158-06

LIU, O. W. *et al.* Systematic Genetic Analysis of Virulence in the Human Fungal Pathogen *Cryptococcus neoformans*. **Cell**, *[S. l.]*, v. 135, n. 1, p. 174–188, 2008. Disponível em: https://doi.org/10.1016/j.cell.2008.07.046

LUBERTO, C. *et al.* Identification of App1 as a regulator of phagocytosis and virulence of *Cryptococcus neoformans*. **Journal of Clinical Investigation**, *[S. l.]*, v. 112, n. 7, p. 1080–1094, 2003. Disponível em: https://doi.org/10.1172/JCI18309

MA, H. *et al.* Expulsion of Live Pathogenic Yeast by Macrophages. **Current Biology**, *[S. l.]*, v. 16, n. 21, p. 2156–2160, 2006. Disponível em: https://doi.org/10.1016/j.cub.2006.09.032

MA, H. *et al.* Direct cell-to-cell spread of a pathogenic yeast. **BMC Immunology**, *[S. l.]*, v. 8, 2007. Disponível em: https://doi.org/10.1186/1471-2172-8-15

MA, H. *et al.* The fatal fungal outbreak on Vancouver Island is characterized by enhanced intracellular parasitism driven by mitochondrial regulation. **Proceedings of the National Academy of Sciences of the United States of America**, *[S. l.]*, v. 106, n. 31, p. 12980–12985, 2009. Disponível em: https://doi.org/10.1073/pnas.0902963106

MA, H.; MAY, R. C. Virulence in *Cryptococcus* Species. *In*: **Advances in applied microbiology**. *[S. l.: s. n.]*. v. 67p. 131–190. *E-book*. Disponível em: https://doi.org/10.1016/S0065-2164(08)01005-8

MACDOUGALL, L. *et al.* Risk Factors for *Cryptococcus gattii* Infection, British Columbia, Canada. **Emerging Infectious Diseases**, *[S. l.]*, v. 17, n. 2, p. 193–199, 2011. Disponível em: https://doi.org/10.3201/eid1702.101020

MAGDITCH, D. A. *et al.* DNA Mutations Mediate Microevolution between Host-Adapted Forms of the Pathogenic Fungus *Cryptococcus neoformans*. **PLoS Pathogens**, *[S. l.]*, v. 8, n. 10, p. e1002936, 2012. Disponível em: https://doi.org/10.1371/journal.ppat.1002936

MAIER, E. J. *et al.* Model-driven mapping of transcriptional networks reveals the circuitry and dynamics of virulence regulation. **Genome Research**, *[S. l.]*, v. 25, n. 5, p. 690–700, 2015. Disponível em: https://doi.org/10.1101/gr.184101.114

MANSOUR, M. K.; LEVITZ, S. M. Interactions of fungi with phagocytes. **Current Opinion in Microbiology**, *[S. l.]*, v. 5, n. 4, p. 359-365, 2002. Disponível em: https://doi.org/10.1016/S1369-5274(02)00342-9

MARESCA, B.; KOBAYASHI, G. S. Dimorphism in *Histoplasma capsulatum* and *Blastomyces dermatitidis*. **Contrib Microbiol**, *[S. l.]*, v. 5, p. 201-216, 2000. Disponível em: https://doi.org/10.1159/000060346

MARUVADA, R. *et al. Cryptococcus neoformans* phospholipase B1 activates host cell Rac1 for traversal across the blood-brain barrier. **Cellular Microbiology**, *[S. l.]*,

v. 14, n. 10, p. 1544–1553, 2012. Disponível em: https://doi.org/10.1111/j.1462-5822.2012.01819.x

MCFADDEN, D. C.; DE JESUS, M.; CASADEVALL, A. The Physical Properties of the Capsular Polysaccharides from *Cryptococcus neoformans* Suggest Features for Capsule Construction. **Journal of Biological Chemistry**, *[S. l.]*, v. 281, n. 4, p. 1868–1875, 2006. Disponível em: https://doi.org/10.1074/jbc.M509465200

MCQUISTON, T. J.; WILLIAMSON, P. R. Paradoxical roles of alveolar macrophages in the host response to *Cryptococcus neoformans*. **Journal of Infection and Chemotherapy**, *[S. l.]*, v. 18, n. 1, p. 1-19, 2012. Disponível em: https://doi.org/10.1007/s10156-011-0306-2

MEYER, W. *et al.* Consensus multi-locus sequence typing scheme for *Cryptococcus neoformans* and *Cryptococcus gattii*. **Medical Micology**, *[S. l.]*, v. 47, n. 6, p. 561-570, 2009. Disponível em: https://doi.org/10.1080/13693780902953886

MISSALL, T. A. *et al.* Distinct Stress Responses of Two Functional Laccases in *Cryptococcus neoformans* Are Revealed in the Absence of the Thiol-Specific Antioxidant Tsa1. **Eukaryotic Cell**, *[S. l.]*, v. 4, n. 1, p. 202–208, 2005. Disponível em: https://doi.org/10.1128/EC.4.1.202-208.2005

MITCHELL, T. G.; PERFECT, J. R. Cryptococcosis in the era of AIDS--100 years after the discovery of *Cryptococcus neoformans*. **Clinical Microbiology Reviews**, *[S. l.]*, v. 8, n. 4, p. 515–548, 1995. Disponível em: https://doi.org/10.1128/cmr.8.4.515-548.1995

MONARI, C.; BISTONI, F.; VECCHIARELLI, A. Glucuronoxylomannan exhibits potent immunosuppressive properties. **FEMS Yeast Research**, *[S. l.]*, v. 6, n. 4, p. 537–542, 2006. Disponível em: https://doi.org/10.1111/j.1567-1364.2006.00072.x

MORANOVA, Z. *et al.* The CRZ1/SP1-like gene links survival under limited aeration, cell integrity and biofilm formation in the pathogenic yeast *Cryptococcus neoformans*. **Biomedical Papers**, *[S. l.]*, v. 158, n. 2, p. 212–220, 2014. Disponível em: https://doi.org/10.5507/bp.2013.024

MOURAD, A.; PERFECT, J. R. Present and Future Therapy of *Cryptococcus* Infections. **Journal of Fungi**, *[S. l.]*, v. 4, n. 3, p. 79, 2018. Disponível em: https://doi.org/10.3390/jof4030079

MOYRAND, F.; FONTAINE, T.; JANBON, G. Systematic capsule gene disruption reveals the central role of galactose metabolism on *Cryptococcus neoformans* virulence. **Molecular Microbiology**, *[S. l.]*, v. 64, n. 3, p. 771–781, 2007. Disponível em: https://doi.org/10.1111/j.1365-2958.2007.05695.x

MUKAREMERA, L. *et al.* Titan cell production in *Cryptococcus neoformans* reshapes the cell wall and capsule composition during infection. **The Cell Surface**, *[S. l.]*, v. 1, p. 15–24, 2018. Disponível em: https://doi.org/10.1016/j.tcsw.2017.12.001

NEAL, L. M. *et al.* CD4+ T Cells Orchestrate Lethal Immune Pathology despite Fungal Clearance during *Cryptococcus neoformans* Meningoencephalitis. **mBio**, *[S. l.]*, v. 8, n. 6, 2017. Disponível em: https://doi.org/10.1128/mBio.01415-17

NGAMSKULRUNGROJ, P. *et al.* The Primary Target Organ of *Cryptococcus gattii* Is Different from That of *Cryptococcus neoformans* in a Murine Model. **mBio**, *[S. l.]*, v. 3, n. 3, p. 1–9, 2012. Disponível em: https://doi.org/10.1128/mBio.00103-12

NIMRICHTER, L. *et al.* Structure, Cellular Distribution, Antigenicity, and Biological Functions of *Fonsecaea pedrosoi* Ceramide Monohexosides. **Infection and Immunity**, *[S. l.]*, v. 73, n. 12, p. 7860–7868, 2005. Disponível em: https://doi.org/10.1128/IAI.73.12.7860-7868.2005

NIMRICHTER, L. *et al.* Self-Aggregation of *Cryptococcus neoformans* Capsular Glucuronoxylomannan Is Dependent on Divalent Cations. **Eukaryotic cell**, *[S. l.]*, v. 6, n. 8, p. 1400–1410, 2007. Disponível em: https://doi.org/10.1128/EC.00122-07

NOSANCHUK, J. D.; CASADEVALL, A. The contribution of melanin to microbial pathogenesis. **Cellular Microbiology**, *[S. l.]*, v. 5, n. 4, p. 203–223, 2003. Disponível em: https://doi.org/10.1046/j.1462-5814.2003.00268.x

NOSANCHUK, J. D.; CASADEVALL, A. Impact of Melanin on Microbial Virulence and Clinical Resistance to Antimicrobial Compounds. **Antimicrobial agents and chemotherapy**, *[S. l.]*, v. 50, n. 11, p. 3519–28, 2006. Disponível em: https://doi.org/10.1128/AAC.00545-06

O'MEARA, T. R. *et al.* Interaction of *Cryptococcus neoformans* Rim101 and Protein Kinase A Regulates Capsule. **PLoS Pathogens**, *[S. l.]*, v. 6, n. 2, p. e1000776, 2010. Disponível em: https://doi.org/10.1371/journal.ppat.1000776

O'MEARA, T. R. *et al.* Global analysis of fungal morphology exposes mechanisms of host cell escape. **Nature Communications**, *[S. l.]*, v. 6, n. 3, p. 1–10, 2015. Disponível em: https://doi.org/10.1038/ncomms7741

O'MEARA, T. R.; ALSPAUGH, J. A. The *Cryptococcus neoformans* Capsule: a Sword and a Shield. **Clinical Microbiology Reviews**, *[S. l.]*, v. 25, n. 3, p. 387–408, 2012. Disponível em: https://doi.org/10.1128/CMR.00001-12

OKAGAKI, L. H. *et al.* Cryptococcal Cell Morphology Affects Host Cell Interactions and Pathogenicity. **PLoS Pathogens**, *[S. l.]*, v. 6, n. 6, p. e1000953, 2010. Disponível em: https://doi.org/10.1371/journal.ppat.1000953

OKAGAKI, L. H.; NIELSEN, K. Titan Cells Confer Protection from Phagocytosis in *Cryptococcus neoformans* Infections. **Eukaryotic Cell**, *[S. l.]*, v. 11, n. 6, p. 820–826, 2012. Disponível em: https://doi.org/10.1128/EC.00121-12

OLIVEIRA, D. L. *et al.* Extracellular vesicles from *Cryptococcus neoformans* modulate macrophage functions. **Infection and Immunity**, *[S. l.]*, v. 78, n. 4, p. 1601–1609, 2010. Disponível em: https://doi.org/10.1128/IAI.01171-09

OLSZEWSKI, M. A. *et al.* Urease Expression by *Cryptococcus neoformans* Promotes Microvascular Sequestration, Thereby Enhancing Central Nervous System Invasion. **The American Journal of Pathology**, *[S. l.]*, v. 164, n. 5, p. 1761–1771, 2004. Disponível em: https://doi.org/10.1016/S0002-9440(10)63734-0

ORSI, C. F. *et al.* The ABC transporter-encoding gene *AFR1* affects the resistance of *Cryptococcus neoformans* to microglia-mediated antifungal activity by delaying

phagosomal maturation. **FEMS Yeast Research**, *[S. l.]*, v. 9, n. 2, p. 301–310, 2009. Disponível em: https://doi.org/10.1111/j.1567-1364.2008.00470.x

OSTERHOLZER, J. J. *et al.* Cryptococcal Urease Promotes the Accumulation of Immature Dendritic Cells and a Non-Protective T2 Immune Response within the Lung. **American Journal of Pathology**, *[S. l.]*, v. 174, n. 3, p. 932–943, 2009. Disponível em: https://doi.org/10.2353/ajpath.2009.080673

PAPPAS, P. G. *et al.* A Phase II Randomized Trial of Amphotericin B Alone or Combined with Fluconazole in the Treatment of HIV-Associated Cryptococcal Meningitis. **Clinical Infectious Diseases**, *[S. l.]*, v. 48, n. 12, p. 1775–1783, 2009. Disponível em: https://doi.org/10.1086/599112

PARK, H. S. *et al.* Calcineurin Targets Involved in Stress Survival and Fungal Virulence. **PLOS Pathogens**, *[S. l.]*, v. 12, n. 9, p. e1005873, 2016. Disponível em: https://doi.org/10.1371/journal.ppat.1005873

PERFECT, J. R. *et al.* Clinical Practice Guidelines for the Management of Cryptococcal Disease: 2010 Update by the Infectious Diseases Society of America. **Clin Infect Dis**, *[S. l.]*, v. 50, n. 3, p. 291–322, 2010. Disponível em: https://doi.org/10.1086/649858

PERFECT, J. R. The Triple Threat of Cryptococcosis: It's the Body Site, the Strain, and/or the Host. **mBio**, *[S. l.]*, v. 3, n. 4, 2012. Disponível em: https://doi.org/10.1128/mBio.00165-12

PERFECT, J. R. Life-saving Antimicrobial Drugs: What Are We Doing to Pricing and Availability?. **Clinical Infectious Diseases**, *[S. l.]*, v. 62, n. 12, p. 1569-1570, 2016. Disponível em: https://doi.org/10.1093/cid/ciw153

PERICOLINI, E. *et al. Cryptococcus neoformans* capsular polysaccharide component galactoxylomannan induces apoptosis of human T-cells through activation of caspase-8. **Cellular Microbiology**, *[S. l.]*, v. 8, n. 2, p. 267–275, 2006. Disponível em: https://doi.org/10.1111/j.1462-5822.2005.00619.x

PIERINI, L. M.; DOERING, T. L. Spatial and temporal sequence of capsule construction in *Cryptococcus neoformans*. **Molecular Microbiology**, *[S. l.]*, v. 41, n. 1, p. 105–115, 2001. Disponível em: https://doi.org/10.1046/j.1365-2958.2001.02504.x

PIROFSKI, L. A.; CASADEVALL, A. Immune-Mediated Damage Completes the Parabola: *Cryptococcus neoformans* Pathogenesis Can Reflect the Outcome of a Weak or Strong Immune Response. **mBio**, *[S. l.]*, v. 8, n. 6, p. e02063-17, 2017. Disponível em: https://doi.org/10.1128/mBio.02063-17

POETA, M. del. Role of Phagocytosis in the Virulence of *Cryptococcus neoformans*. **Eukaryotic Cell**, *[S. l.]*, v. 3, n. 5, p. 1067–1075, 2004. Disponível em: https://doi.org/10.1128/EC.3.5.1067-1075.2004

PRADO, M. *et al.* Mortality due to systemic mycoses as a primary cause of death or in association with AIDS in Brazil: a review from 1996 to 2006. **Memórias do Instituto Oswaldo Cruz**, *[S. l.]*, v. 104, n. 3, p. 513–21, 2009. Disponível em: https://doi.org/10.1590/s0074-02762009000300019

RAJASINGHAM, R. *et al.* Global burden of disease of HIV-associated cryptococcal meningitis: an updated analysis. **The Lancet Infectious Diseases**, *[S. l.]*, v. 17, n. 8, p. 873–881, 2017. Disponível em: https://doi.org/10.1016/S1473-3099(17)30243-8

RAMOS, J.; SYCHROVÁ, H.; KSCHISCHO, M. Yeast Membrane Transport. **Springer**, *[S. l.]*, v. 892, p. 11-31, 2016. *E-book*. Disponível em: https://doi.org/10.1007/978-3-319-25304-6

RANDHAWA, H. S. *et al.* The expanding host tree species spectrum of *Cryptococcus gattii* and *Cryptococcus neoformans* and their isolations from surrounding soil in India. **Medical Mycology**, *[S. l.]*, v. 46, n. 8, p. 823–833, 2008. Disponível em: https://doi.org/10.1080/13693780802124026

REESE, A. J.; DOERING, T. L. Cell wall α-1,3-glucan is required to anchor the *Cryptococcus neoformans* capsule. **Molecular Microbiology**, *[S. l.]*, v. 50, n. 4, p. 1401–1409, 2003. Disponível em: https://doi.org/10.1046/j.1365-2958.2003.03780.x

RETINI, C. *et al.* Specific Activated T Cells Regulate IL-12 Production by Human Monocytes Stimulated with *Cryptococcus neoformans*. **The Journal of Immunology**, *[S. l.]*, v. 162, n. 3, p. 1618–1623, 1999. Disponível em: https://www.jimmunol.org/content/162/3/1618

RETINI, C. *et al.* Interdependency of Interleukin-10 and Interleukin-12 in Regulation of T-Cell Differentiation and Effector Function of Monocytes in Response to Stimulation with *Cryptococcus neoformans*. **Infection and Immunity**, *[S. l.]*, v. 69, n. 10, p. 6064–6073, 2001. Disponível em: https://doi.org/10.1128/IAI.69.10.6064-6073.2001

RHOME, R. *et al.* Biosynthesis and Immunogenicity of Glucosylceramide in *Cryptococcus neoformans* and Other Human Pathogens. **Eukaryotic cell**, *[S. l.]*, v. 6, n. 10, p. 1715-1726, 2007. Disponível em: https://doi.org/10.1128/EC.00208-07

RODRIGUES, M. L. *et al.* Vesicular Polysaccharide Export in *Cryptococcus neoformans* Is a Eukaryotic Solution to the Problem of Fungal Trans-Cell Wall Transport. **Eukaryotic Cell**, *[S. l.]*, v. 6, n. 1, p. 48–59, 2007. Disponível em: https://doi.org/10.1128/EC.00318-06

RODRIGUES, M. L. *et al.* Extracellular Vesicles Produced by *Cryptococcus neoformans* Contain Protein Components Associated with Virulence. **Eukaryotic cell**, *[S. l.]*, v. 7, n. 1, p. 58–67, 2008 a. Disponível em: https://doi.org/10.1128/EC.00370-07

RODRIGUES, M. L. *et al.* Binding of the Wheat Germ Lectin to *Cryptococcus neoformans* Suggests an Association of Chitinlike Structures with Yeast Budding and Capsular Glucuronoxylomannan. **Eukaryotic Cell**, *[S. l.]*, v. 7, n. 4, p. 602–609, 2008 b. Disponível em: https://doi.org/10.1128/EC.00307-07

RODRIGUES, M. L.; NOSANCHUK, J. D. Fungal diseases as neglected pathogens: A wake-up call to public health officials. **PLOS Neglected Tropical Diseases**, *[S. l.]*, v. 14, n. 2, p. e0007964, 2020. Disponível em:

https://doi.org/10.1371/journal.pntd.0007964

ROSAS, Á. L.; NOSANCHUK, J. D.; CASADEVALL, A. Passive Immunization with Melanin-Binding Monoclonal Antibodies Prolongs Survival of Mice with Lethal *Cryptococcus neoformans* Infection. **Infection and Immunity**, *[S. l.]*, v. 69, n. 5, p. 3410–3412, 2001. Disponível em: https://doi.org/10.1128/IAI.69.5.3410-3412.2001

ROY, A. *et al.* Calcium signaling is involved in diverse cellular processes in fungi. **Mycology**, *[S. l.]*, p. 1-15, 2020. Disponível em: https://doi.org/10.1080/21501203.2020.1785962

RUTHERFORD, J. C. The Emerging Role of Urease as a General Microbial Virulence Factor. **PLoS Pathogens**, *[S. l.]*, v. 10, n. 5, 2014. Disponível em: https://doi.org/10.1371/journal.ppat.1004062

SABIITI, W.; MAY, R. C. Mechanisms of infection by the human fungal pathogen *Cryptococcus neoformans*. **Future Microbiology**, *[S. l.]*, v. 7, n. 11, p. 1297–1313, 2012. Disponível em: https://doi.org/10.2217/fmb.12.102

SAKAGUCHI, N. *et al.* Ultrastructural study of *Cryptococcus neoformans* by quick-freezing and deep-etching method. **Mycopathologia**, *[S. l.]*, v. 121, n. 3, p. 133–141, 1993. Disponível em: https://doi.org/10.1007/BF01104068

SANTANGELO, R. *et al.* Role of Extracellular Phospholipases and Mononuclear Phagocytes in Dissemination of Cryptococcosis in a Murine Model. **Infection and immunity**, *[S. l.]*, v. 72, n. 4, p. 2229–39, 2004. Disponível em: https://doi.org/10.1128/IAI.72.4.2229-2239.2004

SANTIAGO-TIRADO, F. H. *et al.* Trojan Horse Transit Contributes to Blood-Brain Barrier Crossing of a Eukaryotic Pathogen. **mBio**, *[S. l.]*, v. 8, n. 1, p. e02183-16, 2017. Disponível em: https://doi.org/10.1128/mBio.02183-16

SCHMIEL, D. H.; MILLER, V. L. Bacterial phospholipases and pathogenesis. **Microbes and Infection**, *[S. l.]*, v. 1, n. 13, p. 1103-1112,1999. Disponível em: https://doi.org/10.1016/S1286-4579(99)00205-1

SCHNEIDER, R. de O. *et al.* Zap1 Regulates Zinc Homeostasis and Modulates Virulence in *Cryptococcus gattii*. **PLoS ONE**, *[S. l.]*, v. 7, n. 8, p. e43773, 2012. Disponível em: https://doi.org/10.1371/journal.pone.0043773

SCHULTZHAUS, Z. *et al.* Transcriptomic analysis reveals the relationship of melanization to growth and resistance to gamma radiation in *Cryptococcus neoformans*. **Environmental Microbiology**, *[S. l.]*, v. 21, n. 8, p. 2613–2628, 2019. Disponível em: https://doi.org/10.1111/1462-2920.14550

SHI, M. *et al.* Real-time imaging of trapping and urease-dependent transmigration of *Cryptococcus neoformans* in mouse brain. **Journal of Clinical Investigation**, *[S. l.]*, v. 120, n. 5, p. 1683–1693, 2010. Disponível em: https://doi.org/10.1172/JCI41963

SIAFAKAS, A. R. *et al.* Lipid Rafts in *Cryptococcus neoformans* Concentrate the Virulence Determinants Phospholipase B1 and Cu/Zn Superoxide Dismutase. **Eukaryotic Cell**, *[S. l.]*, v. 5, n. 3, p. 488–498, 2006. Disponível em:

https://doi.org/10.1128/EC.5.3.488-498.2006

SINGH, A. *et al.* Factors Required for Activation of Urease as a Virulence Determinant in *Cryptococcus neoformans*. **mBio**, *[S. l.]*, v. 4, n. 3, p. e00220-13, 2013. Disponível em: https://doi.org/10.1128/mBio.00220-13

SMITH, L. M.; DIXON, E. F.; MAY, R. C. The fungal pathogen *Cryptococcus neoformans* manipulates macrophage phagosome maturation. **Cellular Microbiology**, *[S. l.]*, v. 17, n. 5, p. 702–713, 2015. Disponível em: https://doi.org/10.1111/cmi.12394

SO, Y.-S. *et al.* Regulatory Mechanism of the Atypical AP-1-Like Transcription Factor Yap1 in *Cryptococcus neoformans*. **mSphere**, *[S. l.]*, v. 4, n. 6, 2019. Disponível em: https://doi.org/10.1128/msphere.00785-19

SPEED, B.; DUNT, D. Clinical and Host Differences Between Infections with the Two Varieties of *Cryptococcus neoformans*. **Clinical Infectious Diseases**, *[S. l.]*, v. 21, n. 1, p. 28–34, 1995. Disponível em: https://doi.org/10.1093/clinids/21.1.28

SQUIZANI, E. D. *et al.* Cryptococcal dissemination to the central nervous system requires the vacuolar calcium transporter Pmc1. **Cellular Microbiology**, *[S. l.]*, v. 20, n. 2, p. e12803, 2018. Disponível em: https://doi.org/10.1111/cmi.12803

SQUIZANI, E. D. *et al.* Calcium Binding Protein Ncs1 Is Calcineurin Regulated in *Cryptococcus neoformans* and Essential for Cell Division and Virulence. **mSphere**, *[S. l.]*, v. 5, n. 5, 2020. Disponível em: https://doi.org/10.1128/mSphere.00761-20

SRIKANTA, D. *et al.* A Sensitive High-Throughput Assay for Evaluating Host-Pathogen Interactions in *Cryptococcus neoformans* Infection. **PLoS ONE**, *[S. l.]*, v. 6, n. 7, p. e22773, 2011. Disponível em: https://doi.org/10.1371/journal.pone.0022773

STANO, P. *et al.* App1: An Antiphagocytic Protein That Binds to Complement Receptors 3 and 2. **Journal of Immunology**, *[S. l.]*, v. 182, n. 1, p. 84–91, 2009. Disponível em: https://doi.org/10.4049/jimmunol.182.1.84

STEENBERGEN, J. N.; SHUMAN, H. A.; CASADEVALL, A. *Cryptococcus neoformans* interactions with amoebae suggest an explanation for its virulence and intracellular pathogenic strategy in macrophages. **Proceedings of the National Academy of Sciences of the United States of America**, *[S. l.]*, v. 98, n. 26, p. 15245–15250, 2001. Disponível em: https://doi.org/10.1073/pnas.261418798

SUMMERS, D. K. *et al.* Coordinate genomic association of transcription factors controlled by an imported quorum sensing peptide in *Cryptococcus neoformans*. **PLOS Genetics**, *[S. l.]*, v. 16, n. 9, p. e1008744, 2020. Disponível em: https://doi.org/10.1371/journal.pgen.1008744

SUN, S. *et al.* The Evolution of Sexual Reproduction and the Mating-Type Locus: Links to Pathogenesis of *Cryptococcus* Human Pathogenic Fungi. **Annual Review of Genetics**, *[S. l.]*, v. 53, n. 1, p. 417–444, 2019. Disponível em: https://doi.org/10.1146/annurev-genet-120116-024755

TAJIMA, K. *et al.* Solubilized melanin suppresses macrophage function. **FEBS**

Open Bio, *[S. l.]*, v. 9, n. 4, p. 791–800, 2019. Disponível em: https://doi.org/10.1002/2211-5463.12615

TAKEDA, T.; YAMAMOTO, M. Analysis and *in vivo* disruption of the gene coding for calmodulin in *Schizosaccharomyces pombe*. **Proceedings of the National Academy of Sciences of the United States of America**, *[S. l.]*, v. 84, n. 11, p. 3580–3584, 1987. Disponível em: https://doi.org/10.1073/pnas.84.11.3580

TEIXEIRA, P. A. C. *et al.* Mannoprotein MP84 mediates the adhesion of *Cryptococcus neoformans* to epithelial lung cells. **Frontiers in cellular and infection microbiology**, *[S. l.]*, v. 4, p. 106, 2014. Disponível em: https://doi.org/10.3389/fcimb.2014.00106

THEWES, S. Calcineurin-Crz1 Signaling in Lower Eukaryotes. **Eukaryotic cell**, *[S. l.]*, v. 13, n. 6, p. 694–705, 2014. Disponível em: https://doi.org/10.1128/EC.00038-14

TIAN, X. *et al. Cryptococcus neoformans* sexual reproduction is controlled by a quorum sensing peptide. **Nature Microbiology**, *[S. l.]*, v. 3, n. 6, p. 698–707, 2018. Disponível em: https://doi.org/10.1038/s41564-018-0160-4

TOPLIS, B. *et al.* The virulence factor urease and its unexplored role in the metabolism of *Cryptococcus neoformans*. **FEMS yeast research**, *[S. l.]*, v. 20, n. 4, 2020. Disponível em: https://doi.org/10.1093/femsyr/foaa031

TREVIJANO-CONTADOR, N. *et al. Cryptococcus neoformans* can form titan-like cells *in vitro* in response to multiple signals. **PLOS Pathogens**, *[S. l.]*, v. 14, n. 5, p. e1007007, 2018. Disponível em: https://doi.org/10.1371/journal.ppat.1007007

TUCKER, S. C.; CASADEVALL, A. Replication of *Cryptococcus neoformans* in macrophages is accompanied by phagosomal permeabilization and accumulation of vesicles containing polysaccharide in the cytoplasm. **Proceedings of the National Academy of Sciences of the United States of America**, *[S. l.]*, v. 99, n. 5, p. 3165–3170, 2002. Disponível em: https://doi.org/10.1073/pnas.052702799

VECCHIARELLI, A. *et al.* Downregulation by cryptococcal polysaccharide of tumor necrosis factor alpha and interleukin-1β secretion from human monocytes. **Infection and Immunity**, *[S. l.]*, v. 63, n. 8, p. 2919–2923, 1995. Disponível em: https://doi.org/10.1128/iai.63.8.2919-2923.1995

VECCHIARELLI, A. *et al.* T lymphocyte and monocyte interaction by CD40/CD40 ligand facilitates a lymphoproliferative response and killing of *Cryptococcus neoformans in vitro*. **European Journal of Immunology**, *[S. l.]*, v. 30, n. 5, p. 1385–1393, 2000. Disponível em: https://doi.org/10.1002/(SICI)1521-4141(200005)30:5<1385::AID-IMMU1385>3.0.CO;2-K

VELAGAPUDI, R. *et al.* Spores as Infectious Propagules of *Cryptococcus neoformans*. **Infection and Immunity**, *[S. l.]*, v. 77, n. 10, p. 4345–4355, 2009. Disponível em: https://doi.org/10.1128/IAI.00542-09

VIJAYAN, K. V. *et al.* Pathophysiology of CD4+ T-Cell Depletion in HIV-1 and HIV-2 Infections. **Frontiers in Immunology**, *[S. l.]*, v. 8, 2017. Disponível em: https://doi.org/10.3389/fimmu.2017.00580

VU, K.; BAUTOS, J. M.; GELLI, A. The Cch1-Mid1 High-Affinity Calcium Channel Contributes to the Virulence of *Cryptococcus neoformans* by Mitigating Oxidative Stress. **Eukaryotic Cell**, *[S. l.]*, v. 14, n. 11, p. 1135–1143, 2015. Disponível em: https://doi.org/10.1128/EC.00100-15

WANG, Y.; AISEN, P.; CASADEVALL, A. *Cryptococcus neoformans* melanin and virulence: mechanism of action. **Infection and Immunity**, *[S. l.]*, v. 63, n. 8, p. 3131–3136, 1995. Disponível em: https://doi.org/10.1128/IAI.63.8.3131-3136.1995

WANG, Y.; CASADEVALL, A. Growth of *Cryptococcus neoformans* in presence of L-Dopa decreases its susceptibility to amphotericin B. **Antimicrobial Agents and Chemotherapy**, *[S. l.]*, v. 38, n. 11, p. 2648-2650, 1994 a. Disponível em: https://doi.org/10.1128/AAC.38.11.2648

WANG, Y.; CASADEVALL, A. Susceptibility of melanized and nonmelanized *Cryptococcus neoformans* to nitrogen- and oxygen-derived oxidants. **Infection and immunity**, *[S. l.]*, v. 62, n. 7, p. 3004–7, 1994 b. Disponível em: https://doi.org/10.1128/IAI.62.7.3004-3007.1994

WHITE, L. P. Melanin: A Naturally Occurring Cation Exchange Material. **Nature**, *[S. l.]*, v. 182, n. 4647, p. 1427–1428, 1958. Disponível em: https://doi.org/10.1038/1821427a0

WICKES, B. L. The role of mating type and morphology in *Cryptococcus neoformans* pathogenesis. **International Journal of Medical Microbiology**, *[S. l.]*, v. 292, n. 5–6, p. 313–329, 2002. Disponível em: https://doi.org/10.1078/1438-4221-00216

WILLIAMSON, P. R. Biochemical and molecular characterization of the diphenol oxidase of *Cryptococcus neoformans*: identification as a laccase. **Journal of Bacteriology**, *[S. l.]*, v. 176, n. 3, p. 656–664, 1994. Disponível em: https://doi.org/10.1128/jb.176.3.656-664.1994

WILLIAMSON, P. R.; WAKAMATSU, K.; ITO, S. Melanin Biosynthesis in *Cryptococcus neoformans*. **Journal of Bacteriology**, *[S. l.]*, v. 180, n. 6, p. 1570–1572, 1998. Disponível em: https://doi.org/10.1128/jb.180.6.1570-1572.1998

WILSON, D. E.; BENNETT, J. E.; BAILEY, J. W. Serologic Grouping of *Cryptococcus neoformans*. **Proceedings of the Society for Experimental Biology and Medicine**, *[S. l.]*, v. 127, n. 3, p. 820–823, 1968. Disponível em: https://doi.org/10.3181/00379727-127-32812

WOLF, J. M. *et al.* Interaction of *Cryptococcus neoformans* Extracellular Vesicles with the Cell Wall. **Eukaryotic Cell**, *[S. l.]*, v. 13, n. 12, p. 1484–1493, 2014. Disponível em: https://doi.org/10.1128/EC.00111-14

WORMLEY, F. L. *et al.* Protection against Cryptococcosis by Using a Murine Gamma Interferon-Producing *Cryptococcus neoformans* Strain. **Infection and Immunity**, *[S. l.]*, v. 75, n. 3, p. 1453–1462, 2007. Disponível em: https://doi.org/10.1128/IAI.00274-06

WOZNIAK, K. L. *et al.* Induction of Protective Immunity Against Cryptococcosis. **Mycopathologia**, *[S. l.]*, v. 173, n. 5-6, p. 387-394, 2012. Disponível em:

https://doi.org/10.1007/s11046-011-9505-8

XUE, C. *et al.* The Human Fungal Pathogen *Cryptococcus* Can Complete Its Sexual Cycle during a Pathogenic Association with Plants. **Cell Host and Microbe**, *[S. l.]*, v. 1, n. 4, p. 263–273, 2007. Disponível em: https://doi.org/10.1016/j.chom.2007.05.005

XUE, C. *Cryptococcus* and Beyond—Inositol Utilization and Its Implications for the Emergence of Fungal Virulence. **PLoS Pathogens**, *[S. l.]*, v. 8, n. 9, p. e1002869, 2012. Disponível em: https://doi.org/10.1371/journal.ppat.1002869

YAUCH, L. E.; LAM, J. S.; LEVITZ, S. M. Direct Inhibition of T-Cell Responses by the *Cryptococcus* Capsular Polysaccharide Glucuronoxylomannan. **PLoS Pathogens**, *[S. l.]*, v. 2, n. 11, p. 1060–1068, 2006. Disponível em: https://doi.org/10.1371/journal.ppat.0020120

YONEDA, A.; DOERING, T. L. A Eukaryotic Capsular Polysaccharide Is Synthesized Intracellularly and Secreted via Exocytosis. **Molecular Biology of the Cell**, *[S. l.]*, v. 17, n. 12, p. 5131–5140, 2006. Disponível em: https://doi.org/10.1091/mbc.E06-08-0701

ZARAGOZA, O. *et al.* The polysaccharide capsule of the pathogenic fungus *Cryptococcus neoformans* enlarges by distal growth and is rearranged during budding. **Molecular Microbiology**, *[S. l.]*, v. 59, n. 1, p. 67–83, 2006. Disponível em: https://doi.org/10.1111/j.1365-2958.2005.04928.x

ZARAGOZA, O. *et al.* Capsule enlargement in *Cryptococcus neoformans* confers resistance to oxidative stress suggesting a mechanism for intracellular survival. **Cellular microbiology**, *[S. l.]*, v. 10, n. 10, p. 2043, 2008. Disponível em: https://doi.org/10.1111/J.1462-5822.2008.01186.X

ZARAGOZA, O. *et al.* The Capsule of the Fungal Pathogen *Cryptococcus neoformans*. **Advances in Applied Microbiology**, *[S. l.]*, v. 2164, n. 09, p. 1–64, 2009. Disponível em: https://doi.org/10.1016/S0065-2164(09)01204-0

ZARAGOZA, O. *et al.* Fungal Cell Gigantism during Mammalian Infection. **PLoS Pathogens**, *[S. l.]*, v. 6, n. 6, p. e1000945, 2010. Disponível em: https://doi.org/10.1371/journal.ppat.1000945

ZARAGOZA, O.; NIELSEN, K. Titan cells in *Cryptococcus neoformans*: cells with a giant impact. **Current Opinion in Microbiology**, *[S. l.]*, v. 16, n. 4, p. 409–413, 2013. Disponível em: https://doi.org/10.1016/j.mib.2013.03.006

ZHANG, Y. *et al.* Robust Th1 and Th17 Immunity Supports Pulmonary Clearance but Cannot Prevent Systemic Dissemination of Highly Virulent *Cryptococcus neoformans* H99. **American Journal of Pathology**, *[S. l.]*, v. 175, n. 6, p. 2489–2500, 2009. Disponível em: https://doi.org/10.2353/ajpath.2009.090530

ZHU, X.; WILLIAMSON, P. R. Role of laccase in the biology and virulence of *Cryptococcus neoformans*. **FEMS Yeast Res**, *[S. l.]*, v. 5, n. 1, p. 1-10, 2004. Disponível em: https://doi.org/10.1016/j.femsyr.2004.04.004

9. Currículo resumido

REUWSAAT, J.C.V.

REUWSAAT, J.

1. Dados pessoais

Nome: Júlia Catarina Vieira Reuwsaat

Local e data de nascimento: São Leopoldo, Rio Grande do Sul, Brasil, 12 de fevereiro de 1992.

Endereço profissional: Centro de Biotecnologia, avenida Bento Gonçalves, 9500, Setor 4, Prédio 43421, laboratório 222, Porto Alegre, RS; CEP 91501-970

Telefone profissional: +55 51 3308-6055; +55 51 3308-6077

E-mail: juliareuwsaat@gmail.com

2. Formação

Curso de graduação: Biotecnologia, ênfase em Biotecnologia Molecular, Universidade Federal do Rio Grande do Sul (UFRGS). Período: 2011-2014.

Título: Expressão da manoproteína Mp43 de *Cryptococcus gattii* com potencial imunoterapêutico para o tratamento da criptococose.

Orientadora: Lívia Kmetzsch

Coorientadora: Marilene Vainstein

Curso de Pós-Graduação concluído: Mestrado *stricto sensu* em Biologia Celular e Molecular pelo Programa de Pós-Graduação em Biologia Celular e Molecular (PPGBCM), UFRGS. Período: 2015-2016.

Título: Avaliação funcional de uma manoproteína predita de *Cryptococcus gattii* na arquitetura capsular e interação com o hospedeiro.

Orientadora: Lívia Kmetzsch

Coorientadora: Marilene Vainstein

Bolsista da Coordenação de Aperfeiçoamento de Pessoal de Nível Superior, CAPES, Brasil.

Curso de Pós-Graduação em andamento: Doutorado *stricto sensu* em Biologia Celular e Molecular pelo Programa de Pós-Graduação em Biologia Celular e Molecular (PPGBCM), UFRGS. Período: 2016-atual.

Título: O fator de transcrição Pdr802 regula a produção de células gigantes, quorum sensing e a patogenicidade de *Cryptococcus neoformans*.

Orientadora: Lívia Kmetzsch

Coorientadora: Marilene Vainstein

Bolsista da Coordenação de Aperfeiçoamento de Pessoal de Nível Superior, CAPES, Brasil.

Doutorado sanduíche: Laboratório da professora Dra. Tamara Doering na Washington University, School of Medicine, St. Louis. Período: 2018-2019.

2.1. Formação complementar

Curso Inglês. Carga horária: 480h. Período: 2014-2017. Universidade do Vale do Rio dos Sinos, UNISINOS, Brasil.

Curso Genética Forense. Carga horária: 10h. Período: 2016-2016. Instituto Galeno, Brasil.

Curso Bioestatística. Carga horária: 45h. Período: 2015-2015. Universidade Federal do Rio Grande do Sul, UFRGS, Brasil.

Curso Bioinformática Básica. Carga horária: 30h. Período: 2015-2015. Universidade Federal do Rio Grande do Sul, UFRGS, Brasil.

Curso Evolução, Análise Filogenética e Filogenômica. Carga horária: 20h. Período: 2014-2014. Universidade Federal do Rio Grande do Sul, UFRGS, Brasil.

Curso PCR em tempo real. Carga horária: 3h. Período: 2014-2014. Universidade Federal do Rio Grande do Sul, UFRGS, Brasil.

Curso Modelagem de Proteínas. Carga horária: 4h. Período: 2014-2014. Universidade Federal do Rio Grande do Sul, UFRGS, Brasil.

Curso Estudo da Sinalização do Câncer. Carga horária: 15h. Período: 2013-2013. Universidade Federal do Rio Grande do Sul, UFRGS, Brasil.

Curso Introdução à metagenômica. Carga horária: 8h. Período: 2013-2013. Universidade Federal do Rio Grande do Sul, UFRGS, Brasil.

Curso Biologia Molecular Básica. Carga horária: 24h. Período: 2012-2012. Universidade Federal do Rio Grande do Sul, UFRGS, Brasil.

Curso Técnicas de Espalhamento de Luz. Carga horária: 20h. Período: 2012-2012. Universidade Federal do Rio Grande do Sul, UFRGS, Brasil.

3. Estágios

Vínculo: Estágio Curricular. Instituição: Laboratório de Diagnóstico Molecular Amplicon, Brasil. Período: 2014-2014.

Projeto: Realização de técnicas de diagnóstico molecular de doenças genéticas e infecciosas e de erros inatos do metabolismo.

Vínculo: Bolsista de Iniciação científica. Instituição: Universidade Federal do Rio Grande do Sul, UFRGS, Brasil. Período: 2014-2014.

Projeto: Estudo funcional de transportadores de cálcio na patogênese de *Cryptococcus neoformans*.

Orientadora: Lívia Kmetzsch

Coorientadora: Marilene Vainstein

Bolsista BIC UFRGS-REUNI.

Vínculo: Bolsista de Iniciação científica. Instituição: Universidade Federal do Rio Grande do Sul, UFRGS, Brasil. Período: 2012-2014.

Projeto: Estudo de novos determinantes de virulência das leveduras patogênicas *Cryptococcus neoformans* e *Cryptococcus gattii*.

Orientadora: Marilene Vainstein

Coorientadora: Lívia Kmetzsch

Bolsista PIBIC CNPq-UFRGS.

Vínculo: Bolsista de Iniciação científica. Instituição: Universidade Federal do Rio Grande do Sul, UFRGS, Brasil. Período: 2012-2012.

Projeto: Caracterização de genes diferencialmente expressos durante os primeiros estágios da infecção de *Metarhizium anisopliae* no carrapato *Boophilus microplus*.

Orientador: Augusto Schrank

4. Prêmios e distinções

Láurea Acadêmica, Universidade Federal do Rio Grande do Sul, 2014.

Bolsa de Pós-doutorado do Conselho Nacional de Desenvolvimento Científico e Tecnológico (CNPq) – PDJ (Processo 150414/2020-0).

5. Experiência profissional ou didática anterior

Projeto de extensão Falaí Biotec. Divulgação da Biotecnologia para alunos do ensino médio de Porto Alegre, através de ações em colégios públicos. Cargo: coordenadora. Período: 2016-2017.

6. Artigos completos publicados

SQUIZANI, E.D., **REUWSAAT, J.C.V.**, MOTTA, H., TAVANTI, A., KMETZSCH, L., 2021. Calcium: a central player in *Cryptococcus* biology. Fungal Biol. Rev. https://doi.org/10.1016/j.fbr.2021.03.004

OLIVEIRA, N.K., FRANK, L.A., SQUIZANI, E.D., **REUWSAAT, J.C.V.**, MARQUES, B.M., MOTTA, H., GARCIA, A.W.A., KINSKOVSKI, U.P., BARCELLOS, V.A., SCHRANK, A., POHLMANN, A.R., STAATS, C.C., GUTERRES, S.S., VAINSTEIN, M.H., KMETZSCH, L., 2021. New nanotechnological formulation based on amiodarone-loaded lipid core nanocapsules displays anticryptococcal effect. Eur. J. Pharm. Sci. 162, 105816. https://doi.org/10.1016/j.ejps.2021.105816

REUWSAAT, J.C. V., DOERING, T.L., KMETZSCH, L., 2021. Too much of a good thing: Overproduction of virulence factors impairs cryptococcal pathogenicity. Microb. Cell 8, 108–110. https://doi.org/10.15698/mic2021.05.750

REUWSAAT, J.C.V., AGUSTINHO, D.P., MOTTA, H., CHANG, A.L., BROWN, H., BRENT, M.R., KMETZSCH, L., DOERING, T.L., 2021. The Transcription Factor Pdr802 Regulates Titan Cell Formation and Pathogenicity of *Cryptococcus neoformans*. MBio 12, 1–20. https://doi.org/10.1128/mBio.03457-20

GARCIA, A.W.A., KINSKOVSKI, U.P., DIEHL, C., **REUWSAAT, J.C.V.**, MOTTA DE SOUZA, H., PINTO, H.B., TRENTIN, D.D.S., DE OLIVEIRA, H.C., RODRIGUES, M.L., BECKER, E.M., KMETZSCH, L., VAINSTEIN, M.H., STAATS, C.C., 2020. Participation of Zip3, a ZIP domain-containing protein, in stress response and virulence in *Cryptococcus gattii*. Fungal Genet. Biol. 144. https://doi.org/10.1016/j.fgb.2020.103438

SILVA E SOUZA, E., BARCELLOS, V. DE A., SBARAINI, N., **REUWSAAT, J.C.V.**, SCHNEIDER, R. DE O., DA SILVA, A.C., GARCIA, A.W.A., VON POSER, G.L.,

BARBOSA, E.G., LIMA, J.P.M.S., VAINSTEIN, M.H., 2020. A Plumieridine-Rich Fraction From *Allamanda polyantha* Inhibits Chitinolytic Activity and Exhibits Antifungal Properties Against *Cryptococcus neoformans*. Front. Microbiol. 11, 2058. https://doi.org/10.3389/fmicb.2020.02058

SQUIZANI, E.D., **REUWSAAT, J.C.V.**, LEV, S., MOTTA, H., SPEROTTO, J., KAUFMAN-FRANCIS, K., DESMARINI, D., HENNING VAINSTEIN, M., CHRISTIAN STAATS, C., DJORDJEVIC, J.T., KMETZSCH, L., 2020. Calcium Binding Protein Ncs1 Is Calcineurin Regulated in *Cryptococcus neoformans* and Essential for Cell Division and Virulence. mSphere 5. https://doi.org/10.1128/mSphere.00761-20

PEREIRA, E., NAPP, A.P., ALLEBRANDT, S., BARBOSA, R., **REUWSAAT, J.**, LOPES, W., KMETZSCH, L., STAATS, C.C., SCHRANK, A., DALLEGRAVE, A., PERALBA, M.D.C.R., PASSAGLIA, L.M.P., BENTO, F.M., VAINSTEIN, M.H., 2019. Biodegradation of aliphatic and polycyclic aromatic hydrocarbons in seawater by autochthonous microorganisms. Int. Biodeterior. Biodegrad. 145. https://doi.org/10.1016/j.ibiod.2019.104789

BARCELLOS, V.A., MARTINS, L.M.S., FONTES, A.C.L., **REUWSAAT, J.C.V.**, SQUIZANI, E.D., DE SOUSA ARAÚJO, G.R., FRASES, S., STAATS, C.C., SCHRANK, A., KMETZSCH, L., VAINSTEIN, M.H., 2018. Genotypic and phenotypic diversity of *Cryptococcus gattii* VGII clinical isolates and its impact on virulence. Front. Microbiol. 9. https://doi.org/10.3389/fmicb.2018.00132

REUWSAAT, J.C.V., MOTTA, H., GARCIA, A.W.A., VASCONCELOS, C.B., MARQUES, B.M., OLIVEIRA, N.K., RODRIGUES, J., FERRAREZE, P.A.G., FRASES, S., LOPES, W., BARCELLOS, V.A., SQUIZANI, E.D., HORTA, J.A., SCHRANK, A., RODRIGUES, M.L., STAATS, C.C., VAINSTEIN, M.H., KMETZSCH, L., 2018. A Predicted Mannoprotein Participates in *Cryptococcus gattii* Capsular Structure. mSphere 3, e00023-18. https://doi.org/10.1128/mSphere.00023-18

LOPES, W., **REUWSAAT, J.C.V.**, HENNING VAINSTEIN, M., STAATS, C., KMETZSCH, L., SCHRANK, A., HENNING VAINSTEIN, M., 2018. The duality of a deadly pathogen. Clin. Microbiol. Infect. 24. https://doi.org/10.1016/j.cmi.2018.07.009

ZIMBRES, A.C.G., **REUWSAAT, J.C.V.**, BARCELLOS, V.A., JOFFE, L.S., FONSECA, F.L., STAATS, C.C., SCHRANK, A., KMETZSCH, L., VAINSTEIN, M.H., RODRIGUES, M.L., 2018. Pharmacological inhibition of pigmentation in *Cryptococcus*. FEMS Yeast Res. 19. https://doi.org/10.1093/femsyr/foy119

SQUIZANI, E.D., OLIVEIRA, N.K., **REUWSAAT, J.C.V.**, MARQUES, B.M., LOPES, W., GERBER, A.L., DE VASCONCELOS, A.T.R., LEV, S., DJORDJEVIC, J.T., SCHRANK, A., VAINSTEIN, M.H., STAATS, C.C., KMETZSCH, L., 2018. Cryptococcal dissemination to the central nervous system requires the vacuolar calcium transporter Pmc1. Cell. Microbiol. 20, e12803.

https://doi.org/10.1111/cmi.12803

OLIVEIRA, D.L., FONSECA, F.L., ZAMITH-MIRANDA, D., NIMRICHTER, L., RODRIGUES, J., PEREIRA, M.D., **REUWSAAT, J.C.V.**, SCHRANK, A., STAATS, C., KMETZSCH, L., VAINSTEIN, M.H., RODRIGUES, M.L., 2016. The putative autophagy regulator Atg7 affects the physiology and pathogenic mechanisms of *Cryptococcus neoformans*. Future Microbiol. 11. https://doi.org/10.2217/fmb-2016-0090

7. Resumos e trabalhos apresentados em congressos

REUWSAAT, J.C.V.; DE SOUZA, H.M.; VASCONCELOS, C.B.; MARQUES, B.M.; RODRIGUES, J.; FRASES, S.; SCHRANK, A.; RODRIGUES, M.L.; STAATS, C.C.; VAINSTEIN, M.H.; KMETZSCH, L., 2017. A predicted mannoprotein is required for capsular architecture in *Cryptococcus gattii*. 10th International Conference on *Cryptococcus* and Cryptococcosis, 2017, Foz do Iguaçu.

DE SOUZA, H.M.; **REUWSAAT, J.C.V.**; MARQUES, B.M.; VASCONCELOS, C.B.; SCHRANK, A.; STAATS, C.C.; VAINSTEIN, M.H.; KMETZSCH, L., 2017. A *Cryptococcus gattii* recombinant mannoprotein as a potential candidate for immunotherapy. 10th International Conference on *Cryptococcus* and Cryptococcosis, 2017, Foz do Iguaçu.

REUWSAAT, J.C.V.; VASCONCELOS, C.B.; STAATS, C.C.; SCHRANK, A.; VAINSTEIN, M.H.; KMETZSCH, L., 2015. Heterologous expression and functional characterization of a hypothetical mannoprotein from *Cryptococcus gattii*. 28º Congresso Brasileiro de Microbiologia, 2015, Florianópolis.

SQUIZANI, E.D.; OLIVEIRA, N.K; **REUWSAAT, J.C.V.**; VASCONCELOS, A.T; SCHRANK, A.; VAINSTEIN, M.H.; STAATS, C.C.; KMETZSCH, L., 2015. Null mutations for vacuolar Ca^{2+} transporters strongly attenuates cryptococcal virulence in a systemic model of cryptococossis. 28º Congresso Brasileiro de Microbiologia, 2015, Florianópolis.

REUWSAAT, J.C.V.; STAATS, C.C.; SCHRANK, A.; VAINSTEIN, M.H.; KMETZSCH, L., 2014. Heterologous expression of *Cryptococcus gattii* mannoprotein Mp43 and evaluation of its immunotherapeutic potential in murine cryptococcosis. 60º Congresso Brasileiro de Genética, 2014, Guarujá.

REUWSAAT, J.C.V.; STAATS, C.C.; SCHRANK, A.; VAINSTEIN, M.H.; KMETZSCH, L., 2014. Expression of a *Cryptococcus gattii* mannoprotein in *Pichia pastoris*. XII International Meeting on Paracoccidioidomycosis, 2014, Brasília.

REUWSAAT, J.C.V.; CUPERTINO, J.B.; STAATS, C.C.; SCHRANK, A.; KMETZSCH, L.; VAINSTEIN, M.H, 2013. Expressão de uma manoproteína de

Cryptococcus gattii recombinante com potencial imunoterapêutico para o tratamento da criptococose. Congresso Brasileiro de Microbiologia, 2013, Natal.

PAIXÃO, R.L.A.; JUNGES, A.; **REUWSAAT, J.C.V.**; STAATS, C.C.; SCHRANK, A., 2012. Construction of bicistronic vectors for the expression of two genes using *IRES* in *Metarhizium anisopliae*. 28º Reunião de Genética de Microorganismos (REGEM), 2012, Foz do Iguaçu.